CRC REVIVALS

Polymers for Electronic Applications

Edited by
Juey H. Lai

CRC Press
Taylor & Francis Group

VISIT…

Polymers for Electronic Applications

Editor
Juey H. Lai, Ph.D.
Lai Laboratories, Inc.
Burnsville, Minnesota

CRC Press
Taylor & Francis Group
Boca Raton London New York

CRC Press is an imprint of the
Taylor & Francis Group, an **informa** business

First published 1989 by CRC Press
Taylor & Francis Group
6000 Broken Sound Parkway NW, Suite 300
Boca Raton, FL 33487-2742

Reissued 2018 by CRC Press

© 1989 by CRC Press, Inc.
CRC Press is an imprint of Taylor & Francis Group, an Informa business

No claim to original U.S. Government works

This book contains information obtained from authentic and highly regarded sources. Reasonable efforts have been made to publish reliable data and information, but the author and publisher cannot assume responsibility for the validity of all materials or the consequences of their use. The authors and publishers have attempted to trace the copyright holders of all material reproduced in this publication and apologize to copyright holders if permission to publish in this form has not been obtained. If any copyright material has not been acknowledged please write and let us know so we may rectify in any future reprint.

Except as permitted under U.S. Copyright Law, no part of this book may be reprinted, reproduced, transmitted, or utilized in any form by any electronic, mechanical, or other means, now known or hereafter invented, including photocopying, microfilming, and recording, or in any information storage or retrieval system, without written permission from the publishers.

For permission to photocopy or use material electronically from this work, please access www.copyright.com (http://www.copyright.com/) or contact the Copyright Clearance Center, Inc. (CCC), 222 Rosewood Drive, Danvers, MA 01923, 978-750-8400. CCC is a not-for-profit organization that provides licenses and registration for a variety of users. For organizations that have been granted a photocopy license by the CCC, a separate system of payment has been arranged.

Trademark Notice: Product or corporate names may be trademarks or registered trademarks, and are used only for identification and explanation without intent to infringe.

Library of Congress Cataloging-in-Publication Data

Polymers for electronic applications, editor, Juey H. Lai
p. cm.
Includes bibliographies and index.
ISBN 0-8493-4704-1
1. Electronics—Materials. 2. Polymers.
I. Lai, J. H. (Juey H.)
TK7871.15.P6P6261989 621‘ .381—dc20 89-9860

A Library of Congress record exists under LC control number: 89009860

Publisher's Note
The publisher has gone to great lengths to ensure the quality of this reprint but points out that some imperfections in the original copies may be apparent.

Disclaimer
The publisher has made every effort to trace copyright holders and welcomes correspondence from those they have been unable to contact.

ISBN 13: 978-1-315-89680-9 (hbk)
ISBN 13: 978-1-351-07590-9 (ebk)

Visit the Taylor & Francis Web site at http://www.taylorandfrancis.com and the
CRC Press Web site at http://www.crcpress.com

PREFACE

Polymers have been increasingly used in many areas of electronics in recent years. This is in part due to the versatility of synthetic methods which can modify polymer properties to fit the need, and in part due to the feasibility of processing and fabrication of polymers into a particular desired form, e.g., a large area thin film with controlled thickness. The objective of this book is to review and discuss some important applications of polymers in electronics. The first three chapters discuss the current primary applications of polymers in semiconductor device manufacturing: polymers as resist materials for integrated circuit fabrication, polyimides as electronics packaging materials, and polymers as integrated circuit encapsulants.

The emergence of conducting polymers as a new class of electronic materials will have a profound effect on future electronic products. Considerable research is currently underway in the field of conducting polymers. Chapters 4 and 5 discuss recent research in electrically conducting polymers and ionically conducting polymer electrolytes, respectively. Chapter 6 describes an emerging area which could be important for future electronics and electro-optics: Langmuir-Blodgett technique for deposition of extremely thin film of controlled film thickness.

The field of polymers for electronic applications has grown very large indeed, and it is not feasible to cover all areas in a single volume. The book covers six important areas which are of current interest. Attempts have been made by the authors to cite many references which should be useful to readers for further reading.

THE EDITOR

Juey H. Lai, Ph.D., is President, Lai Laboratories, Inc., Burnsville, MN. Prior to founding Lai Laboratories in 1987, he was a Staff Scientist at Physical Sciences Center, Honeywell, Inc., Bloomington, MN.

Dr. Lai received his B.S. degree in chemical engineering from National Taiwan University, Taipei, Taiwan, and his M.S. in chemical engineering and Ph.D. in physical chemistry from the University of Washington, Seattle. After completing postdoctoral research at the University of Minnesota, Minneapolis, he joined Honeywell as Principal Research Scientist in 1973. He was appointed Senior Principal Research Scientist in 1978 and Staff Scientist in 1983.

Dr. Lai is a member of the American Chemical Society, a fellow of the American Institute of Chemists and a member of the honor societies Sigma Xi and Phi Lambda Upsilon.

He received Honeywell's highest technical award, the H. W. Sweatt Award, in 1981. He has seven patents and was designated as a Star Inventor by Honeywell. He was the Principal Investigator of several contracts funded by the U.S. Army Electronics Technology and Devices Laboratory and has published over 40 papers in polymer resists, advanced microlithography, polyimides, polymer gas sensor, and polymer liquid crystals. His current interests are in the development of advanced polymeric materials for microelectronics and biomedical applications.

CONTRIBUTORS

Ronald J. Jensen, Ph.D.
Senior Principal Research Scientist
Sensors and Signal Processing Laboratory
Honeywell, Inc.
Bloomington, Minnesota

Juey H. Lai, Ph.D.
President
Lai Laboratories, Inc.
Burnsville, Minnesota

Scott E. Rickert, Ph.D.
President
NanoFilm Corporation
Strongsville, Ohio

Duward F. Shriver, Ph.D.
Professor
Department of Chemistry
Northwestern University
Evanston, Illinois

James S. Tonge, Ph.D.
Project Chemist
Dow Corning
Midland, Michigan

Stephen T. Wellinghoff, Ph.D.
Staff Scientist
Department of Chemistry and Chemical Engineering
Southwest Research Institute
San Antonio, Texas

Ching-Ping Wong, Ph.D.
Distinguished Technical Staff
AT&T Bell Laboratories
Princeton, New Jersey

The editor and authors wish to thank the following persons for their comments and suggestions in reviewing the manuscripts: Mr. Robert Ulmer of Honeywell, Inc. and Dr. Lloyd Shepherd of Cray Research for reading Chapter 1; Mr. David Pitkanene of Honeywell for reading Chapter 3; Dr. Robert Lyle of Southwest Research Institute and Professor Gary Wnek of Rensselaer Polytechnic Institute for reviewing Chapter 4; Professor Austin Angell of Purdue University and Professor B. B. Owens and his colleagues at the University of Minnesota for reviewing Chapter 5; and Professor Jerome Lando of Case Western Reserve University for reviewing Chapter 6. Nora Madson deserves special thanks for her excellent work in typing the manuscripts. I wish to thank my wife, Li, for her support and assistance during the preparation of the volume.

Juey H. Lai
Burnsville, MN
February 1989

TABLE OF CONTENTS

Chapter 1
Polymer Resists for Integrated Circuit (IC) Fabrication 1
Juey H. Lai

Chapter 2
Polyimides: Chemistry, Processing, and Application for Microelectronics 33
R. J. Jensen and Juey H. Lai

Chapter 3
Integrated Circuit Device Encapsulants 63
Ching-Ping Wong

Chapter 4
Electrically Conducting Polymers for Applications 93
S. T. Wellinghoff

Chapter 5
Polymer Electrolytes 157
James S. Tonge and D. F. Shriver

Chapter 6
Langmuir-Blodgett Films: Langmuir Films Prepared by the Blodgett Technique 211
Scott E. Rickert

Index 227

Taylor & Francis
Taylor & Francis Group
http://taylorandfrancis.com

Chapter 1

POLYMER RESISTS FOR INTEGRATED CIRCUIT (IC) FABRICATION

Juey H. Lai

TABLE OF CONTENTS

I. Introduction 2

II. Fundamental Properties of Polymer Resists 2
- A. Application of Polymer Resists for IC Fabrication 2
- B. Brief Introduction to Microlithography 3
  - 1. Photolithography 3
  - 2. Electron-Beam Lithography 5
  - 3. X-Ray Lithography 8
- C. General Requirements of Polymer Resists; Factors Which Affect the Resist Performance 9
  - 1. Sensitivity 9
  - 2. Resolution 11
  - 3. Thermal Stability 11
  - 4. Adhesion 12
  - 5. Dry and Wet Etch Resistance 12

III. Chemistry of Polymer Resists 14
- A. Photoresists 14
- B. Electron Resists 15
  - 1. Positive Resists 16
  - 2. Negative Resists 18
- C. Deep-UV Resists 20
- D. X-Ray Resists 21
- E. Dry Developable Resists 22
- F. Multilayer Resists 24

IV. Recent Developments and Future Outlook 26
- A. Recent Developments 26
  - 1. Nonswelling Negative Photoresists 26
  - 2. Organosilicon Polymer Resists 27
- B. Future Outlook 28

References 28

I. INTRODUCTION

One of the main applications of polymers in electronics is as lithographic resists in integrated circuit (IC) fabrication. The ICs, or modern solid-state devices, consist of patterned thin films of metals, dielectrics, and semiconductors on a monolithic substrate such as a silicon wafer.[1,2] Circuit patterns in IC wafers are formed first by delineating circuit patterns in an imaging medium called a resist, and then transferring the resist patterns to the substrate wafer by etching and/or deposition processes in a single series of operations. The resists currently used in IC fabrication are synthetic organic polymers (with or without additives) which are radiation sensitive.

When the resist is exposed to high-energy radiation such as ultraviolet (UV) light, electrons, or X-rays, certain chemical reactions take place in the exposed area, resulting in a change in its solubility. Utilizing the solubility difference between the exposed and unexposed area, a pattern image can be developed by using a liquid called developer.[3,4]

Resists may be classified according to the nature of radiation used in defining the resist image as photo-, electron-beam or X-ray resists. The corresponding image-forming process is called photolithography, electron-beam lithography, and X-ray lithography.[3,5] Lithographic processes have been used to generate and fabricate circuit patterns in thin films on a semiconductor substrate by the microelectronics industry since 1950.

The basic functional element of ICs is the transistor. Current efforts in the development of very large-scale integration (VLSI) aim to integrate thousands of transistors in a single chip. The manufacture of VLSI circuits has as its primary goal the lowest possible cost per electronic function performed.[2] To achieve this goal, the microelectronics industry has adopted the features of simultaneous fabrication of hundreds of circuits side by side on a single wafer, and continuing miniaturization of the circuit elements and their interconnections.[2]

Photolithography has been the key lithographic technique for solid-state device and IC fabrication. The minimum line width obtained by the photolithographic process, however, has been limited to approximately 1.0 μm. Short wavelength photo-, electron-beam, and X-ray lithographics are the advanced microlithographies which have been pursued to meet the need for fabricating ICs with *submicron* dimensions. Polymer resists designed and developed for advanced microlithographies are critical to the success of VLSI and high-speed solid-state electronics.

II. FUNDAMENTAL PROPERTIES OF POLYMER RESISTS

A. Application of Polymer Resists for IC Fabrication

The application of polymer resists for IC fabrication is based on radiation-induced change in the chemical solubility of the exposed resists. In a typical application, the polymer resist is dissolved in an organic solvent and spin coated onto the surface of the wafer as a thin film (0.5 to 2.0 μm thick). The resist film is prebaked and exposed to high-energy radiation such as UV light, an electron beam, X-rays, or an ion beam. When the resist is irradiated, certain chemical reactions occur in the exposed area resulting in a change in its chemical solubility. Utilizing the solubility difference between exposed and unexposed area, a pattern image can be developed by using a liquid developer to dissolve away the unwanted area. Subsequently, the resist pattern is used as a mask for plasma and ion etching, wet chemical etching, ion implantation, or metal lift-off. The resist is called a negative resist if the solubility of the exposed resist decreases after exposure. Conversely, it is called positive resist if the solubility of the exposed resist increases after exposure.

Current negative photoresists generally consist of a rubber-like polymer, e.g., *cis*-poly(isoprene), and a cross-linking agent called bis-azide, N_3-Ar-N_3, where Ar is an aromatic

group. Upon exposure to UV light of 400 nm wavelength, the bis-azide is excited and forms a highly reactive species known as nitrene :N-Ar-N: which acts as a cross-linking agent to connect the polyisoprene molecules together, thereby decreasing their solubility.

The positive photoresists generally consist of low molecular weight phenolic polymers and a monomeric organic compound called ortho-diazoketone. The dissolution rate of the mixture in alkaline aqueous developer is very low. Upon exposure to UV light, the ortho-diazoketone is photochemically converted to carboxylic acid which renders the exposed resist soluble in the alkaline developer, thus enabling a positive pattern to be developed. The ortho-diazoketone is sometimes called a dissolution inhibitor.

The application of polymer resists in advanced microlithographies such as deep-UV, electron-beam, X-ray, and ion-beam lithography is based on the same principle, but is different from photoresists. Most electron, X-ray, deep-UV, and ion-beam resists are organic polymers without additives. When the polymer resists are exposed to the ionizing radiation, cross-linking or chain scission occurs in the resists. For negative resists, cross-linking occurs predominantly in the exposed area resulting in a decrease in its solubility. For positive resists, chain scission occurs predominantly in the exposed area resulting in an increase in its solubility.

The average IC may require many (10 to 15) lithographic/process steps. A typical lithographic/process cycle is an ion implantation. The objective of an ion implantation is to implant dopant atoms (e.g., phosphorous or arsenic) into the selective area of a silicon wafer. Selective doping can be accomplished by using a patterned resist mask which is created by a lithographic process step as shown in Figure 1. A resist layer is spin coated over the layer of SiO_2 and exposed to high-energy radiation. The resist is developed, i.e., either the exposed (positive resist) or the unexposed (negative resist) area of resist is dissolved and removed. The resist layer is then used as the mask and the ion implantation performed. Finally, the resist layer is removed, completing the doping process.

B. Brief Introduction to Microlithography

1. Photolithography

Photolithography has been the key lithographic technique for solid-state device and IC fabrication. The basic photolithographic equipment consists of a UV light source (300 to 400 nm wavelength), an alignment system, a photomask, and photoresists. The photomask is fabricated either by electron-beam lithography or optical techniques,[6] and consists of circuit patterns defined in a thin film (~1000 Å) of chromium or ion oxide deposited on glass or quartz substrate.

The three exposed techniques currently used in photolithography are contact printing, proximity printing, and projection printing. The contact printing and proximity printing are also called shadow printing (Figure 2). In contact printing, the photoresist and the photomask are in intimate contact and the gap between the mask and the photoresist is practically zero. In proximity printing, a gap ($\geq$10 μm) is maintained between the resist and the photomask. The minimum line width W which can be replicated in shadow printing is given by[7]

$$2W = 3\sqrt{\lambda(S + d/2)}$$

where λ is the wavelength of the UV light, S is the gap width between the mask and the resist film, and d is the thickness of the resist film.

Although high resolution is obtained in contact printing, the intimate contact between the mask and the photoresist often causes damage in both the mask and the wafer (due to contaminant particles) and produces defects which reduce the device yield. Maintaining a small constant gap is difficult to achieve without an extremely flat wafer. The practical gap width is probably limited to 10 μm.[7] The minimum line width which can be replicated by

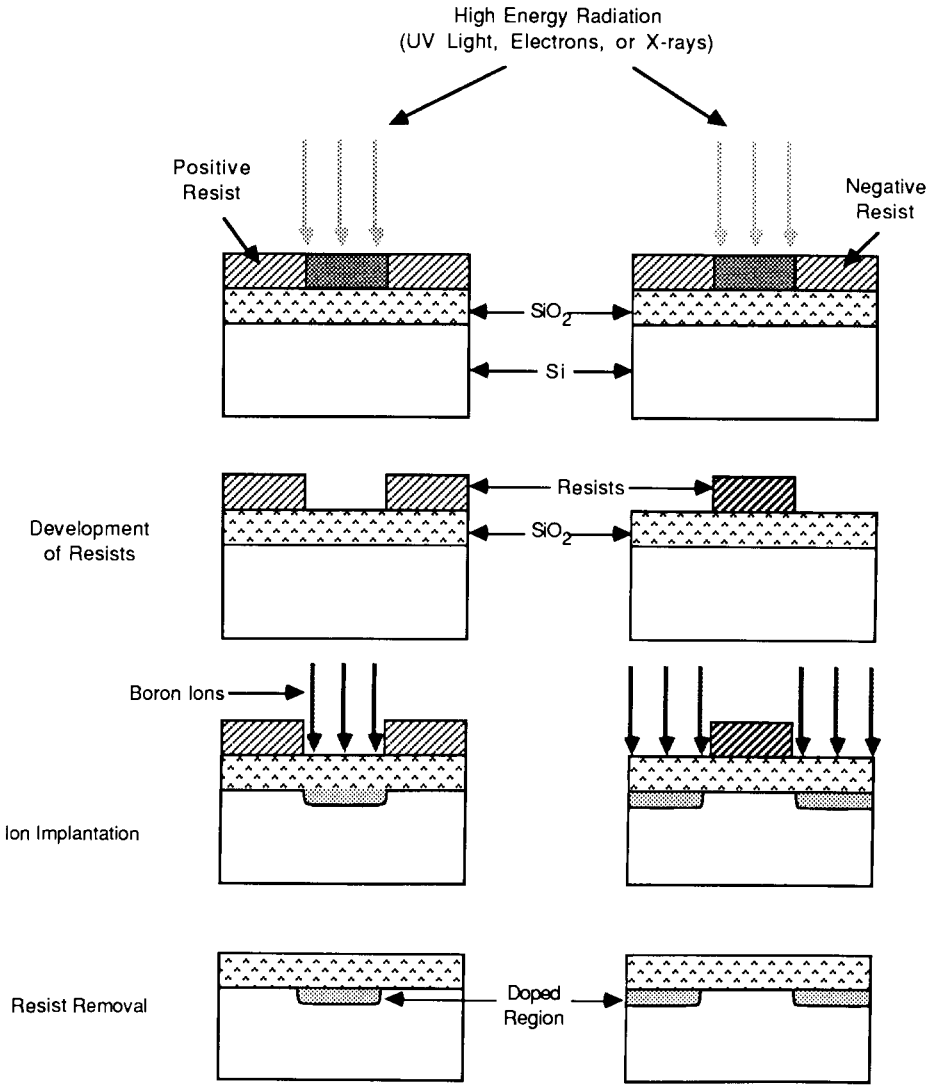

FIGURE 1. A lithographic process, ion implantation.

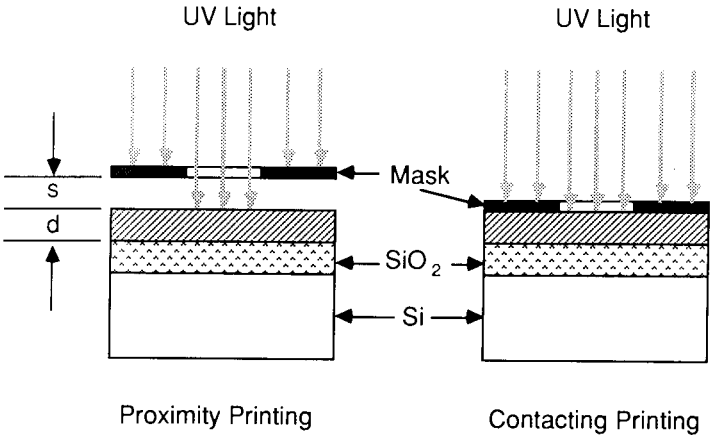

FIGURE 2. Proximity and contact printing.

Table 1
MINIMUM LINE WIDTH W VS. WAVELENGTH λ[a]

	Contact printing (S = 0)		Proximity printing (S = 10 μm)	
λ	200 nm	400 nm	200 nm	400 nm
W	0.5 μm	0.8 μm	2.2 μm	3.1 μm

[a] Photoresist film thickness d is assumed to be 1.5 μm.

shadow printing using a 200- and 400-nm wavelength of UV light is shown in Table 1. Submicron line width is thus seen theoretically possible using short wavelength photolithography such as deep-UV lithography.

Projection printing removes the mask from intimate contact with the wafer and projects the image of a mask to the wafer with either a reflective or a refractive optical system. Two forms of projection system have been developed for IC fabrication. They are 1:1 scanning projection and step-and-repeat projection systems.[5-7]

In the 1:1 scanning projection system, the image of a narrow arc of the mask is projected at a 1:1 ratio to the wafer by spherical reflective mirrors. Since only a small area of the mask is satisfactorily projected, the entire wafer has to be exposed portion by portion. Scanning of the wafer is performed by moving the mask and wafer together while the optics system remains fixed. Since the scanning projection system uses reflective rather than refractive optics, chromatic and spherical aberrations are reduced to zero. The depth of focus is relatively large ($\sim$ 4 μm) and the exposure time is relatively short, less than 1 min.[5]

In the step-and-repeat projection system (commonly called wafer stepper), high-quality refractive lenses are used to project a reticle pattern on the wafer. A typical system consists of a high-intensity mercury light source, a collimating, collection lens system to focus the illumination on a reticle, and a reduction lens system to project the image of the reticle onto the surface of a wafer.[6] The wafer is mounted on a laser-controlled stage, and after each exposure is stepped a distance, realigned, focused, and exposed, until the entire wafer is exposed. Typical steppers project 5× images from chrome reticles at a single wavelength onto wafers which move under the lens in 24-mm or smaller steps. An overlay of ±0.15 μm can be achieved by focusing and aligning at each of the steps as exposure proceeds across the entire wafer. The problem of runout, warpage, and wafer size change during processing which is a problem with the 1:1 scanning projection system is reduced in the stepper by exposing small portions of the wafer at a time, thereby reducing the alignment and focus error. The resolution of wafer stepper is headed toward submicron, as optics are improved in steps by reducing the wavelength from 436—405 to 356 nm and possibly 249 nm (deep-UV region).

2. Electron-Beam Lithography

Electron-beam lithography is an advanced lithographic technique which uses a computer-controlled electron beam (10 to 30 keV) to delineate circuit patterns with submicron features in an electron resist. An electron resist is usually an organic polymer without additive. When a negative electron resist is exposed to a high-energy electron beam, cross-linking occurs predominantly in the exposed resist resulting in a decrease in solubility. On the other hand, when a positive resist is exposed, chain scission occurs predominantly in the exposed resist resulting in an increase in solubility.[4]

An electron-beam lithographic system is basically a computer-controlled scanning electron

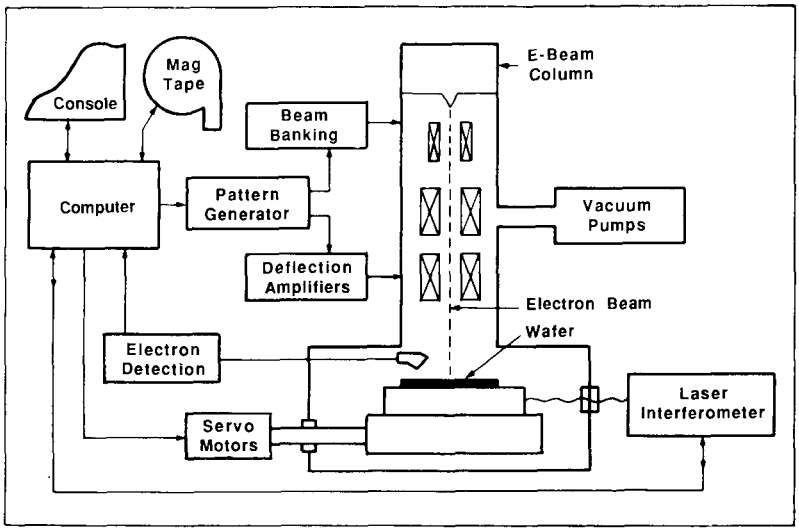

FIGURE 3. An electron-beam lithographic system.

microscope with a precisely controlled stage.[5,8,9] As illustrated in the diagram of a basic electron-beam lithographic system (Figure 3), the circuit pattern is produced by focusing an electron beam and deflecting it on an electron resist-coated wafer situated on an X-Y stage controlled by a laser interferometer. Since the scan field of an electron-optical column is typically a few millimeters (i.e., an electron-beam system can only expose a pattern over a small area at any one time), the resist-coated wafer must be moved many times to expose the entire wafer. The movement of the wafer and its position are usually controlled precisely by the use of a laser interferometer.[9]

The electron-optical column of the scanning electron-beam system consists of an electron gun, electromagnetic lenses, a beam deflection system, and a beam blanking system (Figure 4). An electron gun widely used in the electron-beam system is a lanthanum hexaboride (LaB_6) cathode. The LaB_6 is a thermionic emitter which is brighter and has a longer operating life than the conventional tungsten gun. The electromagnetic lenses are used to focus the electron beam on the surface of the workpiece, and the final beam size is generally $\leq 1/4$ minimum line width desired. The beam deflection system consists of electromagnetic coils used to deflect the beam over a target area called a scan field. The beam blanking system is an electrostatic deflector that deflects the beam out of an adjacent aperture to turn the beam off. Two electron-beam writing strategies to position the beam in the scan field are raster scan and vector scan. In raster scan, the electron beam covers the scan field line by line, and is turned on and off according to the pattern data. In vector scan, the electron beam is deflected to a pattern area requiring exposure, and turned on once it is positioned (Figure 5).[8,10]

Although scanning electron-beam lithography can produce very fine lines (less than 100-Å-wide lines have been produced),[11] the proximity effects due to electron scattering often limit the resolution achievable in a complex circuit pattern.

When high-energy electrons penetrate polymer resists, they encounter both elastic and inelastic collisions with the polymer and substrate molecules.[12,13] Inelastic collisions are small-angle collisions involving primary electrons and the bonding electrons which provide the mechanism of energy transfer. Elastic collisions are the collisions occurring between the primary electrons and the nuclei of the atoms which constitute the polymer and substrate. Elastic scattering is a large-angle scattering which markedly changes the trajectory of the electrons and is responsible for broadening the exposed area from that of the incident beam

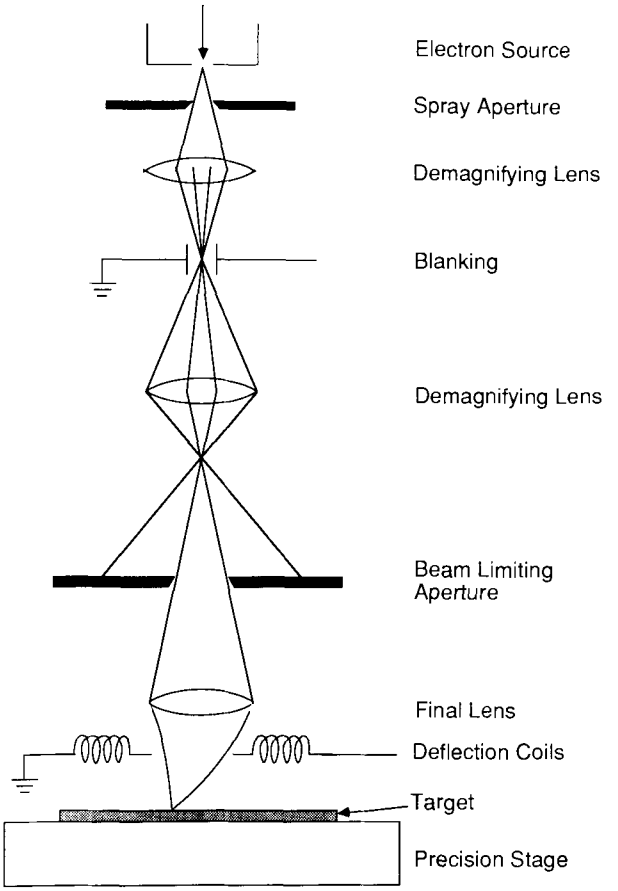

FIGURE 4. Scanning electron-beam system.

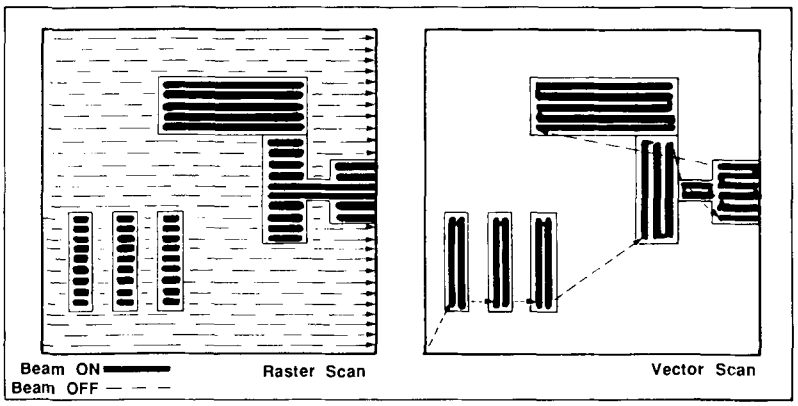

FIGURE 5. Raster scan vs. vector scan in electron-beam lithographic system.

cross section. The scattered electrons (both electrons scattered in the resist and electron backscattered from the substrate) may undergo further inelastic collisions with atoms in the resists outside the area defined by the electron beam, thus creating the proximity effect. To generate a high-resolution pattern, the pattern data generally must be altered to correct for the proximity effect.[8]

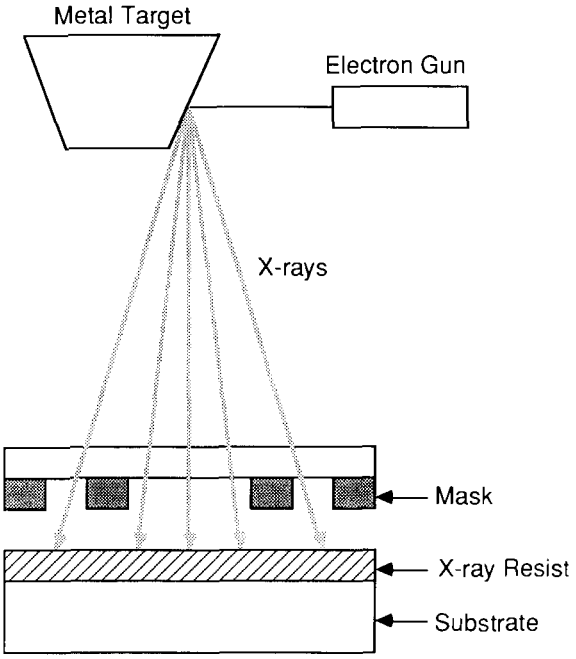

FIGURE 6. An X-ray lithographic system.

3. X-Ray Lithography

In X-ray lithography soft X-rays are used to irradiate X-ray-sensitive polymer resists. X-ray lithography is an extension of photolithography. However, since the wavelength of the X-ray is much shorter (2 to 50 Å) than that of UV light (200 to 400 Å) used in photolithography, the diffraction effects and the standing wave phenomena encountered in photolithography do not pose problems in X-ray lithography.[5,10] The main feature of X-ray lithography is that X-rays can penetrate deep into the resist without undergoing scattering as in electron exposure; therefore, high-resolution patterns can be produced in the thick resist which facilitates pattern transfer.

An X-ray lithographic system generally consists of an X-ray source, a patterned X-ray mask, an alignment system, and X-ray-sensitive resists (Figure 6).[14,15]

X-rays are generated when high-energy electrons (100 kV) impinge on a metal target (e.g., iron, copper, aluminum).[16] Two types of X-ray radiation are produced, a broad band (bremsstrahlung radiation) and characteristic lines. The broad-band X-rays are produced when the incident electrons are accelerated by interacting with the nucleus of the atoms which constitute the target. The line spectra result from an electronic transition that involves innermost atomic orbitals. When the inner-bound electrons of the target (e.g., electrons in the K shell) are ejected by the incident electron beam, the electrons from the other shells fill the hole accompanied by emission of X-rays characteristic of the target materials. The wavelengths of the characteristic radiation λ_c for the common targets are palladium (λ_c = 4.37 Å), aluminum (λ_c = 8.34 Å), copper (λ_c = 13.36 Å), and carbon (λ_c = 43.82 Å).

To obtain an intense X-ray beam, the target must be bombarded with high-energy electrons which heat up the target. A high-flux X-ray source is important for the X-ray lithography since it means shorter exposure time. Typical systems use rotating aluminum anodes[17] which are water cooled. Synchroton radiation and electron storage rings can produce intense, highly collimated X-rays which are suitable for X-ray lithography. The motion of electrons at a relativistic speed (v_c) in a circular orbit generates intense electromagnetic radiation with the peak intensity in the X-ray range. The cost of a synchroton or electron storage ring facility is high and, thus, will probably prevent it from becoming an X-ray source for IC production.

X-ray masks are generally produced by electron-beam lithography. A typical mask consists of a thin substrate (1 to 5 μm) transparent to the X-ray, with the thick X-ray absorber deposited on the substrate forming the circuit patterns.[18] Many materials, both organic and inorganic, have been used as the thin substrate materials.[17] They include Mylar (polyester), polyimides, silicon, silicon nitride, silicon oxide, and silicon carbide. Since the substrate film is very thin, the dimensional stability and the durability of the mask have been a major concern. The common absorber material is gold, and the thickness of gold is typically about 5000 Å. A pattern in gold can be created by using either a deposition (e.g., electroplating or metal lift-off) or an etching method (ion-beam etching or sputter etching).

Exposure of X-ray resists is accomplished by the photoelectrons generated by inelastic collision of X-ray with the bonding electrons of the resist atoms. The photoelectrons undergo both elastic and inelastic scattering as they penetrate the polymer resists. This results in chain scission or cross-linking of the polymer resists similar to that occurring in the electron resists. The energy of the photoelectrons depends on the wavelength of the X-rays, but is in the order of the energy of the incoming photons. The penetration range of the photoelectrons, is smaller than that in the electron-beam lithography, and high-resolution submicron resist patterns are obtainable in a thick X-ray resist.

C. General Requirements of Polymer Resists; Factors Which Affect the Resist Performance

The main requirements of lithographic resists are high sensitivity, high resolution, high thermal stability, good adhesion to the substrate, and adequate wet and dry etch resistance.[3,19] It is important to realize that resist performance depends not only on the intrinsic properties of the materials, but also significantly on the processing parameters. The important intrinsic properties of the polymer resists are chemical structure, molecular weight, molecular weight distribution, and glass transition temperature (T_g). The important processing parameters are resist film thickness, resist film prebake and postbake conditions, developer and development conditions, exposure dose, and the substrate onto which the resist film is deposited.

1. Sensitivity

The sensitivity of a lithographic resist is usually defined as the exposure dose required to induce desired chemical change in the exposed area for complete development. Sensitivity is commonly expressed as J cm^{-2} for photo- and X-ray resists, and C cm^{-2} for electron- and ion-beam resists, where J is joule and C is coulomb. The lithographic sensitivity is determined by plotting normalized film thickness remaining after development vs. logarithm of the exposure dose. For positive resists, the sensitivity is the dose where complete development is obtained (Figure 7). For negative resists, the sensitivity is defined as the dose $Dg^{0.5}$ required to cross-link the resist such that the exposed area retains 50% of original thickness after development (Figure 8). A sensitive resist is required for short exposure time, i.e., high throughput. The sensitivity of photoresists is largely determined by the sensitivity of the monomeric photosensitizer to the UV light and, therefore, is not significantly dependent on the polymer. The sensitivity of electron, X-ray, deep-UV, and ion-beam resists, however, is significantly dependent on the chemical structure of the monomers, the molecular weight, and molecular weight distribution of the polymer. The intrinsic radiation sensitivity of a polymer is related to its chemical structure[12,13,20] and is often characterized by its G_s and G_x values, where G_s and G_x are defined as the number of scission events per 100 eV of energy absorbed and the number of cross-linking events per 100 eV of energy absorbed, respectively. Both G_s and G_x values for a polymer can be determined by measuring M_n (number-average molecular weight) and M_w (weight-average molecular weight) of the irradiated polymer as a function of exposure dose,[12] as shown in the Equations 1 and 2, where D is exposure dose, N_A is Avogadro's number, M_n and M_n° are the number-average molecular weight of exposed and unexposed polymer, and M_w and M_w° are the weight-average molecular weight of exposed and unexposed polymers, respectively.

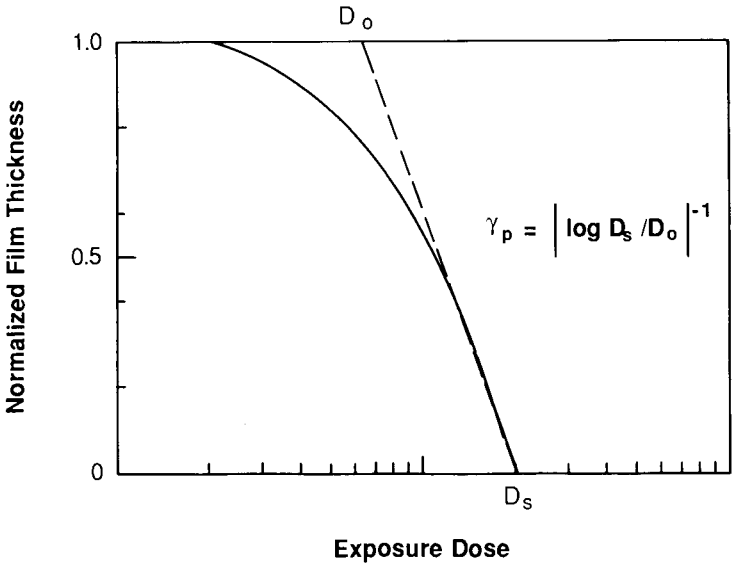

FIGURE 7. Resist film thickness vs. exposure dose (positive resist).

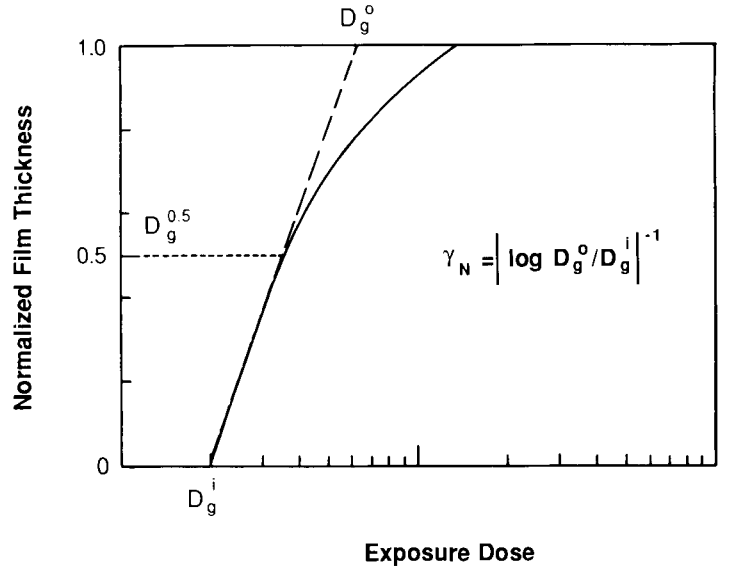

FIGURE 8. Resist film thickness vs. exposure dose (negative resist).

$$M_n^{-1} = M_n^{o-1} + (G_s - G_x)D/100N_A \quad (1)$$

$$M_w^{-1} = M_w^{o-1} + (G_s - 4G_x)D/200N_A \quad (2)$$

The radiation sensitivity and the G values of a number of vinyl polymers have been extensively studied.[21-24]

The effect of molecular weight and molecular weight distribution on the sensitivity of positive electron resists has been found to be significant.[25,26] Increased sensitivity is predicted and observed for the positive electron resist poly(methylmethacrylate) (PMMA) with higher

and narrow molecular weight distribution. The reasons for the increased sensitivity of resists with high molecular weight are that for a given area and thickness of resist, there would be fewer molecules and, therefore, a lower exposure dose would be needed to obtain sufficient chain scission for complete development. Similarly, the narrower the molecular weight distribution, the lower the exposure dose is needed to obtain a sufficient molecular weight difference between unexposed and exposed resists.[25]

2. Resolution

The resolution of a lithographic resist depends significantly on many factors, such as intrinsic properties of the polymer (e.g., chemical structure, molecular weight, and molecular weight distribution), the processing parameters (e.g., prebaking temperature, resist film thickness, developer used, etc.), and exposure techniques (e.g., wavelength of photons and electron-beam energy). The resolution of a resist has been found to be intimately related to the contrast γ of the resist. The contrast of the resist can be experimentally determined from the film thickness after development vs. the exposure dose plots shown in Figures 7 and 8. The contrast is defined as

$$\gamma_p = |\log D_s/D_o|^{-1}$$

for positive resists and

$$\gamma_N = |\log D_g^o/D_g^i|^{-1}$$

for negative resists. It is clear from the definition that the higher the contrast, the higher the resolution. The contrast of the high-resolution positive electron resist PMMA, for example, has a contrast γ_p of 11.7.[27]

The effect of molecular weight and distribution on the sensitivity and resolution of a negative electron resist has been studied using nearly monodisperse and polydisperse polystyrene.[28] It has been found that the sensitivity of the monodisperse polystyrene increases significantly with an increase in molecular weight, monodisperse polystyrene has a very high contrast, and the contrast of polystyrene decreases with an increase in molecular weight distribution.[28] The reason for increased sensitivity in high molecular weight negative resists is similar to that for high molecular weight positive resists. For a polymer resist with a broad molecular weight distribution, gel formation occurs over a large range of exposure dose and, hence, the contrast is low.

3. Thermal Stability

High thermal stability is an important requirement of polymer resists when the resists are used as the etch mask for ion implantation or plasma and ion etching. High thermal stability implies that polymers must have high glass transition temperature T_g. (Glass transition temperature is a second-order phase transition point related to the chain mobility. Below T_g, polymers are brittle and hard. Above T_g, polymers are viscous and rubber-like.) A resist with low T_g could flow or deform when heated during ion implantation or dry etching. The effects of temperature on the profile of the resist patterns are shown in Figure 9 for the positive electron resist EP-25H. The resist EP-25H is a copolymer of methacrylonitrile and methacrylic acid, and has a T_g of 195°C.[29] Although baking the resist at 190°C for 30 min did not induce any significant change (Figure 9B), baking at 200°C caused a noticeable change in the resist line profile (Figure 9C).

Current photoresists cannot withstand a processing temperature higher than 150°C. Efforts have been underway to develop high-temperature photoresists which can withstand temperature near 200°C.[30] Other methods such as use of UV light or plasma to enhance the thermal stability of resist image have also been reported.[31,32]

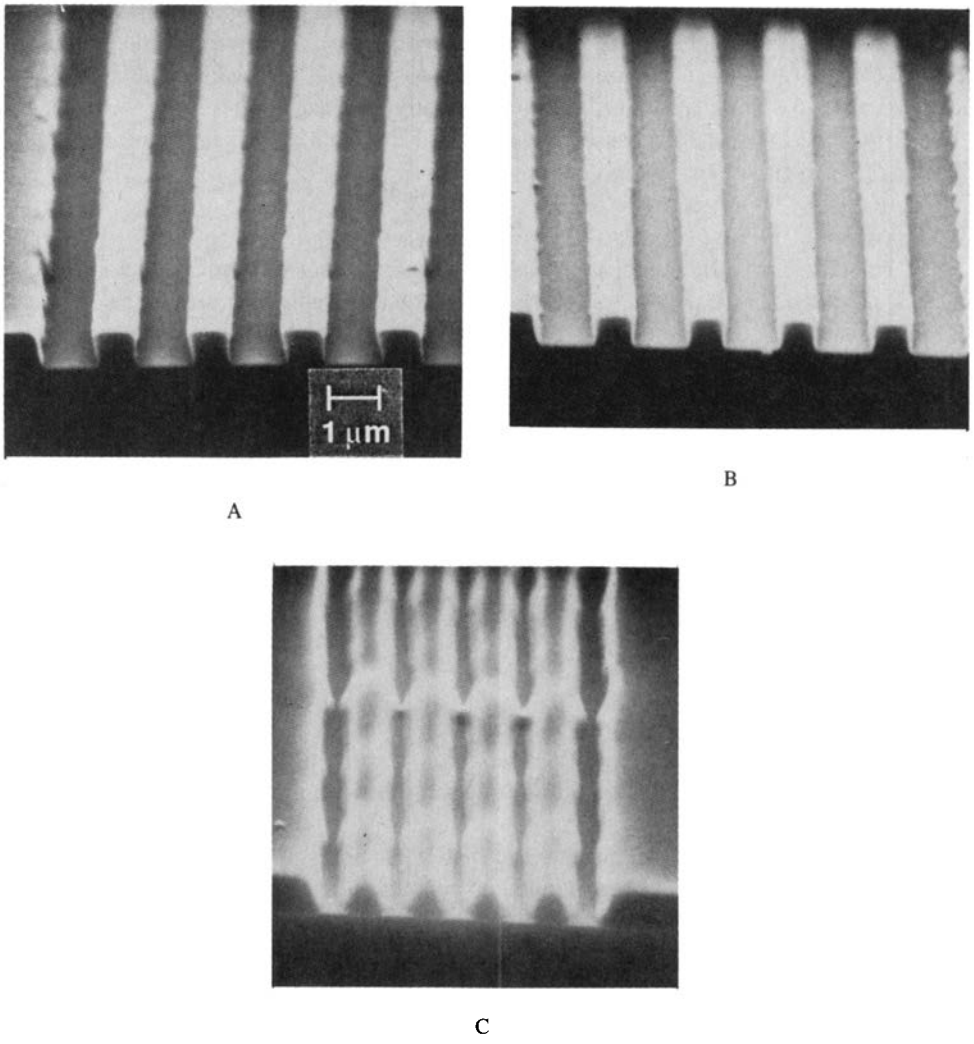

FIGURE 9. Effect of baking temperature on resist line profile. (A) Before bake. (B) After bake at 190°C. (C) After bake at 200°C.

4. Adhesion

Good adhesion to the substrate is also an important requirement of polymer resists. The requirement is critical when the resist is used as the wet etch mask. Poor adhesion allows the liquid etchant to penetrate into the interface causing severe undercutting and loss of line width control. Poor adhesion is often caused by the presence of contaminants on the surface of the substrate or by the presence of particles in the resist solution, and thus can be improved by cleaning the surface or filtering the solution. Adhesion can be improved by applying an adhesion promoter which adheres well to both the substrate and the resist. The adhesion promoter is applied first to the substrate before coating the resist film. One of the widely used adhesion promoters for the photoresists is hexamethyldisilazane (HMDS).

5. Dry and Wet Etch Resistance

The main application of polymer resists in IC fabrication is as etch masks for etching thin films of metals, dielectrics, and semiconductors. The etching can be carried out by either

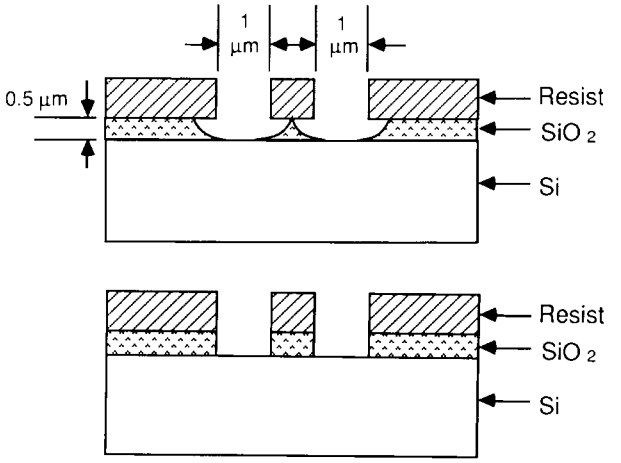

FIGURE 10. Isotropic etching (A) and anisotropic etching (B).

wet etching which uses liquid etchants, or dry etching which uses gases in the form of a plasma. The resists must have adequate resistance to both wet and dry etchants.

A large number of wet etchants have been used.[33] They include acids (e.g., HF, HCl, H_2SO_4, HNO_3, and H_3PO_4), bases (e.g., KOH, NaOH, NH_4OH), and oxidizing agents (e.g., H_2O_2, N_2H_2). Wet etching is an isotropic etching; therefore, it produces undercutting in the pattern edge profile. As the etch mask, the resist must have a much lower etch rate than that of the substrate. Further, the resist must have good adhesion to the substrate.

The current trend in IC fabrication has been the increasing use of dry etching. There are a number of reasons for favoring the dry etching. However, the foremost reason is that while wet etching is generally an isotropic process, anisotropic etching (which is necessary for submicron pattern transfer) can be obtained in dry etching through manipulation of system configuration and process parameters. As the circuit pattern size shrinks to the 1-μm region, the high-resolution pattern transfer by etching is feasible only through anisotropic etching. This is illustrated in Figure 10 which shows that replication of two 1.0-μm-wide lines with 1.0-μm pitch can be replicated in a 0.5-μm-thick film only by an anisotropic etching, but not by the isotropic etching such as wet etching. Further, from economic, safety, and pollution points of view, the chemicals used in wet etching are often more expensive and toxic, and require careful control and disposal.

Dry etching is accomplished by use of gases in the form of a plasma,[34,35] and is sometimes called plasma-assisted etching.[35,36] A plasma can be loosely defined as an assembly of positively and negatively charged particles,[36] and the term discharge is often used interchangeably with plasma. A low-pressure gas discharge is created inside the etch reactor when the electrons in the reactor (generated by photoionization or field emission initially) pick up the energy in an r_f field and collide with the gaseous molecules producing highly reactive ions, electrons, and radicals. The inelastic collisions between the electrons and gases also produce electronically excited atoms and molecules which produce glow.

Dry etching can be (1) completely physical, e.g., ion etching in which inert gases such as Ar ions are used to physically sputter etch material off the surface; (2) a combination of physical and chemical etching, e.g., reactive-ion etching which uses gases such as CF_4 to etch Si; and (3) purely chemical, e.g., use of O_2 plasma to remove (oxidize) the photoresist in a barrel etcher.[37] The etched products are generally volatile gases which are removed by vacuum pumping.

Used as the dry etch mask for high-resolution pattern transfer, the polymer resists must

have a low plasma etch rate. The plasma etch rate of a number of polymers in oxygen plasma has been studied.[38] It has been found that polymers with strong backbone bonds characterized by low G_s, or polymers with aromatic and polar functional groups attached to the main chain and/or side chain are more resistant to plasma etching. Presence of chlorines in the polymers appeared to increase the etch rate of the polymers.[38] The plasma etch rate of a number of vinyl polymers and positive photoresists has also been examined using a CF_4 and O_2 (4%) gas mixture.[39] It has been found that the etch rate of the positive photoresist is at least a factor of 2 lower than the vinyl polymers. Among the vinyl polymers which were studied, poly(methacrylonitrile) has the lowest etch rate. The high etch resistance of positive photoresists is attributed to the aromatic nature of the novolak resins in the photoresists (see the discussion below).

Similar studies to determine the plasma etch rate of various polymers in $CF_4 + O_2$ and CF_4 discharge also indicated that the polymers with aromatic structure were more resistant by a factor of 2 to 4 than the nonaromatic polymers.[40] The etch rate of the aromatic polymers, e.g., polystyrene, poly(*N*-vinylcarbazole), and positive photoresist Az, is in the range of 600 to 700 Å/min. The etch rate of the copolymer of methyl methacrylate and methacrylic acid (a vinyl polymer used as a positive electron resist), on the other hand, is much higher, ~3200 Å/min.[40]

III. CHEMISTRY OF POLYMER RESISTS

A. Photoresists

A photoresist is composed of a polymer, a photosensitizer (also called photoinitiator or photoactive compound), and a solvent.[41] The polymer is the film-forming medium used as the mask for image transfer. The photosensitizer is an organic monomer sensitive to UV light. Upon exposure to UV light, the photosensitizer is photochemically modified which causes a change in the solubility of the polymer. The solvent is used for casting thin polymer film (0.5 to 2.0 μm) by spin coating.

Although there are many positive photoresists commercially available, the basic chemistry of the resist process is similar. The polymers used in positive photoresists are generally low molecular weight phenolic-based polymers such as novolak resins. Novolak resins are low molecular weight polymers derived from condensation polymerization of phenols and formaldehyde (see Table 2). The resins are moderately soluble in aqueous alkaline developers such as metallic or quarternary ammonium hydroxide.

The dissolution rate of the polymer in the developer, however, is significantly reduced (by a factor of ~100)[42] when the polymer is mixed with the photosensitizer. The amount of photosensitizer in the mixture is typically about 25 to 30 wt%. The photosensitizers of positive resists are generally the derivatives of the organic compound 1,2-napthaquinone which are insoluble in alkaline developers, and are called the dissolution inhibitors. Upon exposure to UV light, the photosensitizer 1,2-napthaquinone is converted to ketene, which subsequently reacts with water vapor to form indene carboxylic acid.[43]

The indene carboxylic acid is soluble in the alkaline developer. The effectiveness of the sensitizer as the dissolution inhibitor is thus destroyed by the UV exposure, which renders the exposed photoresist soluble in the alkaline developer, enabling a positive pattern to be developed (see Figure 11).

The application of negative photoresist is based on photo cross-linking of polymer molecules, which decreases polymer solubility enabling a negative pattern to be developed. The polymer resin currently widely used in negative photoresists is cyclized polyisoprene (see Table 2), which has a higher T_g and better film-forming properties than the rubbery, linear polyisoprene.[41] The photosensitizers are generally bis-azide compounds with chemical structures N_3-Ar-N_3 (where Ar is an aromatic group), which absorb UV light of 400 nm wave-

Table 2
PHOTORESIST FORMULATIONS

Type	Sensitizer	Polymer
Positive	1, 2-napthaquinone diazide	Novolak Resin
Negative	Bis-azide e.g. 4,4'-Diazidostilbene	Cyclized polyisoprene

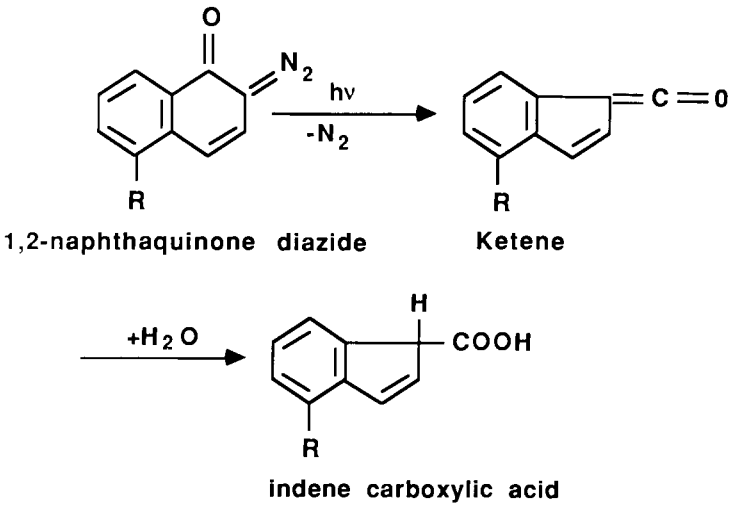

FIGURE 11. Effect of UV light exposure on positive photoresists.

length. Upon exposure to UV light, the bis-azide is excited and forms a highly reactive nitrene, :N-Ar-N:, which acts as a cross-linking agent to connect the polyisoprene molecules, thereby decreasing their solubility[41] (Figure 12). Examples of the sensitizers are 2,6-di-(4'-azidobenzol)-4-methyl cyclohexanone[44] and 4,4'-diazidostilbene.[45]

B. Electron Resists

Most electron resists are single-component organic polymers without additives. The principle of application of electron resists is based on radiation-induced change in solubility.

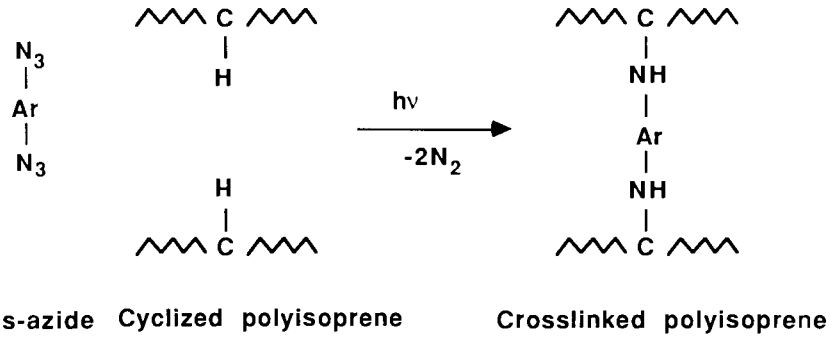

FIGURE 12. Effect of UV light exposure on negative photoresists.

When polymer electron resists are exposed to high-energy electron beam, the polymer molecules are excited and ionized. Although the subsequent reactions are complex, the overall effect of the ionizing radiation on the polymer is well known.[46] The polymers undergo either chain scission or cross-linking or both. Cross-linking means that polymer chains are bonded together through intermolecular bonds which increases the molecular weight. Chain scission means that high molecular weight polymers are broken into several small polymer fragments which decreases polymer molecular weight. One important property of polymers is that both polymer solubility and dissolution rate decrease with an increase in molecular weight.[47] As the polymer chain length increases, the randomly coiled chains are entangled to such an extent that it takes time for polymer chains to separate from one another and dissolve in the solvent developer. Thus, when a positive electron resist is exposed to an electron beam, chain scission occurs predominantly resulting in an increase in solubility. Conversely, when a negative electron resist is exposed to an electron beam, cross-linking occurs predominantly in the polymer resulting in a decrease in solubility. Empirically, the dissolution rate of an amorphous polymer S is related to the molecular weight M by the equation $S = KM^{-a}$, where K and a are constants for a given polymer and solvent.[48,49]

It has been observed that negative resists are generally more sensitive than positive results, but the resolution of negative resists is inherently lower. This is due to the nature of the negative resist process where cross-linked polymers are formed in the exposed area. During the development process in which the unexposed area is removed, the solvent molecules invariably penetrate into the exposed cross-linked polymers, resulting in swelling of the polymer which seriously degrades the resist resolution. Further, the cross-linked resist molecules induced by electron backscattering are difficult to remove cleanly, which results in poor edge acuity (Figure 13). Plasma descum using O_2 plasma is generally applied to improve the edge acuity of developed negative resist patterns.

1. Positive Resists

Three distinct types of polymers have been used as positive electron resists. The first type is vinyl polymer represented by Structure I where X and Y are not hydrogen atoms. For this type of polymer, poly(methacrylates) (Structure II), in particular, have been extensively studied. Some positive resists derived from vinyl polymers are shown in Table 3.

PMMA is probably the earliest polymer used as a positive resist.[50] PMMA has good resolution and acceptable thermal stability (T_g = 100°C), but its sensitivity of 8×10^{-5} C cm^{-2} at 15 kV is low. The search for a more sensitive resist

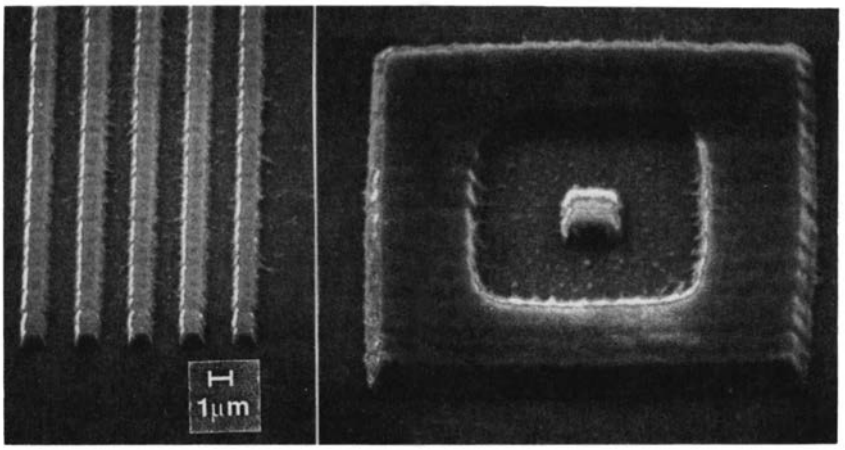

FIGURE 13. Developed negative electron resist patterns prior to plasma descum.

I

II

has led to the development of homopolymers[51-56] and copolymers[29,57-64] of vinyl polymers which act as positive resists. Since degradation of a positive resist occurs through the scission of the main chain, chemical and steric configurations which tend to weaken the main chain stability of a polymer, e.g., a polar substituent at the quarternary carbon or a bulky side group, may increase the radiation degradation susceptibility of the polymer. It has been found that incorporation of fluorine or chlorine atoms into vinyl polymers often leads to an increase in sensitivity.[54-56] The increase in sensitivity, however, is sometimes accompanied by a decrease in thermal stability,[54] a decrease in exposure range where resists act as positive resists,[56,58,62] or a decrease in plasma etch resistance. It has been difficult to find a vinyl polymer which has both high sensitivity and high dry etch resistance. The resist, poly(methacrylonitrile-co-methacrylic acid), probably has the highest thermal stability (T_g = 195°C) among the resists listed in Table 3.[29] It has high resolution (≤0.08 μm) and good sensitivity (15 μC cm^{-2}), and is compatible with semiconductor fabrication.[64] Submicron complemental metal oxide silicon (CMOS) devices have been successfully fabricated using the resist and direct-write e-beam lithography.[65]

The second type of polymer is poly(olefin sulfones), represented by Structure III, which are copolymers of SO_2 and olefin. Poly(butene-l-sulfone) (see Structure IV) is the most well-known example of this type.[66] The polymer is known as PBS and is commercially available. PBS is one of the most sensitive positive electron resists. The G_s of PBS is reported to be about 10, and its electron-beam sensitivity is 1.6×10^{-6} C cm^{-2}, with submicron resolution of 0.5 μm. The dry etch resistance of PBS, however, it extremely low. It is widely used for mask making, but is not suitable for direct wafer exposure application.

Table 3
POSITIVE ELECTRON RESISTS DERIVED FROM VINYL POLYMERS

Polymers	Sensitivity (10^{-6} C cm^2)	T_q (°C)	Ref.
Poly(methyl methacrylate)	100	100	50, 51
Poly(methyl α-chloroacrylate)	10	151	52
Poly(methacrylonitrile)	15	120	53
Poly(hexafluorobutyl methacrylate)	0.4	50	54
Poly(trifluoroethyl α-chloroacrylate)	1—10	133	55
Poly(2,2,2-trichloroethyl methacrylate)	125	138	56
Poly(methyl methacrylate-co-isobutylene)	5	47	57
Poly(methyl methacrylate-co-methyl α-chloroacrylate)	6	127	58
Poly(methyl methacrylate-co-acrylonitrile)	6	97	59
Poly(methyl methacrylate-co-methacrylic acid)	5—10	145	60
Poly(methacrylonitrile-co-methyl α-chloroacrylate)	18	120	61
Poly(methacrylonitrile-co-trichloroethyl methacrylate)	8	123	62
Poly(methyl methacrylate-co-methyl itaconate)	6	150	63
Poly(methacrylonitrile-co-methacrylic acid)	15	195	29, 64

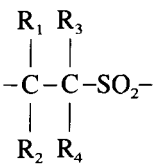

III

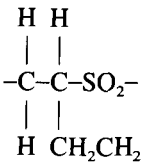

IV

To overcome the weak dry etch resistance of PBS, a two-component positive electron resist has been developed.[67] The resist is composed of a novolak resin in a solid solution with poly(2-methyl-1-pentene sulfone) (PMPS) and was intended to combine the electron-beam sensitivity of poly(olefin sulfone) and high dry etch resistance of the novolak resin. The principle of the application appears to be similar to that of the positive photoresist where PMPS acts as the dissolution inhibitor. Upon exposure to an electron beam, PMPS is depolymerized, which renders the polymer resin soluble in the alkaline developer and thus acts as a positive resist. The sensitivity of the resist (called NPR) is 3 μC cm^{-2} and has improved dry resistance.

The third type is a cross-linked poly(methacrylate) polymer. An example of this is the copolymer of methyl methacrylate and methacryloyl chloride.[68] When the copolymer is heated at a temperature of 160 to 200°C, the carboxyl groups and acid chloride groups react to form carboxylic acid anhydride cross-links. Upon exposure to an electron beam, the cross-links are broken which enable the exposed area to be developed. The cross-linked poly(methacrylates) show considerable improvement in thermal stability and dry etch resistance over those of PMMA, but the sensitivity remains relatively low.[69]

2. Negative Resists

Three types of polymers have been used as negative electron resists (see Table 4). The first type is an epoxide-containing polymer (Structure I) including both homopolymers and copolymers.[70-74] The second type is a polystyrene-based homopolymer and copolymers (Structure II).[75-81] In particular, chlorine-containing polystyrenes have been studied exten-

Table 4
NEGATIVE ELECTRON RESISTS

Polymer	Sensitivity (10^{-6} C cm^{-2})	Ref.
Epoxidized poly(butadiene)	0.1	69
Poly(glycidyl methacrylate)	0.1	69, 70
Poly(glycidyl methacrylate-co-ethyl acrylate)	0.5	71
Poly(glycidyl methacrylate-co-styrene)	1—5	72, 73
Poly(glycidyl acrylate-co-styrene)	0.3—3	72, 73
Poly(styrene)	10	28
Poly(4-chlorostyrene-co-styrene)	5	74
Poly(4-chlorostyrene)	2—5	75
Poly(chloromethylstyrene)	0.4—7	76
Poly(chloromethylstyrene-co-styrene)	2—20	77, 78
Poly(*p*-methylstyrene-co-chloromethyl styrene)	0.3—3	79, 80
Poly(allyl methacrylate-co-2-hydroxyethyl methacrylate)	0.5	81

sively. The third type is a copolymer of poly(methacrylate) with a relatively long side chain which contains unsaturated bonds (Structure III).

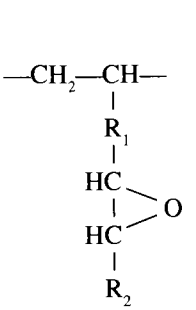

I

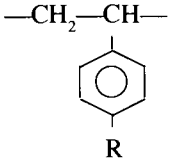

II

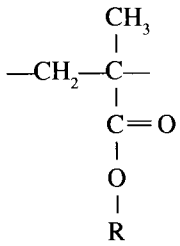

III

The epoxide-containing polymers, such as epoxidized poly(butadiene), poly(glycidyl methacrylate), and poly(glycidyl methacrylate-co-ethyl acrylate), are very sensitive.[70-72] Upon exposure to an electron beam, the epoxy ring is opened which forms intermolecular bonding between neighboring molecules. These polymers, however, have low T_g, and have lower resolution and dry etch resistance than the resists based on polystyrenes. Polystyrene is a high-resolution negative resist with high dry etch resistance.[28] It has acceptable stability (T_g = 100°C) but the sensitivity is relatively low, ~10 μC cm^{-2}. Two approaches have been taken to improve the sensitivity of polystyrene: copolymerization with epoxide-containing monomers or chlorination of polystyrene. The first approach includes copolymerization of styrene with glycidyl methacrylate and glycidyl acrylate which improves the sensitivity while retaining high-resolution characteristics of polystyrene.[73,74] The second approach is to use chlorine-containing polystyrenes such as poly(4-chlorostyrene),[75,76] poly(chloromethylstyrene),[77] and their copolymers with styrene.[78,81] These chlorine-containing polymers have higher sensitivity and higher T_g than polystyrene and they retain the high resolution and high dry etch resistance characteristics of polystyrene. The sensitivity of a negative resist has been found to be proportional to M_w (weight-average molecular weight). The sensitivity value quoted in Table 4 is mostly for the high molecular weight resists. They are more sensitive but have lower resolution than the low molecular weight resists which are less sensitive.[78,79]

Table 5
DEEP-UV RESISTS

Type	Polymer	Sensitizer	Ref.
P	Poly(methyl methacrylate)		83
P	Poly(methyl isopropenyl ketone)	*p*-*t*Butyl benzoic acid	84
P	Poly(methyl methacrylate-co-3-oximino-2-butanone methacrylate)	*p*-*t*Butyl benzoic acid	85, 86
P	Poly(methyl methacrylate-co-indenone)		87
P	Poly(methyl methacrylate-co-glycidyl methacrylate)		88
P	Novolak resin (cresol-formaldehyde)	5-Diazo-Meldrum's acid	89
P	Poly(methyl methacrylate-co-methacrylic acid	*O*-Nitrobenzyl ester of cholic acid	90
N	Poly(*n*-butyl-α-chloroacrylate)		91
N	Chlorinated poly(vinyltoluene)		92
N	Poly(*p*-vinylphenol)	3,3′-Diazidodiphenyl sulfone	93, 94
N	Novolak resin(cresol-formaldehyde)	3,3′-Diazidobenzophenone	95
N, P	Poly[styrene-co-*N*-(*p*-hydroxyphenyl) maleimide]		96

C. Deep-UV Resists

Many electron-beam resists designed for electron beam lithography have been used as deep-UV photoresists. The sensitivity of the resists, however, is generally low, due to their low absorption coefficient in the wavelength region 200 to 300 nm. The widely used electron-beam resist, PMMA, for instance, has been demonstrated to be a high-resolution (0.5 μm), deep-UV resist since 1975.[83] The exposure time required for PMMA, however, is excessively long; therefore, PMMA cannot be considered as a production resist. The classical photoresists which are comprised of novolak resin and diazo naphthoquinone as a sensitizer are designed for use at 400 nm and are unsatisfactory as deep-UV resists. The resists exhibit strong absorption at 254 nm and the sensitizer does not bleach, i.e., the photoproduct absorbs at 254 nm. This renders the resist films virtually opaque at 254 nm resulting in poor resolution and poor edge slope in the developed resists.

Ideally, a high-performance deep-UV resist should have high sensitivity, sharp cutoff in the longer wavelength region, an optimum optical absorption coefficient for high aspect ratio, high thermal stability, and high dry etch resistance for near-micron device fabrication. A list of deep-UV resists is shown in Table 5.

Two types of positive deep-UV resists have been developed. The first type includes homopolymers and copolymers of methacrylate which are used with or without a sensitizer. Upon exposure to deep-UV light, the polymers undergo chain scission resulting in a decrease in polymer molecular weight, thus functioning as a positive resist. The resists of the first type include PMMA,[83] poly(methyl isopropenyl ketone)[84] with *p-tert* butyl benzoic acid as the sensitizer, poly(methyl methacrylate-co-3-oximino-2-butanone methacrylate)[85,86] with *p-tert* butyl benzoic acid as the sensitizer, poly(methylmethacrylate-co-indenone),[87] and poly(methyl methacrylate-co-glycidyl methacrylate).[88] These resists are considerably more sensitive than PMMA.

The second type of positive deep-UV resist is based on the same principle of conventional positive photoresists. A polymer resin is mixed with a dissolution inhibitor which, upon exposure to deep-UV light of 254 nm wavelength, is photochemically converted to a transparent photoproduct no longer capable of retarding the dissolution of the polymer resin, thus enabling the exposed area to be developed. The resists of the second type include a resist

Table 6
X-RAY RESISTS

Type	Polymer	Sensitivity ($mJ\ cm^{-2}$)	Target	Wavelength (Å)	Ref.
P	Poly(methylmethacrylate) (PMMA)	500—2500	Al	8.34	97, 101
P	Poly(butene-1-sulfone) (PBS)	14	Al	8.34	97
P	Poly(hexafluorobutyl methacrylate)	52	Mo	5.40	98
P	Poly(methacrylonitrile)	1800	Al	8.34	53
P	Poly(2,2,2-trifluoroethyl methacrylate)	730	Al	8.34	99
P	Poly(2-fluoroethyl methacrylate)	730	Al	8.34	99
N	Poly(2,3-dichloro-1-propyl acrylate) (DCPA)	7	Pd	4.37	100
N	Chlorinated poly(vinyl ethers)	18—1010	Mo	5.40	101
N	Poly(allyl methacrylate-co-2-hydroxyethyl methacrylate)	9	W	7.0	102
N	Chloromethylated polystyrene	29	Mo	5.4	103
N	Poly(chloromethylstyrene)	25—30	Pd	4.37	104
N	Chlorinated poly(methylstyrene)	17	Pd	4.37	105

consisting of creosol-formaldehyde novolak resin and 5-diazo-Meldrum's acid, with the latter as the dissolution inhibitor,[89] and a resist which consists of poly(methyl methacrylate-co-methacrylic acid) with *O*-nitrobenzyl ester of cholic acids as the dissolution inhibitor.[90]

Two types of negative deep-UV resists have been developed. The first type includes poly(methacrylates) with a long side chain such as poly(*n*-butyl α-chloroacrylate),[91] and chlorinated polystyrenes such as chlorinated poly(vinyltoluene)[92] similar to those polymers used as electron resists. Upon exposure to deep-UV light, the polymers undergo cross-linking resulting in an increase in molecular weight, which enables the polymers to act as negative resists. Since organic solvents are used as the developer for the first type of deep-UV negative resists, the solvent-induced swelling is generally unavoidable, thus reducing the resist resolution.

To overcome the swelling problem, a second type of negative resist has been developed. The resist of the second type consists of a novolak resin (or a phenolic-based polymer) and a cross-linking agent aromatic azide. Upon exposure to deep-UV light the azide acts as a cross-linking agent for the polymer resin, thereby reducing the solubility of the exposed area in alkaline developer. Since the dissolution mechanism of a phenolic resin in alkaline developers is etching and not a conventional dissolution mechanism, swelling-induced pattern deformation does not occur in the resist, which greatly increases its resolution. A negative resist of the second type, consisting of 3,3′-diazidodiphenyl sulfone and poly(vinylphenol), has been termed MRS.[93,94] Similar resists based on the same principle have also been reported.[95]

D. X-Ray Resists

The application of X-ray resists is based on the same principle as that of electron resists. When a polymer resist is exposed to a X-ray, photoelectrons are generated (by the interaction of the X-ray with the polymer resist) which induce chain scission or cross-linking in the polymer, enabling it to act as a resist (see X-ray lithography). In principle, the electron resists discussed in the previous section can all function as X-ray resists; however, not all of them have been evaluated as X-ray resists. A list of representative X-ray resists is shown in Table 6.

Recent efforts in X-ray resist technology has been to develop high-sensitivity, high-resolution resists which are compatible with IC processing. X-ray sources currently used in X-ray lithography have a rather low X-ray flux (10 to 100 $\mu W/cm^2$) and thus a high-

sensitivity resist is required for high throughput. The sensitivity requirement is about 1 to 6 mJ/cm^2 for 60 s exposure time.[106] The strategy for improving the sensitivity has been to use high molecular weight polymers which have high G values (high G_s for positive resists and high G_x for negative resists), and to incorporate high absorbing atoms such as chlorine (which has a high mass absorption coefficient for soft X-ray) in the polymers.[99,100]

Except for PBS, most positive X-ray resists are the poly(methacrylates) type of polymer with fluorine atoms incorporated in the side chains.[98,99] The sensitivity of these resists is significantly higher than that of PMMA, but is far short of the 6-mJ/cm^2 sensitivity required for the high throughput. The plasma etch resistance and thermal stability of these resists are also marginal at best. The PBS resist, although sensitive, has poor plasma etch resistance and cannot be used for producing IC devices.

Negative X-ray resists are generally more sensitive than positive resists. Most negative resists have chlorine atoms incorporated in the side groups or side chains of the polymers to increase X-ray absorption. Except for poly(2,3-dichloro-1-propyl acrylate) (DCPA), which was developed exclusively for X-ray lithography,[100] the other negative resists listed in Table 6 were originally developed and used as electron resists. Two types of negative X-ray resists have been developed. They are poly(acrylates) and the polymers derived from polystyrene. The examples of poly(acrylates) include DCPA and poly(allyl-methacrylate-co-2-hydroxy ethyl methacrylate).[102] These two resists are sensitive, but their resistance to plasma etching is marginal. The polymers derived from polystyrene which also incorporated chlorine atoms have improved sensitivity while retaining high contrast and high dry etch resistance of polystyrene. Further, since polystyrene is currently one of the few polymers which can be obtained in a nearly monodispersed format (i.e., the molecular weight distribution is ~1), the chloromethylated polystryene has the advantage of further improving its contrast due to its narrow molecular weight distribution.[103] The negative resists chloromethylated polystyrene, poly(chloromethyl styrene),[104] and chlorinated poly(methylstyrene)[105] are very sensitive, 17 to 30 mJ/cm^2. However, these resists, similar to other negative resists, are not immune from solvent-induced swelling in the exposed resists. To obtain submicron resolution, less sensitive low molecular weight resists are generally used to minimize swelling and improve resolution.

E. Dry Developable Resists

Negative resists are generally more sensitive than positive resists, but the resolution of negative resists is lower. The dominant effect of UV light, X-ray, or electron-beam exposure on negative resists is a cross-linking process that increases the molecular weight of the polymer, making the exposed area less soluble. During the development of resist image in which the unexposed area is removed, the solvent molecules invariably penetrate into the exposed cross-linked area, resulting in swelling of the polymer which seriously degrades the resist resolution. (This was discussed in Section III.B). Although swelling can be minimized by using a low molecular weight polymer resist with high T_g, and by selecting suitable solvent developers, total elimination of swelling has been very difficult, if not impossible. The swelling problem in the negative resist can be avoided if the differential solubility between exposed and unexposed area does not rely on the cross-linking of the exposed resist, or a dry development process such as plasma process is used to develop the resist patterns.

In recent years there have been reports on dry developable photo-,[107-111] X-ray,[112,113] and electron resists.[114-120] The successful application of the dry developable resists to IC fabrication has also been reported.[107,108] A list of dry developable resists is shown in Table 7.

The majority of dry developable resists are negative resists and the basic approach to the formulation of the resist is similar. The dry developable negative resists generally consist of two components, a monomer and a low plasma-resistant base polymer. Upon exposure to photons, X-rays, or electrons, the monomers are grated to the base polymer and/or

Table 7
PLASMA DEVELOPABLE RESISTS

Resist	Base polymer	Monomer/photoinitiator	Ref.
Photoresist, negative[a]			107
			108
	Poly(2,3-dichloro-l-propyl acrylate)	*N*-Vinyl carbazole/phenanthrenequinone	109
	Poly(methyl isopropenyl ketone)	4-Methyl-2,6-di(4′-azidobenzylidene) cycloexanone-1	110
Deep-UV, positive	Copolymer of methyl methacrylate and SOMA[b]		111
X-ray, negative	Poly(2,3-dichloro-1-propyl acrylate)	*N*-Vinyl carbazole	112
	Poly(2,3-dichloro-l-propyl acrylate)	Bis-acryloxybutyl tetramethyldisiloxane	113
E-beam, positive	Poly(methacrylonitrile)		114
	Poly(acrylonitrile-co-methacrylic acid)		
	Plasma-polymerized methyl methacrylate		115, 116
E-beam, negative	Poly(vinyl acetate)	Vinyl tris-(2-methoxy ethoxy) silane	117
	Poly(methyl isopropenyl ketone)	4,4′-Diazidobiphenyl thioether	118, 119
	Poly(trichloroethyl methacrylate)	*N*-Vinyl carbazole, diphenyl acetylene	120

[a] Resist formulation was not disclosed.
[b] SOMA: 4-(trimethylsilylmethylene)-acetophenoneoxime-methacrylate.

polymerized to a homopolymer. Since the graft copolymer and the homopolymer have a lower plasma etch rate than that of the base polymer by virtue of the formulation, this results in a negative-acting resist. Further, if the monomer can be sublimated or vaporized from the unexposed area by baking prior to plasma development, a thickness difference between exposed and unexposed areas would be obtained. A plasma developable negative electron resist process[120] is shown in Figure 14.

The base polymers used in the negative resists are generally poly(acrylates) which have low plasma etch resistance. Ideally, the base polymers should have good film-forming characteristics, high T_g, and should be compatible with monomers and have low plasma etch resistance. Examples of base polymers include poly(2,3-dichloro-1-propyl acrylate),[109,112,113] poly(vinyl acetate),[117] and poly(trichloroethyl methacrylate).[120]

The required properties of the monomers are that the monomer must be sensitive to high-energy radiation, compatible with the base polymer (i.e., no phase separation occurs in the polymer-monomer mixture), have adequate solubility for spin coating, and high plasma etch resistance. In most dry developable resist processes, O_2 plasma is used to develop the resist image. The monomers used include aromatic-containing monomers such as *N*-vinyl carbazole[112,120] and diphenyl acetylene,[120] or silicon-containing monomers.[113,117] The use of organosilicon monomer is based on the presumption that during plasma development a SiO_2 protective layer is formed in the exposed area which resist further etching by the O_2 plasma.

Dry developable resists based on a different principle have been reported.[110,118,119] The resists consist of poly(methyl isopropenyl ketone) which is used as the base polymer, and an aromatic azide which is used as the photoinitiator. Upon exposure to high-energy radiation, the azide acts as the cross-linking agent which cross-links the base polymer. Upon hardbake after exposure, a hydrogen-bonded product which is a powerful quencher of the electronic

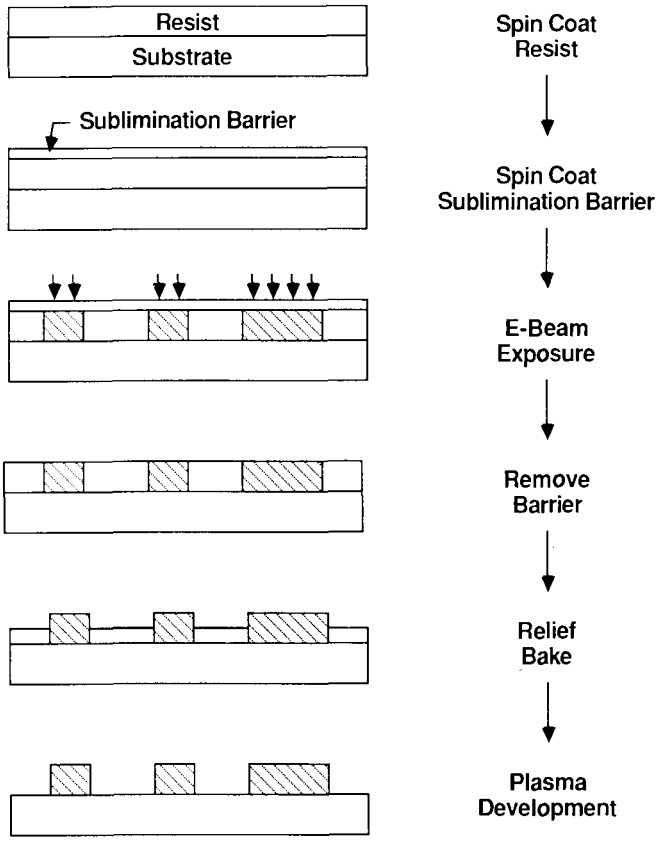

FIGURE 14. A plasma developable negative electron resist.

excitation energy is formed in the exposed area, making the exposed area very plasma etch-resistant. The quencher is more powerful than the aromatic compound arising from the azide by hardbake. The formation of the powerful energy quencher in the exposed area creates a plasma etch rate difference between the exposed and unexposed area. The resists were reported to be effective as dry developable photo-, deep-UV, and electron resists.

Reports on plasma developable *positive* resists have been relatively scarce.[111,114] A resist which consists of a single-component copolymer of methyl methacrylate and silicon-containing monomer (called PDPUV) has been reported to act as a plasma developable deep-UV resist.[111] When PDPUV is exposed to UV light of 254 nm, the silicon-containing side groups in the polymer are split off from the polymer and are removable by hardbake. Since the unexposed area still contains highly O_2 plasma-resistant silicon groups, this creates a plasma etch rate difference between exposed and unexposed areas, enabling the polymer to act as a positive resist. The sensitivity of PDPUV was reported to be 250 mJ/cm_2.

Single-component polymers, poly(methacrylonitrile), and copolymers of acrylonitrile and methacrylic acid were reported to act as plasma developable positive electron resists.[114] The polymers, upon exposure to an electron beam, undergo chain scission creating volatile fragments which can be removed by hardbake. The thickness difference between exposed and unexposed areas is obtained after hardbake, and the resist pattern can be obtained by plasma development.

F. Multilayer Resists

In multilayer resists, more than a single layer of resist films are coated on the wafer for image transfer. Four general methods have been developed.[121,122] The schematic diagrams

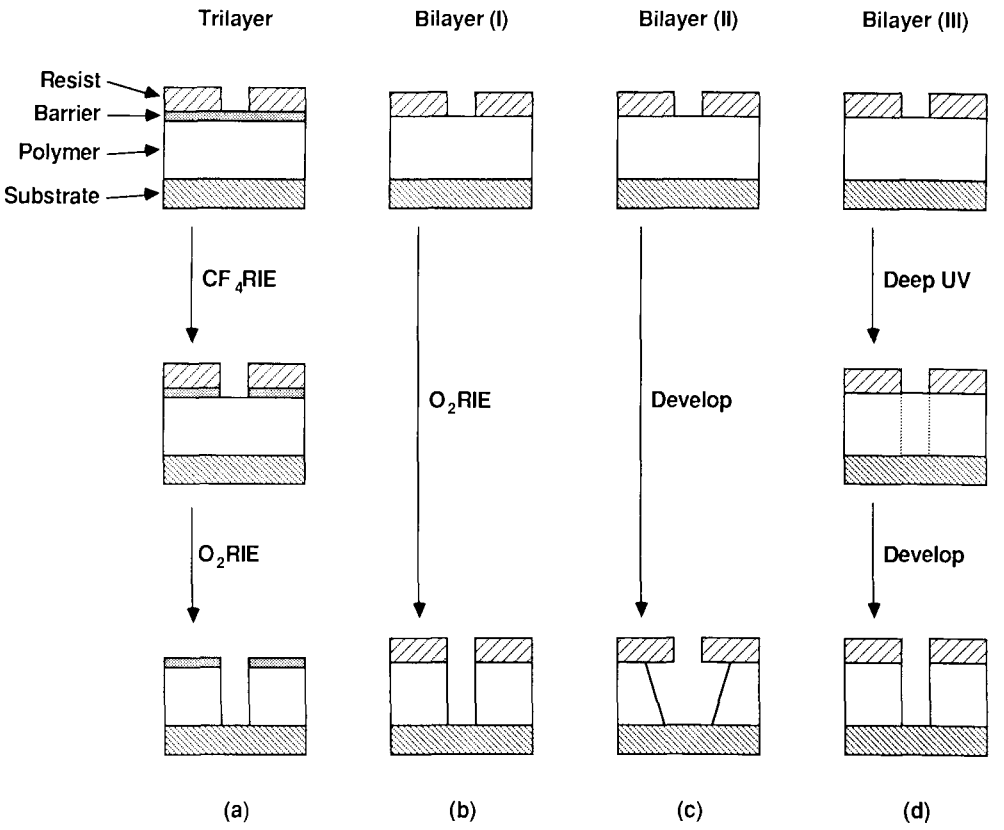

FIGURE 15. Multilayer resists. (a) Trilayer; (b) bilayer (I); (c) bilayer (II); (d) bilayer (III).

of the four methods are shown in Figure 15. In the trilayer resist system (Figure 15a), a thick planarization layer is coated on the bottom. A thin inorganic film (e.g., spin-on glasses, SiO_2, Si_3N_4) which is resistant to O_2 reactive ion etch (RIE) is deposited between the top and bottom layers. The top layer is a thin imaging layer made of a photo-, deep-UV, electron, or X-ray resist. The image in the top layer is transferred to the middle layer (barrier) by CF_4 RIE. Subsequently, the image is transferred to the bottom layer by O_2 RIE.[123,124] A number of polymers have been used as the bottom layer, e.g., conventional photoresist, PMMA, polysulfones, and polyimides.

Double-layer or bilayer resist systems can be further classified into three subsystems. In bilayer resist (I), a photo- or electron-sensitive and O_2 RIE-resistant resist such as an organosilicon polymer is used as the top imaging layer, and the image is transferred to the bottom layer by O_2 RIE. The plasma etch rate of the top layer must be much lower than that of the bottom layer. In bilayer resist (II), a suitable solvent is used to develop the bottom layer to create the undercut profile for metal lift-off. The solvent, of course, must be able to produce a controlled degree of undercutting in the bottom layer without eroding the high-resolution pattern in the top resist. In the bilayer resist (III), image transfer is accomplished by a deep-UV flood exposure and development of the bottom layer. The resist is called portable conformable mask (PCM) which requires that the bottom layer be deep-UV sensitive.[125] Scanning electron-beam micrographs of 0.25-μm metal lines patterned by the bilayer (II) resist structure and the lift-off process are shown in Figure 16. The process which was developed at Honeywell used a 0.3-μm thin electron resist as the imaging layer which was coated on the top of a 0.7-μm thick polymer layer.

Multilayer resist systems require extra processing steps which are both costly and time

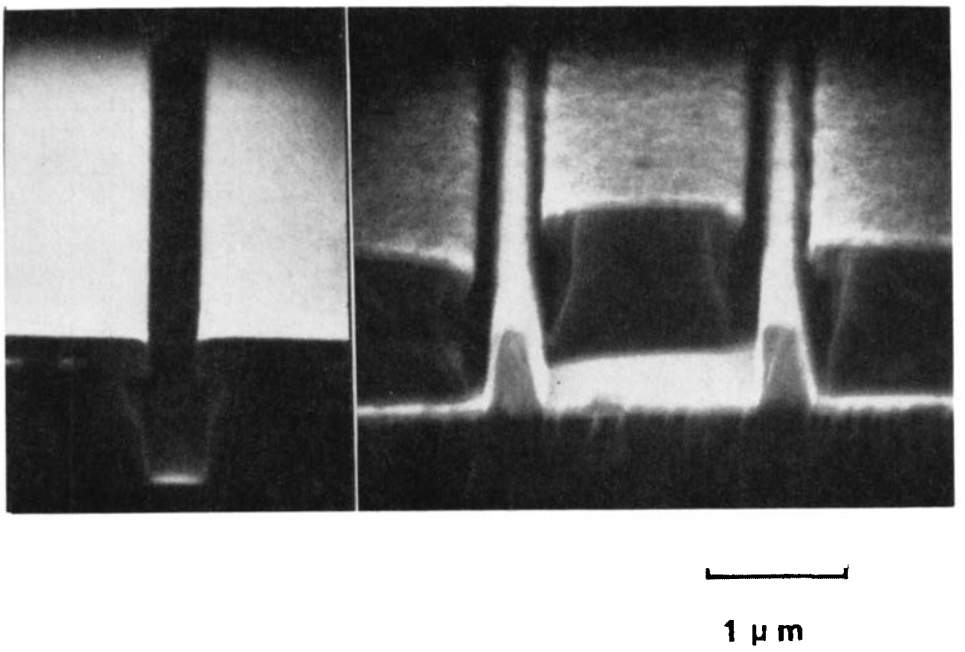

FIGURE 16. Bilayer (II) resist structure for metal lift-off. (A) After electron-beam exposure and development. (B) after metal deposition. (Magnification × 20,000.)

consuming. What then, are the advantages of multilayer resists? It is well known that a thin resist film is required for producing high-resolution patterns and for line width control. The resist thickness, however, must also be sufficiently thick for effective image transfer by etching or metal lift-off. The high aspect ratio requirements can be relatively easily satisfied by a multilayer resist but not by a single layer resist. Further, since a thick polymer layer is coated on the bottom as the planarization layer in the multilayer resist, the line width variation due to resist thickness change over topography, interference effects caused by reflection off topographic features, nonuniformity of reflectivity encountered in optical lithography, and the proximity effect due to electron scattering encountered in electron-beam lithography can be minimized or eliminated in the multilayer resist systems.[122]

IV. RECENT DEVELOPMENTS AND FUTURE OUTLOOK

A. Recent Developments

Recent developments in polymer resists include self-developing resists,[126-128] contrast-enhanced photoresists,[129] nonswelling negative photoresists,[130] and organosilicon polymer resists.[131-137] Two of these recent developments are discussed below.

1. Nonswelling Negative Photoresists

The resolution of the widely used negative photoresist based on cyclized polyisoprene and bisazide has been limited to ~2 μm due to solvent-induced swelling in the exposed area (see Section III.A). In Section III.C, a nonswelling deep-UV negative resist termed MRS was discussed. The resist MRS consists of poly(vinyl phenol) as the host polymer and a bis-azide 3,3′-diazidodiphenyl sulfone as the sensitizer.

Upon exposure to deep UV, the polymer molecules are cross-linked by the sensitizer molecules; however, since the development of the resist pattern is carried out by the aqueous alkaline solution which removes the unexposed polymers by etching, the swelling is avoided.

Similar nonswelling negative photoresist termed MRL, which is applicable in the 300 to 400-nm region, has been reported.[130] The MRL resist consists of poly(vinyl phenol) as the host polymer and a monoazide, 4-azido chalcone (20 wt%), as the sensitizer.

Irradiation by UV light of 300 to 400 wavelength causes the monoazide to attach to the phenolic polymer chain forming basic secondary amine (–RNH–C–) which is far less soluble in the aqueous alkaline solution than the unexposed area, thus enabling the negative resist pattern to be developed without significant swelling.

2. Organosilicon Polymer Resists

A number of organosilicon polymers have been investigated as polymer resists. Among them, polysilanes have been under intensive research in recent years.

Polysilanes designate a class of polymers in which silicon atoms constitute the main chain while the organic groups are bonded to the main chain backbone as the side groups. The chemical structure of the polymers is shown in I, where R_1 and R_2 are either aromatic or are aliphatic groups.

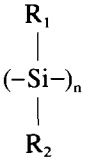

I

Although polysilanes were prepared as early as 1927, use of polysilanes as radiation-sensitive materials was not reported until recently, when soluble high molecular weight polymers were synthesized and characterized.[131]

The nature of substituents R_1 and R_2 is important in determining the physical and chemical properties of polysilanes. Polysilanes with different aromatic and aliphatic substituents have been synthesized, characterized, and some evaluated as lithographic resists.[132] It has been observed that all high molecular weight polysilane derivatives are characterized by a strong electronic absorption in the UV spectral region. The position of the UV absorption and the molar extinction coefficients are functions of both the nature of substituent and the molecular weight. Irradiation of the polysilanes leads predominantly to chain scission and molecular weight reduction, however, scission/cross-linking ratio (i.e., G_s/G_x) is dependent on the nature of the substituents. For example, a study on the effect of irradiation on the absorption spectrum of poly(methyl phenyl silane) found a strong bleaching effect which suggested the occurrence of an extensive chain scission, which was confirmed by GPC analysis of the polymer molecular weight as a function of radiation dose.[132]

Although the processability of the polysilanes as lithographic resists was not fully reported, polysilanes [e.g., poly(*p*-*t*-butylphenylsilane)] were used successfully as the thin imaging layer which showed strong resistance to O_2 reactive ion etching.[132] The stability of the polysilanes has been attributed to the formation of a thin oxide layer in O_2 plasma similar to the behavior of other silicon-containing polymers (see Section II.C.5).

In addition to polysilanes, a variety of other organosilicon polymers were investigated.[133-137] These were used mainly as the thin imaging layers in bilayer resist processes due to their high stability in oxygen plasma. Examples include poly(alkenylsilane sulfones) as positive electron resists,[133] a negative photoresist composed of poly(triallyphenyl silane) and bis-azide,[134] polydimethyl siloxane,[136] and polysiloxane methacrylates as deep-UV positive resists.[137] In most cases, it has been found that a protective SiO_2 layer is formed on the surface of the silicon-containing polymers, and the etch rate of the resist film is inversely proportional to the silicon content of the polymers.

B. Future Outlook

The application of polymer resists for IC processing is expected to continue at a fast pace. New resists and processes that are more compatible with semiconductor processing are being introduced continuously. The general requirements of polymer resists are high sensitivity, high resolution, high thermal stability, and high dry etch resistance. Few of the current polymer resists, however, satisfy all of these requirements. High-temperature positive photoresists and high-resolution negative photoresists are still needed to improve the yield and lower the cost of the photolithographic process. In the advanced microlithographic area, high-sensitivity positive electron and X-ray resists which have both high thermal stability and dry etch resistance are yet to be developed. Similarly, high-resolution negative electron and X-ray resists with high sensitivity have yet to be found. New lithographic processes and resist chemistry, such as multilayer resists, dry developable resists, self-developing resists, contrast-enhanced photoresists, and organosilicon polymer resists, will continue to be explored. It is forseeable that high-performance polymer resists with high sensitivity, high resolution, high thermal stability, and high dry etch resistance will evolve in the future.

REFERENCES

1. **Deckert, C. A. and Ross, D. L.,** Microlithography — key to solid-state device fabrication, *J. Electrochem. Soc.*, 127, 45C, 1980.
2. **Oldham, W. G.,** The fabrication of microelectronic circuits, *Sci. Am.*, 237, 70, 1977.
3. **Thompson, L. F., Willson, C. G., and Bowden, M. J., Ed.,** *Introduction to Microlithography,* ACS Symp. Ser. 219, American Chemical Society, Washington, D.C., 1983.
4. **Thompson, L. F., Willson, C. G., and Frechet, J. M. J., Ed.,** *Materials for Microlithography,* ACS Symp. Ser. 266, American Chemical Society, Washington, D.C., 1984.
5. **Broers, A. N.,** A review of high-resolution microfabrication techniques, *1st Phys. Conf. Ser.*, No. 40, 155, 1978.
6. **Doane, D. A.,** Optical lithography in the 1 μm limit, *Solid State Technol.*, August, 101, 1980.
7. **Bruning, J. H.,** Optical imaging for microfabrication, *J. Vac. Sci. Technol.*, 17, 1147, 1980.
8. **Brewer, G. R., Ed.,** *Electron Beam Technology in Microelectronic Fabrication,* Academic Press, New York, 1980.
9. **Chang, T. H. P., Hatzakis, M., Wilson, A. D., and Broers, A. N.,** Electron-beam lithography draws a finer line, *Electronics,* May, 89, 1977.
10. **Shepherd, L. T. and Carlson, B.,** Photo-, e-beam and x-ray lithography, *Sci. Honeyweller,* 1(4), 1, 1980.
11. **Molzen, W. W., Broers, A. N., Cuomo, J. J., Harper, J. M. E., and Laibowitz, R. B.,** Materials and techniques used in nanostructure fabrication, *J. Vac. Sci. Technol.*, 16(2), 269, 1979.
12. **Charlesby, A.,** *Atomic Radiation and Polymers,* Pergamon Press, London, 1960.
13. **Chapiro, A.,** *Radiation Chemistry of Polymeric Systems,* John Wiley & Sons, New York, 1962.
14. **Spears, D. L. and Smith, H. I.,** High resolution pattern replication using soft x-rays, *Electron. Lett.*, 8(4), 102, 1972.
15. **Spiller, E. and Feder, R.,** X-ray lithography, *Top. Appl. Phys.*, 22, 36, 1977.
16. **Skoog, D. A. and West, D. M.,** *Principles of Instrumental Analysis,* Holt, Reinhard & Winston, New York, 1971, chap. 14.
17. **Hughes, G. P. and Fink, R. C.,** X-ray lithography breaks the VLSI cost barrier, *Electronics,* 11, 99, 1978.
18. **Luthje, H.,** X-ray lithography for VLSI, *Philips Tech. Rev.*, 41, 150, 1983/1984.
19. **Lai, J. H.,** Resist materials for electron-beam lithography, *J. Imaging Technol.*, 11(4), 174, 1985.
20. **Hiroaka, H.,** Radiation chemistry of poly(methacrylates), *IBM J. Res. Dev.*, 21(2), 121, 1977.
21. **Helbert, J. N., Chen, C. Y., Pittman, C. V., Jr., and Hagnauer, G. L.,** Radiation degradation study of poly(methyl α-chloroacrylate) and the methyl methacrylate copolymer, *Macromolecules,* 11, 1105, 1978.
22. **Helbert, J. N., Poindexter, E. H., Stahl, G. A., Chen, C. Y., and Pittman, C. V., Jr.,** Radiation degradation susceptibility of vinyl polymers: nitriles and anhydride, *J. Polym. Sci. Polym. Chem.*, 17, 49, 1979.
23. **Pittman, C. U., Jr., Chen, C. Y., Veda, M., Helbert, J. N., and Kwiatkowski, J.,** Synthesis and radiation degradation of vinyl polymers with fluorine: search for improved lithographic resists, *J. Polym. Sci. Polym. Chem.*, 18, 3413, 1980.

24. **Lai, J. H. and Helbert, J. N.,** Radiation degradation of poly(methacrylates), *Macromolecules*, 11, 617, 1978.
25. **Lai, J. H. and Shepherd, L. T.,** An investigation of the effects of the molecular weight distribution on the sensitivity of positive electron resists, *J. Appl. Polym. Sci.*, 20, 2367, 1976.
26. **Moreau, W. M.,** State of the art of acrylate resists: an overview of polymer structure and lithographic performance, *SPIE*, 333, 2, 1982.
27. **Harada, K., Tamamura, T., and Kogure, O.,** Detailed contrast (r-value) measurements of positive electron resists, *J. Electrochem. Soc.*, 129(11), 2576, 1982.
28. **Lai, J. H. and Shepherd, L. T.,** Experimental observation of nearly monodisperse polystyrene as negative electron resists, *J. Electrochem. Soc.*, 126, 696, 1979.
29. **Lai, J. H., Douglas, R. B., Mao, K., Larson, W. L., and Yau, Y. W.,** High performance electron resists for submicron e-beam lithography, in Proc. 3rd Int. Symp. VLSI Sci. Tech., Electrochemical Society, 1985, 274.
30. **Toukhy, M. A. and Jech, J. A.,** A new high temperature positive photoresist HX-256, *SPIE Adv. Resist Technol.*, 469, 159, 1984.
31. **Hiraoka, H. and Pacansky, J.,** UV hardening of photo- and electron beam resist patterns, *J. Vac. Sci. Technol.*, 19(4), 1132, 1981.
32. **Ma, W. H.,** Plasma resist image stabilization technique (PRIST) update, *SPIE Submicron Lithogr.*, 333, 19, 1982.
33. **Kern, W. and Deckert, C.,** Chemical etching, in *Thin Film Processes,* Vossen, J. L. and Kern, W., Eds., Academic Press, New York, 1978, chap. 5-1.
34. **Mucha, J. A. and Hess, D.W.,** Plasma etching, in *Introduction to Microlithography,* Thompson, L. F., Willson, C. G., and Bowden, M. J., Eds., ACS Symp. Ser. 219, American Chemical Society, Washington, D.C., 1983, chap. 5.
35. **Coburn, J. W.,** Plasma-assisted etching, in *Semiconductor Technology,* Doane, D. A., Fraser, D. B., and Hess, D. W., Eds., Proc. Tutorial Symp. 82-5, Electrochemical Society, 1982, chap. 4.
36. **Melliar-Smith, C. M. and Mogab, C. J.,** Plasma-assisted etching techniques for pattern delineation, in *Thin Film Processes,* Vossen, J. L. and Kern, W., Eds., Academic Press, New York, 1978, chap. 5-1.
37. **Fonash, S. J.,** Advances in dry etching processes — a review, *Solid State Technol.*, January, 150, 1985.
38. **Taylor, G. N. and Wolf, T. M.,** Oxygen plasma removal of thin polymer films, *Polym. Eng. Sci.*, 20(16), 1087, 1980.
39. **Helbert, J. N., Schmidt, M. A., Malkiewicz, C., Wallace, E., and Pittman, C. U.,** Effect of composition on resist dry-etching susceptibility, in *Polymers in Electronics,* Davidson, T., Ed., ACS Symp. Ser. 242, American Chemical Society, Washington, D.C., 1984, chap. 8.
40. **Pederson, L. A.,** Structure composition of polymers relative to their plasma etch characteristics, *J. Electrochem. Soc.*, 129(1), 205, 1982.
41. **DeForest, W. S.,** *Photoresist,* McGraw-Hill, New York, 1975.
42. **Dill, F. H., Hornberger, W. P., Huge, P. S., and Shaw, J. M.,** Characterization of positive photoresists, *IEEE Trans. Electron Devices*, ED-22(7), 445, 1975.
43. **Pacansky, J. and Lyerla, J. R.,** Photochemical decomposition mechanism for AZ-type photoresists, *IBM J. Res. Dev.*, 23, 42, 1979.
44. **Sagura, J. J. and Van Allen, J. A.,** U.S. Patent 2,940,853, 1960.
45. **Hepher, H. and Wagner, H. M.,** U.S. Patent 2,852,679, 1958.
46. **Hill, D. J. T., O'Donnell, J. H., and Pomery, P. J.,** Fundamental aspects of polymer degradation by high-energy radiation, in *Materials for Microlithography,* Thompson, L. F., Willson, C. G., and Frechet, J. M. J., Eds., ACS Symp. Ser. 266, American Chemical Society, Washington, D.C., 1984.
47. **Morawetz, H.,** *Macromolecules in Solution,* Interscience, New York, 1965.
48. **Veberreiter, K.,** *The Solution Process in Diffusion in Polymers,* Crank, J. and Park, G.S., Eds., Academic Press, London, 1968.
49. **Ouano, A.,** A study on the dissolution rate of irradiated poly(methyl methacrylate), *Polym. Eng. Sci.*, 18, 306, 1978.
50. **Haller, I., Hatzakis, M., and Srinivasan, R.,** High resolution positive resists for electron-beam exposure, *IBM J.*, May, 251, 1968.
51. **Greeneich, J.S.,** Developer characteristics of poly(methyl methacrylate) electron resist, *J. Electrochem. Soc.*, 122(7), 970, 1975.
52. **Helbert, J. N., Cook, C. F., Jr., and Poindexter, E. H.,** Poly(methyl α-chloroacrylate) as a positive electron-beam resist, *J. Electrochem. Soc.*, 124(1), 158, 1977.
53. **Helbert, J. N., Cook, C. F., Jr., Chen, C. Y., and Pittman, C. U., Jr.,** Electron beam and x-ray resist behavior of poly(methacrylonitrile), *J. Electrochem. Soc.*, 126(4), 694, 1979.
54. **Kakuchi, M., Sugawara, S., Murase, K., and Matsuyame, K.,** Poly(fluoro methacrylate) as highly sensitive high contrast positive resist, *J. Electrochem. Soc.*, 124(10), 1648, 1977.
55. **Tada, T.,** Poly(trifluoroethyl α-chloroacrylate as a highly sensitive positive electron resist, *J. Electrochem. Soc.*, 126, 1830, 1979.

56. **Tada, T.,** Crosslinked poly(2,2,2trichloroethyl methacrylate) as a highly sensitive positive electron resist, *J. Electrochem. Soc.*, 126, 1635, 1979.
57. **Gipstein, E., Moreau, W., and Need, O.,** Poly(methyl methacrylate-isobutylene) copolymers as highly sensitive electron beam resists, *J. Electrochem. Soc.*, 123(7), 1105, 1976.
58. **Lai, J. H., Shepherd, L. T., Ulmer, R. L., and Griep, C.,** Studies of methyl methacrylate-methyl α-chloroacrylate copolymers and poly(methyl α-chloroacrylate) as electron sensitive positive resists, *Polym. Eng. Sci.*, 17(6), 402, 1977.
59. **Hatano, Y., Shiraishi, H., Taniguchi, Y., Horigome, S., Nonogaki, S., and Naraoka, K.,** Poly(methyl methacrylate-co-acrylonitrile) — a sensitive positive resist, in Proc. 8th Int. Conf. on Electron and Ion Beam Science and Technol., Electrochemical Society, 1978, 332.
60. **Moreau, W., Merritt, D., Moyer, W., Hatzakis, M., Johnson, D., and Pederson, L.,** Speed enhancement of PMMA resist, *J. Vac. Sci. Technol.*, 16(6), 1989, 1979.
61. **Lai, J. H., Helbert, J. N., Cook, C. F., Jr., and Pittman, C. U., Jr.,** Positive electron-beam resist behavior for methacrylonitrile and methyl α-chloroacrylate polymers and copolymers, *J. Vac. Sci. Technol.*, 16(6), 1992, 1979.
62. **Lai, J. H., Kwiatkowski, J. H., and Cook, C. F., Jr.,** Studies of methacrylonitrile and trichloroethyl methacrylate copolymers as electron sensitive positive resists, *J. Electrochem. Soc.*, 129(7), 1596, 1982.
63. **Namaste, Y. M. N., Obendorf, S. K., Anderso, C. C., and Rodriguez, F.,** Electron beam lithographic evaluation and chain scissioning yields of itaconate resists, *SPIE Adv. Resist Technol.*, 469, 144, 1984.
64. **Lai, J. H.,** Resist materials for electron-beam lithography, *J. Imaging Technol.*, 11(4), 164, 1985.
65. **Vyas, H. P., Lutze, R. S. L., and Huang, J. S. T.,** A trench-isolated submicrometer CMOS technology, *IEEE Trans. Electron Devices*, ED-32(5), 926, 1985.
66. **Thompson, L. F. and Bowden, M. J.,** A new family of positive electron resists — poly(olefin sulfones), *J. Electrochem. Soc.*, 120(12), 1722, 1973.
67. **Bowden, M. J., Thompson, L. F., Fuhrenholtz, S. R., and Doerries, E. M.,** A sensitive novolak-based positive electron resist, *J. Electrochem. Soc.*, 128(6), 1304, 1981.
68. **Roberts, E. D.,** A single-component cross-linked methacrylate positive-working electron resist, *Am. Chem. Soc. Div. Org. Coat. Plast. Chem. Prepr.*, 3(2), 36, 1977.
69. **Kitakohji, T., Yoneda, Y., Kitamura, K., Okuyama, H., and Murakawa, K.,** Polymers constituted by methyl methacrylate, methacrylic acid, and methacryloyl chloride as a positive electron resist, *J. Electrochem. Soc.*, 126(11), 1881, 1979.
70. **Hirai, T., Hatano, Y., and Nonogaki, S.,** Epoxide-containing polymers as highly sensitive electron-beam resists, *J. Electrochem. Soc.*, 118(4), 669, 1971.
71. **Taniguchi, Y., Hatano, Y., Shiraishi, H., Horigome, S., Nonogaki, S., and Nanaoka, K.,** PGMA as a high resolution, high sensitivity negative electron beam resist, *Jpn. J. Appl. Phys.*, 18(6), 1143, 1979.
72. **Thompson, L. F., Feit, E. D., and Heidenreich, R. D.,** Lithography and radiation chemistry of epoxy containing negative electron resists, *Polym. Eng. Sci.*, 14(7), 529, 1974.
73. **Lai, J. H. and Shepherd, L. T.,** An investigation of positive and negative resists for electron beam microfabrication, *Am. Chem. Soc. Div. Org. Coat. Plast. Chem. Prepr.*, August 1975.
74. **Thompson, L. F., Stillwagon, L. E., and Doerries, E. M.,** Negative electron resists for direct fabrication of devices, *J. Vac. Sci. Technol.*, 15(3), 938, 1978.
75. **Jagt, J. C. and Whipps, P. W.,** Negative electron resists for VLSI, *Philips Tech. Rev.*, 39(12), 346, 1980.
76. **Liutkus, J., Hatzakis, M., Shaw, J., and Paraszczak, J.,** Poly(4-chlorostyrene), a new high contrast negative e-beam resist, *Polym. Eng. Sci.*, 23(18), 1047, 1983.
77. **Choong, H. S. and Kahn, F. J.,** Molecular parameters and lithographic performance of poly(chloromethylstyrene) — a high performance negative electron resist, *J. Vac. Sci. Technol.*, 19(4), 1121, 1981.
78. **Imamura, S.,** Chloromethylated polystyrene as a dry etching-resistant negative resist for submicron technology, *J. Electrochem. Soc.*, 126, 1628, 1979.
79. **Imamura, S., Tamamura, T., Harada, K., and Sugawara, S.,** High performance negative electron resist, chloromethylated polystyrene. A study on molecular parameters, *J. Appl. Polym. Sci.*, 27, 937, 1982.
80. **Ledwith, A., Mills, M., Hendy, P., Brown, A., Clements, S., and Moody, R.,** An investigation of the lithographic properties of the poly(p-methylstyrene-co-chloromethylstyrene) resist system, *J. Vac. Sci. Technol.*, 3(1), 339, 1985.
81. **Kamoshida, Y., Koshiba, M., Yoshimoto, H., Harita, Y., and Harada, K.,** Application of chlorinated polymethylstyrene, CPMS, to electron beam lithigraphy, *J. Vac. Sci. Technol.*, B1(14), 1156, 1983.
82. **Tan, Z. C. H., Daly, R. C., and Georgia, S. S.,** Novel, negative-working electron-beam resist, *SPIE Adv. Resist Technol.*, 469, 135, 1984.
83. **Lin, B. J.,** Deep UV lithography, *J. Vac. Sci. Technol.*, 12(6), 1317, 1975.

84. **Tsuda, M., Kawa, S. O., Nakamura, Y., Nagata, H., Yokota, Y., Nakane, M. H., Tsumori, T., Nakane, Y., and Mifune, T.,** Spectrally sensitized decomposition of poly(methyl isopropenyl ketone) — novel deep UV resists, *Photogr. Sci. Eng.*, 23, 290, 1979.
85. **Wilkins, C.W., Jr., Reichmanis, E., and Chandross, E. A.,** Preliminary evaluation of copolymers of methyl methacrylate and acryloximino methacrylate as deep UV resists, *J. Electrochem. Soc.*, 127, 2510, 1980.
86. **Reichmanis, E., Wilkin, C. W., Jr., and Chandross, E. A.,** The effect of sensitizers on the photodegradation of poly(methyl methacrylate-co-3-oximino-2-butanone methacrylate), *J. Electrochem. Soc.*, 127, 2514, 1980.
87. **Hartless, R. L. and Chandross, E. A.,** Deep UV photoresists: poly(methyl methacrylate-co-indenone), *J. Vac. Sci. Technol.*, 19, 1333, 1981.
88. **Yamashita, Y., Ogura, K., Kunishi, M., Kowazu, R., Ohno, S., and Mizokami, Y.,** Crosslinking positive resists for deep UV photolithography and its application to LSI fabrication processes, *J. Vac. Sci. Technol.*, 16, 2026, 1979.
89. **Grant, B. D., Clecak, N. J., Twieg, R. J., and Willson, C. G.,** Deep UV photoresist. I. Meldrum's diazo sensitizer, *IEEE Trans. Electron Devices*, ED-28(11), 1300, 1981.
90. **Reichmanis, R., Wilkins, C. W., Jr., and Chandross, E. A.,** A novel approach to o-nitrobenzyl photochemistry for resists, *J. Vac. Sci. Technol.*, 19, 1338, 1981.
91. **Kawazu, T., Kunizuka, M., Yamashita, Y., and Ono, S.,** Deep UV resist with high sensitivity, paper presented at National Convention on Semiconductor and Materials, Japan, 1981.
92. Japan Synthetic Rubber Co., Negative-working deep UV resist, *JST News*, 1(6), 31, 1982.
93. **Iwayanagi, T., Kohashi, T., Nonogaki, S., Matsuzawa, T., Douta, K., and Yanazawa, H.,** Azide-phenolic resin photoresists for deep UV lithography, *IEEE Trans. Electron Devices*, ED-28(11), 1306, 1981.
94. **Matsuzawa, T. and Tomioka, H.,** Deep UV 1:1 projection lithography utilizing negative resist MRS, *IEEE Trans. Electron Devices*, ED-28(11), 1284, 1981.
95. **Yang, J. M., Chiong, K., Yan, H., and Chow, M.,** Negative photoresists for deep-UV lithography, *SPIE Adv. Resist Technol.*, 469, 117, 1984.
96. **Turner, S. R., Ahn, K. D., and Willson, C. G.,** Thermally stable, deep UV resist material, in Proc. ACS Division Polymer Material Science Engineering, American Chemical Society Fall Meeting, 1986, 608.
97. **Thompson, L. F., Feit, E. D., Bowden, M. J., Lenzo, P. V., and Spencer, E. G.,** Polymeric resists for x-ray lithography, *J. Electrochem. Soc.*, 121(11), 1500, 1974.
98. **Kakuchi, M., Sugawara, S., Murase, K., and Matsuyana, K.,** Poly(fluoro methacrylate) as highly sensitive high contrast positive resist, *J. Electrochem. Soc.*, 124(10), 1643, 1977.
99. **Eranian, A., Couttet, A., Datamanti, E., and Dubois, J. C.,** Halogenated poly(methacrylates) for x-ray lithography, in *Photodegradation and Photostabilization of Coatings*, ACS Symp. Ser. 151, American Chemical Society, Washington, D.C., 1981.
100. **Taylor, G. N., Coquin, G. A., and Somekh, S.,** Sensitive chlorine-containing resists for x-ray lithography using 4.37 a pd x-rays, *Polym. Eng. Sci.*, 17, 420, 1977.
101. **Imamura, S., Sugawara, S., and Murase, K.,** Poly(vinylethers) as x-ray resists, *J. Electrochem. Soc.*, 124, 1139, 1977.
102. **Tan, Z. C., Petropoulos, C. C., and Rauner, F. J.,** High sensitivity, high resolution, high-thermal resistant negative electron, x-ray resist, *J. Vac. Sci. Technol.*, 19(4), 1348, 1981.
103. **Imamura, S. and Sugawara, S.,** Chloromethylated polystyrene as deep UV and x-ray resist, *Jpn. J. Appl. Phys.*, 21(5), 776, 1982.
104. **Choong, H. S. and Kahn, F. J.,** Poly(chloromethylstyrene): a high performance x-ray resist, *J. Vac. Sci. Technol.*, 1(4), 1066, 1983.
105. **Yoshioka, N., Suzuki, Y., and Yamazaki, T.,** A high performance negative x-ray resist: CMP-X (pd), *SPIE Electron Beam X-Ray Ion Beam Tech. Submicrom. Lithogr. IV*, 537, 51, 1985.
106. **Taylor, G. N.,** X-ray resists trends, *Solid State Technol.*, June, 124, 1984.
107. **Penn, T. C.,** Forecast of VLSI processing — a historical review of the first dry-processed IC, *IEEE Trans. Electron Devices*, ED-26(4), 640, 1979.
108. **Hughes, H. G., Goodner, W. R., Wood, T. E., Smith, J. N., and Keller, J.,** Photoresist development by plasma, *Polym. Eng. Sci.*, 20, 1093, 1980.
109. **Taylor, G. N., Wolf, T. M., and Goldrick, M. R.,** A negative-working plasma-developed photoresist, *J. Electrochem. Soc.*, 128, 361, 1981.
110. **Tsuda, M. and Oikawa, S.,** Plasma developable photoresist containing electronic excitation energy quenching system, *Polym. Eng. Sci.*, 23, 993, 1983.
111. **Meyer, W. H., Curtis, B. J., and Brunner, J. R.,** Plasma developable positive UV-resists, *Microelectron. Eng.*, 1, 29, 1983.
112. **Taylor, G. N. and Wolf, T. M.,** Plasma developed x-ray resists, *J. Electrochem. Soc.*, 127, 2665, 1980.

113. **Taylor, G. N., Wolf, T. M., and Moran, J. M.,** Organosilicon monomers for plasma-developed x-ray resists, *J. Vac. Sci. Technol.*, 19(4), 872, 1981.
114. **Hiraoka, H.,** All dry lithography processes and mechanistic studies with poly(methacrylonitrile) and related polymers, *J. Electrochem. Soc.*, 128, 1065, 1981.
115. **Morita, S., Tamano, J., Hattori, S., and Ieda, M.,** Plasma polymerized methyl-methacrylate as an electron-beam resist, *Jpn. J. Appl. Phys.*, 51(7), 3938, 1980.
116. **Hattori, S., Tamano, J., Yamada, M., Ieda, M., Morita, S., Yoneda, K., and Ishibashi, S.,** Vacuum lithography using plasma polymerization and plasma development, *Thin Solid Films*, 83(2), 189, 1981.
117. **Whipps, P. W.,** Plasma developable negative e-beam resists, Extended Abstr., 16th Symp. on Electron Ion and Photon Beam Technology, Dallas, May 26 to 29, 1981.
118. **Tsuda, M., Oikawa, S., Kanai, W., Yokota, A., Hijikata, I., Uehara, A., and Nakane, H.,** A principle for the formulation of plasma developable resists and the importance of dry development of submicron lithography, *J. Vac. Sci. Technol.*, 19(2), 259, 1981.
119. **Tsuda, M., Oikawa, S., Kanai, W., Hashimoti, K., Yokota, A., Nuino, K., Hijikata, I., Uehara, A., and Nakane, H.,** Novel plasma developable resist compositions and performance of total dry microfabrications in submicron lithography, *J. Vac. Sci. Technol.*, 19(4), 1351, 1981.
120. **Lai, J. H.,** Plasma developable electron resists, in *Polymers in Electronics*, Davidson, T., Ed., ACS Symp. Ser. 242, American Chemical Society, Washington, D.C., 1984.
121. **Hatzakis, M.,** Multilayer resist systems for lithography, *Solid State Technol.*, August 74, 1981.
122. **Lin, B. J.,** *Multilayer Resist Systems — in Introduction to Microlithography*, Thompson, L. F., Wilson, C. G., and Bowden, M. J., Ed., ACS Symp. Ser. 219, American Chemical Society, Washington, D.C., 1983.
123. **Franco, J., Havas, J., and Levine, H.,** U.S. Patent 3,873,361, 1973.
124. **Brunsvold, W. R., Crockatt, D. M., Hefferon, G. J., and Lyons, C. F.,** Resist technology for submicrometer optical lithography, *Opt. Eng.*, 26(14), 330, 1987.
125. **Lin, B. J.,** Portable conformable mask — a hybrid near-ultraviolet and deep-ultraviolet patterning technique, *Proc. SPIE*, 174, 114, 1979.
126. **Ito, H. and Willson, C. G.,** Chemical amplification in the design of dry developing resist materials, *Polym. Eng. Sci.*, 23(18), 1012, 1983.
127. **Geis, M. W., Randall, J. N., Deutsch, T. F., Efremow, N. N., Donnelly, J. P., and Woodhouse, B.,** Nitrocellulose as a self-developing resist with submicrometer resolution and processing stability, *J. Vac. Sci. Technol.*, B1(4), 1178, 1983.
128. **Srinivasan, R.and Mayne-Banton, V.,** Self-developing photoetching of poly(ethylene terephthalate)films by far-ultraviolet excimer laser radiation, *Appl. Phys. Lett.*, 41(6), 576, 1982.
129. **Griffing, B. F. and West, P. R.,** Contrast enhanced photoresists-processing and modeling, *Polym. Eng. Sci.*, 23(17), 947, 1983.
130. **Iwayanagi, T., Hashimoto, M., and Nonogaki, S.,** Azid-phenolic resin UV resist (MRL) for microlithography, *Polym. Eng. Sci.*, 23(17), 935, 1983.
131. **West, R., David, L.D., Djurovich, P. I., Stearley, K. L., Srinivasin, S. V., and Yu, H.,** Phenylmethylpolysilanes: formable silane copolymers with potential semiconducting properties, *J. Am. Chem. Soc.*, 103, 7352, 1981.
132. **Miller, R. D., Hofer, D., Fickes, G. N., Willson, C. G., Marinero, E., Trefonas, P., and West, R.,** Soluble polysilanes: an interesting new class of radiation sensitive materials, *Polym. Eng. Sci.*, 26(16), 1129, 1986.
133. **Gozdz, A. S., Craighead, H. G., and Bowden, M. J.,** Poly(alkenylsilane sulfone)s as positive electron beam resists for two-layer systems, *Polym. Eng. Sci.*, 26(16), 1123, 1986.
134. **Saigo, K., Ohnishi, Y., Suzuki, M., and Gokan, H.,** A negative photoresist (TAS) for a bi-layer resist system, *J. Vac. Sci. Technol.*, 3(1), 331,1985.
135. **MacDonald, S. A., Ito, H., and Willson, C. G.,** Advances in the design of organic resist materials, *Microelectron. Eng.*, 1(4), 269, 1983.
136. **Chou, N. J., Tang, C. H., Paraszcak, J., and Babich, E.,** Mechanism of oxygen plasma-etching of polydimethyl siloxane films, *Appl. Phys. Lett.*, 46(1), 31, 1985.
137. **Reichmanis, E. and Smolinsky, G.,** Deep UV positive resists for two-level photoresist processes, *Proc. SPIE Int. Soc. Opt. Eng.*, 469, 38, 1984.

Chapter 2

POLYIMIDES: CHEMISTRY, PROCESSING, AND APPLICATION FOR MICROELECTRONICS

Ronald J. Jensen and Juey H. Lai

TABLE OF CONTENTS

I. Introduction 34

II. Polyimide Chemistry 34
- A. Synthesis, Polymerization, and Curing Reactions 34
- B. Types of Polyimides 35
- C. Chemical and Physical Properties 37
- D. Effect of Moisture on the Electrical Properties of Polyimide Thin Films 39

III. Processing of Polyimide Thin Films 39
- A. Deposition and Coating of Polyimide Films 40
  - 1. Spin Coating 40
  - 2. Spray Coating 40
  - 3. Other Deposition Processes 40
- B. Adhesion Promoters 41
- C. Planarization Properties 41
- D. Patterning of Polyimide Thin Films 42
  - 1. Wet Etching 42
  - 2. Dry Etching 44
  - 3. Photosensitive Polyimide 45
  - 4. Laser Ablation 46

IV. Applications 47
- A. Intermetal Dielectrics for Integrated Circuits 47
- B. Electronic Packaging 48
  - 1. High-Performance Packaging Requirements 49
  - 2. Thin-Film Multilayer Packaging Approach 50
  - 3. Advantages and Applications of TFML Interconnections 52
  - 4. Favorable Properties of Polyimides 52
  - 5. Processing of TFML Interconnects 53
  - 6. Demonstrations of TFML Packaging 55
- C. Passivation and Protection 56
- D. Other Applications for Polyimides in Microelectronics 57

V. Conclusions and Future Outlook 57

References 58

I. INTRODUCTION

Polymers are playing an increasingly important role in the protection and interconnection of a variety of electronic components. One class of polymers that has been increasingly used in many areas of electronics is polyimides. Polyimides are characterized by the presence of the phthalimide structure in the polymer backbone.[1] The unique features of polyimides are high thermal stability (400 to 450°C) and processibility. Although there are other polymers that have high thermal stability in the range similar to that of polyimides, these polymers, unlike polyimides, are generally insoluble, intractable, and lack processibility. Polyimides, through a two-step process, solution coating of the polyimide precursor poly(amic acid) and subsequent curing,[2] can be deposited in thin-film form by spin or spray coating and, therefore, are suitable for microelectronic applications.

The application of polyimides in electronics has been mainly in passivation and protection. In recent years, the application has been extended to use as intermetal dielectrics in integrated circuits (ICs)[3] and thin-film multilayer electronic packaging.[4] In addition to high thermal stability and processibility, other favorable properties of polyimides are their low dielectric constant, high resistivity, and high breakdown voltage. Recent advances in photoimagable polyimides[5] has further accelerated the use of polyimides for electronics.

Research on polyimides has been active. Papers on synthesis and characterization of polyimides have been published regularly in the *Journal of Polymer Science, Journal of Applied Polymer Science,* and *Macromolecules.* The research results on characterization, processing, and application of polyimides have been published in the *Journal of Applied Polymer Science, Journal of Electrochemical Society, IEEE Transaction on Components, Hybrids, and Manufacturing Technology,* etc. Papers on microelectronic application of polyimides are mostly found in the *Journal of Electrochemical Society* and American Chemical Society Symposium Series *Polymer Materials for Electronic Applications.* The two-volume book entitled *Polyimides: Synthesis, Characterization and Applications* which was edited by K. L. Mittal and published in 1984 by Plenum Press contains much useful information and data, and is a valuable reference book on polyimides.

II. POLYIMIDE CHEMISTRY

A. Synthesis, Polymerization, and Curing Reactions

Polyimides are long-chain organic polymers characterized by the presence of the phthalimide (I) structure in the polymer backbone. The backbone structure of polyimides can be generally expressed as structure II, where R and R′ are mainly aromatic groups.

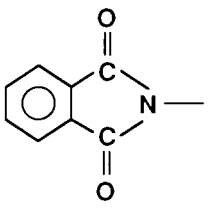

I

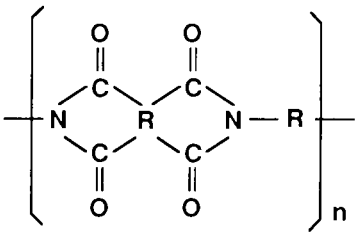

II

Different polyimides have different R and R′ groups.[1,2] Examples for R are and ; and for R′ are , , , etc. Notice that the predominant structures of R and R′ are aromatic, which is responsible for the high thermal stability of the polymers.

Many different polyimides have been synthesized.[1,2] Most polyimides, however, are intractible, insoluble, and lack processibility. The synthesis that make polyimides usable is a

two-step process[1,2] that involves the polymerization of a soluble polyimide precursor called poly(amic acid) that is thermally converted to the polyimide. The soluble precursor poly(amic acid) (V) is commonly prepared by polycondensation reaction between a dianhydride, e.g., pyromellitic dianhydride (III), and a diamine (IV) as shown in the following example:

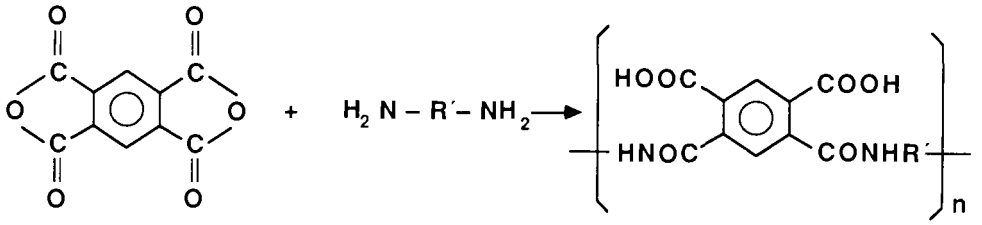

III IV V

The conversion of soluble poly(amic acid) (V) to polyimide (VI) is generally accomplished by heating and is called curing or imidization. The curing reaction involves elimination of H_2O molecules through cyclization as shown in the following:

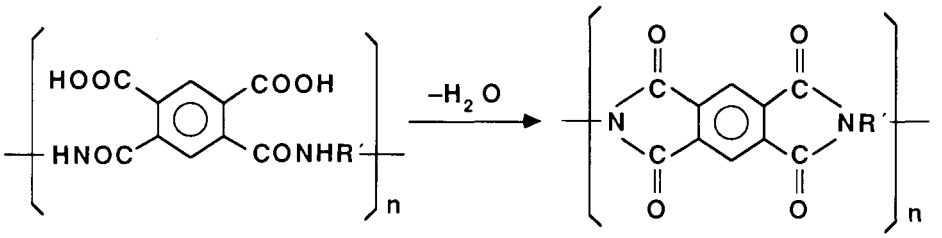

V VI

It is generally accepted that imidization begins at a temperature $\geq$150°C, and complete imidization occurs at a temperature $\geq$300°C. The precursor poly(amic acid) is soluble in polar solvents such as dimethyl formamide and *N*-methylpyrrolidone (NMP). For microelectronic applications, thin films are deposited on the substrates by spin or spray coating of the poly(amic acid) solution, and the thin films are then cured and imidized. The curing is typically performed in two steps. The soft cure, which involves heating the thin film in air at 120 to 250°C, is performed first to remove the coating solvent; this is followed by a hard cure performed at a temperature of 300 to 450°C in a N_2 atmosphere to complete the imidization.[6]

The degree of imidization has a significant effect on the chemical and physical properties of polyimides. Fully cured polyimides, for example, are not soluble in any of the organic solvents, but partially cured polyimides are soluble in the polar solvents. The rate of imidization or degree of cure has been monitored by infrared spectroscopy,[7] thermal analysis (including both thermal gravimetric analysis and differential scanning calorimetry),[3] and dielectrometry (measurement of dissipation factor or dielectric loss).[8,9]

Solution characterization of poly(amic acid) and polyimides has been performed with low-angle light scattering, viscometry, membrane osmometry, and size exclusion chromatography.[10] Comparison of molecular weights of poly(amic acid) and cured polyimide shows little change in molecular weight with cure, indicating minimal degradation during the curing.

B. Types of Polyimides

A large number of polyimides that differ in the chemical structures of R and R′ (see polyimide chemical formula II) have been synthesized.

Some examples of R are 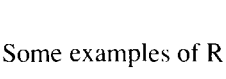 and some examples of R′ are 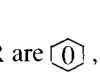 , 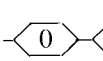 , and 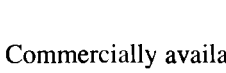 , where X is O, CH_2, S, SO_2, etc.[1,2]

Commercially available polyimides that have been used in electronics include Kapton and Pyralin manufactured by DuPont, and PIQ manufactured by Hitachi Co. of Japan. Kapton polyimides are derived from pyromellitic dianhydride (PMDA) III and 4,4′-diaminodiphenyl ether (DADPE) (VII). Pyralin polyimides (e.g., PI-2400 and PI-2500 series) are sold as a solution of poly(amic acid) derived from PMDA and DADPE or from benzophenone tetracarboxylic dianhydride (BTDA) (VII) and DADPE.[1]

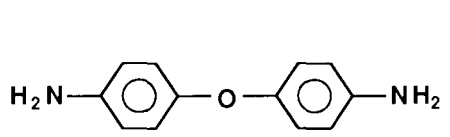

VII

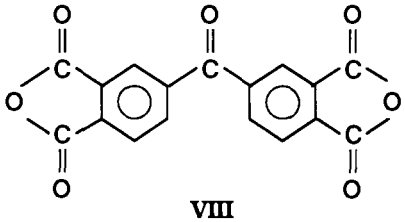

VIII

The chemical structure and composition of PIQ is similar to that of Pyralin but contains an additional ring. The polyimide PIQ designates poly(imide-isoindoloquinazoline-5,6-dione) (IX).[1,11]

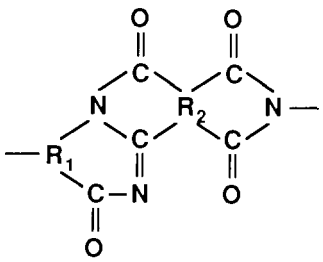

IX

Several commercially available polyimides are supplied as completely imidized polymer in powder form. They include PI-2080 manufactured by Upjohn Co., Rhodia Kermid 600 manufactured by Rhone-Poulenc, and XU-218 manufactured by CIBA-Geigy.[1] The exact composition of these polyimides has not been published. These polyimides, however, are soluble in polar solvents and have lower thermal stability.

Polyimide siloxane is a new class of siloxane-modified polyimide.[12,13] It is available from M & T Chemicals, Inc. The polymer is a block copolymer of BTDA with methylene dianiline (MDA) (X) and bis-gamma aminopropyltetramethyl disiloxane (GAPD) (XI). The polymer has a higher solubility and lower thermal stability (~400°C) than Pyralin-type polyimides. In contrast to Pyralin and PIQ, the siloxane polyimide requires no adhesion promoter when it is coated in thin-film form on silicon wafers for microelectronic applications.

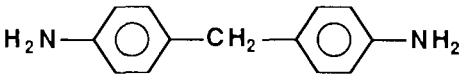

X

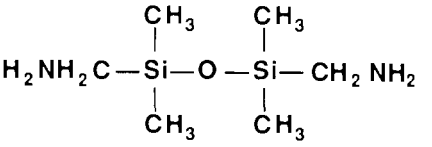

XI

Patterning of polyimide thin films is often required in microelectronic applications. Patterning of polyimides is generally accomplished by use of photolithography. The device pattern is first formed in the photoresist film that is coated on the top of the polyimide film; the resist pattern is then transferred to the polyimide film by wet or dry etching. Since the patterning of polyimide films by conventional processes requires many processing steps, photosensitive polyimides have been under development for a number of years.[5,14,15] Reported photosensitive polyimides have been limited to negative acting, i.e., the exposed area in the polyimide thin film becomes less soluble after ultraviolet (UV) exposure.

Although several formulations of photosensitive polyimides have been reported, the basic formulation is based on the work of Rubner et al.[14] The basic system consists of a photoreactive poly(amic acid) possessing photoreactive side groups R* bound in an ester-like fashion (XII).[14]

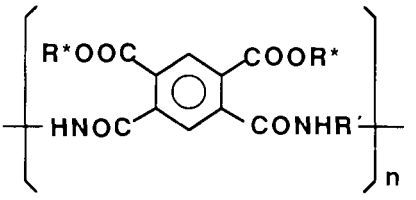

XII

Upon exposure to UV light of 400 Å wavelength, the photoreactive side groups form intermolecular bonding with neighboring polymer molecules, thereby reducing the solubility in the exposed area and enabling the polymer to act as a negative photoresist. After development, the exposed precursor is cured to complete imidization and form polyimide. During the hard curing the photoreactive groups R* that form the cross-linking bridge are volatilized, resulting in a shrinkage of the film. The photoreactive group R* used in photosensitive polyimide was reported to be hydroxyethyl methacrylate,[14,15]

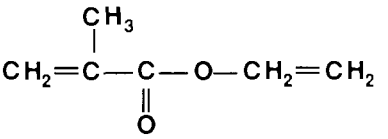

To improve the photosensitivity of the polyimides, monomeric photoinitiators that act as cross-linking agents have been added to the polymers. A vinylsilane-based photoinitiator component, was reported to improve the photosensitivity of the poly(amic acid) ester.[15]

C. Chemical and Physical Properties

The chemical and physical properties of polyimides are significantly dependent on the degree of imidization, the molecular weight, and the chemical structures of R and R′ in the polyimide backbone.

The polyimide precursors, poly(amic acids), are highly soluble polyelectrolytes.[2,16] They are soluble in polar solvents, e.g., *N*-methyl pyrollidone, dimethylformamide, dimethylacetamide, etc., and can readily form salts.[2,17] The molecular weight and molecular weight average of the poly(amic acids) derived from pyromellitic dianhydride and bis(4-aminophenyl)ether have been studied.[7,18] The number-average molecular weights M_n ranged from 13,000 to 55,000 and weight-average molecular weights M_w from 99,000 to 266,000. The viscosity-molecular weight data followed the Mark-Houwink relationship[18]

$$[\eta] = 1.85 \times 10^{-4} M_w^{0.80}$$

The high thermal stability of aromatic polyimides is one of the most important properties responsible for its usefulness in electronics. The thermal decomposition temperature of PIQ is quoted as being 450 to 500°C.[19] TGA (thermogravimetric analysis) has been performed for PI-2555 thin films both soft cured and hard cured.[6] The thermograms show that the onset of thermal decomposition for PI-2555 is approximately at 500°C and significant decomposition occurs at 600°C. Thermograms for the hard-cured film (260°C, 60 min in N_2 atmosphere) show that approximately 2% weight loss occurs in the temperature range 40 to 100°C, which is probably due to the loss of absorbed water. Thermograms of the soft-cured films (120°C, 30 min in air) show that a high degree of imidization was obtained at 250°C; however, even at 400°C, complete imidization was not obtained, which suggests that both curing temperature and time are important in obtaining the complete cure.[6]

The thermal stability of polypyromellitimide films derived from aromatic diamine appears to be dependent on the structure of R′. Introduction of aliphatic linkages into the main chain, or as side chains, results in poorer thermal stability.[2] Thermal stability of the polypyromellitimide derived from *p*-phenylene diamine, for example, is noticeably higher than the one derived from bis(4-aminophenyl)-ether, that in turn, is higher than the one derived from bis(4-aminophenyl)methane.

The glass transition temperature (T_g) of some polyimides has been tabulated.[2,20,21] The T_g of polyimides derived from aliphatic amines is generally lower than the ones derived from aromatic amines which are in the temperature range 280 to 385°C.[1] This is significantly higher than the T_g of most organic polymers. Similar to the behaviors observed for thermal stability, introduction of flexible linkages such as –O–, –S–, $-CH_2-$ have the effect of reducing chain rigidity resulting in a lowering of T_g.[20]

The resistance of aromatic polyimides to ionizing radiation such as high-energy electrons, neutrons, and gamma radiation is excellent. The electrical and mechanical properties are unaffected by exposure to radiation doses of 10^{10} rad of high-energy electrons,[2] and 10^8 rad (Si) of gamma radiation.[35] Polyimides are affected by long-term exposure to UV light, however. Mechanical properties are degraded after 4000 h exposure to UV light.[2]

The solubility of polyimides is dependent on the degree of imidization, the polymer backbone and side chain structures, and the molecular weight of the polymers. In general, the solubility decreases with an increase in degree of imidization and an increase in molecular weight. Fully imidized aromatic polyimides are very resistant to organic solvents and are soluble in concentrated H_2SO_4 and HNO_3.[2,22] Solubility in organic solvents can be improved by modifying the structure of polyimides.[23] The increase in solubility, however, is generally accompanied by a decrease in the thermal stability.

Good adhesion to the substrates is an important requirement of polyimides for microelectronic applications. In general, the aromatic polyimides show good adhesion to the surface of aluminum and chromium, but have poor adhesion to silicon or silicon dioxide.[6,24] Adhesion can be improved by applying an adhesion promoter that adheres well to both the substrates and polyimides. Examples of adhesion promoters include organic aluminum chelate compounds for PIQ[25] and γ-aminopropyltriethoxy silane for PI-2555.[7]

Polyimides possess some favorable properties for application in electronics. The dielectric constant of polyimides is in the range 3.1 to 3.7 at 1000 Hz and room temperature.[1,6,8,24] The dissipation factor of polyimides is in the range 0.001 to 0.003 at the same frequency.[1,6,24] The volume resistivity of polyimides, while a function of both humidity and temperature, is higher than 10^{16} Ωcm at 50% RH and room temperature.[1,19] The dielectric strength is on the order of 10^6 V cm^{-1} at room temperature.[1,19]

Mechanical properties of polyimide thin films have been reported.[1,19,24,26] Young's modulus for the PI-2500 thin films has been measured to be 3 to 4.8 GPa.[24,26] The tensile strength of aromatic polyimides at room temperature is in the range of 170 to 200 MPa.[2,19,24]

D. Effect of Moisture on the Electrical Properties of Polyimide Thin Films

Two concerns for the use of polyimides as dielectrics are the absorption of water vapor and the effect of moisture on electrical and mechanical properties of polyimides. Water vapor absorption isotherms for hard-cured PIQ have been reported.[6] At 23°C and 80% RH, the equilibrium amount of water absorbed by the PIQ was 2.3 wt-%. The effect of temperature on moisture absorption appears to be slight, and the absorption process is slightly exothermic.[6] Moisture transport in PI-2500-type polyimide thin films (1 μm) has been determined.[27] The thin films were exposed to moisture, and both the capacitance and weight change of the films were measured as a function of time to determine the rate of water diffusion. It was found that the water transport in the polyimide films is Fickian, with an activation energy of about 0.25 eV, and the diffusion coefficient of water in the films is about 5×10^{-9} cm^2/s at room temperature.[27]

The effects of humidity and cure conditions on the dielectric constant, dissipation factor, and breakdown voltage of thin films (5 μm) of PI-2555 have been investigated.[24] Parallel plate capacitor structures were fabricated using polyimide films cured in N_2 at different temperature and different pressures. Dielectric properties were measured with a capacitance bridge operating at 1.6 kHz. The dielectric constant (ϵ_r) has been found to increase linearly with increasing relative humidity, with an average value of $\epsilon_r = 3.1$ at 0% RH and a slope of about 0.01/% RH. It has been found that cure conditions have a small effect on ϵ_r, but have a much stronger effect on the dissipation factor. The dissipation factor increases from 0.7 to 3×10^{-3} as percent RH increases from 0 to 100%. Breakdown voltages decrease from 3.3 MV/cm at 0% RH to 1.6 MV/cm at 100% RH, and cure conditions have an insignificant effect on breakdown voltage.[24]

III. PROCESSING OF POLYIMIDE THIN FILMS

Polyimides have a wide range of applications in microelectronics because of their processibility; a variety of techniques can be used to deposit and pattern polyimide films over a wide range of geometries. Polyimides can be obtained in solution form as poly(amic acid) or soluble polyimide (as discussed in Section II.B). These solutions can be deposited by a variety of techniques such as spin or spray coating, screening, dipping, or roll coating to produce a wide range of film thicknesses (1 to 100 μm). The ability of the polyimide solutions to flow before curing promotes the planarization of the underlying substrate or conductor patterns. During curing at moderate temperatures (300 to 420°C), the poly(amic acid) is converted to polyimide, which has excellent thermal, mechanical, and chemical stability and is thus resistant to degradation during subsequent processing steps such as metal deposition, etching, or photolithography. The polyimide films can be patterned by a variety of techniques such as wet etching, plasma or reactive ion etching, ion milling, laser ablation, or direct photopatterning of photosensitive polyimide. These deposition, curing, and patterning processes are discussed in more detail below.

A. Deposition and Coating of Polyimide Films

When polyimides are used as encapsulants or die attach materials, they may be deposited by simple techniques such as dipping or syringe application. In order to deposit thin, uniform films with controlled thickness, more accurate methods such as spin coating, spray coating, screening, or vapor deposition are required.

1. Spin Coating

Spin coating is the most common technique for depositing thin polyimide films. It is a well-characterized process that is used frequently for depositing photoresists in IC processing, and automated spin coating equipment is widely available. Spin coating has also been modeled to predict the effects of a variety of process parameters on coating thickness and uniformity.[28]

The thickness of spin-coated polyimide films depends strongly on the solution viscosity and concentration, and can be accurately controlled over a wide range (e.g., 1 to 8 μm for DuPont 2555 PI) by varying the dispense volume and the time and angular speed of spinning.[24,29] The most sensitive process parameter for controlling film thickness is the spin speed; film thicknesses generally vary with spin speed according to a power law relationship: $t = kw^a$, where t is the film thickness and w is the angular spin frequency. Typical values for soft-cured (120°C) DuPont 2555 polyimide spun for 60 s are $k = 90$ and $a = -0.7$.[24]

The largest practical film thickness achievable by spin coating is on the order of 15 μm. Thicker films, such as those required for interlayer dielectrics in IC packaging applications, are deposited with multiple coatings, with a cure temperature of at least 150°C between coats. In general, the deposition of thick polyimide films by spin coating requires high viscosity solutions that are spun at low angular speeds for short times. All of these factors adversely affect the uniformity of coating thickness. Furthermore, spin coating is limited to square or round substrates a few inches in diameter with no large surface topography.

2. Spray Coating

To overcome these limitations of spin coating, thicker polyimide films can be deposited on larger substrates by spray coating. Spray coating has the additional advantages of high throughput and the ability to coat nonsquare substrates with large topography. Spray coating is thus well suited for high-volume manufacturing operations.

Polyimide can be accurately spray coated in commercial systems in which a spray nozzle passes over the substrates, which are moving on a conveyor belt at right angles to the nozzle motion. The uniformity and thickness of the sprayed films depend of a number of process parameters such as solution viscosity and concentration, solution flow rate, the diameter and shape of the spray nozzle and its distance from the substrates, the atomization pressure, the conveyor speed, and the number of passes of the spray nozzle over the substrates. The selection of a diluting solvent that will rapidly evaporate from the freshly sprayed film is also crucial. Statistically designed experiments are essential in developing an optimized spray coating process.

Very few detailed process descriptions of spray coating have been given in the literature. Spray coating processes developed at Honeywell have been used to deposit polyimide films 2 to 15 μm thick, to an accuracy of ±1 μm, with 20 to 30% planarization of conductor lines per coating and 60% planarization after three coats.[4]

3. Other Deposition Processes

A recently reported alternative to spin or spray coating is screen printing of polyimide solutions.[30-32] Screen printing is a low-cost, high-throughput process capable of directly patterning the polyimide films as they are deposited. In some cases, proprietary fillers, thickeners, and surfactants have been added to the polyimide to improve its printing characteristics,[30] and in other cases the screen printing masks and equipment (especially the squeegee) have been modified.[31]

Another alternative process is the vapor deposition of polyimide, which was recently reported by researchers at IBM, who coevaporated the diamine and dianhydride monomers at stoichiometric rates.[33] The evaporated films had better adhesion and a lower dielectric constant and dissipation factor than spin-coated polyimide. This process offers the possibility of uniform, defect-free, conformal films which can be cured *in situ* during deposition.

B. Adhesion Promoters

The adhesion of polyimide films is highly dependent on the surface chemistry of both the substrate and the polyimide, the substrate roughness and cleanliness, the deposition conditions, and the degree of cure of the polyimide.[34] Long-term environmental effects, particularly the combination of high temperature and humidity, can significantly degrade the adhesion of polyimides to some materials. Adhesion promoters are frequently used to improve the initial adhesion of polyimide to various surfaces or to reduce the degradation in adhesion due to environmental effects. For example, studies at Honeywell have shown that the adhesion of polyimide to Cr is excellent and does not degrade after thermal cycling, thermal shock, accelerated aging at 85°C/85%RH, or exposure to γ-radiation;[24,35] however, a silane adhesion promoter was required to improve the initial adhesion of polyimide to Al_2O_3 ceramic substrates, and to prevent the degradation in adhesion after exposure to high humidity.

The two types of adhesion promoter most commonly used in depositing polyimide films are the silane-based adhesion promoters such as γ-aminopropyltriethoxy silane, and aluminum chelate compounds. The mechanism of silane adhesion promoters has been widely investigated.[7,36] Basically, the ethoxy groups in the silane compound hydrolyze in an aqueous solution and partially polymerize (hence the short shelf-life of these solutions). The hydrolyzed silane oligimer then forms siloxane bonds with the substrate through a condensation reaction with hydroxyl groups on the substrate. The aminopropyl groups on the adhesion promoter react with the poly(amic acid) either through ionic bonding[7] or by forming an imide bond with the amic acid groups.[25]

Aluminum chelate adhesion promoters work by forming a thin amorphous aluminum oxide film (5 nm thick) on the surface of the substrate when the hydrocarbon part of the aluminum chelate decomposes during curing.[25] The adhesion of polyimide to this aluminum oxide film is strong and is not degraded by high temperature and humidity.

Either type of adhesion promoter is applied as a very thin coating, usually by spin coating, prior to deposition of the polyimide. The silane adhesion promoters require only a short bake at temperatures of $\leq$100°C, while the aluminum chelate compounds must be baked at temperatures of 350°C to form the alumina surface. In recent years, polyimide formulations that are self-priming or that contain additives that function as adhesion promoters have become available.

C. Planarization Properties

One of the chief advantages of polyimide as an interlayer dielectric is its ability to planarize underlying conductor topography. The step height of conductor lines is reduced, sidewalls angles are reduced, and sharp corners become more rounded.[37] This planarization effect improves the accuracy, resolution, and yield of subsequent photolithography and patterning operations. Figure 1 shows a cross section of conductor lines 5 μm thick that have been planarized with 25 μm of polyimide deposited in 3 sprayed coatings.

Due to hydrodynamic forces, a freshly coated polyimide solution will initially form a planar surface over any topographical feature whose height is less than the thickness of the deposited film. As the solvents evaporate, however, the viscosity of the polyimide solution increases until it is eventually unable to flow. Further solvent evaporation causes the film to shrink and partially conform to the underlying topography.[38]

The common measure of planarization over a step or conductor line of initial height t_i is the degree of planarization (DOP), defined as

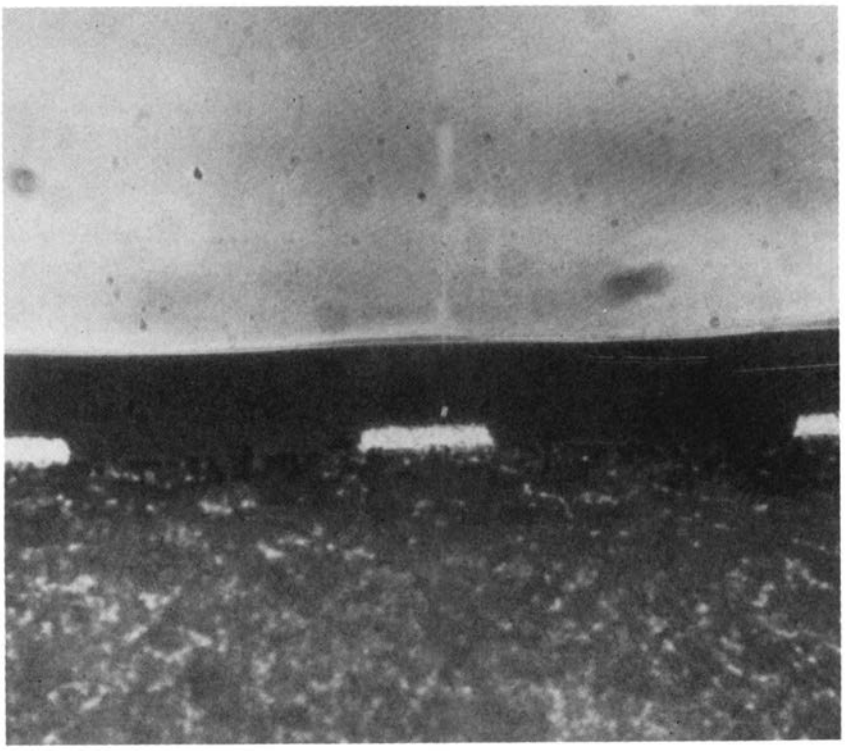

FIGURE 1. Cross-section of 5-μm-thick conductor lines on ceramic planarized with 25 μm of polyimide deposited in three spray coatings.[4]

$$DOP = 1\text{-}t_f/t_i$$

where t_f is the final step height in the polyimide film after curing.[8] The DOP is highly dependent on the solution viscosity and solids content, the molecular weight of the polyimide, and the spacing between conductor features, and it may depend on the thickness of the polyimide film if it is less than the conductor step height t_i.

The DOP increases for multiple coats of polyimide, due to the incremental planarization of each coat. Figure 2 shows planarization measurements for individual and multiple coatings of two different DuPont polyimides.[24] With the exception of a low DOP on the first coating, the incremental DOP for 2555 polyimide is approximately 30% for each coating, resulting in a cumulative DOP of 80% after five coatings or 19 μm total thickness. The higher viscosity 2525 polyimide produces the same film thickness in two coatings, but only achieves 50% planarization. Thus, for a given film thickness, several thin coatings are preferrable over a few thick coatings from the standpoint of planarization.

D. Patterning of Polyimide Thin Films

Polyimide films can be patterned by a variety of techniques, including wet or dry etching through a photolithographically defined mask, direct photopatterning of photosensitive polyimides (discussed in Section II.B), or laser ablation. The process steps involved in wet etching, dry etching, and direct photopatterning are shown in Figure 3.

1. Wet Etching

The earliest technique for patterning polyimide was wet etching. As shown in Figure 3, a pattern is first defined in a positive or negative photoresist film deposited on the polyimide.

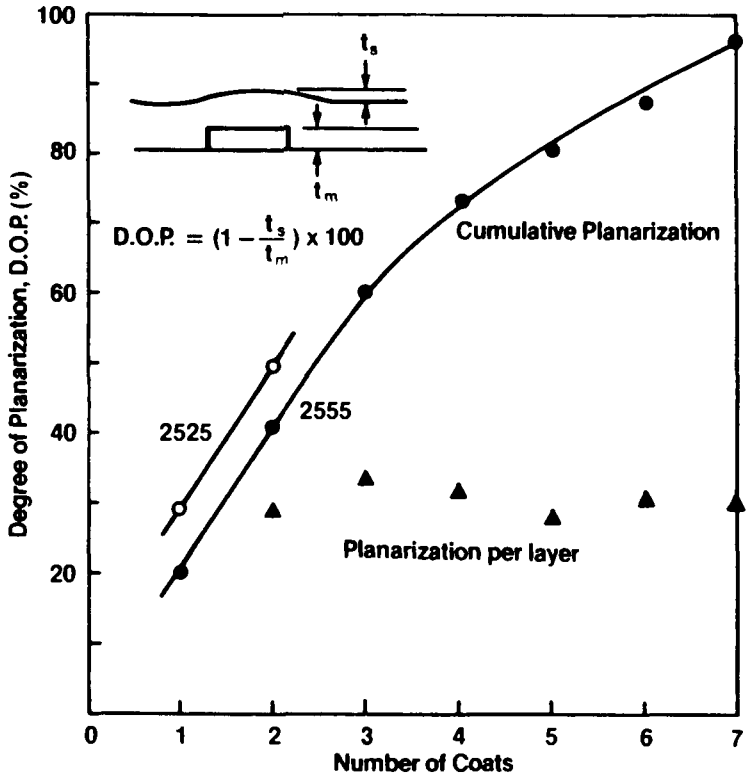

FIGURE 2. Degree of planarization achieved with individual and multiple coatings of two different polyimides.[24]

The unmasked polyimide is then selectively dissolved, and the photoresist is stripped. Fully cured polyimide films can only be etched with a solution containing hydrazine hydrate (H_2NNH_2:H_2O).[39,40] Additives such as ethylene diamine ($NH_2CH_2CH_2NH_2$) have been added to increase the etch rate and improve the linearity of etch rate with time.[39] Although the hydrazine-based etchants are marketed by Hitachi and frequently used in Japan, hydrazine is toxic and highly pyrophoric, and is therefore not widely used in the U.S.

A greater variety of etchants can be used to etch polyimide in the partially imidized state. The alkaline solutions that are used to develop positive photoresists, such as tetralkyl ammonium hydroxide, sodium hydroxide, and potassium hydroxide, will also etch partially cured polyimide.[7] This means that the photoresist can be developed and the polyimide can be etched in a single step. When a negative photoresist is used, the organic developers (such as xylene) will not etch polyimide, and separate solutions such as positive photoresist developers[7] or hydrazine hydrate and ethylenediamine[40] are used to wet etch the polyimide. The residues left by these alkaline etchants must be neutralized with acetic acid and water rinses.[7] The photoresist is then removed with standard photoresist solvents that will not attack the partially cured polyimide. This precludes the use of some strong resist strippers that contain NMP.

The primary limitations of wet etching are the low resolution and small aspect ratio (thickness/width) of the patterned features, which is a limitation of all wet patterning processes. Another drawback of wet etching is that with the exception of the hydrazine etchants, it requires a partially cured polyimide film, and this partial cure is difficult to control. Since the etch rate depends on the degree of cure, it is difficult to reproduce etch rates and control pattern geometries. Finally, the additional shrinkage of the films during the final cure after wet etching may cause further loss of resolution and/or localized cracking due to the stress that is concentrated at patterned features.

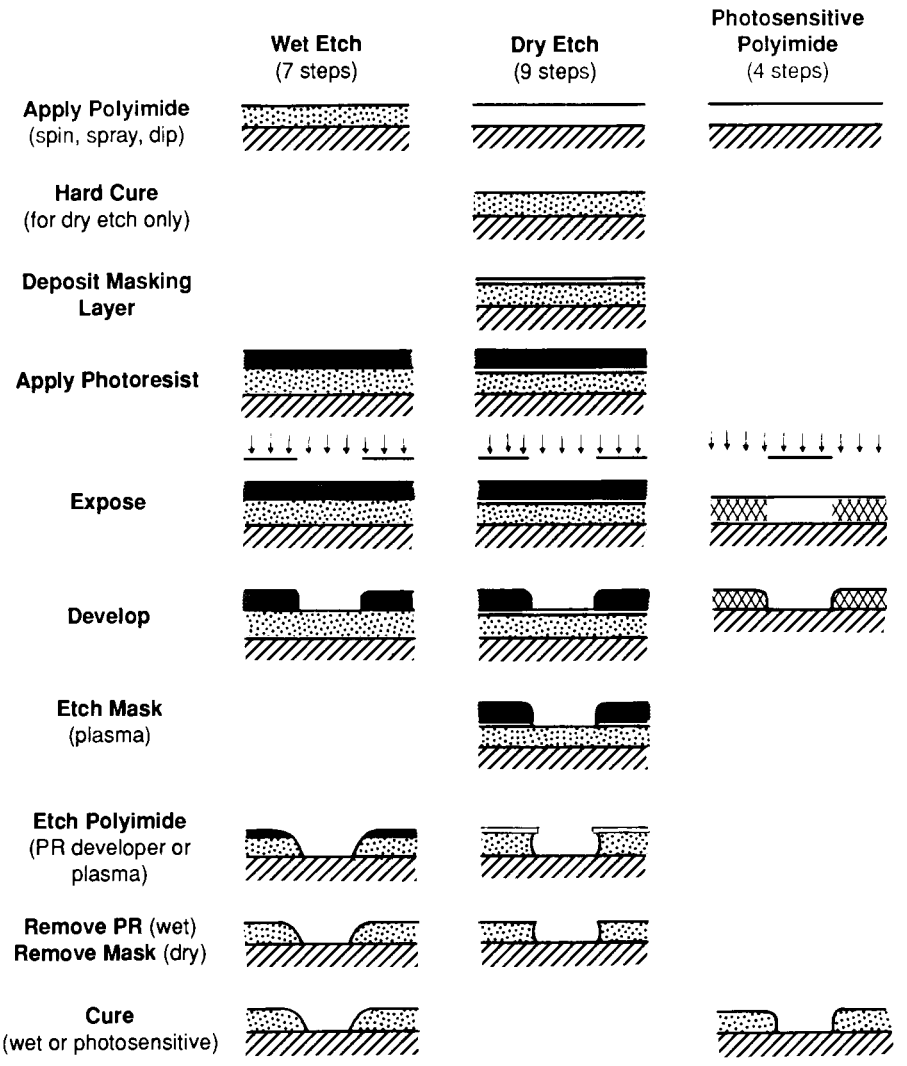

FIGURE 3. Comparison of the process steps involved in patterning polyimide by wet etching, dry etching, and photopatterning of photosensitive polyimide.

2. Dry Etching

Many of these limitations of wet etching are overcome by etching polyimide using "dry" vacuum processes such as plasma etching or reactive ion etching (RIE), in which the substrates are placed on the lower electrode in a parallel plate system sustaining an RF plasma.[24,41,42] Other dry processes include reactive ion beam etching (RIBE) or ion beam-assisted etching (IBAE), in which a beam of reactive ions (e.g., O^+) or inert ions (e.g., Ar^+) are accelerated toward the substrates, which may be flooded with a reactive gas such as O_2.[43] In all of these processes, the etching reactions are initiated by ions that are accelerated perpendicular to the film surface; therefore, these processes can produce high-aspect-ratio features with nearly vertical sidewalls in fully cured polyimide films. These processes are also more reproducible than wet etching, and a variety of process parameters (e.g., reactor pressure, gas composition and flowrate, and RF power or ion beam energy) can be varied to accurately control characteristics such as the etch rate, the selectivity for etching different materials, and the sidewall angle of etched features.

Reactive ion etching, in which the substrates are placed on the powered electrode in a

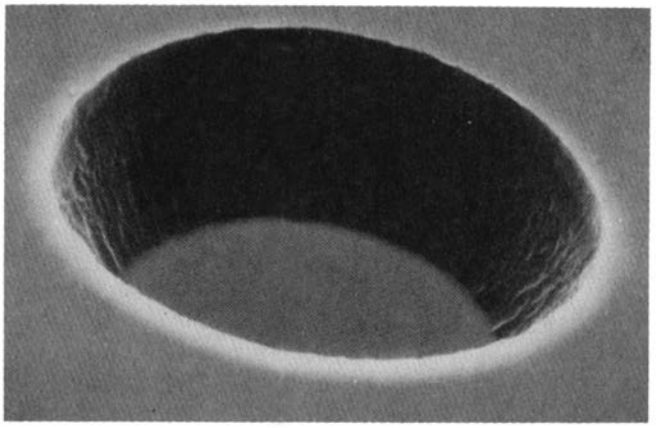

FIGURE 4. SEM micrograph of a via hole 50 μm in diameter reactive-ion etched in polyimide 25 μm thick.[4]

parallel plate plasma system, is the most common dry etching process for polyimide. Polyimide is usually etched in a gas mixture of oxygen and a fluorine-containing gas such as CF_4 or SF_6.[24,41,42] Several investigators have found that the polyimide etch rate increases rapidly with increasing fluorine concentration, reaching a maximum at about 20% CF_4 or 60% SF_6, and then decreasing at higher fluorine concentrations.[41,42] The fluorine concentration is also a sensitive parameter for controlling the sidewall angle of etched features. A tapered sidewall is often desired for good metal step coverage, and this taper can be controlled by adjusting the CF_4 content in the plasma etch gas.[4,44]

Because polyimides etch at nearly the same rate as photoresists, the RIE of thick polyimide films requires that a masking layer of a slow etching material be deposited and patterned on top of the polyimide, as shown in Figure 3. Materials that have been used as masking layers include metals such as aluminum, chromium, titanium,[45] or molybdenum,[46] inorganic materials such as plasma-deposited silicon nitride or silicon dioxide,[4] or spin-on glasses such as SiO_2[47] or aluminum chelate compounds.[48] Figure 4 shows a via hole 50 μm in diameter that has been RIE etched in a polyimide film 25 μm thick, using plasma-deposited SiO_2 as the etch mask.[4] The sidewall has been intentionally tapered to an angle of about 65° from horizontal.

3. Photosensitive Polyimide

The number of process steps required to pattern polyimide films is greatly reduced by directly photopatterning photosensitive polyimide formulations, as shown by the comparison of process steps in Figure 3. The chemistry of photosensitive polyimides was discussed in Section II.B. All of the currently available photosensitive polyimides are negative acting, i.e., they are cross-linked by exposure to near-UV light, and unexposed areas can be selectively dissolved by a developer solution.[5,14,15] The reduction in the number of process steps and the associated process equipment (especially the elimination of plasma deposition and etching systems) offers a significant cost savings and yield advantage over wet or dry etching of polyimide.

The main limitations of photosensitive polyimide are the low resolution and aspect ratio of patterned features. In general, the resolution for positive features (e.g., mesas) is better than for negative features (e.g., holes); unfortunately, holes are the more common pattern for most thin-film applications of polyimide. The via hole aspect ratio (film thickness/via diameter) achievable with photosensitive polyimides is currently limited to about 1:2. Some of the best results have been reported by NTT, where they have achieved a minimum via

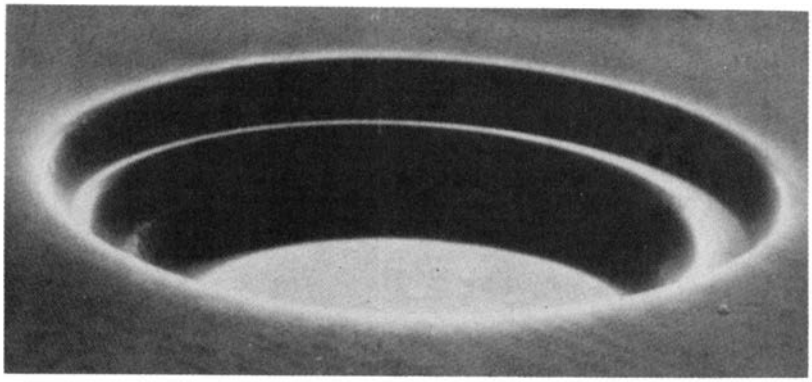

FIGURE 5. SEM micrograph of a via hole 50 μm in diameter × 25 μm deep patterned in photosensitive polyimide.[4]

diameter of 15 μm in 10-μm-thick films,[49] and by Honeywell, where they patterned 50-μm vias in 25-μm-thick films using three coatings and developments.[4] The latter result is shown by the SEM micrograph in Figure 5.

The resolution of negative features in photosensitive polyimide is limited by swelling during development, which is a common problem for negative-acting or cross-linking photoresists. Resolution is also limited by the large amount of film shrinkage that occurs during the final cure after development (typically 50% thickness reduction). The large film shrinkage is due to the large size of the cross-linking groups that are volatilized during curing.

The thickness of photosensitive polyimide films that can be patterned in a single step is limited because UV wavelengths (especially 365 nm) are strongly absorbed by the photosensitive polyimide, which limits the depth of cross-linking in the film.[49-51] During development, the uncross-linked polymer beneath the cross-linked surface layer is dissolved, resulting in undercut and an overhanging sidewall profile. This difficulty in patterning high-aspect-ratio features in thick films limits the use of photosensitive polyimide in high-density packaging applications, where thick dielectric films are required for low interconnect capacitance. The problem may be overcome by repeated coating and development of thin films[4] or by filtering the 365-nm light.[50]

4. Laser Ablation

The most promising future technique for patterning polyimide films is direct patterning by laser ablation. These processes are in the initial stages of development at a number of laboratories.[52-55] Polyimide can be thermally or photochemically decomposed by a variety of lasers and wavelengths, including CO_2, Nd-YAG,[52] and excimer lasers.[53-55] Pulsed excimer lasers operating at wavelengths of 193 to 351 nm have produced the best results, cleanly ablating polyimide without producing by-products of thermal decomposition.

Most of the initial work on excimer laser etching of polyimide has been concerned with reaction mechanisms, as opposed to selective patterning of fine features in polyimide films. In particular, these studies have investigated the relative roles of photothermal and photochemical dissociation, and have concluded that ablation is controlled by photochemical processes at the shorter wavelengths (<193 nm) and by photothermal processes at the longer wavelengths where the photon energy is less than the polymer bond energies.[54]

In a few studies, fine features have been patterned in polyimide films by exposing a large-area laser beam through a contact mask[55] or by using a focused beam.[56] Using the former method, 0.4-μm features were delineated on a polyimide film, although there was a considerable amount of residue due to the low fluence.[55] Direct writing with a focused laser beam offers the possibility of maskless, programmable patterning of polyimide films using a computer-driven translational stage and pulsed laser. Direct writing processes are ideally

Table 1
PHYSICAL PROPERTIES OF POLYIMIDES AND SILICON DIOXIDES[19]

Properties	Polyimides	SiO_2
Coefficient of thermal expansion (1/°C)	5×10^{-5}	0.4×10^{-6}
Thermal stability (°C)	475	1700
Young's modulus (GPa)	3	70
Tensile strength (GPa)	0.1—0.2	0.2
Volume resistivity (Ωcm)	10^{16}	$>10^{16}$
Dielectric strength (V/cm)	10^6	10^6—10^7
Dielectric constant	3.5	3.7

suited to quick-turnaround prototype production. Furthermore, selective laser ablation offers significant cost reduction and yield enhancement by eliminating the masks, alignment equipment, process steps, and defects associated with photolithographic processes. Further development of the process equipment and optics for laser ablation is required to improve the feature resolution and throughput of this process.

IV. APPLICATIONS

A. Intermetal Dielectrics for Integrated Circuits

One of the important applications of polyimides in electronics is as intermetal dielectrics in multilevel interconnections on ICs. Chemical vapor-deposited silicon dioxides (CVD oxides) have been the most widely used intermetal dielectrics. In recent years, however, polyimides have been successfully used in this application.

Chemical, physical, mechanical, and electrical properties of polyimides were discussed in Section II. Many of the mechanical and electrical properties of SiO_2 and polyimides are comparable (see Table 1).[19] The coefficient of thermal expansion of polyimide is approximately an order of magnitude higher than that of SiO_2. The thermal stability and Young's modulus of SiO_2 are higher than that of polyimides. The tensile strength and the electrical properties (volume resistivity, dielectric strength, and dielectric constant) of SiO_2 and polyimide are similar. In fact, the dielectric constant of polyimides is slightly lower.

There are several advantages of using polyimides over CVD oxides: (1) polyimide thin films ranging from 0.5 to 4 μm can be deposited on the silicon wafer by spin coating followed by curing. The deposition process is simple and faster than the deposition process for CVD oxides; (2) the capability of polyimide films to planarize the topography of the substrate is the most important advantage over CVD oxides. Planarization facilitates the patterning of contact vias that is critical to the success of multilevel metallization; (3) since thicker polyimide films can be formed without cracking (i.e., residual stress is less than fracture strength),[11,24] the pinhole density of the films is small. It has been reported that pinhole densities for 1- and 3-μm-thick PI-2545 films are 5 and 0.1 cm^{-2}, respectively;[57] (4) since thick polyimide films are used, the interlevel capacitance is reduced, which enhances high-speed operation of ICs. By using 1.7 μm of PI-2545 films, the interlevel capacitance has been reduced to 2.66×10^{-9} F/cm^{-2}, half that of conventional oxides.[57]

In general, the process sequence required for polyimide films as intermetal dielectrics is the following:

1. Spin coating of polyimide precursors (apply adhesion promoters on substrate first, if necessary)
2. Curing of polyimide films

3. Patterning of contact vias through polyimide films
4. Deposition of contact and interconnect metals
5. Repeat of above processes for multilevel interconnect

Spin coating, curing, and patterning of polyimide films have been discussed (see Section III). Polyimide thin films ranging from 0.5 to 4.0 μm can be obtained by adjusting the precursor solution concentration, spin coating speed, and spin time. Precursor films are generally fully cured after coating; however, partial cure is also done for ease of wet etching of polyimide films. Patterning of via holes is one of the most important steps. Patterning is performed by photolithography followed by wet or dry etching of polyimide films. Although positive photoresists can be used as the etch masks for wet etching of the polyimides,[57] an additional etch mask consisting of a thin Mo film deposited between the polyimide and the photoresist has also been used to control the dimension of via holes.[58] Wet etching of polyimide vias has been accomplished by use of a positive photoresist developer[57] and a mixed solution of hydrazine and ethylene diamine.[58,59] Dry etching of polyimide vias in ICs is generally accomplished by use of an O_2 plasma.[24,60] Although via holes with straight walls provide highest resolution, tapering of vias with a certain angle is required for step coverage, i.e., to ensure uninterrupted metal coverage. Sloped via holes with a dimension of 2 × 2 μm have been obtained.[58,59] Aluminum and its alloy are the most prevalent contact and interconnect metals.[61] During the etching of vias, the surface of the underlying metal can be contaminated that increases the contact resistance. Sputter cleaning has been found to be effective in reducing the via hole resistance to acceptable levels.[58]

Two main issues related to the use of polyimides as intermetal dielectrics are water absorption and polarization. It has been discussed previously (Section II.D) that water absorption has a significant effect on the electrical properties of polyimides. To minimize the water absorption, polyimide thin films must be adequately dehydrated and imidized. To prevent water absorption after bake, thin passivation films of silicon nitride or silicon oxide have been deposited over polyimides as moisture barriers.[61] Of the two, silicon nitride appeared to be more effective than silicon oxides.[62]

Polyimides are long-chain organic polymers which contain polarizable components such as carbonyl groups.[63] Under the influence of an electric field, the dipoles in the polymers could preferentially be aligned, thus inducing an opposite charge at the interface.[64] The charge effects can cause inversion of underlying silicon and consequent undesired communication between doped areas.[65] Effects of polyimide polarization on a typical bipolar structure are shown in Figure 6a, which shows parasitic channel formation due to polyimide polarization.[61] The degree of polarizability in polyimides appears to be related to the chemical structure, with the least hydroscopic polyimide the least polarizable.[63]

Polarization has been a major reliability concern for polyimide applications. The problem, however, has been addressed by eliminating structure within a common silicon island (to prevent inversion), limiting the use of polyimide to low-voltage circuits, or by adding a silicon dioxide film as an underlayer of the polyimide which increases the parasitic device threshold (Figure 6b).[61]

B. Electronic Packaging

Polyimides are used in a variety of applications related to the packaging and interconnection of integrated circuits. Polyimide/glass composites for printed wiring boards are one of the most important alternatives to the standard epoxy/glass boards[66] the main advantage of polyimide/glass is its high thermal stability, which permits the use of high-temperature soldering processes in assembly operations. Polyimide adhesives, sometimes filled with thermally or electrically conductive particles such as silver or ceramic, are also becoming a widely used alternative to epoxies for die attachment, because of their good thermal and chemical stability and their higher degree of purity (especially lower chlorine content).[67]

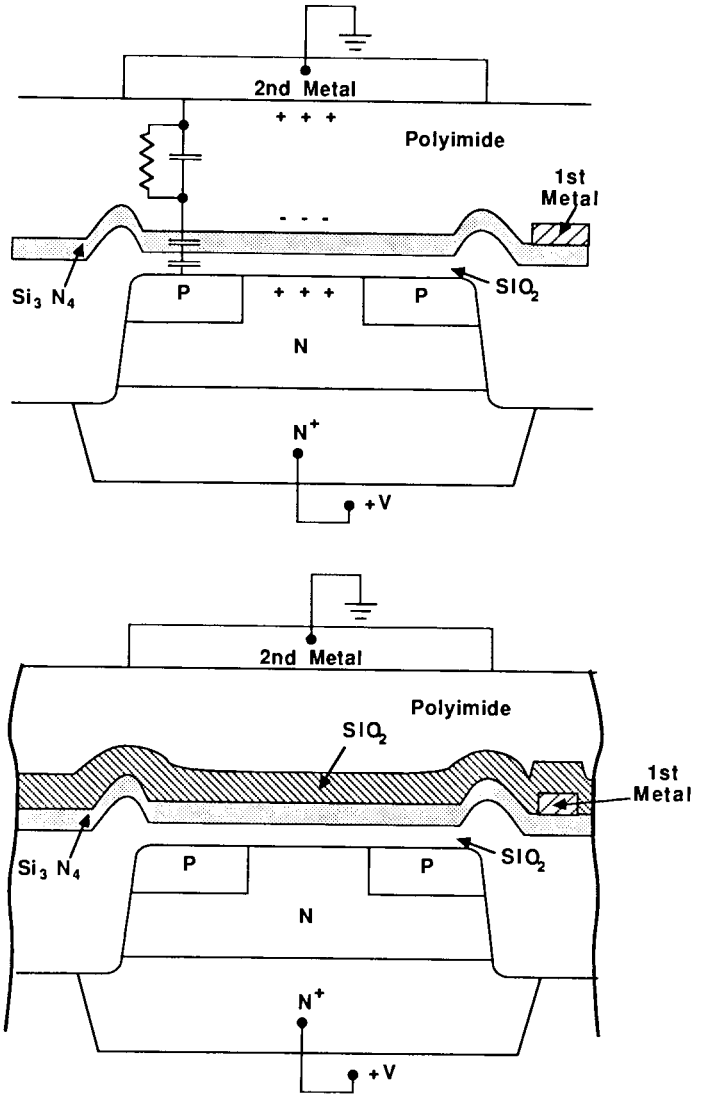

FIGURE 6. (a) Effects of polyimide polarization on typical bipolar structure; (b) one possible solution to the polarization problem.[61]

Free-standing polyimide films (e.g., Kapton) are used as flexible substrates for multichip circuits[68] and for tape-automated-bonding (TAB) leadframes.[69] TAB is becoming a widely used alternative to wire bonding because it can achieve higher bonding density with higher throughput and greater bond strengths than wire bonding, and because it permits ICs to be tested in the leadframe before die attachment.

Finally, polyimides are being used as an interlayer dielectric for multiple-layer interconnections in high-performance IC packages. Because of the current importance of this latter application, the rest of this section will be devoted to a discussion of the use of polyimide as an interlayer dielectric for high-density IC interconnections.

1. High-Performance Packaging Requirements

The high circuit densities and fast switching speeds of advanced very large-scale integration (VLSI), and GaAs ICs have created a need for new technologies to package and interconnect

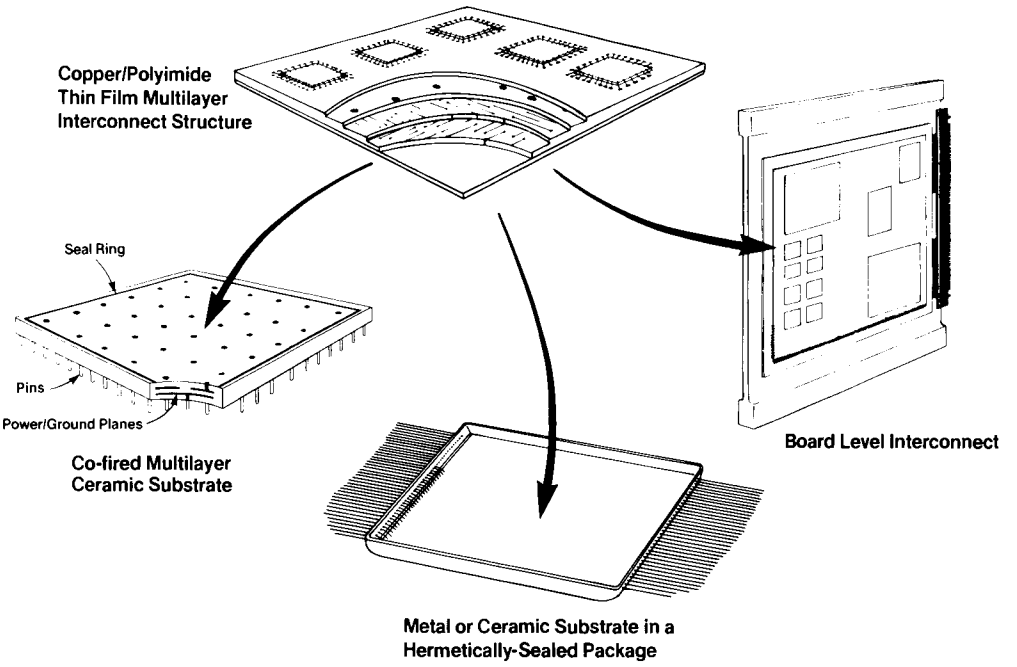

FIGURE 7. Different IC packaging schemes incorporating copper/polyimide thin-film multilayer interconnections.[74]

these devices. For many high-performance systems, multiple-chip packaging approaches are being used to achieve greater chip density, reduce the number of external interconnections, and reduce the interconnect length and thereby reduce the delay time and power consumption required to drive the signals between chips. The high interconnect density of multichip packaging requires processes that can define high-resolution conductor patterns in multiple layers on relatively large substrates. A high-density interconnect technology that is being actively developed throughout the electronics, computer, and IC packaging industries is based on the use of thin-film IC-like processes to pattern multiple layers of a thin-film conductor such as gold, aluminum, or copper and a polymer dielectric, primarily polyimides.[4,24,30-32,45,49,70-75]

2. Thin-Film Multilayer Packaging Approach

The thin-film multilayer (TFML) interconnect structures can be fabricated on a variety of substrates and incorporated into a variety of package designs. The packaging structures shown in Figure 7 have been proposed by Honeywell[4,74] and are representative of many of the packaging approaches being implemented in the industry. In the first approach, the TFML interconnections are patterned on a multilayer cofired ceramic substrate, which may contain additional structures such as internal metal layers for power and ground distribution, a grid array of pins for connecting the package to a printed wiring board (PWB), metallized strips to provide thermal contact to the PWB, and a metallized ring around the perimeter for attachment of a seal ring and lid for hermetic sealing. In the second approach in Figure 7, the TFML interconnections are patterned on a blank metal or ceramic substrate which is then mounted into a hermetically sealable package such as a metal flatpack with perimeter leads. In the third approach, TFML structures are fabricated on larger substrates to create high-density board-level interconnections between single or multichip packages.

In all of these packaging approaches, the high-density interconnections are patterned in TFML structures of copper (or other high-conductivity) conductor and polyimide dielectric.

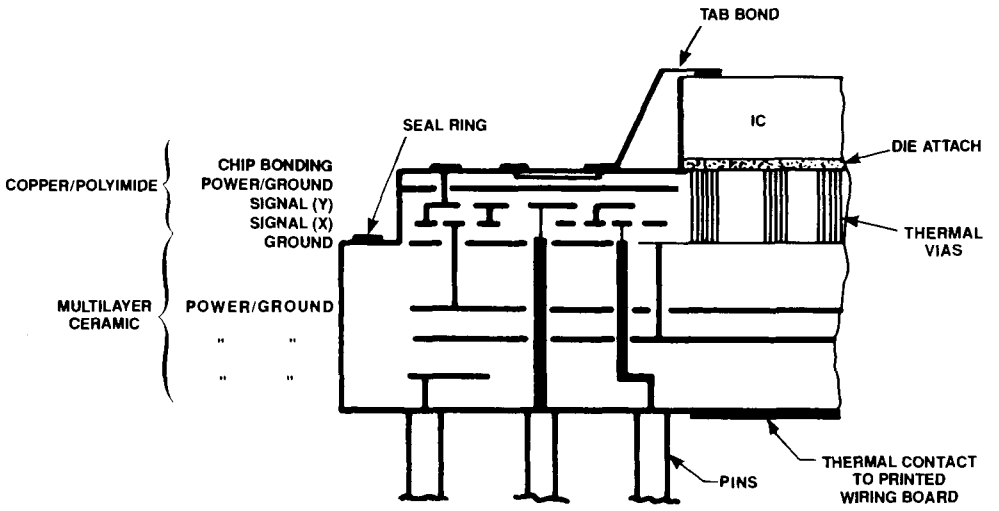

FIGURE 8. Cross section of copper/polyimide thin-film multilayer interconnections on a pinned multilayer ceramic substrate.[74]

Table 2
TYPICAL TFML INTERCONNECT CHARACTERISTICS

Signal Line Dimensions

Conductor thickness	5 μm
Line width	25 μm (0.001 in.)
Line pitch	75—125 μm (0.005 in)
Dielectric thickness	15—25 μm
Via diameter	25—35 μm

Electrical Characteristics (Offset Stripline)

Propagation delay (lossless)	62 ps/cm
Characteristic impedance	50 Ω
Resistance	1.26 Ω/cm
Capacitance	1.2 pf/cm
Inductance	3.1 nH/cm
Max backward crosstalk	−40 dB

Figure 8 shows a typical cross section consisting of two layers of signal lines sandwiched between ground or voltage planes, and a top metal layer for chip attachment and bonding. This places the signal lines in an offset stripline configuration with controlled characteristic impedance. Table 2 shows typical dimensions and electrical characteristics of these offset striplines. For typical 50 Ω signal lines, the conductor lines are 25 μm wide and 5 μm thick and the dielectric thickness is 15 μm between signal layers and 21 μm between signal lines and reference planes. The high conductivity of copper results in a low resistance of 1.3 Ω/cm for the narrow cross-section conductor lines, while the low dielectric constant of polyimide results in a low capacitance of 1.2 pf/cm for the 50-Ω lines. The pitch between signal lines is typically 75 to 125 μm; the minimum pitch will be dictated by yield constraints and permissible cross-talk.

The chips are attached to pads on the surface of the polyimide and electrically bonded to the TFML interconnections by wire bonding (Al or Au wire) or by TAB with a solder bond.

An array of copper vias may be used to conduct heat through the polyimide layers to the substrate.

3. Advantages and Applications of TFML Interconnections

TFML interconnections offer a number of inherent advantages over other interconnect technologies. Table 3 compares the material properties, geometries, and electrical properties of TFML interconnects with the two primary competing technologies: cofired ceramic and multilayer thick film. First, thin-film patterning processes such as photolithography and dry etching can define higher resolution and higher aspect ratio features in the conductor and dielectric materials than the screen printing and hole-punching processes used for cofired ceramic or thick film. The TFML geometries result in high interconnect density and low interconnect resistance and capacitance. Second, thin-film metal deposition processes such as sputtering permit the use of high conductivity metals (Cu, Al) and can achieve nearly bulk resistivity in thin films, as compared to the lower conductivity W and Mo pastes used in cofired ceramic technology or the Cu and Au pastes used for thick film. Third, from a manufacturing standpoint, TFML technology offers cost advantages over thick film and cofired ceramic technology by replacing labor-intensive screen printing processes with automated semiconductor processes, and by replacing hard-tooled punches or screens with fast-turnaround photolithographic masks.

The TFML technology is also highly flexible in that it can be applied to a wide range of substrates, interconnect geometries, and performance requirements. It is being widely developed for multichip packaging of VLSI, VHSIC, and GaAs ICs,[4,24,70] and for high-density hybrid circuits employing lower performance ICs.[31,75] The TFML technology also offers a number of advantages for board-level interconnections between surface-mounted single chip packages or bare chips. Finally, the TFML materials system and process technology can be extended to even finer geometries required for wafer scale integration,[73] or to high-density optical interconnections using thin-film waveguides.[76,77]

4. Favorable Properties of Polyimides

Polyimides possess a combination of physical properties and process characteristics that make them uniquely suited as a dielectric material for TFML interconnections. As discussed in Section II, polyimides can be obtained as very pure solutions of poly(amic acid) or soluble polyimide in a polar solvent such as NMP. These solutions can be deposited by a variety of techniques (discussed in Section III.A) to produce a wide range of film thicknesses (1 to 100 μm). The ability of polyimide to flow before curing enhances the smoothing effect or planarization of underlying conductor topography. After complete imidization at 350 to 450°C, polyimide has high thermal stability (decomposition temperature >450°C) and is chemically inert and insoluble, which prevents degradation during subsequent processing steps involving high temperature (e.g., metal deposition, soldering) or strong solvents and acids (e.g., photolithography, wet etching). Polyimides have relatively high tensile strength (100 to 200 MPa) and a large elongation at break (10 to 25%), making the films resistant to cracking despite the large stresses created by the large thermal expansion mismatch between polyimide and most substrates.

Finally, the dielectric properties of polyimide, particularly its low dielectric constant (ϵ_r), are favorable for high-speed signal propagation. Polyimide has a low ϵ_r of 3.5 (typically), compared to cofired ceramic dielectrics with ϵ_r = 9 to 10 or thick film glass/ceramic dielectrics with ϵ_r = 6 to 9, as shown in Table 3. The low ϵ_r results in low signal propagation delay, since the maximum propagation velocity is determined by the speed of light in the dielectric medium surrounding the signal lines, given by $c/(\epsilon_r)^{1/2}$, where c is the speed of light in vacuum. The low ϵ_r also results in low interconnect capacitance, which reduces RC charging effects and thus minimizes the degradation in signal risetime and the power required

Table 3
COMPARISON OF MULTICHIP PACKAGING TECHNOLOGIES

	Cofired ceramic[b]	Thick-film multilayer[b]	Thin-film multilayer[b]
Conductor material[a]	W (Mo)	Cu (Au)	Cu (Au, Al)
Sheet resistance (Ω/□)	0.01	0.003	0.0035
Thickness (μm)	15	15	5
Line width (μm)	100	100—150	25 → 10
Pitch (w/vias) (μm)	750 → 250	250	125 → 50
Max no. of layers	7 → 30+	5 → 10	5 → ?
Dielectric material	Al_2O_3	Glass/ceramic	Polyimide
Dielectric constant	9.5	6.5—9	3.5
Thickness/layer (μm)	250—500	35—65	10—25
Via diameter (μm)	200 → 100	200	25
Propagation delay (ps/cm)	102	90	62
Min stripline capacitance (pf/cm)	2.0	4.3	1.2
Line resistance (Ω/cm)	1.0	0.3	1.35

[a] Alternative conductor materials are in parentheses; properties are given for primary conductor materials.

[b] Geometries are given for current standard technology; an arrow (→) indicates demonstrated advanced technology.

to drive signals. Finally, a low ϵ_r produces low levels of cross-talk between adjacent conductor lines. Polyimide also has a high breakdown voltage ($V_B \geq 10^6$ V/cm) and a low dissipation factor (tan δ <0.01), resulting in low dielectric losses.

5. Processing of TFML Interconnects

The TFML interconnect geometry presents a number of unique challenges for thin-film processing. The relatively thick conductor and dielectric films, which are required for low interconnect resistance and capacitance, require long processing times and can create significant strain energy due to the thermal expansion mismatch between polyimide and substrates. The high-aspect ratios of conductor lines and polyimide vias require anisotropic patterning processes, and produce large topographies that must be planarized. A wide variety of substrate materials and sizes may be used to support the TFML structures, and each substrate presents unique problems in terms of surface roughness, flatness, mechanical and thermal stability, and compatibility with TFML process equipment and reactants. Finally, the large substrate size places severe demands on process yield; very low defect densities and/or in-process test and repair techniques are required in order to achieve acceptable process yields.

A variety of processes have been used to fabricate TFML structures, including both subtractive[4,24,45] and additive[31,49,73] approaches. The subtractive process sequence shown in Figure 9 has been used at Honeywell for a variety of TFML applications, and is described briefly below as an example.

The conductor layers, consisting of 5 μm of Cu sandwiched between thin (20 to 100 nm) Cr or TiW adhesion layers are deposited by DC and RF sputtering, respectively. Relatively thick (2 to 6 μm) photoresist layers are deposited and patterned, using proximity alignment to accommodate the large warpage of thin substrates and to prevent defects caused by contact between the mask and substrate. The conductor materials are then etched using wet processes for aspect ratios less than 0.5, or ion beam milling[78] for higher aspect ratios.

Poly(amic acid) solutions are deposited by either spinning or spraying (as described in Section III.A) and cured by heating at a controlled rate to a final temperature of 350 to

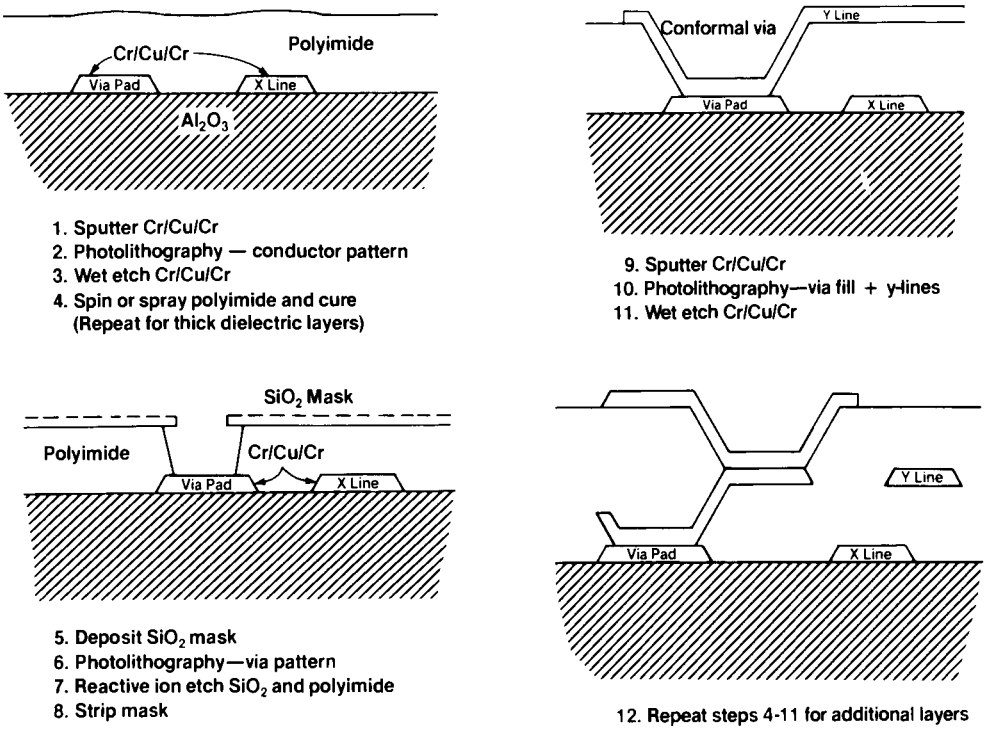

FIGURE 9. Process sequence for patterning copper/polyimide thin-film multilayer interconnect structures.[4]

420°C. Multiple coats are usually deposited to achieve the thick (15 to 40 μm) planarized dielectric layers required for high impedance interconnects. The planarized conductor lines shown in Figure 1 were patterned by wet etching of sputtered copper and planarized with multiple spray coatings of polyimide.

Features such as vias for connection between metal layers are patterned in polyimide by RIE, as described in Section III.D and shown in Figure 4. The vias are metallized by sputtering a conformal metal layer and patterning both the vias and next conductor layer with a single photolithography and etching step. The sequence of deposition and patterning processes is repeated for additional metal layers, using staggered vias to connect through more than one dielectric layer.

A number of other processes have been reported for depositing and patterning the thin-film conductor and dielectric layers. Alternative processes for depositing and patterning polyimide were discussed in Section III, and most of these have beenused for TFML processing. Alternative processes for depositing conductor materials include plating (both electrolytic and electroless), evaporation, cathodic arc deposition, and plasma-enhanced CVD. In addition to the processes discussed above, the conductor layers may be subtractively patterned by RIE, reactive ion-beam milling, or laser-assisted etching.[79]

Several investigators have used additive approaches such as selective electroplating[31,49] or lift-off[73] for defining the conductor patterns. These additive approaches have the important advantage of permitting vertical stacking of vias through several dielectric layers; however, they require additional processing steps because the vias and conductor patterns are defined in separate photolithography steps. A final, very promising additive process is the direct writing of conductor lines using laser-assisted CVD.[80,81] This process is in the early stages of development, but, like laser ablation of polyimide, it offers significant cost reduction and yield enhancement by eliminating masks and photolithography processes from the TFML patterning processes.

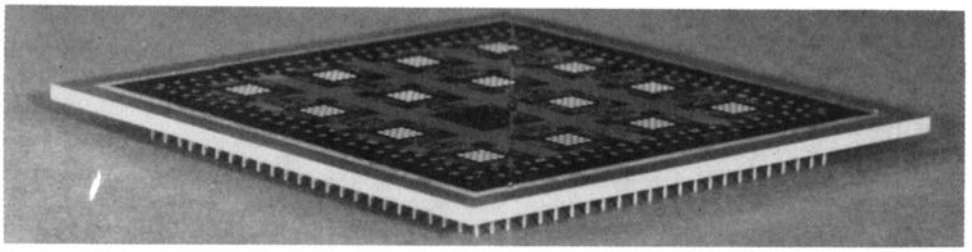

FIGURE 10. Multichip test vehicle for submicron bipolar ICs, containing five metal layers of copper/polyimide interconnections on a 3 × 3″ pinned cofired ceramic substrate.[74]

6. Demonstrations of TFML Packaging

The TFML interconnect technology described above has been under development at a variety of companies for a variety of applications, and several demonstrations of the technology have been described recently in the literature. A number of test vehicles have been developed at Honeywell to evaluate the performance of TFML interconnections. These include: (1) multichip ring oscillator circuits to determine the electrical characteristics of TFML interconnections;[24,82] (2) a thermal test vehicle to test alternative methods of conducting heat through TFML layers;[83] and (3) a multichip test vehicle to test submicron bipolar ICs.[74,83] The latter test vehicle, patterned on a 3 × 3″ pinned cofired ceramic substrate with five metal layers of TFML interconnections, is shown in Figure 10.

Functional packages have also been fabricated at Honeywell to demonstrate the feasibility of TFML technology in various products. Examples include: (1) a microprocessor module for computer applications, containing nine bipolar gate array ICs on an 80-mm square substrate;[4] (2) an 18-chip hybid module for image processing applications, with a 2.25-in.^{2} TFML substrate mounted in a hermetically sealable flatpack;[4,75] and (3) a single-chip package for a digital GaAs IC with 200 I/Os designed to operate at data rates of up to 3 Gbit/s. The latter package contains thin-film TaN resistors patterned very close to the chip to permit the termination of high-speed signal lines and thus prevents signal reflections and ringing.

Other companies that have described TFML-type packaging in the literature include: (1) Mitsubishi, where TFML interconnections are being used in hybrid multichip circuits to increase the interconnect density and reduce costs over the current thick-film technology; (2) Brown, Boverie, and Cie, which has used a two-layer Cu/polyimide interconnect approach for digital cipher electronics in a mobile radio-communication system;[72] and (3) AT & T, which has developed a high-density packaging technology based on flip-chip-bonded ICs interconnected in TFML Cu/polyimide structures on a silicon substrate.[71] In addition, the process technology for TFML interconnect structures has been described in excellent papers from NTT[45,49] and GE.[73]

The most advanced application of TFML technology has been reported by NEC for their SX-1 and SX-2 supercomputers, which are currently in production.[70] The logic module for the computer contains 36 1000-gate current mode logic (CML) chips packaged in individual ceramic carriers that are soldered face down to the multichip substrate through an array of metallic bumps. The 100-mm^2 cofired ceramic substrate contains internal metal planes for power and ground distribution and a pin grid array for connection to a printed wiring board. The high-density interconnections (25-μm lines on a 75-μm pitch) are patterned in five metal/polyimide layers on the ceramic substrate. The multichip module permits the system to achieve a performance of 1300 megaflops (million floating point operations per second) with a machine cycle time of 6 ns.

C. Passivation and Protection

Polyimides have been increasingly used as passivation materials for protecting ICs and device circuits. Traditionally, SiO_2 and Si_3N_4 have been the most widely used passivation materials. These inorganic materials, however, require higher processing temperatures and often cannot provide adequate step coverage. The advantages of using polyimides as passivation materials are spin coatability, patternability, lower processing temperature, good chemical resistance and thermal stability, and planarizability (i.e., providing good step coverage).

The passivation layer must provide protection from physical and mechanical damage, act as a barrier to water molecules and ionic contaminants, and must not modify the performance of ICs and device circuits that it protects. It has been noted that a thin-film overcoat can induce significant mechanical stress that affects the functional characteristics of the device circuits, e.g., the threshold voltage of a metal oxide silicon (MOS) transistor.[3]

Polyimides have been used as α particle barriers to prevent soft errors of memory devices (e.g., RAMs) caused by α particles emitted by a trace amount of naturally occurring thorium and uranium isotopes in packaging materials.[7,84] A layer of polyimide overcoat with a thickness ≥ 75 μm stops most α particles emitted from the packaging materials. The high thermal stability of the polyimides provides adequate thermal resistance to the process temperature required for ceramic or glass sealing.

A polyimide passivation reliability study has been reported.[64] In this study, a polyimide was applied to an n-channel FET (field-effect transistor), and the effect of incompletely cured polyimides on the device's functional reliability was studied. The fully cured polyimide is an effective barrier to sodium and residual ionic contamination, but incompletely cured polyimide behaves as ionic contamination. The behavior of the incompletely cured polyimide was interpreted as due to alignment of dipoles (associated with the incompletely cured polyimides) in the preferential E-field direction that induces charge inversion at the silicon surface, and thus the polyimide behaves as if it were an ionic species.[64]

Polyimides have been used to passivate thin-film microwave hybrid circuits.[85] Thin films (5 μm) of PI-2550 were spin coated on the circuits, partially cured, patterned with a positive photoresist to open the bonding pad, and fully cured. The developer for the positive photoresist, an alkaline solution, was used to etch the polyimide in patterning the bonding pad. Since the etching was an isotropic process that resulted in a severe undercutting, a proper sizing of the photomask was required. Environmental testing showed that the polyimide met the requirements as the passivation material. The adhesion and step coverage were excellent, and it provided adequate protection for resistor films in a high-humidity environment.

A similar passivation study for thin-film resistors has also been reported.[86] The polyimide used in this study was PIQ, and a negative photoresist was used to pattern the partially cured polyimide. Both adhesion testing and environmental testing substantiated the adequate performance of polyimide passivation.

Electromigration has been one of the principal failure modes in ICs. Electromigration is a mass transport occurring in metal thin-film conductors due to the momentum exchange between conduction electrons and the metal atoms as an electric current is passed through the conductor.[87] Electromigration is typically characterized by resistance changes and open circuit failures, and is often due to void formation in the conductor. It has been found that a passivation layer on top of the metallization can enhance the reliability of the conductor.[88] Although CVD SiO_2 has been the most commonly used passivant for ICs, recent studies indicate that polyimide passivation can significantly retard electromigration and thus enhance the reliability of the underlying conductors.[87]

Although both positive and negative photoresists have been used to pattern polyimide thin films for passivation, the use of conventional photoresists requires many processing steps and considerable process control. Recent development of photoimageable polyimides is expected to accelerate the use of polyimides for passivation.

D. Other Applications for Polyimides in Microelectronics

Because of their excellent thermal and chemical stability and their processibility, polyimides have found a number of other applications in microelectronics. An important application of polyimides is their use as a temporary masking or planarizing layer to aid in the fabrication of microelectronic structures. For example, polyimides are frequently used as the bottom planarizing layer in trilevel photoresist processes. In this approach a thin metal or dielectric layer is deposited on the polyimide and patterned using a thin, high-resolution resist (such as an e-beam resist), and the high-aspect-ratio pattern is then transferred into the thick underlying polyimide layer, usually by RIE. (This process is discussed in more detail in Chapter 1, Section III.F). Polyimides are an ideal planarizing material because they can be deposited over a wide range of thicknesses, they have good planarizing properties, and they are not degraded by high temperatures or chemicals involved in subsequent processing steps.

The high-aspect-ratio patterns formed in the polyimide can serve as masks for dry etching processes in which a relatively thick masking layer is required, or they can serve as a mask for ion implantation[89,90] or ion-beam lithography.[91] In these applications polyimide has the advantage of good thermal and dimensional stability compared to conventional photoresists. The trilevel resist structures can also be used as a lift-off stencil for patterning fine metal lines. In this process, the polyimide can be fully stripped, usually with an O_2 plasma, to leave behind the metal pattern,[92] or it can remain in the area between metal lines to planarize the structure.[93]

Polyimides have been used as a flexible substrate for X-ray masks.[94] The X-ray absorbing material (e.g., gold) is patterned on a polyimide film that is coated onto a silicon wafer; the backside of the wafer is then etched away to leave a thin polyimide diaphram with the X-ray absorbing pattern. The good dimensional stability of polyimide and its transparency to X-rays makes it well suited to this application. Another unique application of polyimides is in the fabrication of micro-Fresnel zone plates, in which high-aspect-ratio patterns in polyimide serve as a master mold for the replication of zone plates.[95]

Finally, some specialized electronic products also employ polyimide as a dielectric material. Several researchers have reported the use of polyimides as planarizing dielectric layers in densely wound coils for thin-film magnetic recording heads.[96,97] Polyimide thin films have also been used as the dielectric sensing element in a capacitance humidity sensor that is IC compatible.[98]

V. CONCLUSIONS AND FUTURE OUTLOOK

Most of the polyimide applications discussed above have been developed over the last 5 to 10 years and are just now being introduced into production. The performance advantages offered by polyimides include: (1) high-density patterning, due to the planarization and processibility of polyimides; (2) high-speed signal propagation, due to the low dielectric constant of polyimide; and (3) high reliability, due to the excellent thermal, chemical, and mechanical stability of polyimide. These advantages will become increasingly important as speed, density, and reliability requirements of ICs and other microelectronic devices continue to grow.

As the applications of polyimide broaden, new polyimide chemistries will also be developed. In the last 3 to 4 years there has been a tremendous growth in the number of new polyimide formulations available from a growing number of manufacturers. Preimidized polyimides are gaining rapid acceptance because of their longer shelf life, lower cure temperatures, and, in many cases, lower moisture absorption. Photosensitive polyimides are perhaps the most important development in polyimide chemistry because of their ease of patterning.

Polyimide properties that can benefit most from further improvement and that are being actively developed include: (1) lower moisture absorption, (2) a lower dielectric constant, (3) a lower thermal expansion coefficient to match silicon or ceramic packaging substrates, (4) improved fracture strength and failure strain, and (5) better self-adhesion to silicon and other substrate materials. A number of new polyimide formulations have already been introduced with one or more of these improvements. A notable example is a polyimide with a very low coefficient of thermal expansion (CTE = 3×10^{-6}/°C), introduced recently by Hatachi.[99] Although low CTE polymers usually have a high modulus and low tensile strength, this polyimide consists of low-CTE rigid-rod domains in a low modulus matrix, and it has a high tensile strength, comparable to that of conventional polyimides (Structure IV in Section II.A).

As polyimide chemistries are improved, alternative high-temperature polymers with similar processibility and dielectric properties are being developed and may replace polyimides in some applications. An example is the polybenzocyclobutenes recently introduced by Dow Chemical.[100]

In addition to advances in polyimide chemistry, the material systems and processes used in multilayer interconnections for ICs and electronic packages (as discussed in Sections IV.A and IV.B) will also be improved. Significant research effort is now being devoted to the interfaces between polyimide and various metals, ceramics, and polyimide itself, from the standpoint of adhesion, interface chemistry, and metal migration or solvent penetration into polyimide. Improved patterning processes for multilayer interconnect structures are also being actively developed. The most significant advancements are the use of additive processes such as lift-off for higher resolution, and the development of direct-write laser-assisted processes for patterning polyimide and for writing conductor lines.

REFERENCES

1. **Cassidy, P. E. and Fawcett, N. C.,** Polyimides, in *Kirk-Othmer Encyclopedia of Chemical Technology,* Vol. 18, Grayson, M. and Eckroth, D., Eds., John Wiley & Sons, New York, 1982, 704.
2. **Sroog, C. E.,** Polyimides, *J. Polym. Sci. Macromol. Rev.,* 11, 161, 1976.
3. **Wilson, A. M.,** Polyimide insulators for multilevel interconnections, *Thin Solid Films,* 83, 145, 1981.
4. **Jensen, R. J.,** Polyimides as interlayer dielectrics for high-performance interconnections of integrated circuits, in *Polymers for High Technology: Electronics and Photonics,* Bowden, M. J. and Turner, S. R., Eds., ACS Symp. Ser. 346, American Chemical Society, Washington, D.C., 1987, chap. 40.
5. **Rohde, O., Riediker, M., Shaffner, A., and Bateman, J.,** Recent advances in photoimagable polyimides, *SPIE Adv. Resist. Technol. Process. II,* 539, 175, 1985.
6. **Lai, J. H., Douglas, R. B., and Donohoe, K.,** Characterization and processing of polyimide thin films for microelectronics application, *Ind. Eng. Chem. Prod. Res. Dev.* 25(1), 38, 1986.
7. **Lee, Y. K. and Craig, J. D.,** Polyimide coating for microelectronic application, in *Polymeric Materials for Electronic Applications,* ACS Symp. Ser. 184, American Chemical Society, Washington, D.C., 1982.
8. **Rothman, L. B.,** Properties of thin polyimide films, *J. Electrochem. Soc.,* 127, 2216, 1980.
9. **Day, D.R. and Senturia, S. E.,** In-situ monitoring of polyamic acid imidization with microdielectrometry, in *Polyimides: Synthesis, Characterization and Application,* Vol. 1, Mittal, K. L., Ed., Plenum Press, New York, 1984, 249.
10. **Cotts, P. M.,** Solution characterization of polyamic acids and polyimides, *Org. Coat. Appl. Polym. Sci. Proc.,* 18, 278, 1983.
11. **Saiki, A., Harada, S., Okubo, T., Mukai, K., and Kimura, T.,** A new transistor with two-level metal electrodes, *J. Electrochem.Soc.,* 124(10), 1619, 1977.
12. **Davis, G. C., Heath, B. A., and Gildenblat, R.,** Polyimide siloxane: properties and characterization for thin film electronic applications, in *Polyimides: Synthesis, Characterization and Application,* Vol. 2, Mittal, K. L., Ed., Plenum Press, New York, 1984, 847.
13. **Berger, A.,** Modified polyimides by silicone block incorporation, in *Polyimides: Synthesis, Characterization and Application,* Vol. 1, Mittal, K. L., Ed., Plenum Press, New York, 1984, 67.

14. **Rubner, R., Ahne, H., Kuhn, E., and Kolodziej, G.,** A photopolymer — the direct way to polyimide patterns, *Photogr. Sci. Eng.*, 23(5), 303, 1979.
15. **Merrem, H. J., Klug, R., and Hartner, H.,** New developments in photosensitive polyimides, in *Polyimides: Synthesis Characterization and Application,* Mittal, K. L., Ed., Plenum Press, New York, 1984, 919.
16. **Bower, G. M. and Frost, L. W.,** Aromatic polyimide, *J. Polym. Sci.*, A-1, 3135, 1963.
17. **Endrey, A. L.,** U.S. Patent 3,242,136, 1966.
18. **Wallach, M. L.,** Structure-property relation of polyimide films, *J. Polym. Sci.*, A-2, 5953, 1967.
19. "PIQ" Heat Resistance Fine Polymers for Semiconductor Devices, Data Chemical Sheet No. Y-100, Hitachi Chemicals Co., Tokyo,1981.
20. **Fryd, M.,** Structure-Tg relationship in polyimides, in *Polyimides: Synthesis, Characterization and Application,* Vol. 1, Mittal, K. L., Ed., Plenum Press, New York, 1984, 377.
21. **Bessonov, M. I. and Kuznetsov, N. P.,** Softening and melting temperatures of aromatic polyimides, in *Polyimides: Synthesis, Characterization and Application,* Vol. 1, Mittal, K. L., Ed., Plenum Press, New York, 1984, 385.
22. **Wallach, M. L.,** Polyimide solution properties, *J. Polym. Sci.*, A-2(7), 1995, 1969.
23. **Kurita, K. and Williams, R. L.,** Heat resistant polymers containing bipyridyl units. I. Polyimides, *J. Polym. Sci.*, 11, 3125, 1973.
24. **Jensen, R. J., Cummings, J. P., and Vora, H.,** Copper/polyimide materials system for high performance packaging, *IEEE Trans. Components Hybrids Manuf. Technol.*, CHMT-7(4), 384, 1984.
25. **Saiki, A. and Harada, S.,** New coupling method for polyimide adhesion to LSI surface, *J. Electrochem. Soc.*, 129(10), 2278, 1982.
26. **Allen, M. G., Mehregany, M., Howe, R. T., and Senturia, S. D.,** Microfabricated structures for the in situ measurements of residual stress, Young's modulus, and ultimate strain of thin films, *Appl. Phys. Lett.*, 51(4), 241, 1987.
27. **Denton, D. D., Ray, D. R., Priore, D. F., Senturia, S. D., Anolick, E. S., and Scheider, D.,** Moisture diffusion in polyimide films in integrated circuits, *J. Electron. Mater.*, 14, 119, 1985.
28. **Jenekhe, S. A.,** Polymer processing to thin films for microelectronic applications, in *Polymers for High Technology; Electronics and Photonics,* Bowden, M. J. and Turner, R. S., Eds., ACS Symp. Ser. 346, American Chemical Society, Washington, D.C., 1987, chap. 22.
29. **Givens, F. L. and Daughton, W. J.,** On the uniformity of thin films: a new technique applied to polyimides, *J. Electrochem. Soc.*, 126, 269, 1979.
30. **Nguyen, P. H. and Russo, F. R.,** New polyimide system for multilayering, *Proc. Int. Symp. Microelectron.*, p. 702, 1986.
31. **Takasago, H., Takada, M., Adachi, K., Endo, A., Yamada, K., Makita, T., Gofuku, E., and Onishi, Y.,** Advanced copper/polyimide hybrid technology, *Proc. Electron. Components Conf.*, p. 481, 1986.
32. **Nguyen, P. H., Falletta, C. E., and Fusso, F. R.,** Multilayering with polyimide dielectric and metallo-organic conductors, *Proc. Int. Symp. Microelectron.*, p. 258, 1985.
33. **Salem, J. R., Sequeda, F. O., Duran, J., Lee, W. Y., and Yang, R. M.,** Solventless polyimide films by vapor deposition, *J. Vac. Sci. Technol.*, A4, 369, 1986.
34. **Narechania, R. G., Bruce, J. A., and Fridmann, S. A.,** Polyimide adhesion: mechanical and surface analytical characterization, *J. Electrochem. Soc.*, 132, 2700, 1985.
35. **Jensen, R. J., Douglas, R. B., Smeby, J. M., and Moravec, T. J.,** Characteristics of polyimide material for use in hermetic packaging, *Proc. VHSIC Packag. Conf.*, p. 193, 1987.
36. **Pleuddemann, E. P.,** *Silane Coupling Agents,* Plenum Press, New York, 1982, chap. 5.
37. **White, L. K.,** Planarization phenomena in multilayer resist processing, *J. Vac. Sci. Technol.*, B1, 1235, 1983.
38. **Day, D. R., Ridley, D., Mario, J., and Senturia, S. D.,** Polyimide planarization in integrated circuits, in *Polyimides: Synthesis, Characterization and Applications,* Mittal, K. L., Ed., Plenum Press, New York, 1984, 767.
39. **Mukai, K., Saiki, A., Yamanaka, K., Harada, S., and Shoji, S.,** Planar multilevel interconnection technology employing a polyimide, *IEEE J. Solid State Circuits,* SC-13, 462, 1978.
40. **Harada, Y., Matsumoto, F., and Nakakado, T.,** A novel polyimide film preparation and its preferential-like chemical etching techniques for GaAs devices, *J. Electrochem. Soc.*, 130, 129, 1983.
41. **Turban, G. and Rapeaux, M.,** Dry etching of polyimide in O_2-CF_4 and O_2-SF_6 plasmas, *J. Electrochem. Soc.*, 130, 2231, 1983.
42. **Egitto, F. D., Emmi, F., and Horwath, R. S.,** Plasma etching of organic materials. I. Polyimide in O_2-CF_4, *J. Vac. Sci. Technol.*, B3, 893, 1985.
43. **Gokan, H., Itoh, M., and Esho, S.,** Oxygen ion beam etching for pattern transfer, *J. Vac. Sci. Technol.*, B2, 34, 1984.
44. **Sun, C. P.,** Polyimide etch profile control by plasma processing, extended abstr., Electrochemical Society Fall Meet., Vol. 87-2, Electrochemical Society, Pennington, NJ, 1987, 674.

45. **Tsunetsugu, H., Takagi, A., and Moriya, K.,** Multilayer interconnections using polyimide dielectrics and aluminum conductors, *Int. J. Hybrid Microelectron.*, 8, 21, 1985.
46. **Shiiki, K., Yuitoo, I., and Shiroishi, Y.,** Fabrication of coils with high aspect ratios for thin-film magnetic heads, *J. Vac. Sci. Technol.*, A3, 1996, 1985.
47. **Ting, C. H., Yeh, S., and Liauw, K. L.,** Sloped vias in polyimides by RIE, *Semicond. Int.*, 82, February 1985.
48. **Gobrecht, J. and Rossinelli, M.,** Al_2O_3 spin on glass as highly selective mask for reactive ion etching, extended abstr., Electrochemical Society Fall Meet., Vol. 84-2, Electrochemical Society, Pennington, NJ, 1984, 374.
49. **Moriya, K., Ohsaki, T., and Katsura, K.,** High-density multilayer interconnection with photo-sensitive polyimide dielectric and electroplating conductor, *Proc. Electron. Components Conf.*, p. 82, 1984.
50. **Deutsch, A. S. and Schulz, R.,** A high resolution photosensitive polyimide precursor, *Proc. Int. Electron. Packag. Conf.*, p. 331, 1986.
51. **Endo, A., Takada, M., Adachi, K., Takasago, H., Yada, T., and Onishi, Y.,** Material and processing technologies of polyimide for advanced electronic devices, *J. Electrochem. Soc.*, 134, 2523, 1987.
52. **Perry, P. B., Ray, S. K., and Hodgson, R.,** Optical optimization of line deletion and personalization parameters on polyimide films, *Thin Solid Films*, 85, 111, 1981.
53. **Brannon, J. H., Lankard, J. R., Baise, A. I., Burns, F., and Kaufman, J.,** Excimer laser etching of polyimide, *J. Appl. Phys.*, 58, 2036, 1985.
54. **Yeh, J. T. C.,** Laser ablation of polymers, *J. Vac. Sci. Technol.*, A4, 653, 1986.
55. **Srinivasan, V., Smirtic, M. A., and Babu, S. V.,** Excimer laser etching of polymers, *J. Appl. Phys.*, 59, 3861, 1986.
56. **Braren, B. and Srinivasan, R.,** Optical and photochemical factors which influence etching of polymers by ablative photodecomposition, *J. Vac. Sci. Technol.*, B3, 913, 1985.
57. **Shah, P., Laks, D., and Wilson, A.,** High performance, high density MOS process using polyimide interlevel insulation, *IEDM Abstr.*, 465, 1979.
58. **Nishida, T., Saiki, A., Homma, Y., and Mukai, K.,** Advanced planar metallization with polymer for VLSI, *IEDM Abstr.*, 552, 1982.
59. **Jones, J. I.,** The reactions of hydrazine with polyimides and its utility, *J. Polym. Sci.*, 22, 773, 1969.
60. **Herndon, T. O. and Burke, R. L.,** Inter-metal polyimide insulator for VLSI, *Kodak '79 Interface*, 146, October 1979.
61. **Mastroianni, S. T.,** Multilevel metallization device structures and process options, *Solid State Technol.*, 156, May 1984.
62. **Lin, J. W.,** Use of polyimide as interlayer dielectric for microelectronic packaging and passivation layer for IC chips, Short Course on Polyimides for Microelectronics Applications, University of California, Berkeley, August 1981.
63. **Samuelson, G. and Lytle, S.,** Reliability of polyimide in semiconductor devices, in *Polyimides: Synthesis, Characterization and Application*, Mittal, K. L., Ed., Plenum Press, New York, 1984, 751.
64. *Gregoritsch, A. J.*, Polyimide passivation reliability study, 14th Annual Proc. Rel. Physics, p. 228, 1976.
65. **Brown, G. A.,** Reliability implications of polyimide multilevel insulators, in Int. Reliability Phys. Symp. Proc., Orlando, FL, April 1981, 282.
66. **Mather, J. C.,** A status report on multilayer circuit boards, *Proc. Electron. Components Conf.*, p. 302, 1980.
67. **Bolger, J. C. and Mooney, C. T.,** Die attach in hi-rel P-DIPs: polyimides or low chlorine epoxies?, *Proc. Electron. Components Conf.*, p. 63, 1984.
68. **Ballard, W. V. and Cardashian, V. S.,** Semi-conductor packaging featuring copper polyimide multilayer tape, *Proc. Electron. Components Conf.*, p. 556, 1986.
69. **Scharr, T. A.,** TAB bonding a 200 lead die, *Int. J. Hybrid Microelectron.*, 6, 561, 1983.
70. **Watari, T. and Murano, H.,** Packaging technology for the NEC SX supercomputer, *IEEE Trans. Components Hybrids Manufact. Technol.*, CHMT-8, 462, 1985.
71. **Bartlett, C. J., Segelken, J. M., and Teneketges, N. A.,** Multi-chip packaging design for VLSI-based systems, *Proc. Electron. Components Conf.*, p. 518, 1987.
72. **Ackerman, K.-P., Hug, R., and Berner, G.,** Multilayer thin film technology, *Proc. Int. Soc. Hybrid Microelectron*, p. 519, 1986.
73. **McDonald, J. F., Steckl, A. J., Neugebauer, C. A., Carlson, R. O., and Bergendahl, A. S.,** Multilevel interconnections for wafer scale integration, *J. Vac. Sci. Technol.*, A4, 3127, 1986.
74. **Jensen, R. J.,** Recent advances in thin film multilayer interconnect technology for IC packaging, in *Electronic Packaging Materials Science III*, MRS Symp. Ser. 108, Jaccodine R., Jackson, D. A., and Sundahl, R. C., Eds., Materials Researach Society, Pittsburgh, 1988, 73
75. **Kompelien, D., Moravec, T. J., and DeFlumere, M.,** A new hybrid technology: high density thin film copper/polyimide multilayer system, *Proc. Int. Soc. Hybrid Microelectron.*, p. 749, 1986.
76. **Franke, H. and Crow, J. D.,** Optical waveguiding in polyimide, *SPIE Integrated Circuit Eng. III*, 651, 102, 1986.

77. **Selvaraj, R., McDonald,J. F., Lin, H. T., and Gupta, S.,** Optical interconnections using integrated waveguides in polyimide for wafer scale integration, *Proc. 4th Int. IEEE VLSI Multilevel Interconnect. Conf.*, p. 306, 1987.
78. **Cummings, J. P., Jensen, R. J., Kompelien, D. J., and Moravec, T. J.,** Technology base for high performance packaging, *Proc. Electron. Components Conf.*, p. 465, 1982.
79. **Lankard, J. R.,** Laser assisted etching of chromium and copper, extended abstr., Electrochemical Society Fall Meet., Vol. 87-2, Electrochemical Society, Pennington, NJ, 1987, 611.
80. **Baum, T. H.,** Laser chemical vapor deposition of gold, *J. Electrochem. Soc.*, 134, 2616, 1987.
81. **Gupta, A. and Jagannathan, R.,** Laser writing of copper lines from metalorganic films, *Appl. Phys. Lett.*, 51, 2254, 1987.
82. **Lane, T. A., Belcourt, F. J., and Jensen, R. J.,** Electrical characteristics of copper/polyimide thin film multilayer interconnects, *IEEE Trans. Components Hybrids Manufact. Technol.*, CHMT-10, 577, 1987.
83. **Speerschneider, C. J., Belcourt, F. J., Jensen, R. J., and Smeby, J. M.,** Honeywell's VHSIC phase 2 packaging technology, *Proc. VHSIC Packag. Conf.*, p. 131, 1987.
84. Polyimide film-not liquid-shields rams from alpha particles, *Electron. Des.*, p. 36, November 22, 1980.
85. **Miller, S. C.,** Passivating thin film hybrids with polyimide, *Circuit Manufact.*, 17, 54, 1977.
86. **Scheiman, G. R.,** Characterization of a polyimide passivation on thin film resistor network, *Int. J. Hybrid Microelectron.*, 5, 202, 1982.
87. **Anolick, E. S., Lloyd, J. R., Chiu, G. T., and Korobov, V.,** The effects of polyimide passivation on the electromigration of Al-Cu thin films, in *Polyimides: Synthesis, Characterization and Applications,* Mittal, K. L., Ed., Plenum Press, New York, 1984, 889.
88. **Lloyd, J. R.,** Electromigration in Al-Cu thin films with polyimide passivation, *Thin Solid Films*, 91, 207, 1982.
89. **Hu, E. L., Howard, R. E., Grabbe, P., and Tennant, D. M.,** Ion beam processing using metal on polymer masks, *J. Electrochem. Soc.*, 130, 1171, 1983.
90. **Herndon, T. O., Burke, R. L., and Yasaitis, J. A.,** Polyimide for high resolution ion implantation masking, *Solid State Technol.*, 27(11), 179, 1984.
91. **Economou, N. P., Flanders, D. C., and Donnelly, J. P.,** High resolution ion beam lithography, *J. Vac. Sci. Technol.*, 19, 1172, 1981.
92. **Homma, Y., Nozawa, H., and Harada, S.,** Polyimide liftoff technology for high-density LSI metallization, *IEEE Trans. Electron. Devices,* ED-28, 552, 1981.
93. **Rothman, L. B.,** Process for forming passivated metal interconnection system with a planar surface, *J. Electrochem. Soc.*, 130, 1131, 1983.
94. **Wada, T., Sakurai, S., and Kawabuchi, K.,** Fabrication of polyimide X-ray masks with high dimensional stability, *J. Vac. Sci. Technol.*, 19, 1208, 1981.
95. **Glocker, D. and Wiseman, R.,** A new method for the batch production of micro-fresnel zone plates, *J. Vac. Sci. Technol.*, 20, 1098, 1982.
96. **Hanazono, M., Narishige, S., Kawakami, K., Saito, N., and Takagi, M.,** Fabrication of a thin film head using polyimide resin and sputtered Ni-Fe films, *J. Appl. Phys.*, 53, 2608, 1982.
97. **Shiiki, K., Yuitoo, I., and Shiroishi, Y.,** Fabrication of coils with high aspect ratios for thin-film magnetic heads, *J. Vac. Sci. Technol.*, A3, 1996, 1985.
98. **Glenn, M. C. and Schuetz, J. A.,** An IC-compatible polymer humidity sensor, in *Proc. Honeywell Polymer Conf.*, Lai, J. H., Ed., Honeywell, Minnetonka, MN, 1985, 3.
99. **Numata, S., Miwa, T., Makino, D., Imaizumi, J., and Kinjo, N.,** Low thermal expansion polyimides and their applications, in *Electronic Packaging Materials Science III,* MRS Symp. Ser. 108, Jaccodine, R., Jackson, K. A., and Sundahl, R. C., Eds., Materials Research Society, Pittsburgh, 1988, 113.
100. **Kirchhoff, R. A., Baker, C. E., Gilpin, J. A., Hahn, S. F., and Schrock, A. K.,** Benzocyclobutenes in polymer synthesis, *Int. SAMPE Tech. Conf.*, 18, 478, 1986.

Taylor & Francis
Taylor & Francis Group
http://taylorandfrancis.com

Chapter 3

INTEGRATED CIRCUIT DEVICE ENCAPSULANTS

C. P. Wong

TABLE OF CONTENTS

I. Introduction 64

II. Purpose of Encapsulation 64
- A. Moisture 64
- B. Mobile Ion Contaminants 64
- C. UV-Visible Light Radiation 66
- D. Hostile Environments 66

III. Encapsulation Techniques 67
- A. Four Types of Chip-to-Substrate Interconnection 67
  - 1. Wire Bonding 67
  - 2. Tape Automated Bonding 67
  - 3. Flip-Chip Bonding 67
  - 4. Beam-Leaded Devices 67
- B. On-Chip Encapsulation Technique 69
  - 1. Thermal Deposition 69
    - a. Hot-Wall, Reduced-Pressure Reactor Process 69
    - b. Continuous, Atmospheric Pressure Reactor 70
  - 2. Plasma Depositions 70
    - a. Parallel-Plate Plasma-Assisted CVD 71
    - b. Hot-Wall Plasma-Assisted CVD 71
  - 3. Radiation-Stimulated Deposition 72
- C. Chip Packaging Encapsulation Techniques 73
  - 1. Cavity-Filling Processes 73
  - 2. Saturation and Coating Processes 74

IV. Device Encapsulants 74
- A. Inorganic Encapsulants 74
- B. Organic Encapsulants 74
  - 1. Epoxies 75
  - 2. Silicones 79
  - 3. Polyurethanes 80
  - 4. Polyimides 81
  - 5. Parylene®: Poly-(Para-Xylylene) 83

V. Temperature Humidity Bias (THB) Accelerating Testing of Potential IC Encapsulants 84
- A. Triple-Track Testing Devices 85
- B. Triple-Track Device Cleaning and Coating 86

VI. Reliability 86

VII. Conclusions 89

References 90

I. INTRODUCTION

The rapid development of integrated circuit (IC) technology from small-scale integration (SSI) to very large-scale integration (VLSI) has had great technological and economic impact on the electronic industry throughout the world. The exponential growth of the number of components per chip, the exponential decrease of device dimensions[1-2] (Figure 1), and the steady increase in IC chip size (Figure 2) have imposed stringent requirements, not only on the IC physical design and fabrication, but also on the IC encapsulants. The increase of integration in VLSI technology has resulted in the miniaturization of the device size which has reduced the propagation delay due to higher density packaging and interconnection. VLSI technology operates at a faster speed, consumes less power, and, consequently, dissipates less heat during operation. As a consequence, VLSI technology has increased the reliability and reduced the cost per function of the devices, which have had profound impact on the electronics industry.

What are the future trends and limitations of silicone IC technology? At this point in time, the ultimate production limitation feature size would be ~0.1 μm. It is not due to the limitation of device physics or chemistry. As far as complimental metal oxide silicon (CMOS) technology is concerned, the IC gate oxide with thickness of 10 Å or more could prevent the electron tunneling; theoretically, this 10-Å thickness of gate oxide should be the feature size limit; however, the production feature size limitation is mainly due to economic factors. For IC device feature size down to 0.1 μm, we need to use the step and repeat and electron-beam or X-ray exposure lithographic processes which are very expensive, not only in terms of capital expenditures, but also tedious and time-consuming processes. On the other aspects of IC technology, we predict that the chip size will continue to increase up to ~10 cm^2/chip. This is limited by the manufacturability. The ultimate speed of the silicon device will be increased up to the electron mobility in silicon (10×10^{-12} s). When fast device speed in excess of the electron mobility in silicon is needed, GaAs device should be used. Nevertheless, we expect silicon IC devices to stay with us for some time to come.

II. PURPOSE OF ENCAPSULATION

The purpose of encapsulation is to protect the electronic IC devices and prolong their reliability. Moisture, mobile ion contaminants, ultraviolet (UV), visible, and α-particle radiation, and hostile environmental conditions are some of the possible modes of degradation or interaction which could negatively affect device performance or lifetime. These will be discussed

A. Moisture

Moisture is one of the major sources of corrosion for IC devices. Electrooxidation and metal migration are associated with the presence of moisture. The diffusion rate of moisture depends on the encapsulant material.[3] Figure 3 shows the permeability of various materials. Pure crystals and metals are the best materials for moisture for moisture barrier. Glass (silicon dioxide) is an excellent moisture barrier, but it is slightly inferior to pure crystals and metals. Organic polymers, such as fluorocarbons, epoxies, and silicones, are one to two orders of magnitude more permeable to moisture as compared with glass. Gases are the most permeable to moisture of all materials. In general, for each particular material the moisture diffusion rate is proportional to the water vapor partial pressure and inversely proportional to the material thickness.

B. Mobile Ion Contaminants

Mobile ions, such as sodium or potassium, tend to migrate to the p-n junction of the IC device where it picks up an electron and deposits as the correspondent metal on the p-n

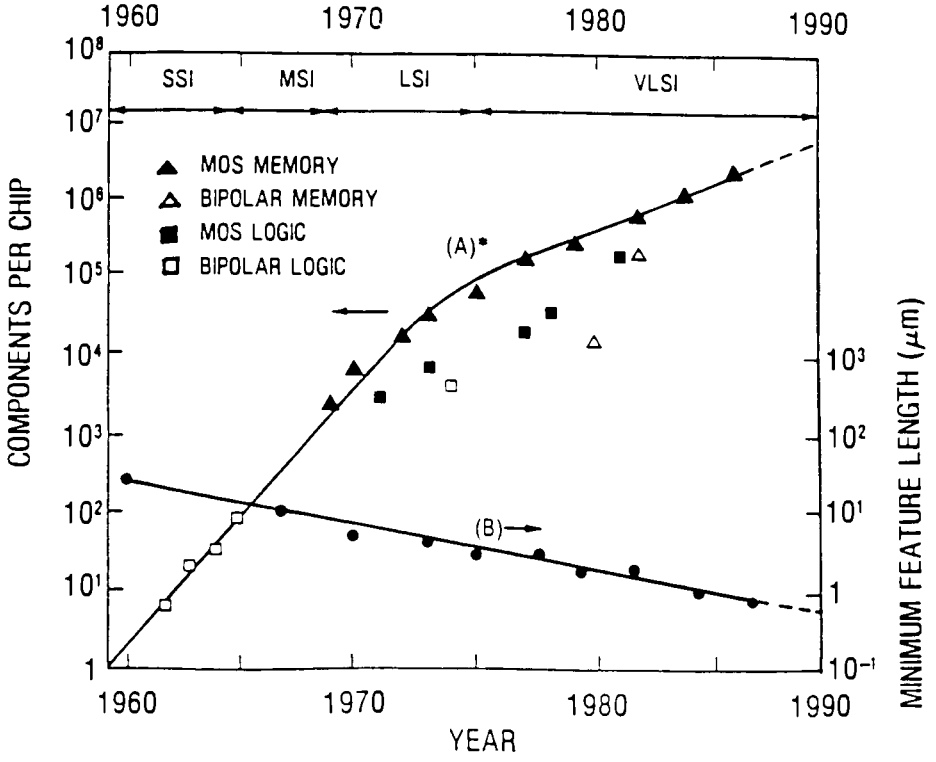

FIGURE 1. IC technological trends.[1]

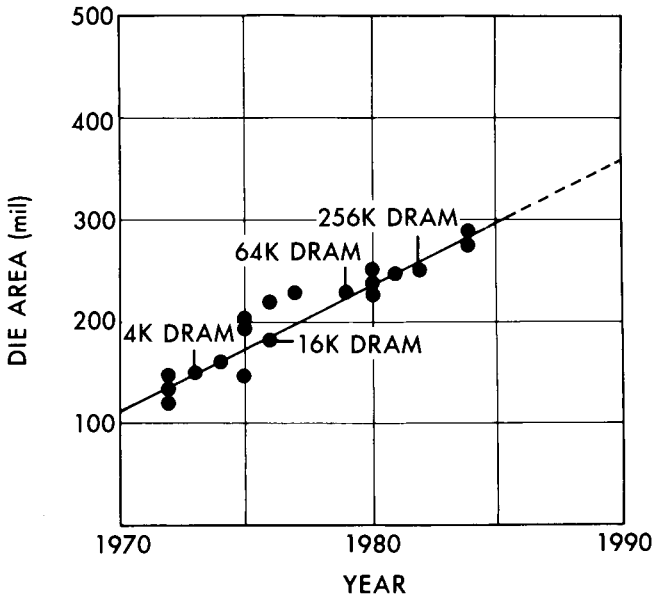

FIGURE 2. IC chip dimension trends.[2]

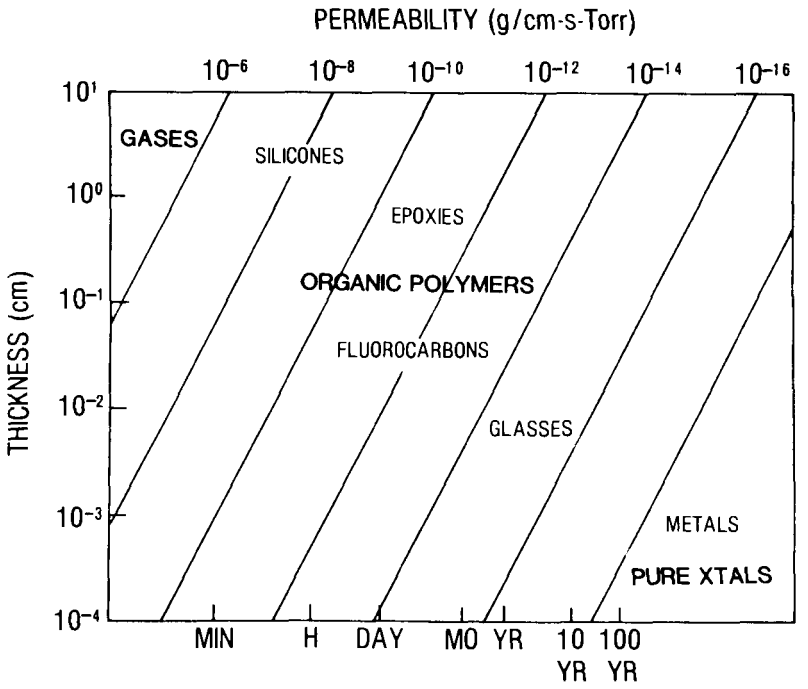

FIGURE 3. Diffusion of moisture in various materials.[3]

junction which destroys the device.[4] Chloride ions, even in trace amounts (in ppm level), could cause the dissolution of aluminum metallization of CMOS semiconductor devices. Unfortunately, CMOS is likely to be the trend of the VLSI technology and sodium chloride is a common contaminant. The protection of these devices from the effects of these mobile ions is an absolute requirement.

C. UV-Visible Light Radiation

There is an increasing amount of light-sensitive optodevices that need UV-VIS protection. α-Particle radiation is caused by a very low level or uranium and cosmic radiation present as background radiation in the device package and the atmosphere, respectively, which could generate a temporary "soft error" in operating dynamic random access memory (DRAM) devices. This type of α-particle radiation has become a major concern, especially in high-density memory devices. Good encapsulants must have radiation purity less than 0.001 α particles per square centimeter per hour. Since the α particle is a weak radiation, a thin (a few micrometers thickness) encapsulant usually will prevent this radiation damage of the DRAM devices.

D. Hostile Environments

Hostile environments, such as extreme temperatures, high relative humidity, and operating bias of the device, are part of the real-life operation. It is critical for the device to survive these operation-life cycles. Besides, encapsulants must also enhance the mechanical and physical properties of the IC devices.

In addition to the above functions, the encapsulant must be an ultrapure material, with superior electrical and physical properties, and ease of application and repair in production and service. With the proper choice of encapsulant, the encapsulation could enhance the fragile IC device, improve its mechanical and physical properties and its manufacturing yields, and prolong the reliability of the IC device which is the ultimate goal of the encapsulation.[5]

III. ENCAPSULATION TECHNIQUES

Prior to the discussion of encapsulation techniques, the IC assembly sequence is reviewed.

A. Four Types of Chip-to-Substrate Interconnection

For IC chip bonding to outside substrate interconnection, there are four major types of IC chip interconnection techniques: (1) wire bonding, (2) tape automated bonding (TAB), (3) flip-chip bonding, and (4) beam-leaded bonding.

1. Wire Bonding

Wire bonding is the most popular technique for IC chip-to-substrate interconnection. It accounts for 70% of the IC chip-to-substrate interconnection used in the IC industry. A thin (1.0 to 1.25 mil diameter) gold or aluminum wire is used in this process. Thermocompression and ultrasonic and thermosonic techniques are usually used for this bonding technology. Wedge-wedge or ball-wedge techniques, which are used in the manufacture of aluminum and gold wires, respectively, are some of the common wire-bond technologies. Due to the physical orientation of the wedge-wedge bonds, the wedge bonding must be in line with the chip and that package wedge bond with less bonding configuration, ball-wedge bonding has greater potential for automation process. With the advances of the automatic wire-bonding machine, this technique is quite effective in interconnection of the IC device. To minimize the intermetallic compound formation which weakens the bonding, aluminum wire bonding to aluminum bond pad is preferred to aluminum wire bonding to gold bond pad. Ultrasonic energy bonding tends to break up the surface oxides and exposes a fresh surface for bonding and creates a better bond. Bonding of gold wire to gold pad wire seems to provide the best bonding of all.

2. Tape Automated Bonding

The TAB process uses a chemically etched, prefabricated copper lead frame which is adhesively attached in a continuously etched tape of repetitive sites. This repetitive lead frame is continuously bonded by thermocompression or gold-tin eutectic bond to the bumped chip. This is a highly automatic process and each device could be tested and burned in before bonding. TAB associated with surface mount is a growing technology and will have significant potential in the near future.

3. Flip-Chip Bonding

Flip-chip technology has been mainly developed by IBM.[6] The IC chip is bonded face forward to the substrate through solder balls interconnection technology. The solder balls are processed through a sequential evaporation, chromium (Cr), copper (Cu), and gold (Au), through a mask onto the aluminum bond pad on a wafer. Lead-tin (Pb-Sn) solder preform is then evaporated onto the Cr-Cu-Au cap. The advantage of this technology is the short interconnection path which results in faster speed. In addition, the flip-chip technology allows arrays of bond pads which are not limited to peripheral edge pads in most devices. This array of bonding pads increases the interconnection density; however, the disadvantages of this technology are complex routing of the array of device bond pads and poor heat dissipation from this flip-chip configuration.

4. Beam-Leaded Devices

Beam-leaded device bonding was developed by AT&T.[7] Metallization of beam leads is plated on the beam-leaded bonds while the device is in the wafer form. These device leads are further etched out to form leads. Thermocompression bonding is used to attach the chip to substrate. The active side of the device is bonded face down toward the substrate, such

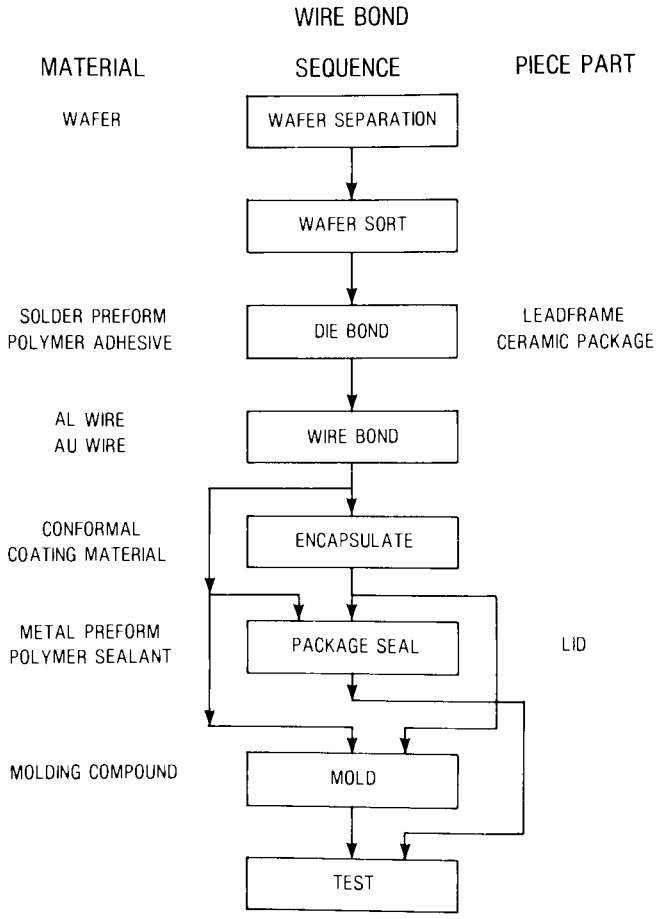

FIGURE 4. Flow chart of IC packaging.[8]

as the flip-chip technology configuration. This beam-leaded bonding technology provides an effective "one-shot" bonding with excellent bond strength; however, it is an expensive process because it consumes some valuable silicon real estate for the leads formation. AT&T has been using this technology since the 1960s and it has proven to be an effective IC chip-to-substrate interconnection in their hybrid IC technology.

The wire-bonded IC device will be used as an example of a common IC package. This IC packaging example will provide a better understanding of the packaging sequence and encapsulation process. Let us assume that the IC devices have gone through the completed fabrication process and are still in a wafer form. These devices are then tested for functions and defects, and separated or sorted by dicing. The functional devices are then die bonded to the package or lead frame with a solder preform (tin-lead solder eutectic) or polymer adhesive (typically silver-filled epoxy, metal-filled silicone, polyimide, or silicone-polyimide die attach adhesives.) The IC device is further wire bonded with a thin (1.0 to 1.25 mil diameter) gold or aluminum wire to the package or to the lead frame for outside chip interconnection. The wire-bonded chip is now ready for encapsulation with the encapsulant and package lid sealing with metal preform or polymer sealant in the package, or for some lead frame package, an epoxy-type molding compound is used to postmold the package. At this stage, the package is ready for testing. A flow chart is shown in Figure 4 for this packaging sequence.[8] Since the package step is close to the end of the IC device manufacturing process, the major concerns are the ease of the encapsulation process, high yield,

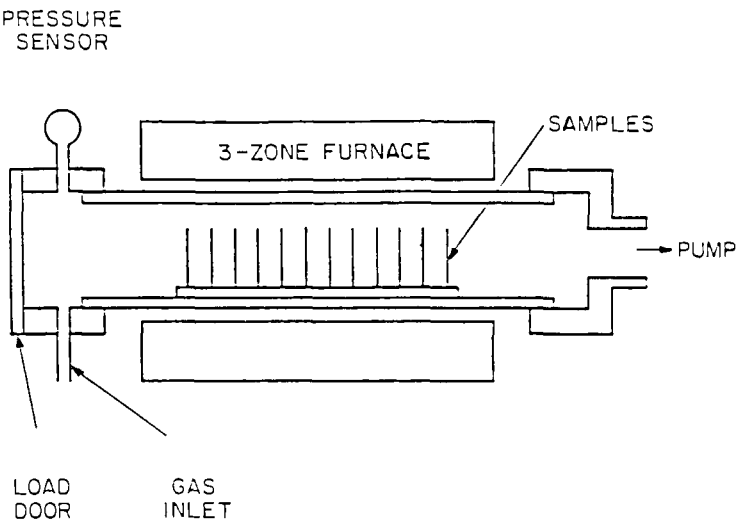

FIGURE 5. Chemical vapor deposition: hot-wall, reduced-pressure reactor process.[9]

and repairability, especially in terms of the high-cost customer-designed VLSI devices. Encapsulation techniques consist of two major levels: (1) on-chip encapsulation (deposition of passivation dielective layers right after IC chips are fabricated), prior to chip testing, dicing, and sorting steps; and (2) chip packaging encapsulation, where devices are being fabricated and going through final packaging process.

B. On-Chip Encapsulation Technique

Silicon dioxide, silicon nitride, silicon-oxy-nitrite, and polyimides are commonly used in device passivation. These passivation layers are known to have excellent moisture and mobile ion barriers of the devices. As for the sodium ion barrier, silicon dioxide is inferior to silicon nitride; however, the use of phosphorous-a (few weight percent, usually less than 6%) doped silicon dioxide has greatly improved its mobile ion barrier property. A thin layer (in 1 to 2 μm thickness) of one of these dielectric materials is deposited uniformly on the finished device, except at the bond pad areas for bonding. Most of these inorganics are deposited in one of the three major processes.[9-12]

1. Thermal Deposition

Chemical vapor deposition (CVD), a thermal process, is one of the widely used methods in preparing silicon dioxide, polysilicon, silicon nitride, or silicon-oxy-nitride passivation layers.[13-24] The thermal process can be divided into two methods.

a. Hot-Wall, Reduced-Pressure Reactor Process (Figure 5)

In this process, the reactive gases (see Table 1) are passed from one end of a reactor and pumped out through a quartz tube reactor chamber. The fabricated devices which are in wafer form (from 50 to 200 wafers per run) are vertically stacked in the reactor chamber. Since the deposition rate is a function of both reactive gas concentration and temperature, there is a reactive gas concentration gradient in the reactor chamber — being rich at the beginning of the reactor and poor at the end of the reactor. Therefore, the oxide or nitrite tends to deposit faster at the beginning of the chamber and progressively less as they move down from the reaction chamber. A nonuniform thickness deposit could result. To resolve this nonuniform deposition problem, a three-zone heating furnace with increasing furnace

Table 1
TYPICAL REACTIONS FOR DEPOSITING DIELECTRICS AND POLYSILICON

Reactants	Deposition temperature (°C)	Product
$SiH_4 + CO_2 + H_2$	850—950	Silicon dioxide
$SiCl_2H_2 + N_2O$	850—900	
$SiH_4 + N_2O$	750—850	
$SiH_4 + NO$	650—750	
$Si(OC_2H_5)_4$	650—750	
$SiH_4 + O_2$	400—450	
$SiH_4 + NH_3$	700—900	Silicon nitride
$SiCl_2H_2 + NH_3$	650—750	
$SiH_4 + NH_3$	200—350	Plasma silicon nitride
$SiH_4 + N_2$	200—350	
$SiH_4 + N_2O$	200—350	Plasma silicon dioxide
SiH_4	600—650	Polysilicon
$SiH_4 + N_2O + NH_3$	200—350	Silicon-oxy-nitride

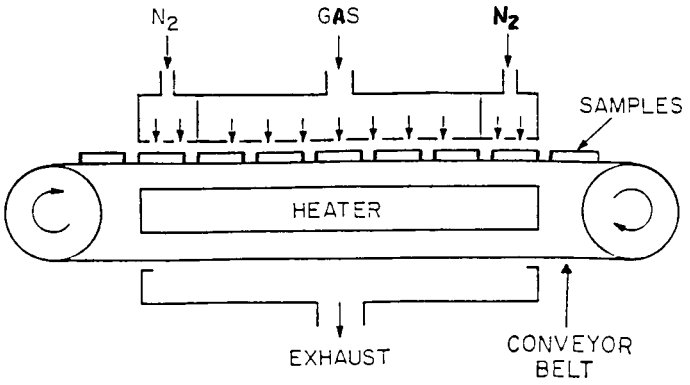

FIGURE 6. Chemical vapor deposition: continuous, atmospheric pressure reactor process.[9]

temperature range between 300 and 900°C is used to compensate for the difference in this type of deposition. The pressure of the reactant chamber is maintained at ~0.25 to 2.0 torr and the gas flow is between 100 and 1000 stdcc/min. The advantages of this process are high-quality uniform films, large loading, and batch process in production; however, the disadvantages are the toxic reactive gases used in this process.

b. Continuous, Atmospheric Pressure Reactor (Figure 6)

An alternative CVD process employs a continuous throughput, conveyor belt process. The reactive gas is purged from the center of the reactor and flows uniformly through the entire conveyor-heated wafers at atmospheric pressure. Silicon dioxide and silicon nitride are usually formed in this process. The advantage of this process is the high throughput, good quality, and uniform films. The disadvantages are, however, a large consumption of reactive gas and the formation of particulates that require frequent chamber cleaning.

2. Plasma Depositions

Thermal processes previously discussed, in general, provide high-quality and good uniform films, however, a higher deposition temperature is required. For CMOS technology, the

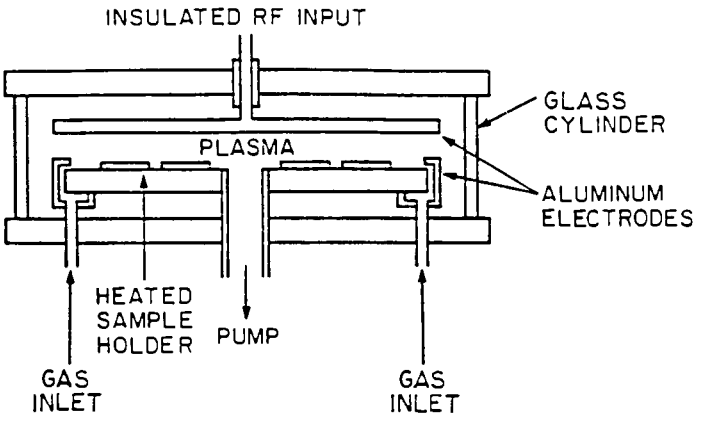

FIGURE 7. Plasma-assisted chemical vapor deposition: parallel-plate process.[9]

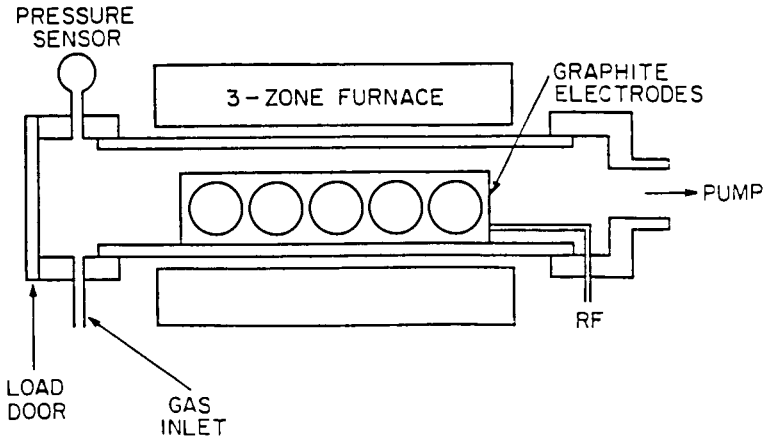

FIGURE 8. Plasma-assisted chemical vapor deposition: hot-wall process.[9]

aluminum metallization tends to have intermetallic diffusion problems at high temperatures and results in the formation of "Hillocks" which are mainly due to the high-temperature deposition-generated stress-release phenomena. The low-temperature (~400°C) plasma-assisted CVD becomes an attractive alternative. There are generally two plasma CVD processes.[25-33]

a. Parallel-Plate Plasma-Assisted CVD (Figure 7)

Parallel-plate plasma-assisted CVD is typically a cylinder glass reactor with parallel aluminum plates acting as electrodes on the top and bottom. The lower plate is the grounded electrode whose wafers are horizontally placed on the heated electrode (~100 to 400°C). A radio frequency voltage is applied on the top electrode to generate a glow discharge between the two plates. Reactive gases (see Table 1) flow through the discharged area and deposit on the wafer. Silicon nitride and silicon oxide are usually deposited by this process. The advantage of this process is the lower temperature deposition. The disadvantages are (1) low throughput, (2) manual process for each wafer, and (3) particles and particulates generated in the reactor may damage the reactor.

b. Hot-Wall Plasma-Assisted CVD (Figure 8)

This hot-wall plasma-assisted CVD process eliminates most of the parallel-plate plasma process problems as mentioned before. The process usually takes place in a three-zone heated

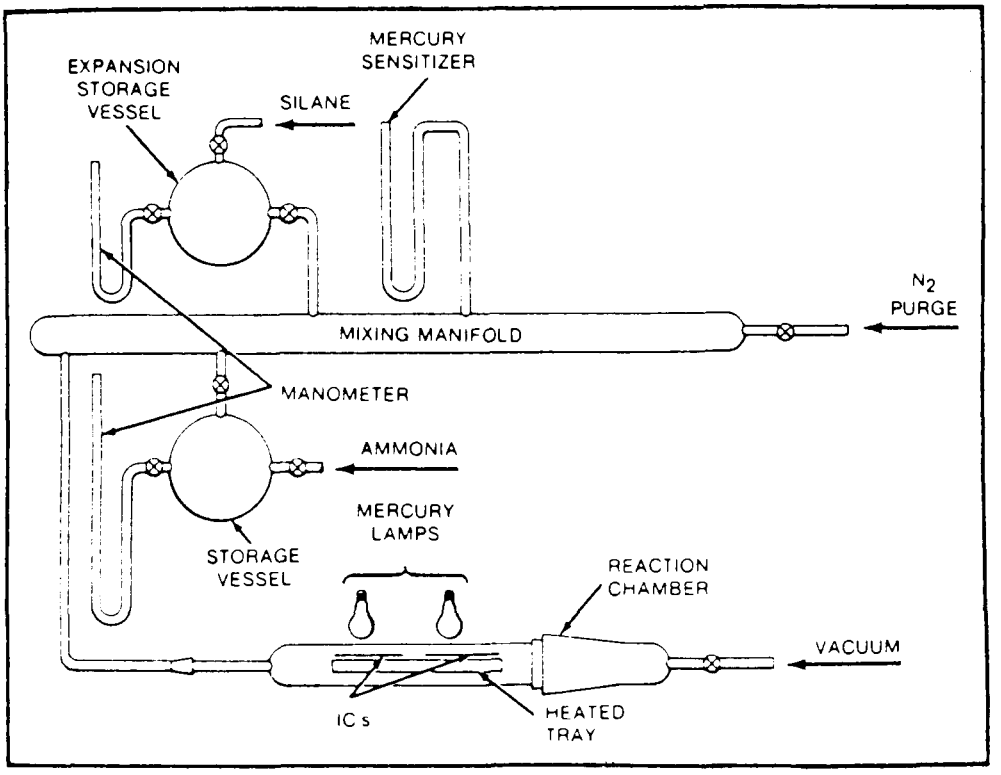

FIGURE 9. Radiation-stimulated deposition process.[35]

quartz reactor with wafers vertically placed parallel to the reactive gas flow. The reactive gases flow from one end to the other with the similar setup as the hot-wall, reduced-pressure CVD process. The radio frequency electrode which supports the wafers consists of aluminum or graphite slabs. Alternate electrodes are located on top of the furnace for plasma discharge. The major advantage of this process is low-temperature deposition. The disadvantages are that particulates are generated from the furnace and the process requires the manual loading and unloading of wafers. Recently developed magnetically enhanced plasma has increased the slow deposition rate. Silicon nitride, silicon-oxy-nitride, and silicon dioxide are readily prepared by this process (see Table 1).

3. Radiation-Stimulated Deposition

Radiation-stimulated deposition is a more recently developed process by Peters of Hughes Aircraft Company.[34,35] The process uses UV radiation to stimulate a mercury catalyst, silane, and ammonia (or hydrazine) reaction for the deposition of the silicon nitride passivation layer. Photodeposition does not rely on thermal energy to initiate the deposition. The UV photon energy is first absorbed by the reactants which lead to the dissociation of their chemical bonds. In addition, Ehrlich and co-workers[36] of MIT Lincoln Laboratories and Boyer and co-workers of Colorado State University[37] developed a low-temperature laser deposition process. The laser provides a high-intensity deep-UV source with a wavelength of 200 nm for the photodissociation or reactive gases (metal hydrides) which then deposits metal without masking. The high cost of the UV laser and the purity of film prevent its commercial application; however, the mercury-sensitized radiation-stimulated process which uses only low-cost UV lamps has become quite attractive. Recently, Tylan Company has licensed and commercialized this process. Figure 9 shows the reaction diagram where ni-

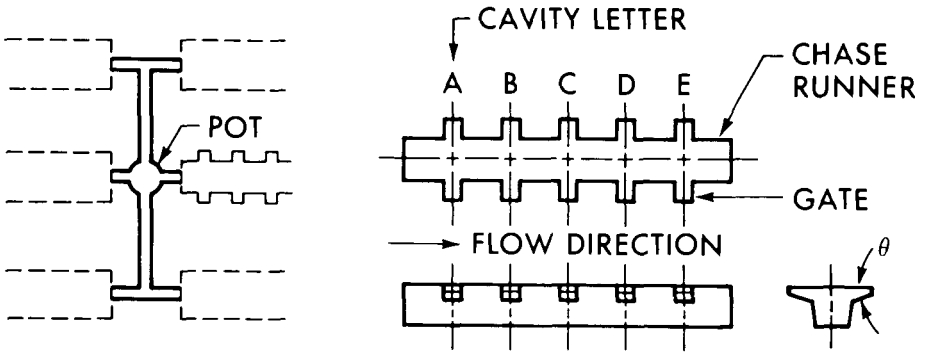

FIGURE 10. Plastic molding process.[39]

trogen carrier gas was used to purge the reaction chamber. Silane, ammonia, or hydrazine (gases) and mercury catalyst were premixed in a manifold chamber and introduced to an UV-activated chamber. Wafers were loaded horizontally on the heated tray (~100°C) and silicon nitride was deposited on the wafer. The quality of the film is inferior to the thermal growth films and trace amounts of mercury contaminants (incorporated in the deposited film) may cause some reliability concern in certain VLSI processes.[38] This film has potential, however, as a passivation layer for mercury-cadmium-tellurate (Hg-Cd-Te) temperature sensors (II to VI compound sensors).

C. Chip Packaging Encapsulation Techniques

Chip packaging encapsulation techniques consist mainly of cavity filling and saturation and coating.[39]

1. Cavity-Filling Processes

Potting, casting, and molding are common processes for cavity filling. Potting is the simplest. It involves filling the electronic component within a container with a liquid resin and then curing the material as an integral part of the component. Polymeric resins (such as epoxies, silicones, polyurethanes, etc.) are usually used as potting materials. Containers (such as metal can or rugged polymeric casing) enhance the effectiveness of the encapsulant. In the fast-growing automation manufacturing process, rugged machine-insertable components such as surface-mounted chip carriers, dual-in-line (DIP), single-in-line (SIP) packages, and discrete components are highly desirable for automation processes.

Casting is similar to potting, except the outer casing is removed after the polymer cavity-filling process is completed and cured. No heat or pressure is applied in the process.

Molding has become an increasingly important process in modern device encapsulation. It involves injecting a polymeric resin (one of the molding compounds) into a mold and then curing. The process involves the following steps: (1) the molding compound is preheated until it melts and the resin flows through runners, gates, and finally fills up the cavities; (2) the resin is then cured (hardened) and released from the mold to predetermined shapes. The exact control of the mold pressure, viscosity of the molten molding compound, and the delicate balance of runners, gates, and cavity designs are very critical in optimizing the increasing molding plastic IC.[40] Finite element analyses of the plastic molding process are becoming an integral part in solving this process. Pressure, injection, and conformal moldings are some of current molding processes. Figures 10 and 11 illustrate the typical conformal molding process and the old and new molded components. New advances of low-stress molding compounds and techniques, such as the new transfer molding with the aperture plate molding, and reactive injection molding, are becoming popular and economic ways to encapsulate and package the new IC devices.

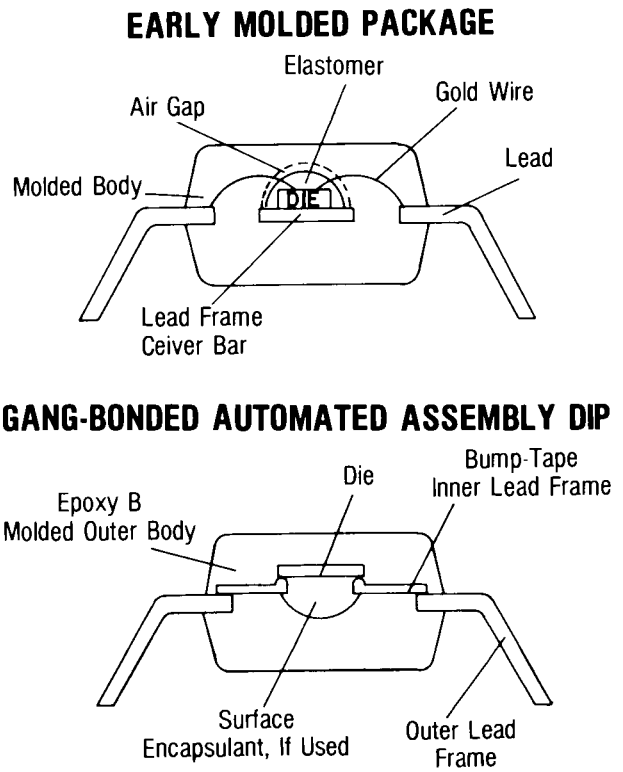

FIGURE 11. New and old molded device parts.

2. Saturation and Coating Processes

Impregnation, dip, conformal, and surface coatings are common saturation coatings. Impregnation coating is performed by the saturation of a low-viscosity resin to the component which also includes a thin film coated on the component surface. This process is usually used with a cavity filling or conformal coating process. Dip coating is performed by dipping the component into a encapsulant resin. The component is then withdrawn, dried, then cured. Coating thickness is usually a function of resin viscosity, withdrawal rate, and temperature of resin.

Conformal coating is the most common technique used in IC device encapsulation. Spin coating and flow coating are also commonly used. Suitable rheological properties of the encapsulant (such as viscosity, yield stress, G′ [storage modulus], and G″ [loss modulus]) are critical in obtaining a good flow coating package, especially in hydrid IC encapsulation, where the encapsulant tends to run over from the substrate and wick the leads of the hybrid devices.[41]

IV. DEVICE ENCAPSULANTS

Device encapsulants are divided in two groups of materials.

A. Inorganic Encapsulants

Silicon dioxide, silicon nitride, and silicon-oxy-nitride, which have previously been described in Sections III.B.1 through III.B.3, are commonly used inorganic encapsulants.

B. Organic Encapsulants

Organic polymeric encapsulants are divided into three categories: (1) thermosetting materials, (2) thermoplastic polymers, and (3) elastomers. Thermosetting materials are cross-

linking polymers which cannot be reversed to original polymer after curing. Silicones, polyimides, epoxies, silicone-modified polyimides, polyesters, butadiene-styrenes, alkyd resins, allyl esters, and silicone-epoxies are examples. Thermoplastic polymers, when subjected to heat, will flow and solidify upon cooling without cross-linking. These thermoplastic processes are reversible and become a suitable engineering plastic material. Polyvinyl chloride, polystyrene, polyethylene, fluorocarbon polymers, asphalt, acrylics, tars, Parylene® (trademark from Union Carbide's poly-para-xylylene), and recently developed preimidized silicone-modified polyimides by GE, M & T Chemicals, and Occidental Chemicals are examples of thermoplastic polymers. Elastomers are materials that have high elongation or elasticity properties, have cross-linking in their systems, and belong to thermosetting polymers. These types of material consist of a long, linear, flexible molecular chain which is joined by interval covalent chemical cross-linking. Silicone rubbers, silicone gel, natural rubbers, and polyurethanes are examples (see Table 2); however, for IC technology applications, only a few of the above which have ultrapure properties, such as epoxies, silicones, polyurethanes, Parylene®, polyimides, and silicone-polyimides, have been shown to be acceptable IC encapsulants.

1. Epoxies

Commercial epoxies were first prepared in early 1930. They have become one of the most utilized polymeric materials used for electronics. Their unique chemical and physical properties such as excellent chemical and corrosion resistances, electrical and physical properties, excellent adhesion, insulation, low shrinkage properties, and reasonable material cost have made epoxy resins very attractive in electronic applications.[42-45] The commercial preparation of epoxies are based on bisphenol A, which upon reaction with epichlorohydrin produces bisglycidyl ethers (see Figure 12). The repetitive group, n, varies from 0 (liquid) to approximately 30 (hard solid). The reactants ratio (bisphenol A vs. epichlorohydrin) determines the final viscosity of the epoxies. In addition to the bisphenol A resins, the novolac resins (see Figure 13) with multifunctional groups which lead to higher cross-link density and better thermal and chemical resistance have gained increasing acceptance in electronic applications. Typical epoxy curing agents are amines, anhydrides, dicyanodiamides, melamine/formaldehydes, urea/formaldehydes, phenol/formaldehydes, and catalytic curing agents. Anhydrides and amines are two of the most frequently used curing agents.

Selecting the proper curing agents is dependent on application techniques, curing conditions, pot-life required, and the desired physical properties. Besides affecting viscosity and reactivities of the epoxy formulations, curing agents determine the degree of cross-linking and the formation of chemical bond in the cured epoxy system. The reactivity of some anhydrides with epoxies is slow; therefore, an accelerator, usually a tertiary amine, is used to assist the cure. "Novolacs" and "Resole" are two major commonly used phenolformaldehyde epoxies. A novolac is a phenol-formaldehyde, acid-catalyzed epoxy polymer. The phenolic groups in the polymer are linked by a methylene bridge which provides highly cross-linked systems and a high-temperature and excellent chemical resistance polymer. "Resole" is a base-catalyzed phenol-formaldehyde epoxy polymer. In most phenolic resins commonly used with epoxies, the phenolic group is converted into an ether to give improved base resistance. Phenolic resins are cured through the secondary hydroxyl group on the epoxy backbone. High-temperature curing is required in this system and it provides excellent chemical-resistance epoxies. Recently developed high-purity epoxies have become very attractive encapsulants for electronics.

These new types of resin contain greatly reduced amounts of chloride and other mobile ions, such as sodium and potassium, and have become widely used in device encapsulation and molding compounds. The incorporation of fused silica as filler in the epoxy system has drastically reduced the thermal coefficient of expansion of these materials which makes them

Table 2
TYPICAL CURED PROPERTIES OF BASIC ENCAPSULANTS[39,55]

	Electrical						Thermal			Physical[a]				
Polymer system	Dielectric strength (V/mil)	Specific resistivity Ωcm)	Water absorption (%)[b]	Dielectric constant (10^{10} cps)	Loss tangent (10^{10} cps)	Relative arc track resistance[6]	Heat distortion temperature (°F)	Safe use temperature (°F)	Linear expansion × 10^5/°F	Ultimate tensile strength (psi)	Ultimate elongation (%)	Hardness[d]	Relative adhesion[c]	Remarks
Thermoplastic														
Asphalt and tars[e]	300	10^{10}	0.08	3.5	0.04	5	130	160	8	600	5	SD 60	4	Lowest cost
Fluorocarbon	450	10^{18}	0.00	2.1	0.0003	1	250	500	5.5	3,000	200	SD 60	None	Good solvent resistance
Polyethylene[e]	500	10^{16}	<0.01	2.3	0.0005	3	—	240	9.5	4,000	1,000	SD 65	5	Flexible
Polystyrene[e]	550	10^{18}	0.04	2.5	0.0003	3	180	185	4	7,000	1.5	M 80	4	Rigid
Polyvinyl chloride[e]	400	10^{15}	0.15	2.8	0.006	3	150	210	3	3,000	100	SD 80	3	Coating material
Wax[e]	400	10^{17}	0.02	2.6	0.001	3	80	135	11	300	5	SD 30	4	Melt, pour, and chill
Silicone-polyimide[f]	1,500—2,800	10^{15-17}	<1	3.0	0.007	2	300—460	750	30—47 (C)	2,000	200	—	1	Good solvent resistance, high temp
Parylene[g]	500—7,000	10^{13-16}	0.03	2.8	0.01—0.003	2	535—760	250	3.5—6.9	10,000	200	—	4	Conformal coating
Thermosets														
Alkyd[e]	350	10^{14}	0.4	3.8	0.025	2	220	250	4	8,000	—	SD 90	2	
Allyl ester[e]	400	10^{14}	0.7	—	—	3	>190	210	4	5,500	—	M 70	3	
Butadiene-styrene[e]	600	10^{16}	0.03	2.4	0.006	3	260	475	5	4,000	4	SD 80	4	
Epoxide[e]	450	10^{14}	0.20	2.9	0.018	2	400	450	3	10,000	<1	M 90	1	Excellent solvent resistance
Phenolaldehyde[e]	350	10^{12}	0.3	4.7	0.04	4	175	175	4	7,000	1.5	M 126	2	
Polyester[e]	350	10^{13}	0.4	3.5	0.05	3	190	325	6	8,000	<5	M 100	3	
Silicone[e]	600	10^{15}	0.03	2.8	0.002	2	100	500	7	2,500	8	M 60	4	Excellent THB performance
Polyimides[h]	3,400	10^{16}	—	3.6	0.002	2	>600	<800	2—7	14,000—20,000	10—80	—	3	Good solvent resistance, high temp
Silicone-epoxy[i]	246—338	10^{15}	0.1	3.6	0.004	2	—	<390	3—6	8,000	—	SD 60	3	Good for molding

Elastomers														
Buna-S rubber	500	10^{14}	—	2.5	0.01	4	—	250	6	300	400	SA 50	2	Flexible
Chloro rubber	400	10^{12}	—	2.7	0.05	3	—	—	9	2,500	500	SA 70	3	Flexible
Natural rubber	500	10^{16}	—	2.1	0.03	4	—	150	4	3,000	700	SA 50	2	Flexible
Silicone rubber[e]	600	10^{13}	—	3.0	0.05	2	>450	500	—	650	100	SA 60	4	Flexible
Thioplast[e]	150	10^{11}	—	14	0.15	4	—	250	10	300	400	SA 40	2	Poor electrical properties, high temp
Urethane[e]	350	10^{11}	0.4	3.5	0.04	4	>150	200	10	5,000	400	SA 40	1	Poor electrical properties, high temp
Inorganics														
SiO_2	5,000	$>10^{16}$		3.5—4		1	1,400	1,400	0.3—0.5	14,000—56,000	0		4	Excellent passivation properties
Si_3N_4	5,000	10^{12}		7—10		1	1,400	700—1,400	2.5—3	14,000—140,000	0		4	Excellent passivation property

[a] At 70—90°F.
[b] In 24 h, $^1/_8$ in. thick.
[c] 1 best, 5 poorest.
[d] M = Rockwell M; SA = Shore Durometer A; SD = Shore Durometer D.
[e] Unfilled.
[f] M&T Chemical Co.
[g] Union Carbide.
[h] DuPont.
[i] Dow Corning.

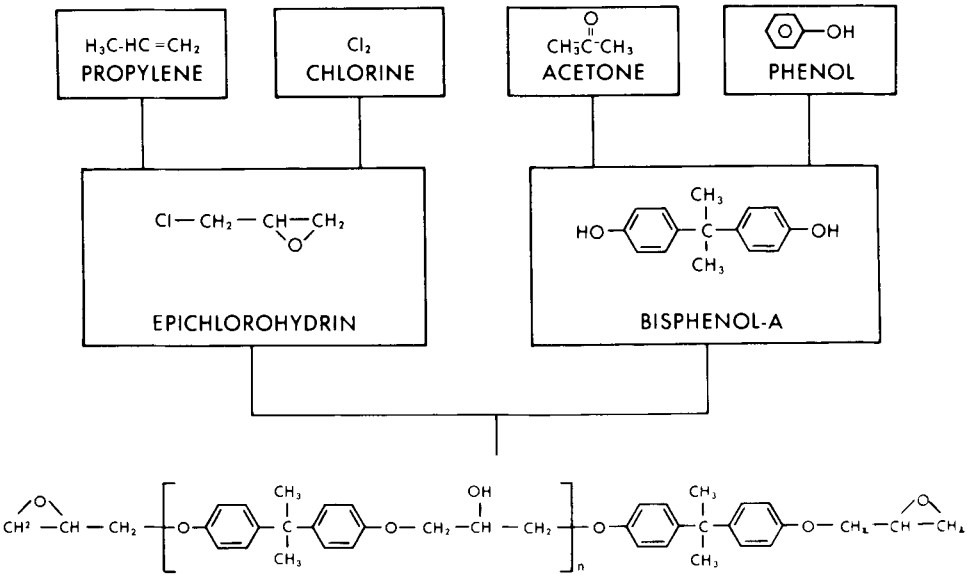

FIGURE 12. Commercial epoxy preparation scheme.

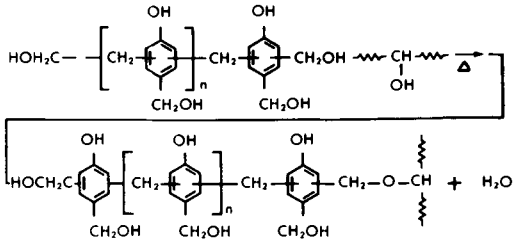

"RESOLE" (PHENOL—FORMALDEHYDE)

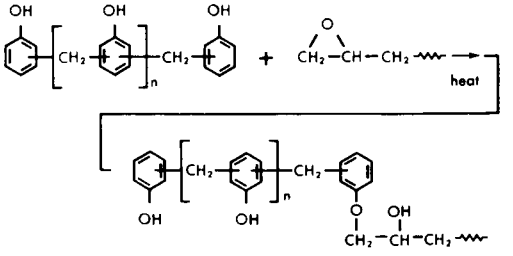

"NOVOLACS" (PHENOL—FORMALDEHYDE)

FIGURE 13. Novolac epoxy chemical structures.

more comparable with the IC die-attached substrate materials. The incorporation of a small amount of an elastomeric materials (such as silicone elastomer) to the rigid epoxy has drastically reduced the modulus of the material and reduced the thermal stress of the epoxy material.[46] This new type of low-stress epoxy encapsulant has great potential application in molding large IC devices. The "glob-top"-type epoxy material is becoming increasingly more acceptable as an encapsulant for the higher reliability electronic device and system. When the epoxy materials are properly formulated and applied and their stress-related issues have been properly considered and reduced, they could be a very attractive high-performance encapsulant. The continuous advancements in epoxy material development will have a great impact in device packaging.

2. Silicones

Although organosilicon compounds have been known since 1840, it was not until the 1930s that research directed toward obtaining heat-resistant electrical insulating materials led Corning Glass Works and General Electric into the manufacturing of silicone polymers.

Room-temperature vulcanized (RTV) silicone elastomer, an organosiloxane, cured by a moisture-initiated, catalyst-assisted process, is one of the most effective encapsulants used for temperature cycling and moisture protection of IC devices. Since World War II, silicones (organosiloxane polymers) have been used in a variety of applications where properties of high thermal stability, hydrophobicity, and low dielectric constant are necessary, e.g., as encapsulants or conformal coatings for integrated circuits. In 1969 it was demonstrated that RTV silicones exhibited excellent performance as moisture protection barriers for IC devices and a number of different RTV silicones have been adapted for use in the electronics industry.[47-64]

The basis of commercial production of the silicones is that chlorosilanes are readily hydrolyzed to give disilanols which are unstable and condense to form siloxane oligomers and polymers. Depending on the reaction conditions, a mixture of linear polymers and cyclic oligomers is produced. The cyclic components can be ring opened to linear polymers and it is these linear polymers that are of commercial importance (see Figure 14). The linear polymers are typically liquids of low viscosity and, as such, are not suited for use as encapsulants. These must be cross-linked (or vulcanized) in order to increase the molecular weight to a sufficient level where the properties are useful. Two methods of cross-linking are used: those which can be classified as condensation cures (see Figure 15) and those which are addition cure systems (see Figure 16). For electronic applications, only the RTV silicone which uses alkoxide cure, and platinum catalyzed additional heat cure vinyl and hydride silicone systems are suitable for device encapsulation.

Ionic materials, whether from the device surface, encapsulation materials, or the environment, affect the electrical reliability of encapsulated IC devices. For this reason, the silicones are subjected to intense purification. The concentration of Na^+, K^+, and Cl^- mobile ions is less than a few ppm, and α-particle emission is less than 0.001 α/cm^2 h. Thus, it offers excellent α particle shielding for eliminating soft error in DRAM devices, such as 64K, 256K, and megabit chips.[65] The drawbacks of RTV silicone as an IC encapsulant are both its poor solvent resistance and weak mechanical properties.[66] Highly fluorinated alkyl-substituted siloxanes have shown improvement in solvent resistance, although a recently developed silicone material with high cross-linking density and high filler loading system seems to significantly improve the solvent resistance of the silicone encapsulant.[67,68]

Heat-curable silicone (either elastomer or gel) has become an attractive device encapsulant. Its curing time is much faster than the RTV-type silicone. Besides, heat-curable silicone gels tend to have slightly better thermal properties than conventional RTV silicone. With its excellent jelly-like (very low modulus) intrinsic softness, silicone gel is a very attractive encapsulant in wire-bonded large-chip-size IC devices. The two-part heat-curable system

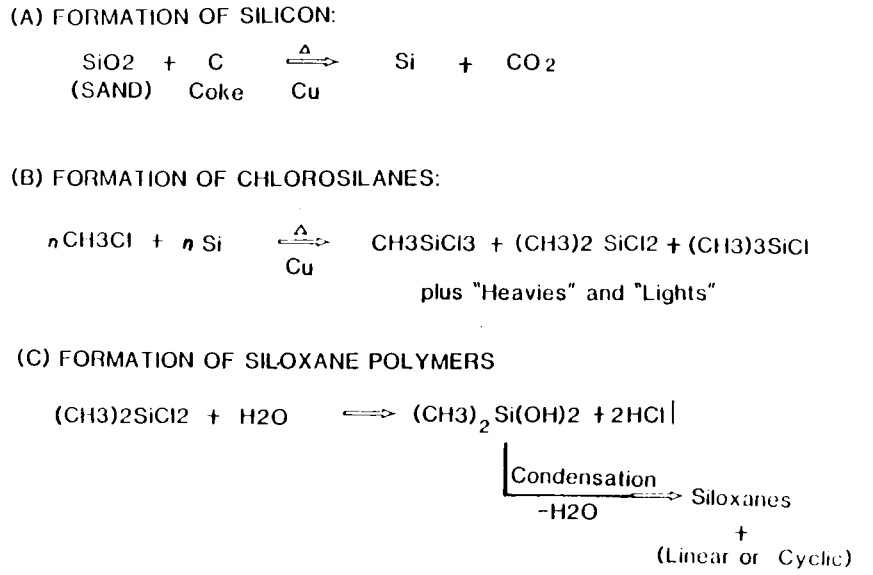

FIGURE 14. Commercial preparation of silicone.

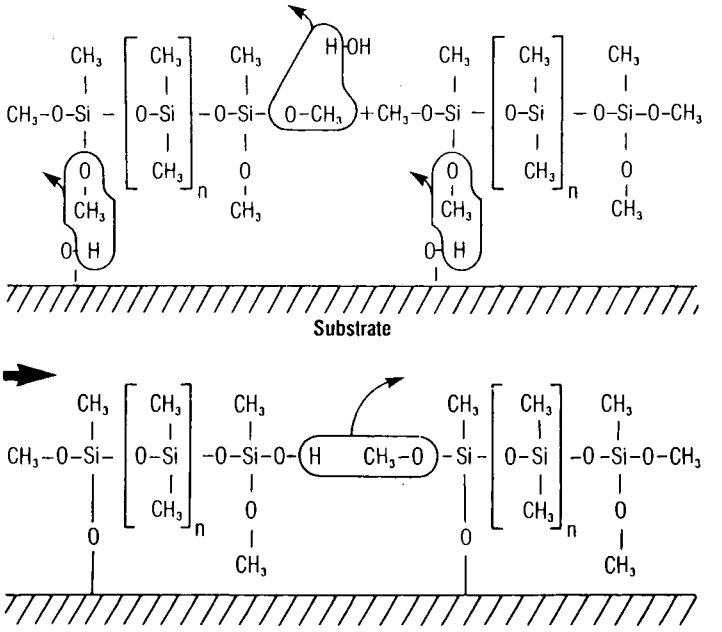

FIGURE 15. RTV silicone: condensation cure mechanism.

which consists of the vinyl and hydride reactive functional groups and the platinum catalyst additional cure system provides a fast-cure system without any by-product (see Figure 16 for cure mechanism). This solventless type of heat-curable silicone gel will have increased usage in electronic applications.

3. Polyurethanes

Polyurethane was first made available by Otto Bayer in the late 1930s in Germany.[69] The early study of polyurethane was simply based on di-isocyanates and diols, however, recent

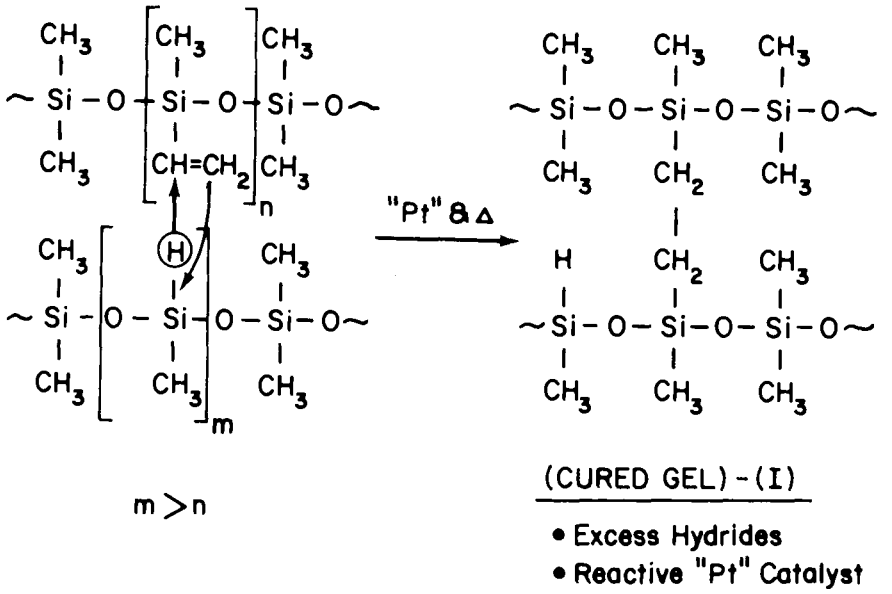

FIGURE 16. Additional heat-curable silicone cure mechanism.

work is focused on the use of intermediates which are low molecular weights, polyesters, and polyethers with reactive functional groups such as the hydroxyl or isocyanate group capable of further cross-linking, chain extension, or branching with other chain extenders to higher molecular weight polyurethanes. Diamine and diol are chain extended with the prepolymer (either polyester or polyether) to form polyurethanes with urea or urethane linkages, respectively.[70] The morphology of polyurethane is well characterized. Hard and soft segments from diisocynates and polyols, respectively, are the key to excellent physical properties of this material (see Figure 17).

Base is a more widely used catalyst than acid as polyurethane polymerization. The increasing basicity is proportional to its catalytic activity. Amines, such as tertiary alkylamines, and organic metal salts, such as tin or lead octoates, promote the reaction of isocyanate and hydroxyl functional groups in the polyurethane system and accelerate the cross-linking. The hydrolytic stability of the final property of polyurethane could, however, be affected by the catalyst used. UV stabilizers are usually added to reduce the radiation effect of the material. In addition, polyurethane has unique high strength, high modulus, high hardness, and high elongation. It is one of the toughest elastomers used today. High-performance polyurethane elastomers are used in potting and in reactive injection molding of IC devices.

4. Polyimides

Polyimide is one of the fastest growing material areas in polymers for electronic applications. It was first developed at DuPont in the 1950s. During the past couple of decades, there has been tremendous interest in this material for electronic applications. The superior thermal (up to 500°C), mechanical, and electrical properties of polyimide have made its use possible in many high-performance applications, from aerospace to microelectronics. In addition, polyimides show very low electrical leakage in surface or bulk. They form excellent interlayer dielectric insulators and also provide excellent step coverage which is important in multilayer IC structures. They have excellent solvent resistance and ease of application. They could be easily either spun-on or flow-coated and imaged by a conventional photolithography and etch process.

Most polyimides are aromatic diamine and dianhydride compositions (see Figure 18). Polyamic acids are precursors of the polyimides. Thermal cyclization of polyamic acid is a

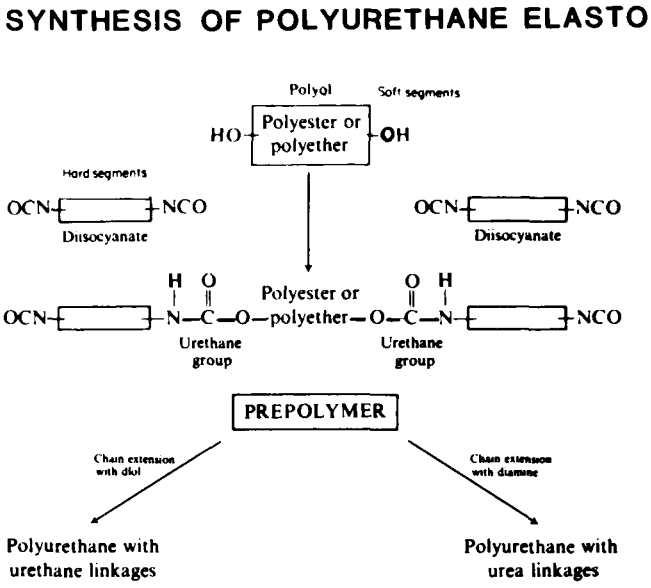

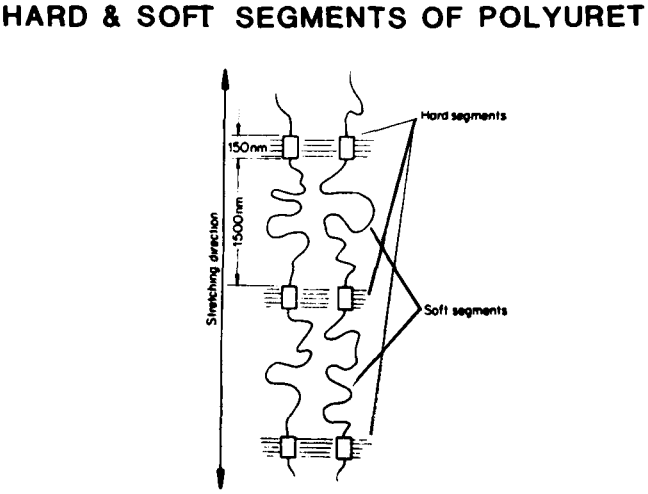

FIGURE 17. Synthesis and morphology of polyurethanes.

simple curing mechanism for this material (see Figure 19). Siemens of Germany developed the first photodefinable polyimide material,[71] however, Ciba Geigy has recently announced a new type of photodefinable polyimide which does not require a photoinitiator.[72] Both of these photodefinable materials are negative resist-type polyimides. A positive resist-type polyimide which reduces the processing step in IC fabrication is not yet commercially available. Hitachi has recently announced an ultralow thermal coefficient expansion (TCE) polyimide which has some potential in reducing the thermal stress of the silicon chip and the polyimide encapsulant. The rod-like, rigid structure of the polyimide backbone structure is the key in preparing a low TCE polyimide.[73] By simply blending a high and a low TCE polyimide, one will be able to achieve a desirable TCE encapsulant which could match the TCE on the substrate and reduce the thermal stress problem in encapsulated device temperature cycling testing. The affinity for moisture absorption, a high-temperature cure, and high cost of the polyimide are the only drawbacks that prevent its use in general electronic application. Preimidized polyimides which cure by evaporation of dissolved solvent may

POLYMER TYPE	GROUP	ANHYDRIDE	DIAMINE	MODULUS OF ELASTICITY Kg/cm²	ELONGATION AT BREAK	Tg
PMDA - Benzidine	1	RIGID	RIGID	120K	2	NONE
ODPA - PPDA	2	FLEXIBLE	RIGID	65K	5	NONE
PMDA - ODA	3	RIGID	FLEXIBLE	35K	100	"CROSS-LINKS"
ODPA - ODA	4	FLEXIBLE	FLEXIBLE	30K	100	270°C FUSIBLE

FIGURE 18. Examples of some aromatic polyimides.

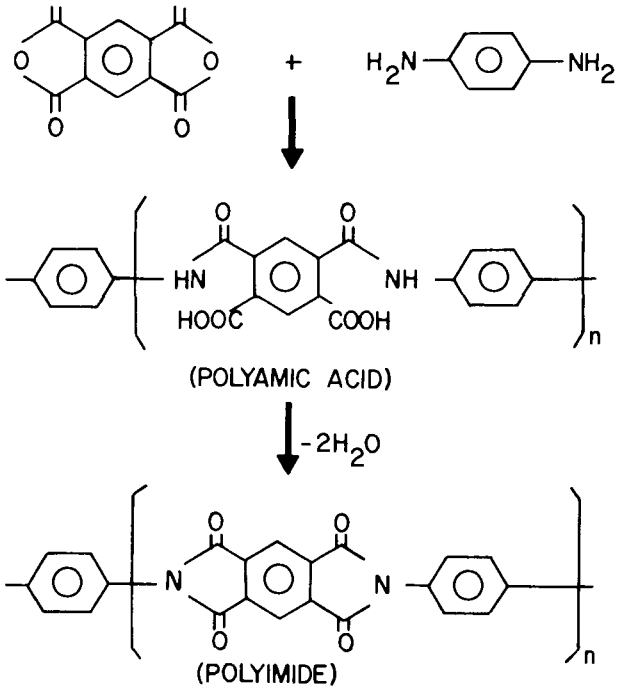

FIGURE 19. Polyimide cure mechanism.

reduce the drawback of high-temperature cure of the material. Advances in polyimide synthesis have reduced the material moisture absorption and improved the adhesion of the material. These new types of polyimide systems will have significant implications in device packaging. Recently, a siloxane-polyimide copolymer, which combines both the silicone and polyimide properties, has gained acceptance as an IC device encapsulant.

5. Parylene®: Poly-(Para-Xylylene)

Parylene®, a poly-(para-xylylene) (see Figure 20), was first developed by Union Carbide Corporation.[74,75] The process uses a thermal reactor to first vaporize (at 150°C, 1 torr pressure)

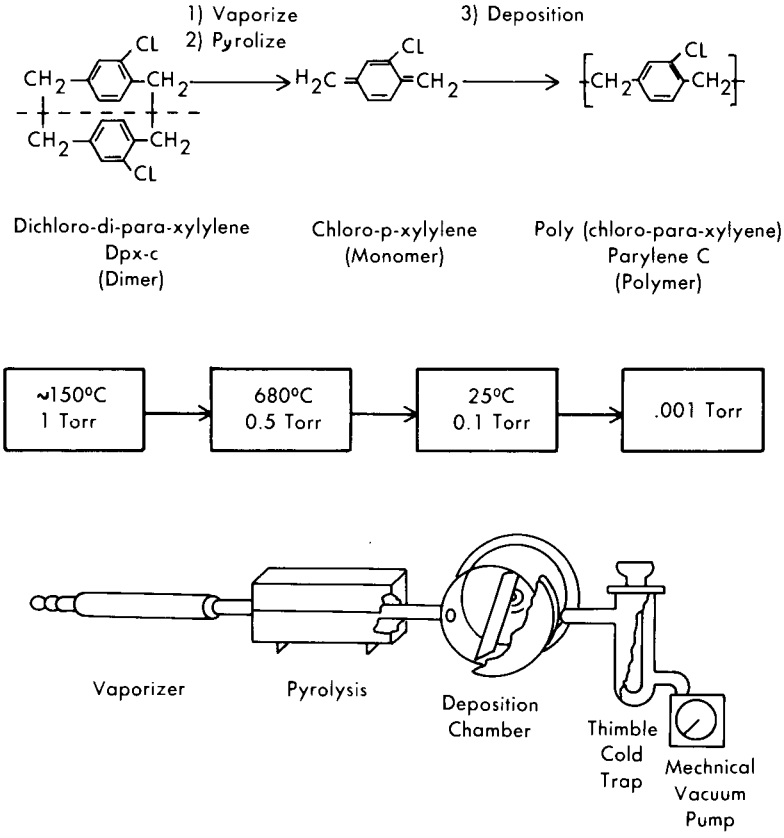

FIGURE 20. Parylene® deposition process.[74]

and pyrolyze (at 680°C, 0.5 torr pressure) the di-para-xylylene to para-xylylene, an intermediate, then deposit as para-xylylene-Parylene® polymer at room temperature. This room-temperature deposition is a very attractive encapsulation process, especially for temperature-sensitive, low-transition substrate materials. This Parylene® deposition provides an excellent conformal coating with excellent step coverage thin film (1 to 2 mil thickness). Since it is a room-temperature, spontaneous, and gas-to-solid deposition process, encapsulated electronic parts only experience a minimal stress and it is an excellent, reliable, and labor-saving process. In addition, the deposition rate of Parylene® depends on different types of Parylene® used. The dichloro and monochloro substituted on the benzene ring of the Parylene®, D and C, respectively, have a faster deposition rate than the normal unsubstituted Parylene® N. The deposited Parylene® film has excellent chemical resistance and electrical properties. Since this process only pyrolysis the dimer to a tough polymer, there are no solvents, catalysts, etc. to create impurity in formed film. Besides, this is a vapor phase deposition; it is suitable for depositing continuous film at hard-to-reach areas, such as underchip coverage of the flip-chip or beam-leaded devices. Currently, this process is widely used in conformal coating of military application circuit boards for severe environmental protection or hard abrasive electronic parts.

V. TEMPERATURE HUMIDITY BIAS (THB) ACCELERATING TESTING OF POTENTIAL IC ENCAPSULANTS

THB accelerating testing is used to screen potential encapsulants. The THB testing devices (triple-track coupons), testing hardwares, and interpretation of good and bad encapsulants will be addressed as follows.

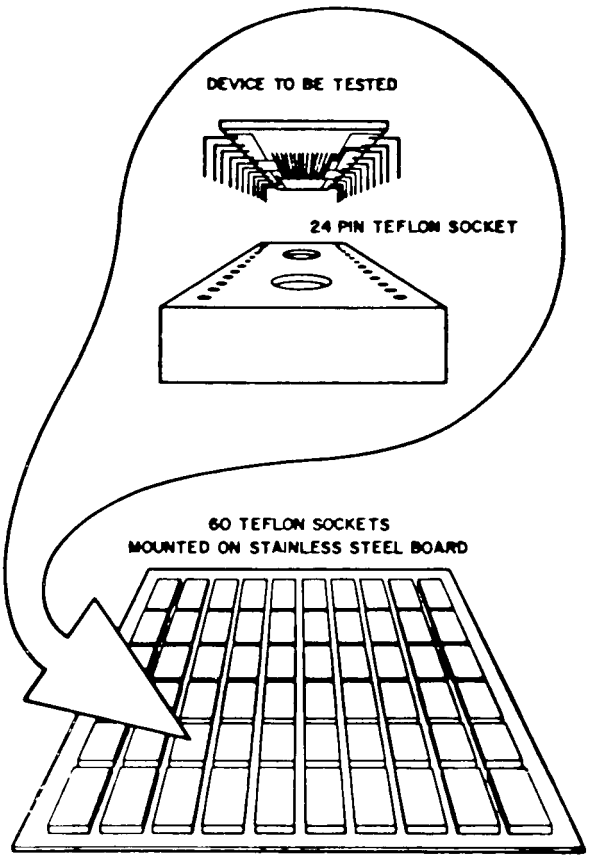

FIGURE 21. Triple-track testing setup.[76]

A. Triple-Track Testing Devices

The primary purpose of an encapsulant is to maintain the electrical integrity of the device for long periods over a broad range of environmental conditions. A modification of the THB procedure developed by AT&T Bell Laboratories was used to evaluate the performance of encapsulants.[76] THB testing is performed with a tantalum nitride *T*riple-*T*rack *R*esistor (TTR). A triple-track test device consists of three tantalum nitride metal tracks deposited on a ceramic substrate; each track is 3 mil wide and the spacing between tracks is 3 mil with a meandering pattern. The triple-track device is encapsulated, with the testing encapsulant mounted in Teflon sockets on stainless steel plates (see Figure 21) and placed in a 85°C, 85% relative humidity environment. The two outer tracks were grounded and the center track was biased at +180 Vdc (see Figure 22). Under these conditions, water vapor penetrating the coating can form layers of continuous water path which cause anodization of the tantalum nitride resulting an increase in the resistance of the biased track. The presence of ionic contaminants, either in the encapsulant or on the substrate, will accelerate the rate of increase in resistance. At set intervals, usually 24, 48, or 72...etc., h, the resistance of the center track was measured. The change in resistance, $\Delta R/R$, which attributed to the electrooxidation of the biased track, was then calculated and plotted as a function of time. A perfect encapsulant would have a $\Delta R/R$ of 0, but an increase in resistance of less than 1% in 100 h with the accelerated conditions of 85°C, 85% RH has been considered satisfactory for some materials (see Figure 23). A number of formulations were also tested using *T*riple-*T*rack *C*onductors (TTC). TTCs are similar to TTRs, with the only difference being that the metallization is titanium-palladium-gold. In this instance, leakage current is measured as a

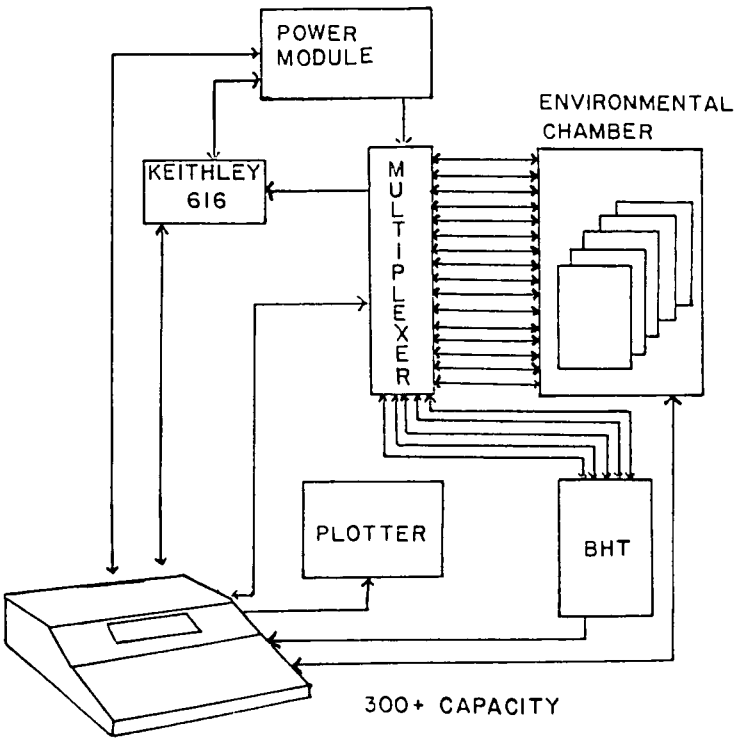

FIGURE 22. THB testing hardware.[76]

function of time under the accelerated aging conditions. In general, the encapsulated TTC will have a lower leakage current at a longer testing time. We could attribute this lower leakage current with longer testing time to the sweeping out of contaminated ions. A good encapsulant should have a lower leakage current. For IC device encapsulants, a minimum of 10^{-9} A at 1000 h is preferred (see Figure 24).

B. Triple-Track Device Cleaning and Coating

TTRs and TTCs should be cleaned just before coating to insure a minimum amount of surface contamination. This contamination is typically dust and organics. A standard cleaning procedure used was boiling peroxide, Freon, and deionized water to remove all contamination. UV-ozone, microwave discharge plasma cleanings are also very effective in cleaning these devices prior to encapsulant coating. After this cleaning procedure, the TTRs and TTCs were flow coated with the encapsulant. The encapsulants were cured at their prescribed temperature and then ready for electrical testing. It must be noted that cleanliness is the most critical factor in encapsulation of IC devices. Device reliability is greatly dependent on the cleaning process as well as the suitable encapsulant.

VI. RELIABILITY

Reliability is generally defined as a probability that an item will perform a certain required function under certain stated conditions for a stated period of time. Many people would like to define reliability with certain mathematical terms, such as failure rate, mean time to failure, reliability function, probability density function, failure unit, etc. There are many mathematical models that predict the failure rate of certain device life cycles. The most common one is the well-known "bathtub" model (see Figure 25). In the bathtub model, a

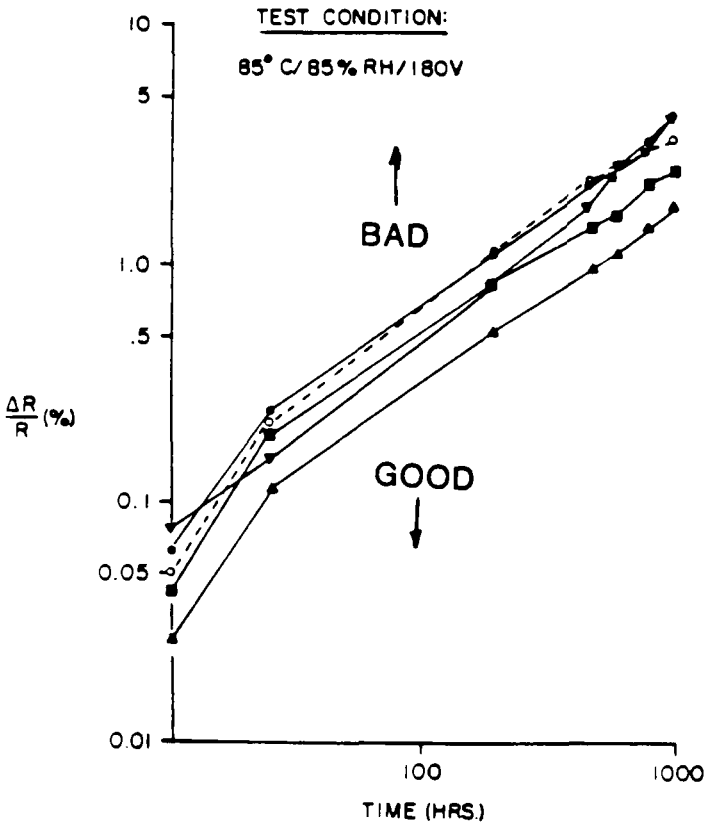

FIGURE 23. THB testing of resistance change with testing time.

failure rate is usually plotted vs. time for device failure. At the beginning of the device's entire life, there tends to be a high failure rate. This early device failure or infant mortality is usually due to manufacturing defects, such as photoresist residue, etching defects, oxide pinholes, ionic contaminations on chip and/or device packaging, poor metallization, weak wire bonds, scratches and cracks in chips, or poor packaging and device encapsulants.[77] The Weibull model and others are usually used to predict the accelerating factor of this type of early failure of devices.[78-81]

The burn-in testing process in device manufacturing is usually used to eliminate the high early failure rate. During the burn-in procedure, devices are subjected to higher than normal operation temperatures. Most of the device accelerating failures are associated with the Arrhenius equation, which depends largely on the activation energy and temperature. The Arrhenius equation is defined as $R = Ro \exp(-Ea/kT)$, where R is the reaction rate, Ro is the initial reaction rate, Ea is the activation energy, k is the Boltzman constant, equal to 8.6×10^{-5} eV/deg, and T is the absolute temperature. A higher temperature burn-in could weed out the manufacturing defects and reduce the early infant mortality failure (see Figure 26). After the early failure state, the device failure rate is at a steady state. At this steady state, the failure rate is usually low and steady. The length of this steady state depends on the physical design, manufacture durability, and operating environments. For solid-state IC devices, this is usually a problem-free period. After this steady-state period, the device will enter its wearout, final period. In some devices, corrosion, electromigration, mobile contaminant ions are some of the failure modes; however, the exact wearout mechanism is still not too well defined.

In addition to the failure rate model, it would be of benefit to us to understand the effect

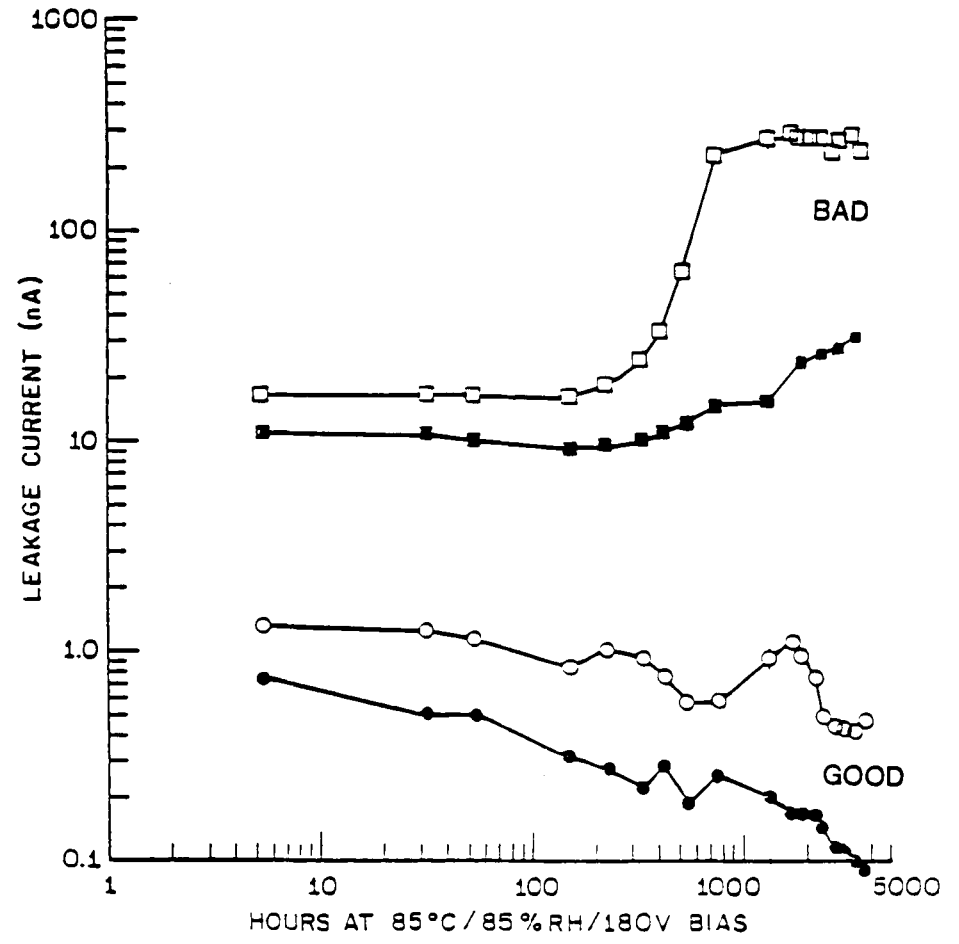

FIGURE 24. THB testing of leakage current change with testing time.

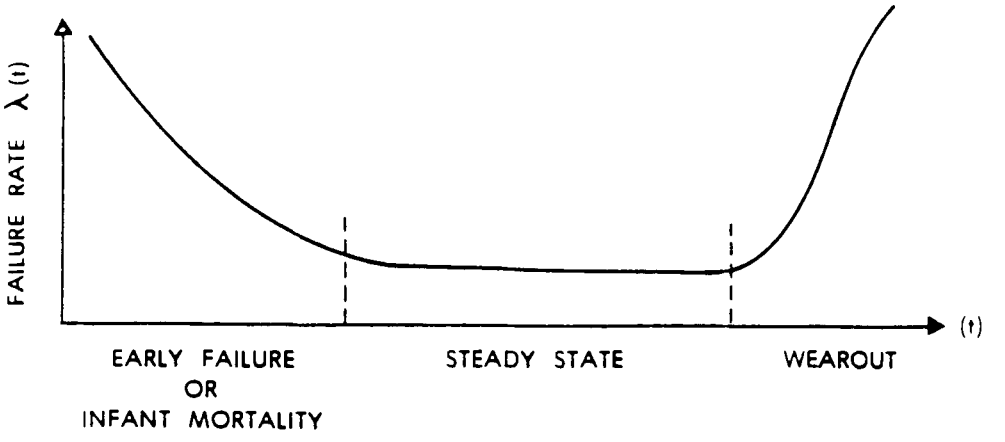

FIGURE 25. Model for device failure rate vs. time.

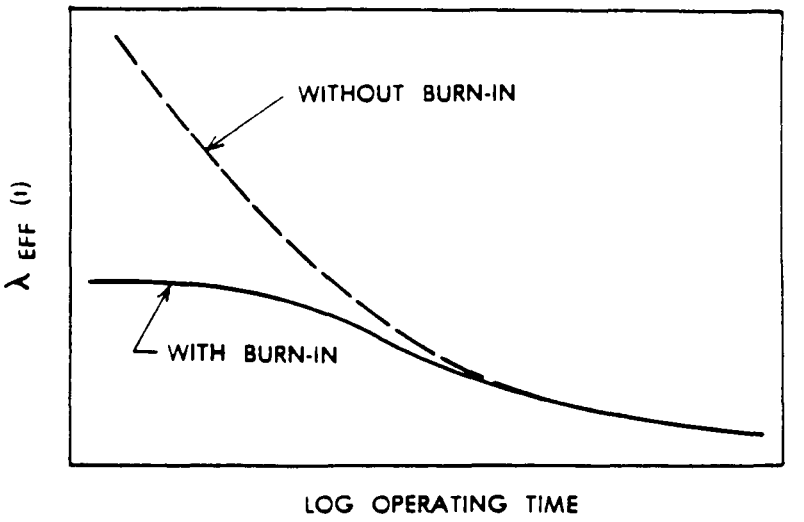

FIGURE 26. Failure rate vs. time in use for device with and without burn-in.[82]

of failure on an electronic system. A simple example by Bertram[82] to define the *F*ailure Un*it* (FIT) in an electronic switching system (ESS) which consists of 100,000 components, transistor, and others provides a clear picture of the effect of failure rate. Let us assume there is one device failure per month as our goal; this system will have a failure rate (λ) of:

$$\lambda < \frac{1 \text{ failure}}{10^5 \text{ device} \times 720 \text{ h}} = 14 \times 10^{-9} \text{ failure/device hours}$$

$$1 \text{ FIT} = 1 \text{ failure}/10^9 \text{ device hours}$$

Therefore, our hypothetical failure rate of the ESS is

$$\lambda < 14 \text{ FIT}$$

During the 10 years in service, the ESS may have 120 device failures which is equivalent to 0.1% device in the whole ESS. For the high reliable ESS, a FIT rate of 10 is desirable, 100 will probably be acceptable, and 1000 is unacceptable. Furthermore, the acceptable FIT rate is also dependent on the designed system. The highly reliable ESS requires low FIT rate and short life-cycle consumer product accepts higher FIT rate. The complexity and the expected lifetime of the system are critical parameters in deciding the FIT rate. In addition, in the accelerated reliability testing, a large testing sample size with reasonable testing time, and a large collected data base are essential for developing a reliability accelerated test system. Inadequate reliability testing which results in early product failure could be expensive and highly undesirable in IC manufacturing. For an IC technology to have an excellent yield and reliability, thorough circuit design, well process control, and well reliability will provide a high yield and reliable product. The high yield and reliable processes are critical to the survival of the IC technology at the current competitive marketplace.

VII. CONCLUSIONS

The rapid development of IC technology has created a critical need for advanced polymeric materials as device interlayer dielectrics, passivation layers, encapsulants, and packagings.

Recent advances in high-performance polymeric materials, such as improved silicone elastomers, ultrasoft silicone gels, low-stress epoxies, and low thermal expansion coefficient polyimides, have provided polymers which are compatible with VLSI technology;[83] however, the demands for improved properties of materials in the areas of low dielectric constants, high breakdown voltage strength, high sheet resistance, and less dielectric change with humidity will continue to require the developing of high-performance polymeric materials. Their application in on-chip interconnections and wafer-scale integration architecture structure with very fast interconnecting network and high-performance packaging will become apparent.[84] It is a challenge that the collaborative efforts among polymer chemists, material scientists, and device engineers will face in the near future.

REFERENCES

1. **Moore, G.,** VLSI, What does the future hold, *Electron. Aust.*, 42, 14, 1980.
2. **Sze, S. M., Ed.,** *VLSI Technology,* McGraw-Hill, New York, 1983.
3. **Traeger, R. K.,** Hermeticity of polymeric lid sealants, *Proc. 25th Electron. Components Conf.*, p. 361, 1976.
4. **Grove, A. S.,** *Physics and Technology of Semiconductor,* John Wiley & Sons, New York, 1967.
5. **Wong, C. P.,** Integrated circuit encapsulants, in *Polymers in Electronics,* Vol. 5, John Wiley & Sons, New York, 1986, 638.
6. **Totta, P. A. and Sopher, R. P.,** SLT device metallurgy and its monolithic extension, *IBM J. Res. Dev.*, 13, 226, 1969.
7. **Lepselter, M. P.,** Beam leaded silicon IC, *Bell Syst. Tech. J.*, 45, 233, 1966.
8. **Steidel, C. A.,** Assembly techniques and packaging, in *VLSI Technology,* Sze, S. M., Ed., McGraw-Hill, New York, 1983, 551.
9. **Adams, A. C.,** Dielectric and polysilicon film deposition, in *VLSI Technology,* Sze, S. M., Ed., McGraw-Hill, New York, 1983, 93.
10. **Kern, W. and Ban, V. S.,** Chemical vapor deposition of inorganic thin films, in *Thin Film Processes,* Vossen, J. L. and Ker, W., Eds., Academic Press, New York, 1978, 257.
11. **Kern, W. and Schnable, G. L.,** Low-pressure chemical vapor deposition for very large-scale integration processing — a review, *IEEE Trans. Electron Devices,* ED-26, 647, 1979.
12. **Douglas, E. C.,** Advanced process technology for VLSI circuits, *Solid State Technol.*, 22, 61, 1979.
13. **Vossen, J. L. and Kern, W.,** Thin film formation, *Phys. Today,* 33, 26, 1980.
14. **Hammond, M. L.,** Introduction to chemical vapor deposition, *Solid State Technol.*, 23, 104, 1980.
15. **Rosler, R. S.,** Low pressure CVD production processes for poly, nitride, and oxide, *Solid State Technol.*, 20, 63, 1977.
16. **Brown, W. A. and Kaminus, T. I.,** An analysis of LPCVD system parameters for polysilicon, silicon nitride and silicon dioxide deposition, *Solid State Technol.*, 22, 51, 1979.
17. **Gieske, R. J., McMullen, J. J., Donaghey, L. F., Rai-Choudhury, P., and Tauber, R. N., Eds.,** *Chemical Vapor Deposition — 6th Int. Conf.*, Electrochemical Society, Princeton, NJ, 1977.
18. **Hitchman, M. L.,** Kinetics and mechanism of low pressure CVD of polysilicon, in *Chemical Vapor Deposition — 7th Int. Conf.*, Sedgwick, T. O. and Lydtin, H., Eds., Electrochemical Society, Princeton, NJ, 1979.
19. **Bryant, W. A.,** The kinetics of the deposition of silicon by silane pyrolysis at low temperatures and atmospheric pressure, *Thin Solid Films,* 60, 19, 1979.
20. **Van Den Brekel, C. H. J. and Bollen, L. J. M.,** Low pressure deposition of polycrystalline silicon from silane, *J. Cryst. Growth,* 54, 310, 1981.
21. **Kamins, T. I.,** Structure and properties of LPCVD silicon films, *J. Electrochem. Soc.*, 127, 686, 1980.
22. **Mandurah, M. M., Saraswat, K. C., and Kamins, T. I.,** Phosphorus doping of low pressure chemically vapor-deposited silicon films, *J. Electrochem. Soc.*, 126, 1019, 1979.
23. **Logar, R. E., Wauk, M. T., and Rosler, R. S.,** Low pressure deposition of phosphorus-doped silicon dioxide at 400°C in a hot wall furnace, in *Chemical Vapor Deposition — 6th Int. Conf.*, Donaghey, L. F., Rai-Choudhury, P., and Tauber, R. N., Eds., Electrochemical Society, Princeton, NJ, 1977.
24. **Huppertz, H. and Engl, W. L.,** Modeling of low-pressure deposition of SiO_2 by decomposition of TEOS, *IEEE Trans. Electron Devices,* ED-26, 658, 1979.

25. **Adams, A. C. and Capio, C. D.,** The deposition of silicon dioxide films at reduced pressure, *J. Electrochem. Soc.*, 126, 1042, 1979.
26. **Watanabe, K., Tanigake, T., and Wakayama, S.,** The properties of LPCVD SiO_2 film deposited by SiH_2Cl_2 and N_2O mixtures, *J. Electrochem. Soc.*, 128, 2630, 1981.
27. **Maeda, M. and Nakamura, H.,** Deposition kinetics of SiO_2 film, *J. Appl. Phys.*, 52, 6651, 1981.
28. **Tobin, P. J., Price, J. B., and Campbell, L. M.,** Gas phase composition in the low pressure chemical vapor deposition of silicon dioxide, *J. Electrochem. Soc.*, 127, 222, 1980.
29. **Adams, A. C. and Capio, C. D.,** Planarization of phosphorous-doped silicon dioxide, *J. Electrochem. Soc.*, 128, 423, 1981.
30. **Pliskin, W. A.,** Comparison of properties of dielectric films deposited by various methods, *J. Vac. Sci. Technol.*, 14, 1064, 1977.
31. **Adams, A. C., Schnike, D. P., and Capio, C. D.,** An evaluation of the prism coupler for measuring the thickness and the refractive index of dielectric films on silicon substrates, *J. Electrochem. Soc.*, 126, 1539, 1979.
32. **Nagasima, N.,** Structure analysis of silicon dioxide films formed by oxidation of silane, *J. Appl. Phys.*, 43, 3378, 1972.
33. **Percy, P. S., Stein, H. J., Doyle, B. L., and Picraus, S. T.,** Hydrogen concentration profiles and chemical bonding in silicon nitride, *J. Electron. Mater.*, 8, 111, 1979.
34. **Peters, J. W.,** U.S. Patent 4,371,587, 1981.
35. **Hall, T. C. and Peters, J. W.,** Photonitride passivating coating enhances IC reliability and simplifies fabrication, *Insul. Circuits*, 27(1), 22, 1981.
36. **Ehrlich, D. J., Osgood, R. M., Jr., and Deutsch, T. F.,** Laser microphotochemistry for use in solid-state electronics, *IEEE J. Quantum Electron.*, 16(11), 1233, 1980.
37. **Boyer, P. K., Roche, G. A., and Collins, G. J.,** Laser photodeposition of silicon oxides and silicon nitrides, *Electrochem. Soc. Extended Abstr.*, 82-1, 102, 1982.
38. **Okake, H.,** *Photochemistry of Small Molecules*, John Wiley & Sons, New York, 1978, 219.
39. **Volk, M. C., Lefforge, J. W., and Stetson, R.,** *Electrical Encapsulations*, Reinhold Publishing, New York, 1962.
40. **Kaneda, A. et al.,** Modifications of flow channels in multi-cavity mold die for resin molding of IC devices, *Proc. Int. Conf. Polym. Process.*, p. 349, 1979.
41. **Wong, C. P. and Rose, D. M.,** Alcohol modified RTV silicone for IC device packaging, *IEEE Trans. Components Hybrids Manuf. Technol.*, CHMT-6(4), 485, 1983.
42. **Lee, H. and Neville, K.,** *Handbook of Epoxy Resins*, McGraw-Hill, New York, 1967.
43. **May, C. A. and Tanaka, Y.,** *Epoxy Resins*, Marcel Dekker, New York, 1973.
44. *Encyclopedia of Polymer Science and Technology*, Vol. 6, John Wiley & Sons, New York, 1967, 209.
45. *Advances in Electronic Circuit Packaging*, Vol. 1 to 4, Plenum Press, New York, 1960 to 1963.
46. **Ito, S., Uhara, Y., Tabata, H., and Suzuki, H.,** Special properties of molding compounds for small-outline packaged devices, *36th Electron. Components Conf. Proc.*, p. 360, 1986.
47. **White, M. L.,** Encapsulation of integrated circuits, *Proc. IEEE*, 57, 1610, 1969.
48. **Mancke, R. G.,** A moisture protection screening test for hybrid circuit encapsulants, *IEEE Trans. Components Hybrids Manuf. Technol.*, 4(4), 492, 1981.
49. **Jaffe, D. and Soos, N.,** Encapsulation of large beam leaded devices, *Proc. Electron. Components Conf.*, p. 213, 1978.
50. **Wong, C. P.,** High performance RTV silicones as IC encapsulants, *Int. J. Hybrids Microelectron.*, 4(2), 315, 1981.
51. **Wong, C. P. and Maurer, D. E.,** Improved RTV Silicone for IC Encapsulants, Special Publ. 400-72, Semiconductor Moisture Measurement Technology, National Bureau of Standards, U.S. Government Printing Office, Washington, D.C., 1982, 275.
52. **Wong, C. P.,** Improved room-temperature vulcanized silicone elastomers as integrated circuit encapsulants, in *Polymer Materials for Electronic Applications*, ACS Symp. Ser. 184, American Chemical Society, Washington, D.C., 1982, 171.
53. **Wong, C. P.,** Thermogravimetric analysis of silicone elastomers as integrated circuit device encapsulants, *Am. Chem. Soc. Org. Coat. Appl. Polym. Sci. Proc.*, 48, 602, 1983.
54. **Wong, C. P. and Rose, D. M.,** Modified RTV silicone as device packagings, *33rd Electron. Components Conf. Proc.*, p. 505, 1983.
55. **Wong, C. P.,** Integrated Circuit Device Encapsulants, an intensive short course in Polymers in Electronics, University Extension, University of California, Berkeley, August 1 to 30, 1983.
56. **Wong, C. P.,** IC Encapsulants, in Polymers for Electronic Applications P1-35, Materials Research Laboratory and Center for Continuing Education, State University of New York, New Paltz, November 1983.
57. **Wong, C. P.,** Thermogravimetric analysis of silicone elastomers and IC device encapsulants, in *Polymers in Electronics*, ACS Symp. Ser. 242, American Chemical Society, Washington, D.C., 1984, 285.

58. **Wong, C. P.,** Effects of RTV silicone cure in device packagings, *ACS Polym. Sci. Eng. Proc.,* 55, 803, 1986.
59. **Wong, C. P.,** U.S. Patent 4,278,784, July 14, 1981.
60. **Wong, C. P.,** U.S. Patent 4,318,939, March 9, 1982.
61. **Wong, C. P.,** U.S. Patent 4,330,637, May 18, 1982.
62. **Wong, C. P.,** U.S. Patent 4,396,796, August 2, 1983.
63. **Wong, C. P.,** U.S. Patent 4,508,758, April 2, 1985.
64. **Wong, C. P.,** U.S. Patent 4,552,818, November 12, 1985.
65. **Riley, J. E.,** Ultrahigh sensitive uranium analyses using fission track counting: further analysis of semiconductor packaging materials, *J. Radioanal. Chem.,* 72, 89, 1982.
66. **Noll, W.,** *Chemistry and Technology of Silicones,* Academic Press, New York, 1968.
67. **Wong, C. P.,** U.S. Patent 4,564,562, January 14, 1986.
68. **Wong, C. P.,** U.S. Patent 4,592,959, June 3, 1986.
69. **Saunder, J. H. and Frisch, K. C.,** *Polyurethanes: Chemistry and Technology,* Vol. 1 and 2, Interscience, New York, 1962.
70. **Hepburn, C.,** *Polyurethane Elastomers,* Applied Science Publishers, Englewood, NJ, 1982.
71. **Rubner, R.,** *Production of Highly Heat-Resistant Film Patterns from Photo-Reactive Polymeric Precursors,* Vol. 5, Springer-Verlag, Berlin, 1976, 92.
72. **Pfeifer, J. and Rhode, O.,** Direct photoimaging of fully imidized solvent-soluble polyimide, in Proc. 2nd Int. Conf. on Polyimides, Ellenville, NY, 1985, 130.
73. **Numata, S., Fujisaki, K., Makino, D., and Kinjo, N.,** Chemical structures and properties of low thermal expansion polyimides, in Proc. 2nd Int. Conf. on Polyimides, Ellenville, NY, 1985, 492.
74. **Gorham, W. F.,** A new, general synthetic method for the preparation of linear poly-p-xylylenes, *J. Polym. Sci.,* 4, 3027, 1966.
75. **Bachman, B. J.,** Poly-p-xylylene as dielectric material, *1st Int. Soc. Adv. Mater. Process. Conf.,* 1, 431, 1987.
76. **Sbar, N. L. and Kozakiewicz, R.,** New acceleration factors for temperature, humidity, bias testing, *IEEE Trans. CHMT,* ED-26, 56, 1979.
77. **Wood, J.,** Reliability and degradation of silicon devices and integrated circuits, in *Reliability and Degradation,* Howes, M. J. and Morgan, D. V., Eds., John Wiley & Sons, New York, 1981.
78. **Peck, D. S.,** New concerns about integrated circuit reliability, *Reliability Phys. 16th Annu. Proc.,* p. 1, 1978.
79. **Bailey, C. M.,** Basic integrated circuit failure mechanisms, in *Large Scale Integrate Circuits: State of the Art and Prospects,* Esaki, L., Ed., Lange Voorkout, The Hague, 1982.
80. **Peck, D. S.,** The analysis of data from accelerated stress tests, *Reliability Phys. 9th Annu. Proc.,* p. 69, 1971.
81. **Peck, D. S.,** Practical applications of accelerated testing-introduction, *Reliability Phys. 13th Annu. Proc.,* p. 253, 1975.
82. **Bertram, W. J.,** Yield and reliability, in *VLSI Technology,* Sze, S. M., Ed., McGraw-Hill, New York 1983, 599.
83. **Wong, C. P.,** Can IC surface protection replace hermetic ceramic VLSI packaging?, Program and Extended Abstr., 5th VLSI Packaging Workshop, cosponsored by IEEE-CHMT Society and National Bureau of Standards, Paris, November 17 and 18, 1986, 45.
84. **Neugebauer, C. A.,** Comparison of wafer scale integration with VLSI packaging approaches, *IEEE Trans. Hybrids Manuf. Technol.,* CHMT-10(2), 184, 1987.

Chapter 4

ELECTRICALLY CONDUCTING POLYMERS FOR APPLICATIONS

Stephen T. Wellinghoff

TABLE OF CONTENTS

I. Introduction 94
   A. General Comparison of Materials 94
   B. Limits to Commercial Applications of Conducting Polymers 95
      1. Chemical Instability 96
      2. Processibility of Conducting Polymers 96
   C. Statement of the Problem — Can Intrinsically Conducting Polymers Be Competitive Commercial Products? 98

II. Mechanism of Charge Transport in Conducting Polymers 99
   A. Charge Transport — Simple One-Electron Band Theories 99
   B. Intrachain Transport by Mobile Defects in Conducting Polymers 107
   C. Electronic Interchain Charge Transport in Conducting Polymers 111
   D. Organometallic Charge Transfer Complexes 117
   E. Proton-Assisted Electron Transport 119

III. Processibility and Environmental Stability of Conducting Polymers 121
   A. Environmental Stability of Conducting Polymers 121
   B. Processing Conducting Polymers 126
      1. Rigid Rod Polymers — Nascent Morphology and Liquid Crystal Processing 126
      2. Insoluble Polymers by Thermolysis of Soluble Precursors 128
      3. Hydronium and Hydride Abstraction Route from Precursor to Conductor 129
      4. Solutions of Conducting Polymers in Exotic Solvents 130
      5. Copolymers, Grafting, and Side Chain Modification 131
      6. Composites of Conducting Polymers 134

IV. Some More Applications of Conducting Polymers 134
   A. Linear Optical Properties of Polymeric Conductors 134
   B. Photoconductivity and Devices 139
   C. Nonlinear Optical Properties of Conducting Polymers 142
   D. Electrochemical Devices — Batteries and Chemical Sensors 146

V. Concluding Remarks 149

Acknowledgments 149

References 150

I. INTRODUCTION

In recent times chemists have become increasingly interested in designing new materials which exhibit unique electronic, optical, and mechanical properties. The success of new composite materials which combine the advantages of polymeric, ceramic, and metal components has given rise to a new materials chemistry approach. A prime example of this approach is the recent synthesis of ceramics based on copper oxide that are already achieving superconducting transition temperatures close to 95K.[1] Prior to this, the highest temperature that had been achieved in metal-metalloid alloys was in Nb_3Ge at 24 K.[2] Superconductivity has also been observed in mixed valence charge transfer complexes of organic metals around 1 K[3] and also in polysulfurnitride produced by the solid-state polymerization of cyclic tetramer.[4] Recently, tremendous advances have been made in preparing organic polymers of very high room-temperature conductivities. Using a new synthesis method which avoids defects in the polymer chain, a polyacetylene having almost the same conductivity of copper ($6 \times 10^5\ \Omega^{-1}\ cm^{-1}$) on a comparative volume basis has been developed.[5] This is quite surprising since graphite, which has a two-dimensional network of strong covalent bonds, conducts at an order of magnitude lower level. This is an achievement since most polymers are insulators with a conductivity of less than $10^{-10}\ \Omega^{-1}\ cm^{-1}$.

A. General Comparison of Materials

All these new materials offer certain advantages, but also disadvantages, when compared to elemental metals or their alloys with metalloids. Ceramics, besides having a much higher transition temperature for superconductivity, can be made either in film or monolithic form by low-temperature methods such as sol gel casting.[6] A larger variety of structures, even metastable ones, can probably be made by this technique. Lower energy processes for producing elemental metal alloys of unusual structure are also available, but organometallic vapor deposition,[7] sputtering,[8] and electron beam evaporation[9] are useful only for the manufacture of thin films. Ceramics do have the disadvantage of having no mode of easy dislocation movement as do elemental metals, and are thus very brittle, regardless of the way that they are made. Cold or even hot drawing methods normally used for making wire probably will not be successful for ceramic materials. Some ductility has been seen in thin films of ceramics or inorganic glasses that are strongly bound to substrates[10] or in transformation-toughened zirconia monoliths,[11] but these materials are exceptions. Ceramics are superior to elemental metal alloys in high-temperature creep resistance for this same reason.

Polymeric materials are usually characterized by strong covalent bonds along the polymer chain, while bonding forces between chains are considerably weaker. Polymers thus have lower glass transition temperatures, melting points, and thermal stabilities than ceramics and metals. Solubilities in solvents and low-temperature melt processing are usually advantages that polymers have when it comes to making films and monolith objects. Another advantage is the very large design flexibility that one has with these materials. Not only are there very large numbers of organic monomers available to make organic polymers like polyacetylene and polypyrrole, but organometallic and totally inorganic polymers now can be made. Examples would include polymeric phthalocyanine complexes of elemental metals and metalloids[12] and polysulfur nitride.[4]

In the years since the discovery of conducting polyacetylene in 1977,[13] the hope was that low processing temperatures and design flexibility expected for conducting polymers would lead to a myriad of new applications that originally had included replacing copper in transmission lines, but later, more realistically, settled on predominantly thin-film applications as transparent top contacts on photovoltaics, static dissipation in thin films, electrochromic displays, and battery electrodes (Table 1). At the time of this writing, however, only electrochemically produced polypyrrole latex suspensions with polyanionomeric counterions

Table 1
APPLICATIONS OF MOLECULAR ELECTRONIC MATERIALS[142]

Application	Materials	Significance
Rechargeable battery	Polyaniline; polypyrrole	High energy capacity: 341 W h kg^{-1}; lightweight rechargeable system
	Poly(vinyl pyridine)-I_2	Comprises cathode in LiI battery
Chemical sensors	Phthalocyanine metal complexes in polyphenylene and polypyrrole	
Wiring, coatings, and shielding	Poly(vinyl acetate) doped with $Et_2NH^+(TCNQ)_2$	10^4 Ω cm resistivity, easily produced and fabricated
	Polyacetylene doped with iodine; polypyrrole, electrochemically doped	Conductivity can be varied by selectively doping material (from 1—165,000 Ωcm^{-1})
Transparent conductive thin films	Polypyrrole polymer complexes; polybenzothiophene complexes	Antistatic packaging for semiconductor and electronics industries; high optical transmission and electrical conductivity
Electronic devices	Poly(*N,N'*-dibenzyl-4,4'-bipyridium)	Demonstration of molecule-based rectifier, threshold voltage varied by altering molecular materials used
	Polypyrrole on Si polyaniline between metal electrodes	Used to make organic transistor
Optical display devices	Conducting polythiophene complexes	Produces colored displays with fast switching times and better viewing geometry (no polarizing elements) than LCD devices
	Tetrathiafulvalence or pyrazoline in polymethacrylonitrile doped with $LiClO_4$	
	Poly (3-bromo-*N*-vinylcarbazole); *N,N'*di(*n*-heptyl)-4,4'-bypyridinium dibromide	Very fast (<200 ms) photochromic changes observed High speed, reversible, and exhibits memory effects
Electrophotography	Poly(vinyl carbazole)-trinitrofluorenone	High quantum efficiency CuTCNQ + poly(*N*-vinyl carbazole)-trinitrofluorenone charged by halogen lamp, multiduplication up to 50 copies
	Polycarbonate-triphenylalanine *N,N'*-diphenyl-*N,N'*-bis(3-methyl phenyl)-(1,1'-biphenyl)-4,4'-diamine in polycarbonate	
Photovoltaics	Polyacetylene/n-ZnS	Used in Schottky barrier configuration: polyacetylene bandgap matches solar spectrum well
	Electrochemically doped poly(*N*-vinyl carbozole) mecrocyanine dyes	Conversion efficiencies 0.015—2.00%
Photonic devices (solid-state optical switching elements)	Electrochemically doped polythiophenes	Optoelectronic switching accompanied by optically induced doping; subsequent updoping occurs electrochemically
	Polyacetylene	Highest known nonresonant $\chi^3 = 10^{-8}$ esu

(Polaroid),[14] polypyrrole film (BASF), and perhaps polyphenylene (Allied) and polyaniline (Sieko) can be called even experimental commercial products.

B. Limits to Commercial Application of Conducting Polymers

It is interesting to explore the reasons behind this current lack of commercial acceptance. Before a new product is developed to replace the old, it must be much cheaper to make,

easier to process, more reliable, or safer. Up until very recently no conducting polymer has achieved this combination of properties. Very soon workers in the area realized that polymers such as polyacetylene and polyphenylene would conduct only if their basic structures as wide gap semiconductors were modified by chemical or electrochemical redox reactions to produce mobile enionic or cationic, radical or nonradical species, similar to the introduction of impurity bands in heavily doped III-IV semiconductors. Unfortunately, in most cases these charged carriers were not truly delocalized and noticeable charge would appear at atomic positions that were susceptible to chemical attack.[15]

1. Chemical Instability

For instance, the chemical instability of polyacetylene is caused by an initial reaction with oxygen to produce a p-type semiconductor with a superoxide counterion O_2-. Although an initially stable conducting polymer is formed the counterion eventually attacks the polymer chain at defect positions (sp^3). The product ketone then interrupts transport of charge. This chemical instability can be protected against only by performing the oxidation in strong protonic acids (HBF_4) so the superoxide counterion is immediately destroyed.[16] The other way is to make very perfect, highly crystalline polymeric conductors as has been done recently with polyacetylene.[5] Since the carriers are so delocalized this form of polyacetylene is air stable for days rather than for hours. Oxygen diffusion is also retarded by high crystallinity; however, it is not clear at present whether synthetic methods will be found to produce this perfection of structure in other polymers.

The other strategy is to make polymers whose most reactive positions are protected by substitution with unreactive chemical groups or polymer chain linkages. This approach is successful with heteroaromatic polycationic conductors based on thiophene,[17] pyrrole, and carbazole.[18] Even at the present time, however, there is no effective way to stabilize the very highly reactive n-type polymers in air. This latter fact effectively precludes the development of total polymeric p-n junctions unless steps are taken to encapsulate the junction. Potential microelectronic applications are now limited to Schottkey-type barriers on metals.[19]

Another difficulty that presents itself for making stable gradations in charge density which are necessary for junctions in conducting polymer chains is the self- and electroinduced diffusion of the small counterions. Stable gradations in charge density are impossible due to the diffusion of these carriers between weakly bound polymer chains.[20] Polypyrrole latex materials with polyanionic counterions mentioned above presumably would not have some of these difficulties, but even polymeric chains will diffuse if the matrix is not a rigid glass.[21] A promising approach to this problem is to bind the counterion to the polymer by means of a side chain that is attached at a position that does not interrrupt carrier transport down the chain.[22] This polymeric zwitterion is also stable and soluble in water.

2. Processibility of Conducting Polymers

Polyacetylene appears as a fibrous net (Plate 1*) with enormous surface area when acetylene is polymerized on a catalyst-coated surface. Very good access to an electrolyte would permit this morphology to undergo fast, relatively uniform electrochemical oxidation or reduction.[23] The high potential charge density and access to electrolyte suggest storage batteries with very high-power densities.[24] Polyacetylene is insoluble in all known solvents in which it might be chemically stable and must be used in the nascent, polymerized state. In fact, this is a general property of all rigid rod conjugated or aromatic polymers with no solubilizing groups.[25] The very strong cooperative van der Waals interaction between apolar rigid rod chains and cross-linking either during polymerization or redox doping precludes solubility.

Some rigid rod polymers are soluble in very aggressive protonic acids such as methanesulfonic, fluorosulfonic, and phosphoric acids. These include the polymeric

*See Plate 1 following p. 120.

phthalocyanines[26] and the polybenzobisthiazole materials or ladder-like polymers,[27] all of which can be oxidized to a conducting state after being processed into fibers or films. The former materials can even be cospun with ultrahigh-strength aromatic polyimides out of the same solvent which is removed ultimately by water extraction. Protonation of the polymer on nitrogen positions with unpaired electron density and subsequent generation of a polyelectrolyte is the mechanism of solubilization.

An alternative method for making soluble polymers is to perform the polymerization in a highly polar or polarizable solvent where the solvent can oxidize the polymer *in situ* to a soluble polyelectrolyte. Polyphenylene sulfide conductors are made in the solvent AsF_3-AsF_5,[28,29] while a number of polycarbazole conductors have been made by casting from liquid iodine solution. In the latter case the carbazole monomer is simultaneously cationically polymerized by I^+ and oxidized to conducting polymer in a homogeneous fashion.[30] Although the former method requires a rather poisonous and aggressive medium, the iodine casting process is quite convenient, can be performed in air, and the iodine solvent can be recovered for reuse.

Similar to the approach now being taken in ceramic technology where processible preceramic polymers are first made before conversion to ceramics of limited processibility, soluble precursors to conducting methine-linked heteroaromatics[31] and polyvinylene heteroaromatics[32] or polyacetylene[33] itself have been made. In the former case the oxidant dehydrogenates a solubilizing methylene linkage to a methine linkage which supports charge transport. In the latter situations a fragment is removed from a soluble percursor by thermolysis to yield an apolar conjugated structure which can be oxidized to a conductor.

Electrochemical polymerizations are similar to the above-referenced liquid iodine polymerizations except that an anode initiates the polymerization of the heteroaromatic (pyrrole, thiophene, carbazole, etc.) by generation of a radical cation at the electrode surface, which will then go on to couple with neutral molecules or other radical cations to produce polymer. The electrode will then also oxidize the polymer to a conducting film. Composite conducting films of improved mechanical properties have been made by swelling an electroinactive polymer film with monomer and then electrolyzing to a percolating, fibrous conductor morphology that bridges the carrier film in the form of an inhomogeneous blend.

A clever adaptation of these simultaneous polymerization and doping processes has been made by Japanese workers who have photomasked a substrate to initiate polymerization and conducting polymer formation in selected patterns on a surface that had been pretreated with an initiator.[34] Patterning of sensors and waveguides for certain specialty applications is envisioned for this method.

Inhomogeneous blend films of polyacetylene and other alkene polymers have been made with block and graft copolymerization.[35] The objective was to make soluble copolymers that would form phase-separated blends with topologically connected polyacetylene phases upon casting. The connected polyacetylene phase would then support the current flow after it has been diffusion doped. The approach was quite successful in making some very interesting blends, but problems with environmental stability of the polyacetylene still remained. As mentioned briefly above, the most successful application of blend technology has been to swell nonconducting polymer particles in aqueous or nonaqueous suspension with pyrrole monomer, which is then electropolymerized when the latex particle impinges on the electrode surface. The latex polymer can deprotonate to form a polymeric counterion in response to the formation of an electropositive polymer in its interior. Since the polypyrrole bridges the particle from surface to surface, the latex emulsion can be cast into conductive films. In principle there is no reason why the latex could not be centrifugally cast in the manner of ceramic powder processing[36] to produce thick monoliths that could be annealed (or sintered) void free and subsequently machined to specifications.

Simple powder metallurgical techniques such as vacuum sintering have been employed

to make thick battery plaques of thermally stable polymers such as polyphenylene and its oligomers.[37] Invariably, these objects are of low strength because of the unavoidable growth of voids during the sintering process. This type of process is of considerable interest in the manufacture of ceramic monoliths from powders. Polyphenylene is really no different from ceramics from the mechanical point of view, since its rigid chain structure precludes any low-temperature dynamic mechanical relaxation processes that might induce ductility. The problem of void generation and embrittlement is still present in ceramics processing, but is probably avoidable once mixtures of precisely monosized particles can be made.[38] There is considerable potential to use the well-known emulsion polymerization techniques to produce lattices of 500 Å, which can then be swollen by electroactive monomer to monosized particles ten times larger and then polymerized to almost pure conductive polymer.[39]

Spurred perhaps by the observation that highly conducting polypyrrole charge transfer complexes could be formed even with long, surfactant-like counterions, chemists have recently synthesized monosubstituted polythiophenes with attached alkyl and alkoxyether side chains longer than butyl[40-43] that are soluble in a wide variety of solvents at DP (degree of polymerization) greater than 300. In some cases the conducting charge transfer complex is also soluble and will produce films of 1 to 1000 Ω^{-1} cm^{-1} upon recasting. Recently, random copolymers of thiophene with methyl methacrylate have also been made.[44] Coupled with the conducting, water-soluble, zwitterionic side-chain derivatives of polythiophene mentioned above, it is clear that a new class of especially processible conducting polymers has been made.

C. Statement of the Problem — Can Intrinsically Conducting Polymers Be Competitive Commercial Products?

The above overview was meant only to give an introduction to the problems that face the commercial introduction of intrinsically conducting polymers. Until the development of the new ultrahighly conducting polyacetylene there was no hope that conducting polymers could be used in bulk applications, like wire or cable. Even the new polyacetylene needs improved environmental stability before it can even hope to compete with aluminum alloy lightweight conductors which are already well established. Of course, a breakthrough such as close-to-room temperature superconductivity would change all this. In fact, this author believes that the usefulness of this new material will be predominantly theoretical, leading to synthetic design concepts which will ultimately produce tough superconducting wire and films with high superconducting transition temperatures. The wise materials chemist will position himself so that he might be able to take advantage of concepts that might drop out from junctures between this field and the superconducting ceramics area.

Electromagnetic insulation (EMI) of electric components has been proposed as an application of conducting polymers, but metal and graphite-filled epoxy and composites with engineering thermoplastics[45a,45b] will be very difficult to dislodge from this market. At present there is also much activity in preparing conducting polymers for the secondary battery market where p-type polyphenylene,[46] polypyrrole,[47] polythiophene,[48] and polyaniline[49] anodes are coupled with Li metal cathodes. All polymer batteries are considered hopeless now because of the absence of an appropriate n-type polymeric cathode material. Polyacetylene anodes are no longer a factor because of coulombic inefficiencies[50] and chemical instabilities during deep discharge.[51] The hope for polymeric anodes lies in improving their charge density so that greater watt hours/liter can be obtained.[52]

There has been some effort in the area of polymer thin-film heterojunctions with III-IV semiconductors[53] and Schottkey barriers with elemental metals.[54] Every application, however, is plagued with very high interfacial trap densities due to defects and disorder in the polymer, in addition to the previously mentioned counterion diffusion problems.[22] This leaves applications such as cheap solar cells and photoelectrochemical conversion in doubt.

In the former area amorphous and polycrystalline silicon solar cells already have much higher efficiencies, are quite inexpensive, and still will have a hard time competing with single-crystal cells. Recently, polymeric conductors that are transparent in the visible have been made.[55,56] Conductivities and environmental stability are still problems. On the other hand, new cheap, organometallic precursor routes to indium tin oxide (ITO) alloys are under intense development, as any superficial perusal of the recent Japanese patent literature will attest to.[57] ITO alloys have much higher conductivity ($10^4\ \Omega^{-1}\ cm^{-1}$) and higher environmental stabilities, at least at present,[58] and thus they will probably remain preeminent in transparent contacts for displays and other transparent contacts for some time.

Polymers could have a strong market position in areas where a designed complicated structure is an advantage. Electrochromic displays or filters are a strong possibility in that the optical absorbance of electrically conducting polymers is a strong function of the degree of oxidation.[59] Considering the myriad of copolymers that can be made, the redox switched absorption characteristics one could build in are almost limitless. The only problem that might arise is switching speed limitations caused diffusion speeds of counterions into the films.

The necessary absorption and release of counterions that occur upon redox of a conducting polymer that is a problem in battery technology and fast electrochromic displays can be turned into an advantage. For example, polythiophene-type polymers have been used to store glutamate counterion anions that can be released upon reduction of the polymer.[60a] One can envision such a system for controlled release of drugs, but the market potential is significant only for the release of cationic drugs. Recently, the same authors have released the protonated form of dopamine by using a complex of poly *n*-methyl pyrrole cation and polystyrenesulfonate counterion.[60b] Drug cation is incorporated into the polymer film by reduction of the polymer chain. The drug is then released by oxidizing the film with the polymeric anion remaining bound to the polymeric cation. Electrically controlled ion exchange resins or ion barriers are other similar applications.

During studies of conducting polymers for battery applications, conducting polymer electrodes have been found to catalyze the decomposition of the electrolyte. There is still clear and as yet relatively unexplored application for polymeric conductors in electrocatalysis.

A very recent effort has been made to measure the nonlinear optical properties of conducting polymers.[61] Nonconducting polydiacetylene already was known to have the highest nonresonant third-order nonlinear optical coefficients of any material[62] because of its very extensive π-conjugated backbone and highly nonparabolic band edges.[63] If carriers are introduced there is every reason to believe that much higher coefficients will be obtained in these highly anisotropic materials.[64] The secret to success here will be to make materials that have wide band gaps (or windows of transparency) at low intensities, but will reversibly switch to narrow gap materials in the picosecond time scale to induce nonlinear absorption or reflection effects.

As the above discussion indicates, there is substantial application for conducting polymers, but their present disadvantages must be realized and taken into account. The materials and applications chemist wanting to make or use conducting polymers must have a better understanding of the theoretical underpinnings to conductivity in conducting polymers and more details about the experimental results than the above discussion provides.

II. MECHANISM OF CHARGE TRANSPORT IN CONDUCTING POLYMERS

A. Charge Transport — Simple One-Electron Band Theories

Characteristically, the conductivity of metals even semimetals such as graphite decreases with increase in temperature.[65] So far only polysulfurnitride among polymers has clearly shown this behavior; however, molecular metals such as tetrathiofulvalene (TTF) charge

Alternate Single-Double Bond Polyacetylene

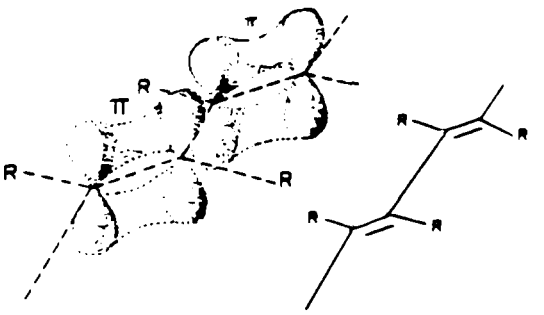

FIGURE 1. π-Electron-conjugated structure.[62]

transfer complexes with tetracyanoquinodimethane (TCNQ) also exhibit this behavior in single crystals.[66] The rationale for this temperature dependency is that the extended orbital network is fragmented by transient lattice vibrations (phonons) which become more numerous as the temperature increases. The one-dimensional nature of the orbital network and very strong coupling between the orbitals responsible for covalent binding and those responsible for electron delocalization assures that there will be very strong coupling between phonons and carriers in materials such as polyacetylene and polyphenylene. Permanent distortions such as those present at crystalline grain boundaries also contribute to reducing the electron mobility and, thus, usually the conductivity. This type of defect carrier scattering, however, yields no temperature dependence of the conductivity.

Electron orbitals in a periodic solid have a quantized energy range of values that increases as the binding between adjacent atoms increases. The collection of p_z orbitals (one from each of the two carbons in the unit cell of *trans*-polyacetylene) that interact in the x direction of the carbon chain of polyacetylene overlaps to form the uppermost filled π crystal orbital (HOMO). The remaining three electrons of carbon fit into sp^2 orbitals which form σ bonds with adjacent carbons and the attached hydrogen and are unimportant in conduction (see Figure 1 for the corresponding example of polydiacetylene).

The exact form the extended wavefunctions take in the crystal, along with their corresponding energy values, can be calculated by a variety of methods which include various approximations to the energy hamiltonian.[67] The specific details of these methods are beyond the scope of this review; but we will discuss one-dimensional conductors in terms of an approximate tight binding method, the rudiments of which can be found in Reference 68, so that the reader can get the flavor of conduction processes.

The hamiltonian that is used to describe the motion of electrons in a solid consists of two parts, an operator (p^2, $p = -ih\,d/dx$) that yields the kinetic energy of the electron and a part that describes the potential energy the electron experiences in the lattice [U(x)]. Both of these factors operate on the electron amplitude function to yield the energy eigenvalue, e_k, of each specific wavefunction solution.

$$[(1/2m)(p^2) + U(x)]\exp(ikx)u_o(x) = e_k \exp(ikx)u_o(x) \quad (1)$$

where m = the mass of the carrier and k = 2π/(wavelength) of the electron particle in the

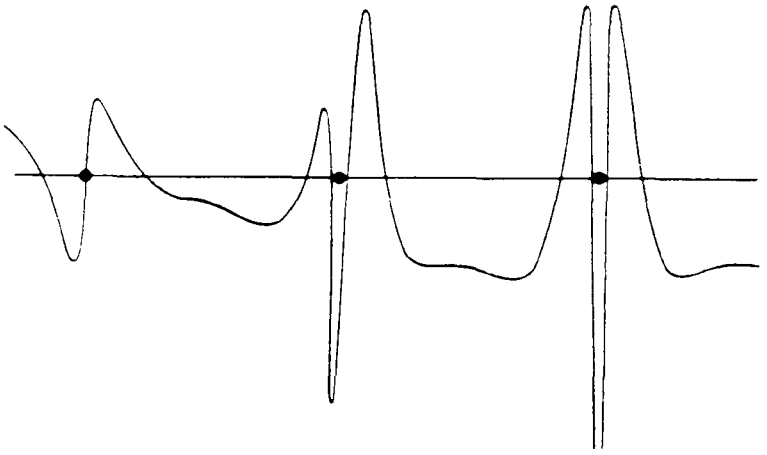

FIGURE 2. Real part of wavefunction, ϕ, plotted as a function of distance along a line of atom centers in sodium. (Adapted from Slater, J. C., *Phys. Rev.*, 445, 794, 1934.)

lattice, $i = (-1)^{1/2}$. u_o represents the simple additive contributions of the p_z orbitals of the carbon atoms in the lattice (Figure 2) and is rapidly varying in amplitude in the vicinity of the carbon nucleus. In Figure 2 the overall behavior of a p orbital is simulated by an s orbital for clarity of presentation because of the complicated node structure of the p orbital. This wavefunction is simply the most highly symmetric bound state that most chemists are familiar with and will contain two electrons.

In a periodic solid, however, N atoms in a line of length L is modeled by closing a long-enough line of atoms into a loop by attaching the beginning and end of the string. The electron amplitude must have the same value at the start and end of the string to maintain continuity. However, since once attached, the beginning is no longer known, the amplitude of the wavefunction is not preferentially maximum at any point over time and its probability of being found on any part of the string must be uniform. The so-called traveling wave, $\Phi = \exp(ikx)$, meets these specifications, since $\Phi\Phi^*$ = probability of finding the electron at x is a constant. Φ is a solution of Equation 1 when $U(x) = 0$ and the energies are quantized in quantum number, k, with $-k$ and $+k$ being degenerate solutions, each holding two electrons. $-k$ and $+k$ represent electrons with momenta; $p = -hk$ or $+hk$ in opposite directions.

The energy of the electrons is purely kinetic ($p^2/2m$). In order to meet the periodic boundary conditions of the problem $k = 0, \pm 2\pi/L, \pm 4\pi/L, \ldots, \pm n\pi/L$. The ground state of the material with N atoms in length L will then consist of filled levels between $k = 0$ and $n = 2(N/4)$ for large-enough N. For very large N and L, typical for a truly electron-delocalized solid, the energy level spacing will be much less than kT and no activation energy will be required to change k state. The density of states in this band of energies, $D(E) = d(\text{states})/dE$, is a more convenient factor to work with when extended states are considered.

Of course, no solid consists of free electrons that are unaffected by the attractive potential of the ion cores, their own coulomb repulsion, or stabilizing exchange interactions. Surprisingly, the last two interactions often can be ignored to get a basic idea of the band structure; therefore, we will consider only the first.

Polyacetylene has two atoms per unit cell of length a, each contributing one electron to the π system, and, thus, a set of M cells, each of length a, will have a total length $L = Ma$, and contribute 2M electrons to the band which will then fill up to level, $k = \pm M\pi/L$ or $k = \pm\pi/a$. At these first Brillouin zone boundaries, $k = \pm\pi/a$, the uppermost occupied level consists equally of waves traveling to the right and to the left; the only time-independent solutions are

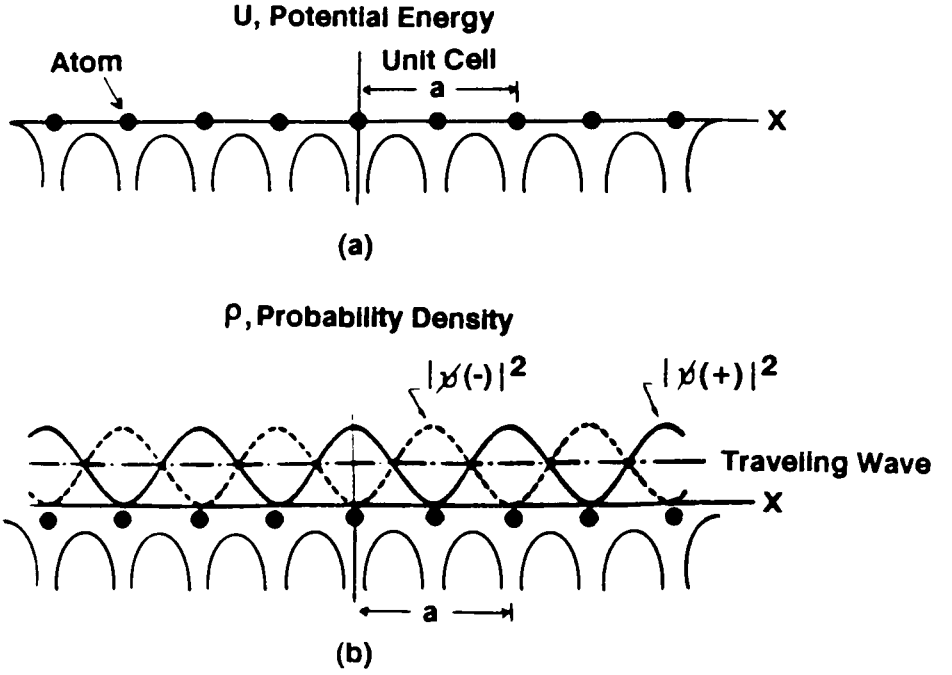

FIGURE 3. (a) Potential energy of conduction electron in field of ion cores; (b) distribution of the probability density of $|\phi(+)|^2$ and $|\phi(-)|^2$ in a linear lattice of *trans*-polyacetylene.[2]

$$\Phi(+) = \exp(i\pi\chi/a) + \exp(-i\pi\chi/a) = 2\cos(\pi\chi/a), \quad |\Phi(+)|^2 \overset{2}{\approx} \cos^2\pi\chi/a$$

$$\Phi(-) = \exp(i\pi x/a) - \exp(-i\pi x/a) = 2i\sin(\pi x/a), \quad |\Phi(-)|^2 \overset{2}{\approx} \sin^2\pi x/a \qquad (2)$$

The now-standing wave electron probability, $\rho = |\phi|^2$, maximizes at the unit cell center and edges, respectively, for $\phi(+)$ and $\phi(-)$ (Figure 3).

In the case of *trans*-polyacetylene the two atoms in the unit cell are related by a screw translation symmetry, which makes the p orbitals indistinguishable insofar as the one-dimensional crystal potential goes. Thus, the potential can be modeled as

$$U(x) = U_{<200>}\cos\pi x/a \qquad (3)$$

which maximizes at the atomic positions located at the (200) planes of the unit cell. This crystal potential will give rise to an energy difference between the two standing wave states or energy gap, E_g, at $k = \pm 2\pi/a$ (Figure 4).

$$E_g = 2U_{<200>} \int_{+1}^{-1} dx(\cos\pi x/a)[\cos^2(\pi x/a) - \sin^2(\pi x/a)] = U_{<200>} \qquad (4)$$

We thus conclude that *trans*-polyacetylene will be a material with a half-filled band.

A more accurate picture would, of course, include the p orbital, $u(x - x_j)$, positioned at each j site in the lattice right from the very beginning of the calculation. In effect, this inclusion would simply set the potential energy of the band at $k = 0$; kinetic energy contributions from the occupied traveling wave levels would determine the band width up to the k where the energy gap appeared. Wigner and Seitz showed that this was a good

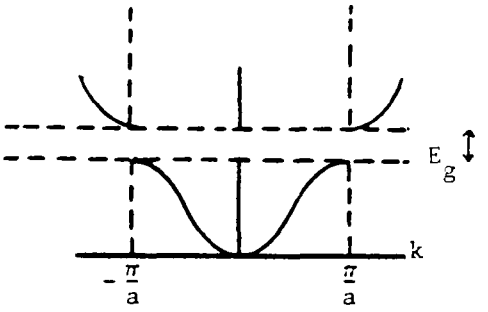

FIGURE 4. (a) Plot of energy vs. wavevector for a free electron; (b) plot of energy vs. wavevector for an electron in a monatomic lattice of lattice constant, a.[2]

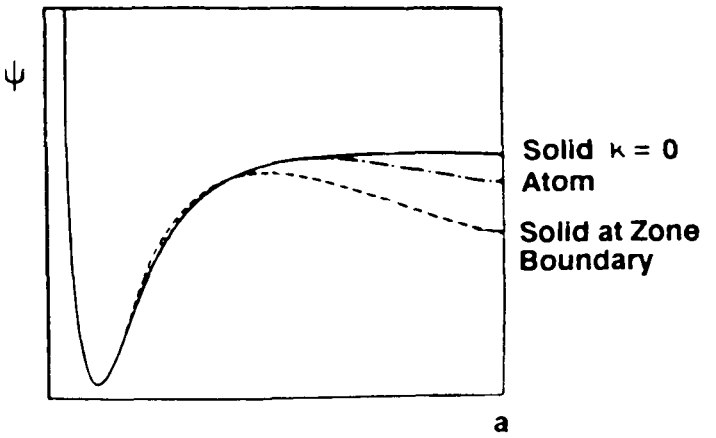

FIGURE 5. Radial wavefunctions for the 3s orbital of free sodium atom and for the 3s conduction band in sodium metal.[2]

approximation for the band structure of alkali metals and their method, in essence, involves solving Equation 1 with an appropriately simple potential coefficient as in Equation 3. Figure 5 shows that the wavefunction is perturbed only at distances far from the atom core at $k = 0$ and $k = \pi/a$.

The final degree of sophistication we will consider will be the so-called tight binding method, since this relates directly to the Huckel molecular orbital description familiar to most chemists. Here, the wavefunction of the crystal is described by

$$\phi_k(x) = M^{-1/2} \sum_j \exp(ikx_j)u(x - x_j) \tag{5}$$

where the summation is over all atomic positions M — u, in our case, being p_z. The first-order energy for this wavefunction is the diagonal matrix element of the crystal hamiltonian, where if only nearest-neighbor interactions are considered is

$$\langle k|H|k\rangle = -\alpha - \beta \sum_m \exp(-iky_j) \tag{6}$$

where $\alpha \equiv$ coulomb integral $= \int u\, H_m u\, {}^*{}_m dV$ and $\beta \equiv$ resonance integral $= \int u_m H u_n dV$ between nearest neighbors.

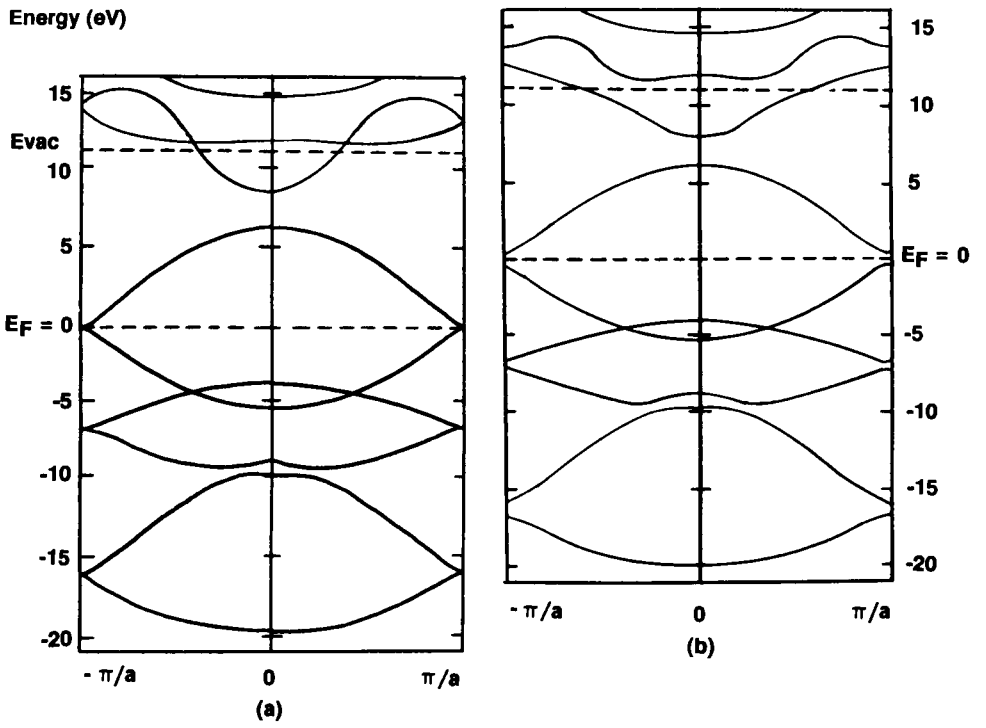

FIGURE 6. Band structure of one-dimensional *trans*-polyacetylene for two choices of bond length: (a) uniform (1.39 Å); (b) weakly alternating (C=C: 1.36 Å, C–C: 1.43 Å).[69]

In *trans*-polyacetylene nearest neighbors are present at $\pm a/2$; therefore,

$$e_k = -\alpha - 2\beta(\cos ka/2) \tag{7}$$

A plot of this band structure for *trans*-polyacetylene is shown in Figure 6a[69] in the reduced zone scheme. At $k = 0$ the resonance interaction is the strongest and the energy is at its most negative ($-\alpha - 2\beta$). The energy increases with wavevector until π/a, where the highest occupied or Fermi level lies at α. Since π/a and $2\pi/a$ are connected by a unit cell translation vector, a, the branch of the energy curve from π/a to $2\pi/a$ is reflected back to $k = 0$ (or equivalently $2\pi/a$), where the energy reaches $-\alpha + 2\beta$. The total bandwidth is thus 4β up to the energy gap that is defined by the crystal structure. Clearly, the stronger the bonding between atoms the wider the band.

It is now time to consider what happens when an electric field is applied to electrons pictured in band scheme Figure 6a. In the absence of an electric field, since $-k$ and $+k$ orbitals are equally occupied for each energy, no net carrier transport occurs. Once the field is applied, however, carriers are attracted to the positive electrode, biasing the electron distribution toward, for example, $+k$ momentum states at the expense of $-k$ states. The electrons which once resided in a $-k$ state will be promoted to a higher $+k$ state by the field. Each of the carriers across the entire band will experience this shift and be continuously accelerated toward the electrode until scattered either elastically by a phonon or inelastically by some static defect back in the opposite direction (e.g., $+k \rightarrow -k$). Thus, the electron distribution does not continually grow in kinetic energy, but dissipates its energy into heat. The effect on electron flow is that there is a biased drift of electrons toward the electrode at a drift velocity.

$$v_d = eE_f\gamma/m \tag{8}$$

where e is unit charge, m = carrier mass, γ = time from v = 0 to maximum v_d at scattering, and E_f = electric field.

If there are N electrons per cubic centimeter, the electric current density in terms of number of charges/square centimeter/second is

$$j = Nev_d \tag{9}$$

or since $j = \sigma E_f$, $\sigma = Ne^2\gamma/m$ or Ohm's law, or if $\mu = e\gamma/m$

$$\sigma = Ne\mu \tag{10}$$

where Ne is coulombs/cubic centimeter and μ = cm²/V-s (in CGS units μ is 300 times higher and is expressed in cm²/statV-s). Since V = IR, an ohm is defined as a current, I, in coulombs/second dropping through a potential difference of 1 V; the conductivity, σ, is expressed in Ω^{-1} cm^{-1}.

One is now rapidly able to distinguish the important factors for high electrical conductivity. A high electron density, N, is obviously important as is a high electron mobility. If all the p_z electrons of the polyacetylene participate in the conduction process, the conduction electron density will be 4.2×10^{22}/cc vs. 8.4×10^{22}/cm³ for copper. If the mobilities are similar we would expect similar conductivities $\approx 10^5$ Ω^{-1} cm^{-1}.

Since the electrons are not completely free in polyacetylene but move instead in a lattice, the carrier mass is not that of a free electron; instead an effective mass, m*, is observed. This mass is inversely proportional to the curvature of the e vs. k relationship

$$m^* = \hbar^2(d^2e_k/dk^2)^{-1} \tag{11}$$

or, using Equation 7,

$$m^* = 2\hbar^2/\beta a^2 \tag{12}$$

Table 2[69] lists the resonance integrals for organic metals and organic conductors of various kinds. The carrier masses expected for π delocalized polymers at resonance integral values of several electronvolts is comparable to the mass of a free electron at least in the direction of strong bonding. Since the bands of elemental metals are also several electronvolts wide, the carrier-effective masses should be about the same. If the time between scattering, γ, is also comparable, polyacetylene should therefore conduct just as well as copper in the chain direction. "Intrinsic" *trans*-polyacetylene has a conductivity of 10^{-5} Ω^{-1} cm^{-1}, however, ten orders of magnitude lower than copper!

What has caused this disagreement with expectations is the instability of a uniform π electron density to bond alternation in a one-dimensional system, the Peierls instability. This distortion is periodic in the lattice and will open up a band gap at the Fermi level at $\pm\pi/a$ (Figure 6b). The experimentally observed gap is 1.5 eV, which is less than the 2.3 eV expected for alternate double and single bonds. The structurally related $(SN)_x$, a three-dimensionally bound structure, is not susceptible to this distortion and thus behaves as a metal.[70]

Since the electrons all exist in completely filled bands, an electric field cannot perturb the momentum distribution of the electrons at absolute zero and no current may flow. At finite temperatures the Fermi-Dirac distribution which defines the occupation probability of the orbitals is no longer a box function with a dropoff at the Fermi energy, but develops a Boltzman-like tail with the Fermi energy, E_o, now appearing at midgap (Figure 7). The Fermi-Dirac distribution is

Table 2
VALUES OF THE RESONANCE INTEGRAL (β), EFFECTIVE MASS (m*), AND BAND GAP (E_G) FOR VARIOUS ORGANIC CRYSTALS AND POLYMERS[69]

Compound	β (eV)	|m*/m|
Anthracene	2.5×10^{-3}	11
(TTF) (TCNQ)	0.15 (‖)	2.5
	1.7×10^{-3} (⊥)	
$(SN)_x$	2.50 (‖)	1.0
	0.25 (⊥)	2.0
trans-$(CH)_x$	3.00 (‖)	0.5
cis-$(CH)_x$	2.60 (‖)	0.5
	0.10 (⊥)	
Polypyrrole	3.0 (‖)	0.5
Poly(*p*-phenylene)	2.0 (‖)	0.5

Note: ‖ Refer to the chain axis or direction of high conductivity.

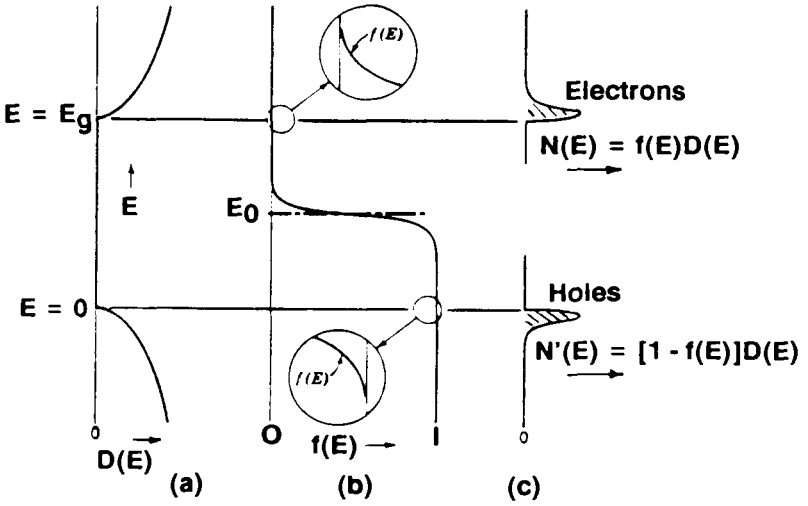

FIGURE 7. Carrier population in intrinsic semiconductor. (a) Density of states; (b) Fermi function; (c) densities of holes and electrons.[65]

$$f(E) = \{\exp[(E - E_o)/kT] + 1\}^{-1} \tag{13}$$

When the electrons leave the filled band they leave an equal number of holes (positively charged carriers) behind. The Fermi energy (or electrochemical potential) appears at midgap so the distribution function may balance the population of the two bands properly.

When the conductivity equation is written for semiconductor such as this, the total number of carriers contributing to the conduction process will be much less than a good metal and will depend in an exponential fashion on the band gap.

$$\sigma = N_e e\mu_e + N_h e\mu_h \tag{14}$$

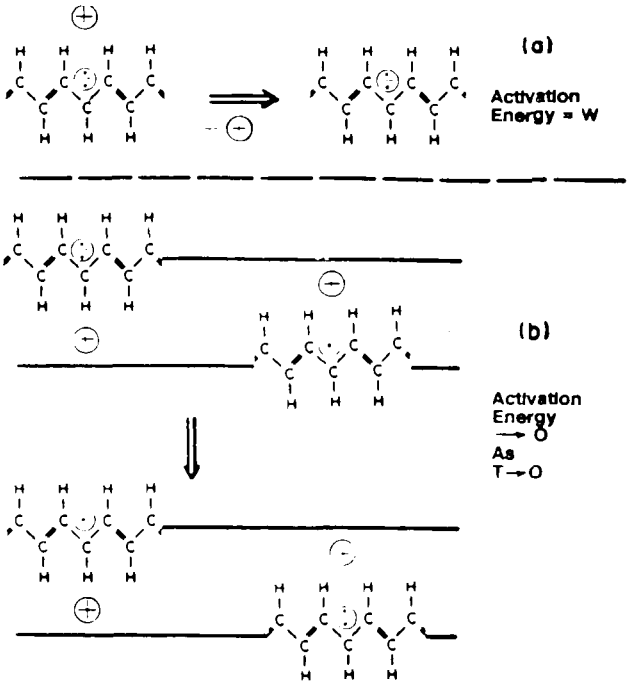

FIGURE 8. Schematic representation of soliton conduction. (a) Free soliton in which a bound charged soliton is thermally liberated; (b) hopping of an electron between soliton-bound states. The + represents a positively charged impurity.[72]

where electron and hole mobilities must be considered separately. Because of the temperature dependence of the population of phonon levels the mobilities are temperature dependent. For example, at 4 K the electron mobility in PbTe is 5×10^6 cm^2/V-s, while at room temperature it is 1.6×10^3 cm^2/V-s. The thermal population of levels is much more important in the high temperature range and the conductivity can be expressed as

$$\sigma = Ce(\mu_e + \mu_h)\exp(-E_g/2kT) \tag{15}$$

where C contains factors related to the density of states in relevant parts of the bands.

B. Intrachain Transport by Mobile Defects in Conducting Polymers

The temperature dependence of the conductivity of intrinsic polyacetylene does not seem to obey relationship 15, however. The conductivity of polyacetylene at low impurity level is quite "subactivated" in that a plot of $-\ln\sigma$ vs. $(1/T)^{(1/m)}$ is linear with $m > 1$.[71] A fairly strong electron spin resonance signal is also observed for "intrinsic" *trans*-polyacetylene which always contains minute amounts of charged impurities and defects due to the *cis-trans* isomerization process. The first of these generates charged solitons which have no spin, and the latter solitons with spin. A soliton in this system is a domain wall between alternate phases of double- and single-bond alternation. Since there is no change in net energy when the domain wall moves one bond, the ground state is degenerate, a necessary condition for soliton existence. The soliton state appears at midgap at π/a.

When an electron is removed from a soliton by a catalyst impurity a charged soliton is formed which is pinned to the impurity center. If, however, two impurity sites are close together, there is potential for the pinned, charged soliton to exchange with a propagating soliton on an adjacent chain with little change in net energy (Figure 8). Lattice phonons

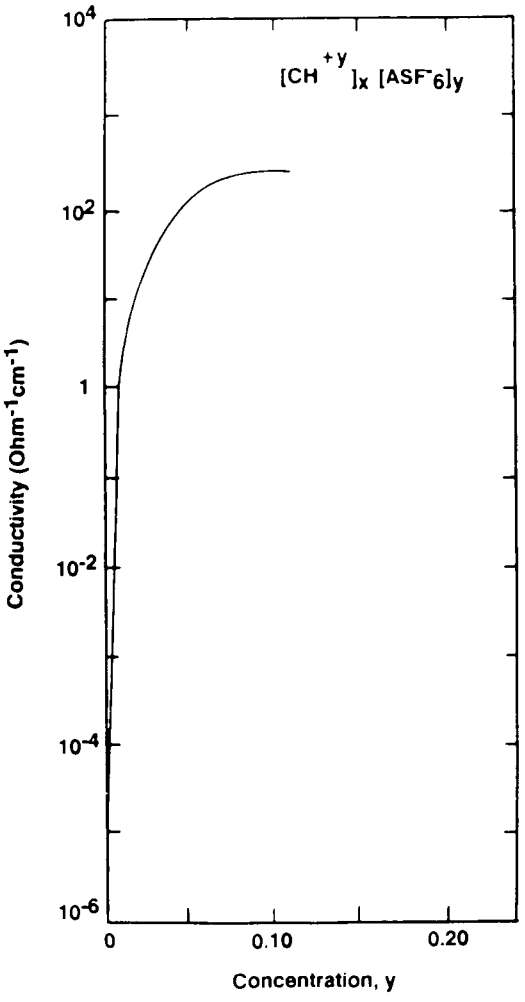

FIGURE 9. Electrical conductivity of doped *trans*-polyacetylene film as a function of degree of oxidation.[13]

will thus induce a hop of the charge between chains. Kivelson[72] has shown that a theory of this sort explains the transport properties of *trans*-polyacetylene quite well in the close-to-intrinsic region. This theory bears some similarity to the fixed-range hopping model for conduction in amorphous semiconductors, with the exception that at least one of the defects is dynamic in polyacetylene. In the strict fixed-range hopping model the carriers tunnel between totally pinned states of similar energy.[73]

Early on workers found that polyacetylene could be oxidized or reduced with the appropriate acceptors or donors. The same could be accomplished at a controlled potential on an electrode surface to generate mobile radical cations or anions in the polymer chain associated with an "inert" counterion.[16] In order to match convention with solid-state physics practice the polymeric cation-rich materials were called p-doped, while the polymeric anion-rich materials were called n-doped. The conductivities rose over ten orders of magnitude (Figure 9) with the addition of only a few percent of the redox agent. Of great interest, besides the obvious practical interest in the existence of such a highly conducting polymer, was the observation that the Pauli magnetic susceptibility did not increase markedly until well into the metallic regime beyond 7% added oxidant. Large Pauli susceptibilities are obviously characteristic of free electrons with spins in the conduction bands of metals. Spinless carriers seemed to be carrying the current in even metallic-like polyacetylene!

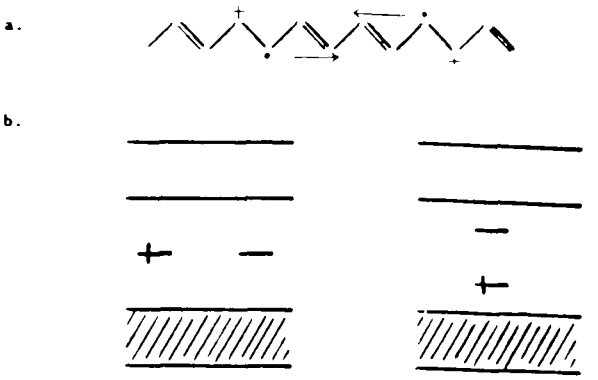

FIGURE 10. (a) Generation of two charged solitons by the annihilation of unpaired electrons; (b) singly occupied, degenerate soliton level at midgap (left); singly occupied polaron level.[74]

Further theoretical calculations[74] solved this problem by showing that, first of all, solitons could not be generated intrinsically as pairs (soliton-antisoliton) without collapse, and therefore could be important only as extrinsic impurities at very low doping levels. If, on the other hand, an electron was added to or removed from the pair, a stable polaron-soliton pair would be generated with very weak binding between the two chain defects. Because of the interaction between the wavefunctions of the two defects two new states are created in the gap, one bonding level occupied by one electron in the case of oxidative doping and an empty antibonding level (Figure 10). Further, because of significant binding between the polaron and a counterion, the solitons diffuse away from their associated polaron to annihilate with another soliton from an adjacent polaron-soliton pair to produce a new double bond and a spinless charged soliton pair (Figure 10). An empty charged soliton band arises midgap the material conducts by a spinless mechanism as observed.

At high concentrations of charged solitons the wavefunctions of these defects will interact sufficiently to broaden the charged soliton band into the valence and conduction bands eliminating the energy gap. At this point ordinary metallic conductivity with spin is observed.

A similar situation arises with aromatics such as polythiophene, poly *p*-phenylene, polypyrrole, and many others. As background, a listing of several of these intrinsic insulators or semiconductors appears in Table 3[76] along with their band gaps. Unlike polyacetylene and poly *p*-phenylene a number of electron-rich polymers with low electron affinities do not form reduced conducting states. These include polypyrrole and polythiophenes; however, all will form p-type materials. At present no truly electron-deficient polymers have been made that would show n-type behavior preferentially. Most of the listed materials have similar conduction mechanisms when doped, in that, unlike polyacetylene, they have no degenerate ground state and thus no solitonic carriers, but like polyacetylene, exhibit a spinless carrier mechanism as the transition to a metal takes place.

Figure 11 represents the evolution of the band structure in the prototypical n-doped poly *p*-phenylene. First, polarons are generated by adding an electron to an extended quinoidal segment. This carrier will proceed down the chain under the influence of the applied electric field by means of a phonon-assisted hopping mechanism and the material will conduct as a semiconductor with finite spin carriers. The radical is strongly coupled to the charge by a rather strong lattice relaxation, thus defining a width of about four to five quinoidal-type rings over which the radical anion is delocalized. Two polaron states are present in the gap. In the case of n-doping the upper band is half filled while the lower band is half filled for p-doping. Calculations predict that two of these polarons are unstable to condensation to a bipolaron or dianion with no spin.[75,76] At high-enough doping levels two in-gap bipolaron

Table 3
EXPERIMENTAL E_gs FOR CONDUCTING POLYMERS

Polymer	Experimental (EG/eV)
	1.8
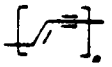	2.1
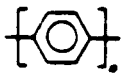	3.4
	4.9
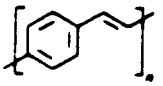	3.0
	3.0
	2.7
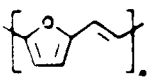	2.4
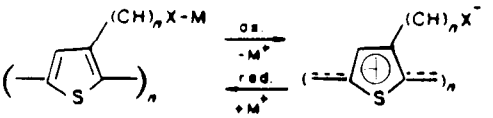	2.2
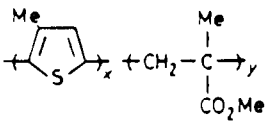	3.4
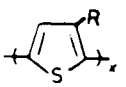	1.5

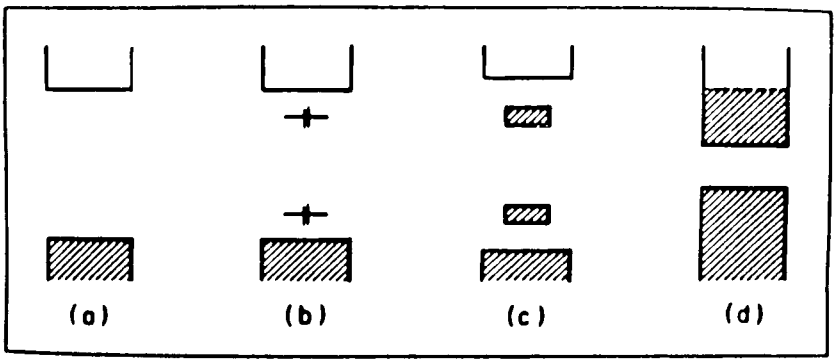

FIGURE 11. Evolution of the band structure of polyparaphenylene anion. (a) Neutral; (b) intermediate level with bipolaron states (delocalized dianion) in the gap; (c) 50% reduction and formation of bipolaron bands; (d) 100% reduction level (one anion/monomer).[75]

bands will appear at the expense of the polaron bands. These will be completely filled in the case of n-doping or empty for p-doping. Metallic-type conductivities are achieved at this stage even in the presence of completely filled bands! As in polyacetylene these dynamic impurity bands will finally close with both the conduction band and valence bands to generate an orthodox metal. This situation is certainly much different than the usual semiconductors and metals and is directly assignable to the reduced dimensionality of the polymer system, where electron phonon coupling processes give localized states a very important role in the conduction processes.

C. Electronic Interchain Charge Transport in Conducting Polymers

So far we have neglected the transport between chains, which is, of course, necessary before any DC conduction process can be observed. The crystal structures of undoped polyacetylene and poly *p*-phenylene reveal that there is little chance of π-π overlap between chains in the form of a sandwich complex. However, upon oxidation or reduction, the polyionomeric chains appear to form separate stacks with channels of counterions in-between.[77] Polypyrrole can also be prepared with very long soap-like counterions in highly conducting form with sandwich-like stacks of partially oxidized polypyrrole chains and separate lamellae of soap molecules (Figure 12). DC conduction in this latter structure can be rationalized only if the stacks of polypyrrole chains interpenetrate by sharing chains, since the soap channels would not be expected to be electronically conducting.

There is massive literature on low molecular weight organic metals, or even superconductors, that form separate adjacent stacks of donor and acceptors.[78-81] In the case of intercalation between donor and acceptor molecules insulating states are always generated, except for the case of two-dimensional graphite intercalates.[82] Another requirement for good conduction is partial charge transfer between the donor stack and acceptor stack. Complete charge transfer invariably prevents electron hopping between the aromatic molecules that make up the stack or even metallic band formation because of mutual electron repulsion. A Wigner lattice of frozen spins is formed in this case. If only partial charge transfer takes place, as in the one-to-one salt of the acceptor, TCNQ, and the donor, TTF, very high conductivities of $10^4\ \Omega^{-1}\ cm^{-1}$ and metallic temperature dependency are obtained.

In order for the charge to jump from one chain to the other, there must be extensive intramolecular charge delocalization over the jump position. Figure 13 illustrates this requirement. In (a) the dimeric unit A-B contains a delocalized charge which can jump to an uncharged A-B of the same symmetry with little change in energy. The dimeric unit in (c), on the other hand, contains a relatively localized charge. The intermolecular jump then

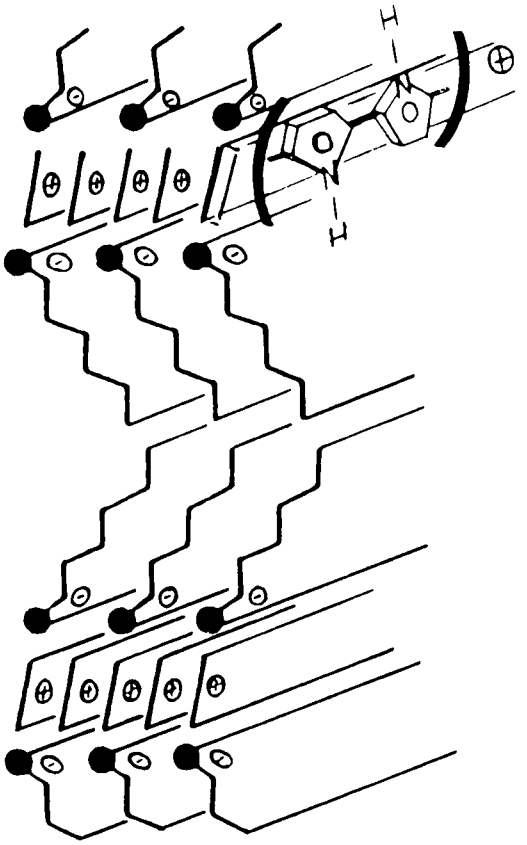

FIGURE 12. Possible multilayer stacked order in the polypyrrole salts. The zig-zag lines symbolize the alkylchains, the black dots stand for the ionic $-SO_3$ or $-OSO_3^-$ groups (see Wegner[172]).

requires a significant distortional activation energy to destroy first a relatively stable arrangement in the original charged species before the jump can occur (d).

TTF is an example of a delocalized radical cation where the charge resonates between the two rings with no activation barrier (Figure 13), as there is no net change in the number of aromatic sextets during the charge transfer. In annellated forms of TTF the transfer of charge from the small ring to the large annellated ring requires the destruction of the very stable benzene ring aromatic structure (Figure 13) which requires about 0.8 eV. As we know, TTF forms very highly conducting charge transfer complexes, unlike the benzo derivative which forms only poor conductors.

The polymers of 3,6-linked carbazoles are good conductors ($1\ \Omega^{-1}\ cm^{-1}$) when they are oxidized by halogens.[83-86] All these conductors are amorphous and, thus, breaks in the good π-π overlap must occur at frequent intervals. An extended band structure would then be a poor approximation to the describe transport in this system. Thus, intramolecular charge transport must proceed only a few monomer units before an interchain jump must occur. That the radical cation carrier is delocalized over at least two mer units is not in doubt, since even though $+1.2$ V vs. SCE (standard calomel electrode) is required to oxidize carbazole, 3,3′-linked dicarbazoles can be oxidized at $+0.7$ V,[87,88] and oligomeric materials at even slightly lower voltages.[89]

The charge in this material probably flows by phonon-assisted intramolecular jumps of the dimer-delocalized radical cation between dimer units (Figure 14). A strong intensification

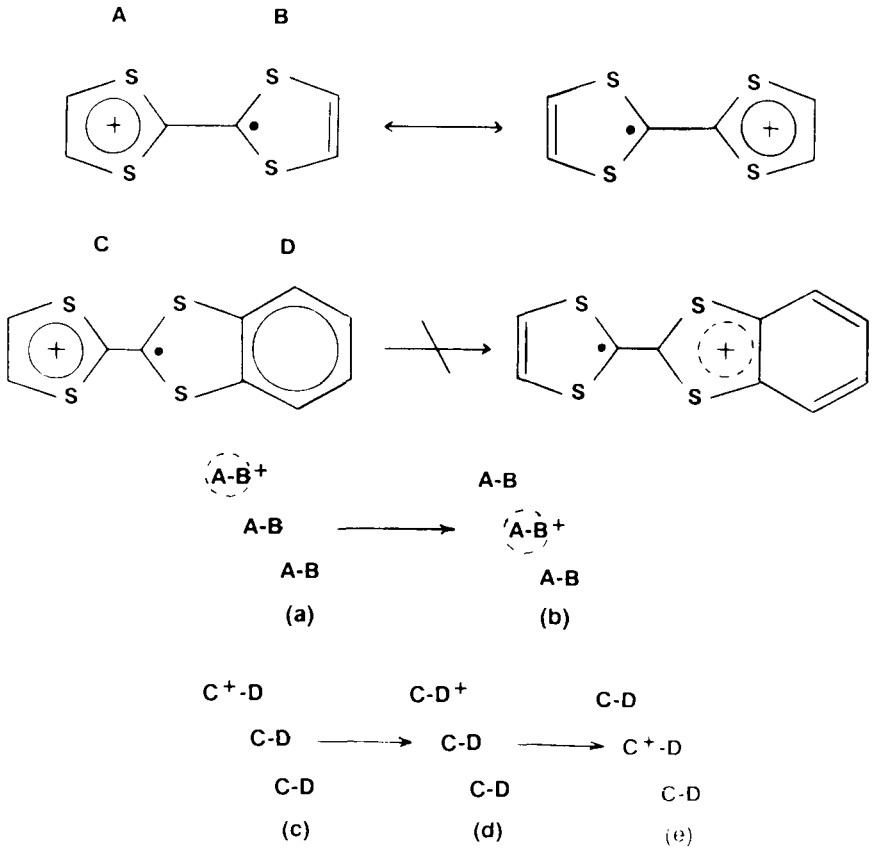

FIGURE 13. (a) Ordered array of A-B molecules with one electron delocalized over a single site (dotted line). In this configuration, nuclear symmetry of $(A\text{-}B)^{\cdot +}$ will be the same as for $(A\text{-}B)^{o}$; (b) charge transport occurs. Delocalized state has readily moved to second site; (c) charge localized on C with large symmetry change in C-D; (d) charge must overcome distortional energy barrier involving dearomatization of D; (e) intermolecular charge transfer occurs.[78]

of the ring carbon-carbon stretch around 1600 cm^{-1} verifies that this vibration is strongly coupled to the carrier. The disorder around biaryl bonds, of course, requires an electron transfer between chains in a fairly short distance and this is demonstrated in Figure 15 in direct analogy with Figure 13. The polycarbazole complexes clearly meet the requirement for partial charge transfer, since in all cases of oxidation no more than one third of the carbazole units are oxidized. Work on low molecular weight oligomers of other polymers has also revealed that intramolecular delocalization over only three to four monomomer units is necessary to realize the full conduction potential of aromatic and heteroaromatic polymers.[90]

Another observation that is of interest is the very low 0.05 free spins/mer even when one third of the carbazole units have been oxidized. As reported in the previous section, spinless carrier transport has been rationalized in terms of bipolaron transport. In the carbazole case this would require the generation of a very highly localized, doubly charged diimine structure (Figure 16). In dimer model compounds this state is observed only at voltages above +1.4 V (SCE) and can be readily seen in the cyclic voltammetry (CV) (Figure 17a). In carbazole oligomers, although two oxidation waves are seen, only one broad reduction wave appears providing evidence that the initially generated dications decompose into radical cations which then migrate away from the initial location of double oxidation (Figure 17b).

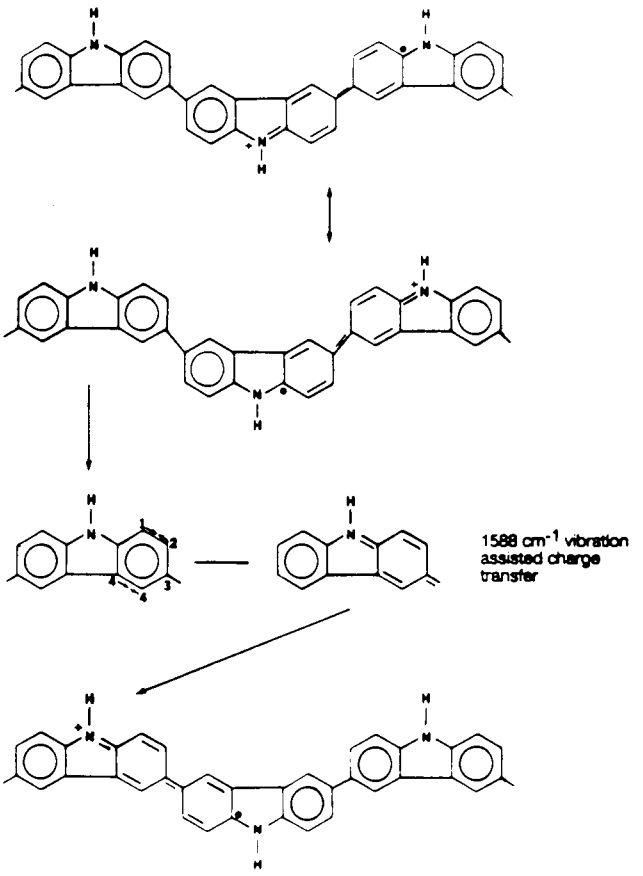

FIGURE 14. Schematic of intramolecular radical cation motion in polycarbazole.[86]

The ESR analysis of model compound, *N,N'*dimethyl carbazole 3,3'-dicarbazolyl tetrafluoroborate reveals that the spin concentration increases from 0.01 radical/mer in the solid state to 1 radical/dimer as the solution is diluted to 6.7 m*M* in nitrobenzene. Apparently, in the solid state there is sufficient intermolecular overlap so that there is spin pairing and the material precipitates into a diamagnetic singlet state. This must also explain the low spin concentration in heavily oxidized polymeric materials, since there does not appear to be any good electrochemical evidence for the presence of dications.

From the above discussion it is quite logical to conclude that radical cations carry the charge in polycarbazoles and probably a number of other heteroaromatic conducting polymers. Charge transport in these materials appears to be rather similar to low-dimensional stacked materials. The more isotropic forms of conduction are obviously important especially in amorphous or partially crystalline polymers.

Returning finally to polyacetylene, several very low molecular weight charge transfer complexes and CO copolymers of this polymer were made and were found to conduct as well as doped high molecular weight homopolymer.[91] This result showed that only very short delocalized sequences were required to generate a significant probability for intermolecular hopping. These authors postulated that the insulator-to-metal transition in conducting polymers is caused by a type of "glass transition" to mobile carriers when a critical radical ion concentration is reached. At low concentrations radical ion carriers are pinned at their respective counterions; however, at a critical concentration, the counterions are shielded by the large carrier density. This permits the radical ions to hop through the lattice

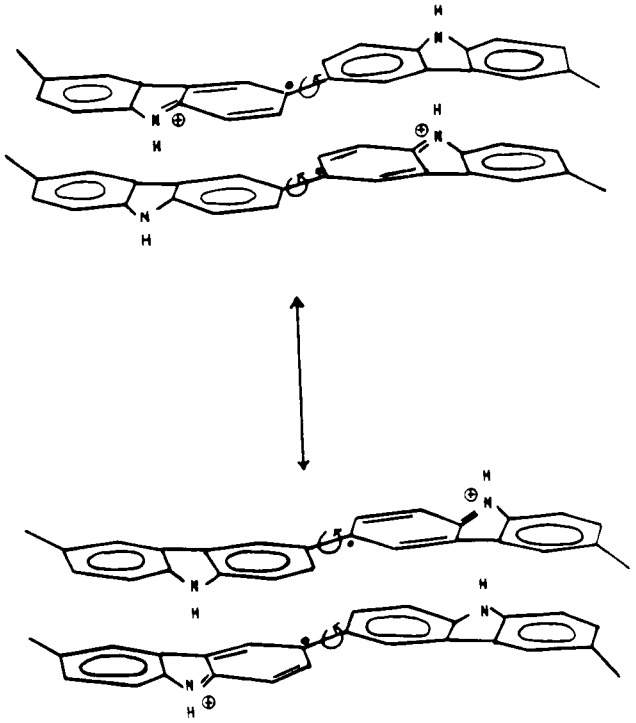

FIGURE 15. Radical cation readily transfers across biaryl bond with small activation energy involving coupling of electron with biphenyl torsion and ring breathing modes. This charge transfer is induced by near-IR radiation. Sandwich complex formation aligns molecules for intermolecular electron hop and minimizes torsional angle responsible for NIR absorbance.[86]

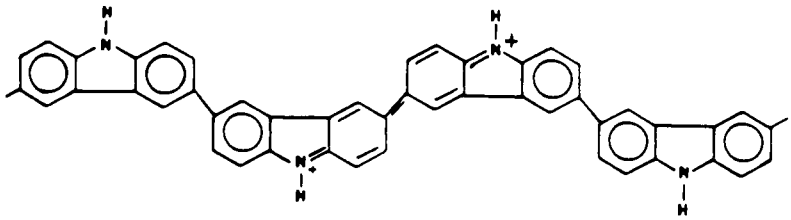

FIGURE 16. Relatively unstable diimine dication in polycarbazole.

by a fixed-range phonon-assisted tunneling process in agreement with the inverse fourth power dependence of the conductivity observed in many samples. In polyacetylene this "glass" or mobility transition occurs at degrees of oxidation <1%, much below the 7% where a large increase in Pauli susceptibility signals the presence of true conduction band electrons.

This latter approach to the mechanism of conductivity, of course, focuses more attention on morphological features such as degree of crystallinity, crystal size, and paracrystalline order. For example, the large anisotropies in conductivity obtained when highly oriented polyacetylene is stretched might simply be a consequence of extended chain crystals whose length-to-width ratio is large. Since the long axis of these crystals will orient in the stretch direction, the crystal size and, thus, the conductivity in this direction will be larger even if the carrier mobility is isotropic within the crystal.

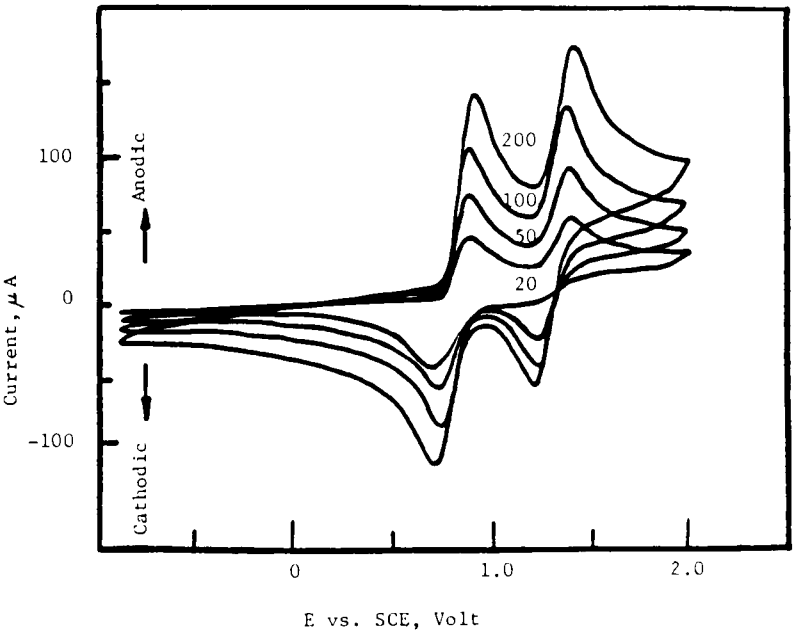

A

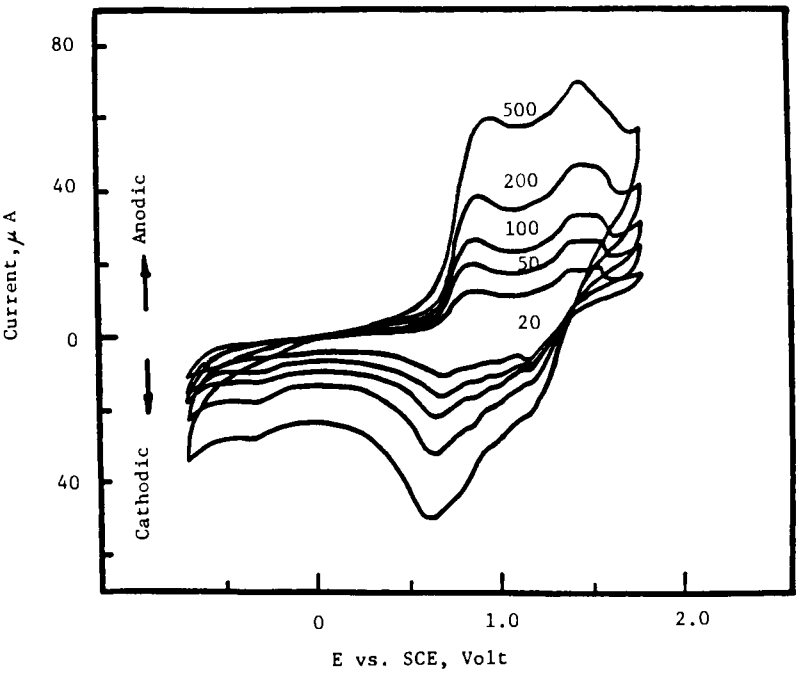

B

FIGURE 17. (A) 1.65×10^{-2} *M* of *N,N'*-dimethyl-3,3'-dicarbazolyl in 0.1 *M* $TBAPF_6$ acetonitrile solution with Au electrode (A = 7.1×10^{-2} cm^2); (B) 2.67 mg/ml of poly-3,6-*N*-methylcarbazole in 0.102 *M* $TBAPF_6$-acetonitrile with Au electrode. Scan rates (mV/s). (Adapted from Smyrl, W. and Deng, Z., unpublished data.)

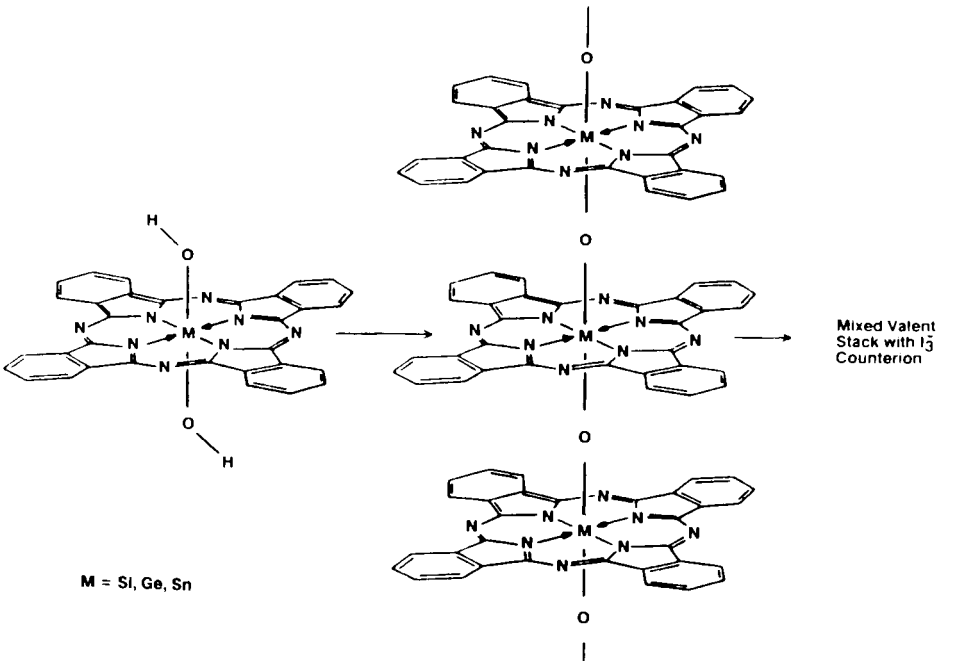

FIGURE 18. Crystal structure and preparation of stacked metalloid phthalocyanine iodine complexes (see Marks et al.[174]).

D. Organometallic Charge Transfer Complexes

The ultimate in stacked low-dimensional metals is made from sandwich-type stacks of the phthalocyanine or other macroligand complexes of the main group[92] and transition metal complexes[93] (Figure 18). The strategy initially was to use the central metal or metalloid atom as a substrate to which would be attached a bridge group that would set the interstack spacing precisely. The synthetic chemist would thus be freed from the uncertainty of whether the donor acceptor complex would form conducting separate stacks of insulating mixed stacks. The conduction mechanism would, of course, require partial charge transfer from the macroligand so that the appropriate partially filled Hubbard band would form and enable interligand charge transfer against minimal electrostatic repulsion. Many such polymers have been formed with a variety of linkages and, as expected, the best conductivities are at a degree of charge transfer around $^1/_3$. Maximum conductivities of 100 Ω^{-1} cm^{-1} at room temperature are found for well-oriented fibers spun from liquid crystalline dopes in strong acids. Interchain charge transport must occur in a substantially different fashion in these polymers because of the orientation of the delocalized rings relative to the polymer chain axis. Since intercalation between rings on adjacent chains is impossible, interchain hopping must occur by transfer between macrocyclic edges.

It is also possible to obtain electron transport through the central bond which bonds the macrocyle together if groups with empty low lying π^* orbitals are used as μ bridges between transition elements with d orbitals. In fact, a phthalocyanine polymer connected together by an alternating chain of Fe(+3) and CN^- moieties conducted at 0.2 Ω^{-1} cm^{-1} with no redox required! Significant conductivities were also seen in transition metals linked by pyrazine. Characteristically, the long axis of the π-deficient ligand did not lie perpendicular to the ring, but was bent significantly away from this angle.

The electronic structure of the complex in Figure 19 is quite interesting, since during the synthesis the macrocycle is doubly reduced to a delocalized dianion. The charge is then balanced by the central Co(+3) and the CN^- bridge. Since the macrocycle π^* state is

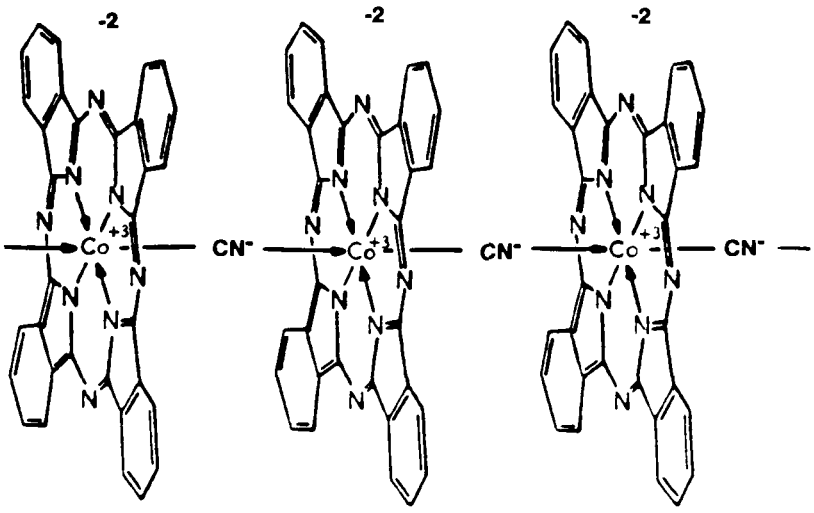

FIGURE 19. Intrinsically conducting metal phthalocyanine-bridged polymers with Co(III) (see Hanack[175]).

occupied it must lie rather close in energy to the d^6 level of Co(+3), with which there must be significant d-π mixing. The cyanide bridge ion also has an empty π^* into which the metal d orbitals can donate to form a σ bond. The other end of the cyanide can form a weaker coordinate bond to the adjacent metal ion. In some systems with d^{10} shells [AgCN, $Zn(CN)_2$, etc.] linear chains of alternate, covalently bound metals and cyanides are found. It is not unreasonable to expect the covalent bond to resonate across the CN linkage binding the entire system in a synergistic fashion.

Bridge complexes between two metal atoms or chains of atoms have been quite popular since the discovery of the Creutz-Taube complex in 1972.[94-96] In this complex two hexa coordinate tetraammonia ruthenium ions are bridged by μ-pyrazine and the total complex charge is +5. Originally, the complex was thought to be mixed valence with an asymmetric charge distribution between metals, however, a completely delocalized ground state has now been proven.[97,98] Very soluble, linear, monodisperse oligomers containing up to six pyrazine-bridged rutheniums were also made (Figure 20) and proven to be valence delocalized at degrees of oxidation between completely oxidized $Ru(+3)_n$ and reduced $Ru(+2)_n$.[97] Surprisingly, the electrical conductivity of these compounds was not measured, although this author would expect that solids of the mixed valent oligomers would conduct very well. The existence of this type of compound provides evidence that some of the electron-deficient, ligand-bridged, metal phthalocyanine compounds could be valence delocalized through the central thread. However, there must be very careful attention paid to the energies and symmetries of the metal d orbitals and bridge ligand so that the correct orbital mixing occurs.

Similar mixed valent osmium (+3, +2)[98] and osmium-ruthenium dimers have also been made,[101] in addition to a wide variety of asymmetric binuclear complexes with different nonbridging ligand substitutions. The controlled stepwise polymerization of ligand metal fragments such as these might lead to characterizable linear homo- and copolymers with interesting electrical, magnetic, and catalytic properties.

There are several variants of these sorts of metal ligand chain compounds that have been actually shown to exhibit high intrinsic conductivities. The most recent of these includes poly(nickel tetrathioxalates)[99] and poly(iron benzodithiolenes)[100] (Figure 21). The Mössbauer spectrum of the iron benzodithiolene compounds reveals that all the iron atoms have been oxidized to Fe(+3), implying that each benzodithiolate anion has a charge of −3, which

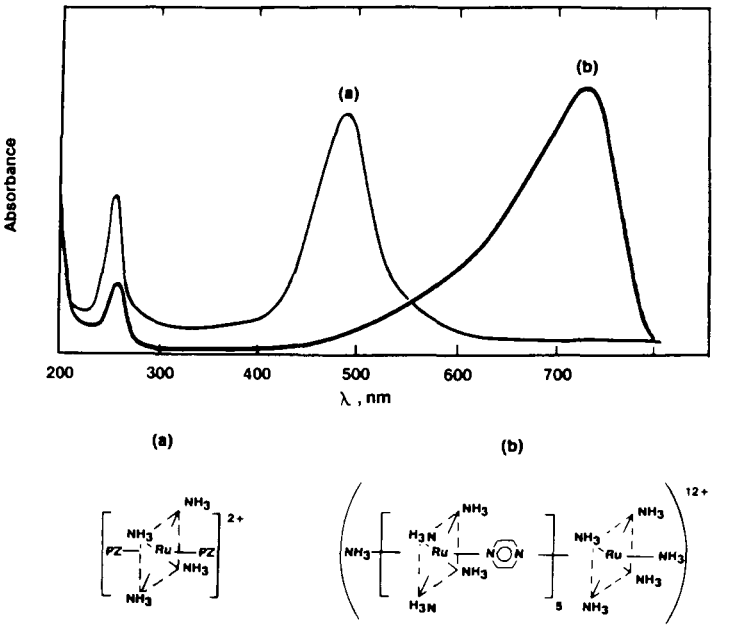

FIGURE 20. Spectra for $[pzRu(pz)]^{2+}$ and $[NH_3Ru_6NH_3]^{+12}$ compounds in the UV-visible region.[97]

might be consistent with a delocalized radical trianion. Unfortunately, as in so many other cases, the spins couple into a S=O ground state and no direct information about radical anion generation can be obtained. Since there is no mixed valence, delocalization along the chain is unlikely. Charge is then probably transported in these compounds intermolecularly through a stacked arrangement.

E. Proton-Assisted Electron Transport

Recently, there has been considerable interest in the conduction processes taking place in polyaniline charge transfer complexes. Understanding these mechanisms in this material is important, since polyaniline secondary batteries seem to be making the strongest bid for application.[101] Oxidized forms of polyaniline are also highly conducting (10 Ω^{-1} cm^{-1}) and air and water stable.

Polyaniline film is made by a very cheap and facile chemical or electrochemical oxidation of aniline in acid solution; however, the material is probably a mixture of octamers, the relative proportion of each form being related to the redox state of the film[102] (Figure 22). The most highly oxidized form, pernigraniline, is unstable. In fact, polyaniline films cannot be oxidized beyond +0.5 V (SCE) without permanent structural changes such as ring closures to carbazole or phenazine or fragmentation.

In situ ESR experiments during the CV of polyaniline films provide strong evidence that radical cations are responsible for conduction. A massive generation of unpaired electrons at +0.2 V (SCE) at the first oxidation wave in the CV[103] is coincident with the insulator-to-"metallic" transition. The conducting state cannot be a true metal, since the T_1 relaxation time of metallic electrons is too short to permit an observable ESR signal. The highest conductivities are obtained when the polymer is oxidized in strong acid, suggesting that protonation steps are inherently involved in the conduction process. The ESR signal is also very narrow and the spin diffusion completely isotropic. The highly delocalized nature of the conduction was rationalized by proposing that a dynamic (<5 ns) proton exchange between adjacent mer units was occurring in concert with carrier transport.

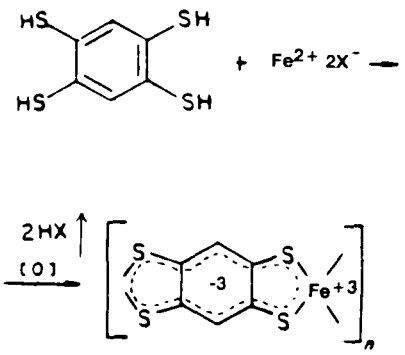

FIGURE 21. Preparation of intrinsically conducting iron poly(benzodithiolenes).[100]

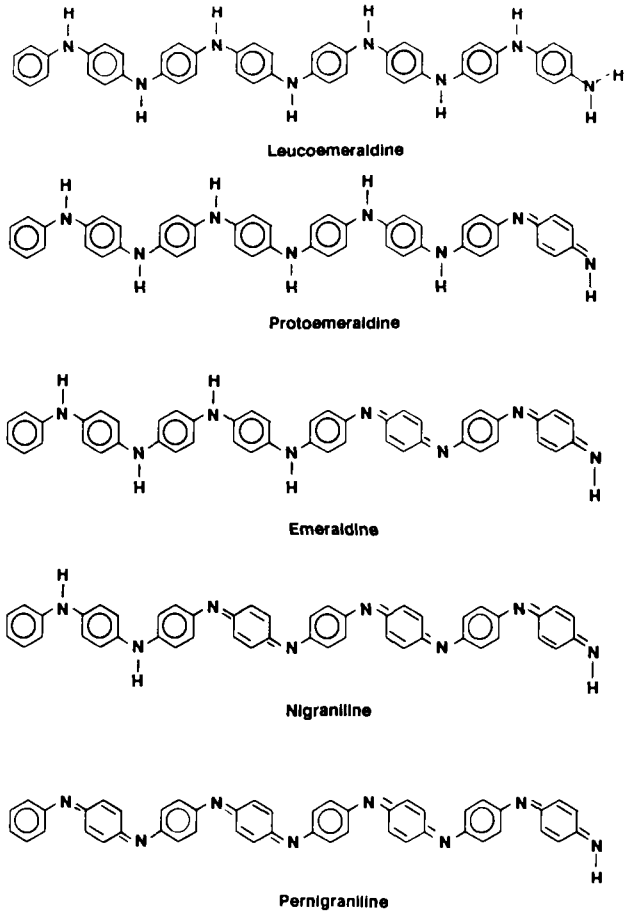

FIGURE 22. Various levels of oxidation of the linear octamer of aniline.[102]

The most logical explanation[102] for the conduction process is based upon the known stabilization of delocalized radical semiquinone by nitrogen protonation. As the number of these radical cations increases the potential for intermolecular charge transfer with neutral segments will also increase. At a higher degree of oxidation the oligomer will look more like pernigraniline and become less conductive because of the high concentration of diimine sequences.

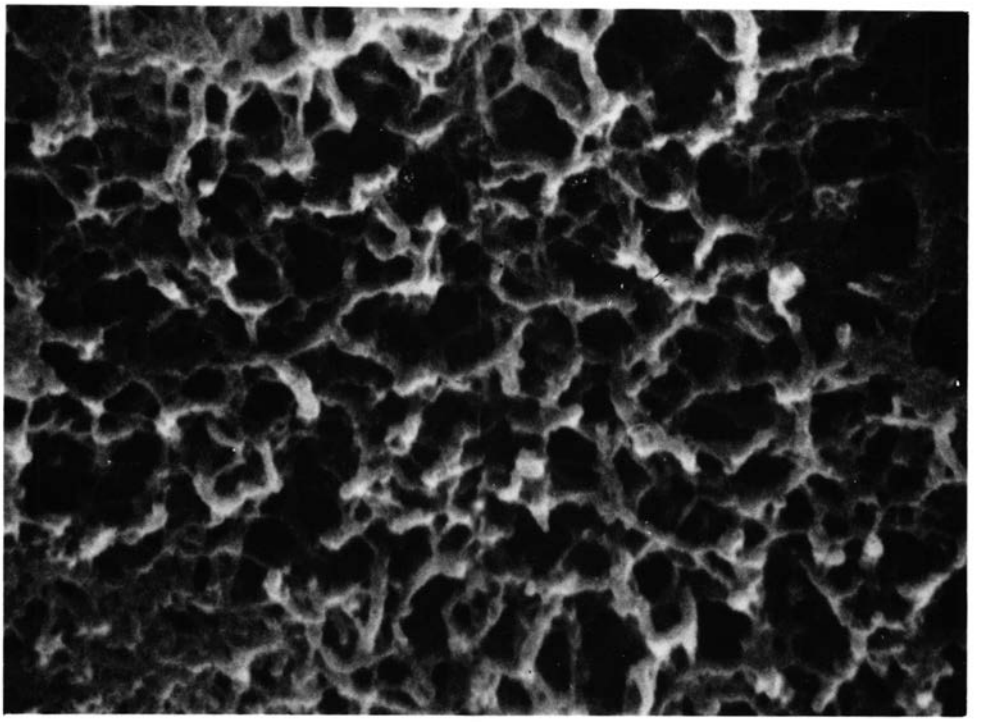

PLATE 1. Scanning electron micrograph of Ziegler-Natta polyacetylene with fibril diameter about 500 Å.[29]

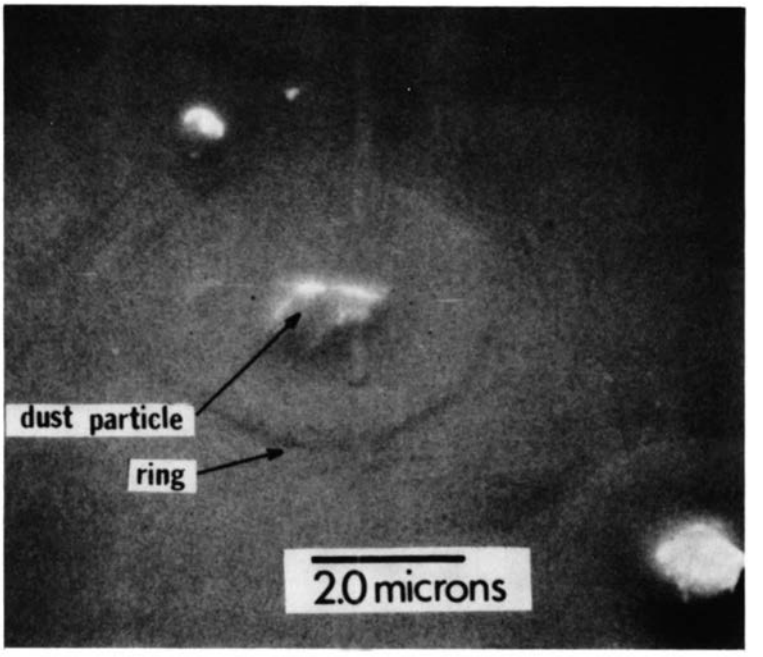

PLATE 2. Typical dust particle and resulting film defects in the film prepared without benefit of clean room standards.

Taylor & Francis
Taylor & Francis Group
http://taylorandfrancis.com

Table 4
REDUCTION POTENTIALS OF SELECTED POLYACETYLENE COUPLES AND OTHER COUPLES[16]

Couple	E°_{red} (vs. SCE)
1 $Li^+ + e^- \rightleftarrows Li$	−3.28
2 $(CH^{-0.1+a})_x + (ax)e^- \rightleftarrows (CH^{-0.1})_x$	−2.43
3 $(CH^{-q+a})_x + (ax)e^- \rightleftarrows (CH^{-q})$	−1.53
4 $N_2 + 4H_2O + 4e^- \rightleftarrows N_2H_4 + 40H^-$	−1.39
5 $(CH^{+a})_x + (ax)e^- \rightleftarrows (CH)_x$	−0.93
6 $Cr^{+3} + e^- \rightleftarrows Cr^{2+}$	−0.63
7 $Pb^{+2} + 2e^- \rightleftarrows Pb$	−0.26
8 $H^+ + e^- \rightleftarrows 1/2\ H_2$	−0.23
9 $(CH^{+q+a})_x + (ax)e^- \rightleftarrows (CH^{+q})_x$	−0.23
10 $SO_4^{-2} + 4H^+ + 2e^- \rightleftarrows H_2SO_3 + H_2O$	−0.03
11 $I_2 + 2e^- \rightleftarrows 2I^-$	+0.21
12 $(CH^{+0.06+a})_x + (ax)e^- \rightleftarrows (CH^{+0.06})_x$	+0.37
13 $O_2 + 2H^+ + 2e^- \rightleftarrows H_2O_2$	+0.45
14 $O{=}(C_6H_4){=}O + 2H^+ + 2e^- \rightleftarrows HO(C_6H_4)OH$	+0.47
15 $(CH^{+0.1+a})_x + (ax)e^- \rightleftarrows (CH^{+0.1})_x$	+0.47
16 $Ag^+ + e^- \rightleftarrows Ag$	+0.57
17 $O_2 + 4H^+ + 4e^- \rightleftarrows 2H_2O$	+1.00
18 $ClO_4^- + 8H^+ + 8e^- \rightleftarrows Cl^- + 4H_2O$	+1.15
19 $H_2O_2 + 2H^+ + 2e^- \rightleftarrows 2H_2O$	+1.55

III. PROCESSIBILITY AND ENVIRONMENTAL STABILITY OF CONDUCTING POLYMERS

A. Environmental Stability of Conducting Polymers

The above mechanisms of charge conduction rely heavily on species which are inherently unstable in the presence of water and oxygen, namely, radical anions and cations. In order to employ these materials in practical application, of course one can always encapsulate with an impermeable barrier. That is a technology unto itself and it is always preferable to have inherently stable materials.

A table of the electromotive series for polyacetylene and oxidants and reductants makes it clear why polyacetylene polyionomers are so unstable in the atmosphere (Table 4).[16] Neutral polyacetylene is stable between −2.44 and −0.24 V (SCE). Any redox couple outside these limits will, respectively, reduce or oxidize the polymer. As electron density is withdrawn from the polymer by continued oxidation, the Fermi level will drop, moving the electrochemical potential of the polymer more positive vs. SCE. Because of the slow transport of the counterions into the crystalline fibers, equilibrium at each potential requires *circa* 8 d; however, the open circuit potential of a doped polyacetylene film can be estimated as:

$$V_{oc} = +0.25 + 0.14\ln X \tag{16}$$

where X is the percent oxidation.

Reference to Table 4 shows that oxidation by oxygen in the presence of protons lies at +0.98 V, still above the rest potential of the most highly oxidized form of polyacetylene. Thus, oxygen should further oxidize even heavily *p*-polyacetylene. The first step in this process is tranfer of an electron to oxygen to form superoxide ion, O_2^-, and then a subsequent reaction of this ion with hydrogen ion to form water or hydrogen peroxide, depending on the electrochemical potential of the polyacetylene. Unfortunately, the superoxide counterion

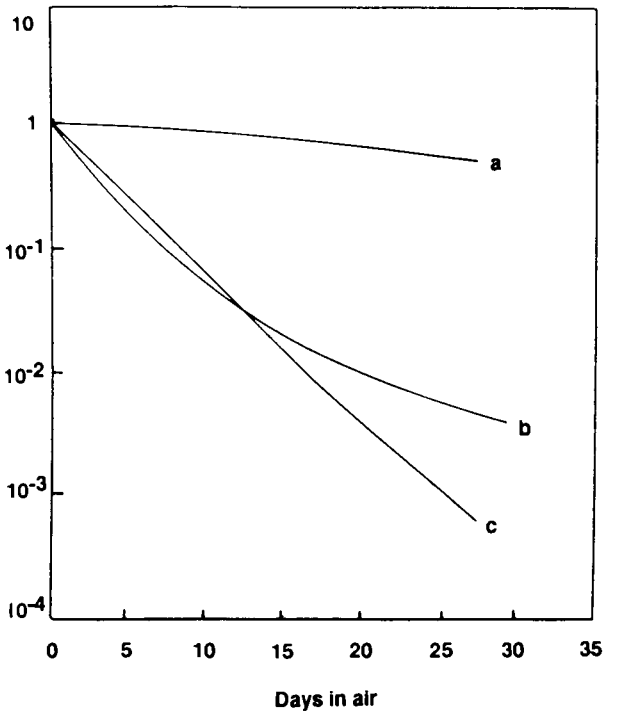

FIGURE 23. Environmental stability of low defect polyacetylene complex, a, vs. polyacetylene with sp^3-type defects; b, film; c, powder. Vertical axis is conductivity ratio = conductivity at t/conductivity at t = O (see Reference 176).

has a strong tendency to reaction with polycarbocations to form C-OH or ultimately, ketone, which will destroy both inter- and intramolecular order, and, thus, conductivity. In the presence of high concentrations of nonoxidizing acid (HBF_4) the reaction with the counterion is prevented even after oxidation to form the superoxide ion. Fast protonation of the oxide to inert products and counterion replacement with BF_4^- evidently precludes oxidative attack.

The other way to prevent oxidative attack and decomposition of the polyacetylene conductors is to generate very high crystallinities and miniminize sp^3-type defects in the chain. Since polyacetylene can become metallic-like in behavior at oxidant concentrations less than 1% (redox at very slow rates), the polyradical ions are highly delocalized. The radical ion concentration is thus rather low on any carbon atom and this would obviously retard attack by water and oxygen. However, the carriers could be trapped at defects where they would be much more susceptible to reaction. Higher crystallinities would also retard reaction by slowing ingress of reactants.

These factors are clearly demonstrated in Figure 23, which compares the new sp^3 defect-free polyacetylene with the older material which contains significant numbers of these defects. Unfortunately, most conducting polymers cannot be made in such defect-free or in highly crystalline form and other mechanisms must be developed to environmentally stabilize the carriers.

Several years ago 3,3′-dicarbazole dimer radical cations were found to be quite stable[83,84] even in air, because of delocalization of the electron over two carbazole units. Especially stable materials were also found in the radical-rich (nitrogen) and carbon positions *ortho* and *para* to it were substituted with protective groups. This was in agreement with the ESR results which showed that the radical concentrations were highest at these positions. The very good environmental stability of these potential carriers suggested the preparation of

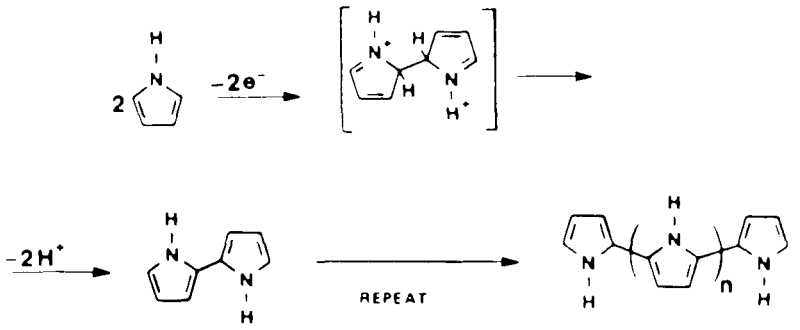

FIGURE 24. Mechanism for the anodic polymerization of pyrrole.[35]

coupled polycarbazole charge transfer complexes that were N substituted with methyl groups so as to protect what were at the time thought to be sensitive 1- and 8-positions. As expected, the stability in air of the radical cationic complexes with polyhalogen, BF_4^-, and PF_6^- counterions was quite good in that no deterioration in conductivity was seen over several months.[83]

What was surprising to us were the good complexes the *N*-methyl-substituted carbazole polymers made with iodine, since the redox for radical cation generation in the polymer is close to +0.6 V (SCE). The iodine couple I_2/I_3^- appears at +0.29 V and thus we would not expect iodine to oxidize the polymer. However, in the adsorbed, condensed state on the surface, some I^+ is undoubtedly in equilibrium with polyiodide[104] and could therefore oxidize the polymer. The molecular weight was also increased upon iodine oxidation of cast films, suggesting that radical cations could couple at active chain ends to form a biaryl bond. This redox-induced cationic polymerization has been found in many aromatic and heteroaromatic polymers. In effect, the electrochemically induced version of this process is responsible for the polymerization of pyrrole to high molecular weight, insoluble films on electrode surfaces (Figure 24).

We also made polymers with an unprotected nitrogen by polymerizing an *N*-trityl-substituted 3,6-diodocarbazole by a nickel-catalyzed organometallic coupling scheme, cleaving the protecting group and casting a film.[86] Because of the slightly higher oxidation potential of this material when compared to the more electron-rich methyl-substituted polymer, iodine formed a complex with rather high iodine vapor pressure. Bromine formed complexes with conductivities of $10^{-2}\ \Omega^{-1}\ cm^{-1}$, but the conductivity rapidly deteriorated due to complexation with the nitrogen and then subsequent ring bromination. Bromination of the ring would also take place in *N*-methyl derivatives with cleavage of the methyl group if the exposure to bromine was permitted to exceed a certain time; otherwise the complex was stable indefinitely in air. When the *N*-hydro derivative was oxidized by NO^+ salts in the absence of water so that no strong nucleophiles were present, the conducting complexes were again stable in air.

3,6-Diiodo carbazole was also polymerized with a copper catalyst to make a polymer with mixed 3,3′- and 9,3′-linkages[56] whose bromine complexes initially conducted at $1\Omega^{-1}\ cm^{-1}$. The specific interest in this polymer was the wide absorption minimum that the conducting complex exhibited in the visible with all the applications such a material would have. Under dry nitrogen the radical cations produced by NO^+ showed a strong tendency to couple through the remaining iodine-substituted 6-positions. This process occurred over a period of hours with subsequent evolution of the spectrum to one reminiscent of localized, monomeric carbazole radical cation. In the presence of moist air the visible absorption decreased drastically with the formation of brominated or hydroxylated derivatives.

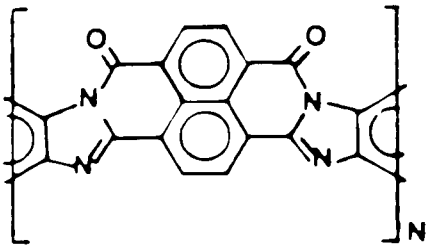

FIGURE 25. Ladder polymer of the benzimidazobenzophenanthrolin type.[27]

The above illustrates that the correct way to design a conducting polymer for environmental stability is to perform ESR measurements on the radical ion of the monomer and dimer to deduce the positions of highest spin density, and it also illustrates whether this spin can delocalize into an adjacent mer to reduce its reactivity. The polymer should then be synthesized with attention to protecting the appropriate positions without large perturbance of the material's packing.

Polypyrrole and polyaniline charge transfer complexes have outstanding hydrolytic and oxidative stability. In the former case the rather extensive delocalization of the charge in the pyrrole ring system and the electron donating effect of the nitrogen stabilize the charge. Similarly, in polyaniline the spin has even a stronger tendency than even in carbazole to reside on the unreactive nitrogen position and the 3,6-positions which are blocked by the biaryl bonds of polymerization.[105] Polypyrrole complexes are even stable to 200°C.

Poly 2,2′-coupled thiophene complexes are also air stable (although there is apparently some long-term stability problem with moisture[106]), because the electron-rich sulfur atom and extensive delocalization of the charge stabilize the radical cation. Many 3-substituted derivatives have also been made and fairly good environmental stability seems to be a general feature, although sulfur has a richer oxidative chemistry than N-H. This same kind of stability is to be expected in such "bridged *cis*-polyacetylene" if the heteroatom is an electron donor.

Overall, achieving good environmental stability in oxidized polymer complexes does not present an overwhelming problem. This is definitely not true for reduced complexes which are very air and water sensitive — without exception. This is certainly a difficulty in application, since no all-polymer p-n junction can be made or n-type catalytic system designed without elaborate sealing techniques. The diffculty of this problem is demonstrated by the air instability of alkali metal-reduced graphite.[107] Since this presents the maximum chance for radical anion to delocalize into a two-dimensional net the potential stability should be large for this structure. It is then rather doubtful whether any aromatic linear or even ladder polymer polyanion can be stable even if extensively delocalized. Some workers have tried to surmount this problem by preparing electron-deficient azaaromatic polymers such as polyquinolines,[108] but all these materials, even though they were very good n-conductors, were very air sensitive.

A possible exception to this rule might be the rather good air stability of potassium metal-reduced BBL ladder polymer (Figure 25).[27,109] Conductivities of 0.1 Ω^{-1} cm^{-1} decreased only one order of magnitude over 1 month in air. Initially, one might expect that the potassium would attack the carbonyl group to generate a type of potassium metal radical anion which is so air sensitive that it is used as an indicator for water and oxygen in solvents. Conceivably, in this case the radical is delocalized into the ladder polymer where it is resonance stabilized. Oddly enough, naphthalide ion, a weaker reducing agent, reduces the polymer to 1.0 Ω^{-1} cm^{-1}; but the conductivity decays very rapidly even in vacuum! These results indicate that there is a critical excess electron concentration that is required for carrier destruction probably by carrier coupling and major structural distortion.

Table 5
SOLUTION PROCESSIBLE POLYTHIOPHENE DERIVATIVES

Water-soluble zwitterion[22]

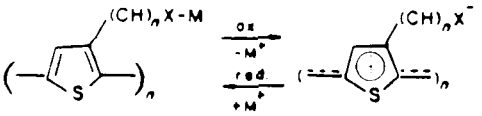

Random copolymer[44]

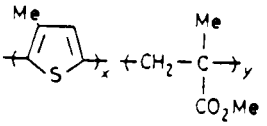

Flexible side groups[40]

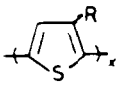

(1) $-(CH_2)_n$ Me [n = 5, 7, 11, 17, 19]
(2) $-CH_2OMe$
(3) $-CH_2O[CH_2]_2OMe$
(4) $-CH_2O[CH_2]_2O[CH_2]_2OMe$
(5) $-CH_2NHC(O)[CH_2]_{10}Me$
(6) $-O[CH_2]_2O[CH_2]_2OMe$

BBL complexes also can be pyrrolized to what could be graphitic-like structures at only 280°C to form conducting solids with conductivities of $10^4\ \Omega^{-1}\ cm^{-1}$.[109] This is in the range of temperature where a laser beam could be used to pyrrolize to an intrinsic semimetal locally. Undoping of the unexposed matrix would generate conductive patterns in an insulating matrix. Presently, the best way to perform this patterning is to graphitize aromatic or unsaturated polymers with ion beams. Massive ionization to free radicals results in radical coupling to amorphous carbon.[110]

The difficulty of this problem is further emphasized by looking at the TCNQ radical anion, which is one of the best acceptors known with a reduction potential of +0.13 V (SCE).[111] The strategy with the design of this molecule is to maximize the electron deficiency of the π orbital system through substitution with highly electron-withdrawing cyano groups. Although fairly good air stability is noted for solid-state complexes of the compound, TCNQ radical anion solutions are not air stable over long periods of time, as can be rationalized from reference to Table 5. True air stability results only when the oxidation potential of the radical anion is close to +0.16 or +1.0 V, in basic or acid solution, respectively.

As mentioned above in the mechanism section, some of the inherent conductors such as thiolate metal complexes showed a large negative thermopower characteristic of n-type semiconduction, perhaps deriving from an excess radical anion mobility in ligand stacks. These complexes were quite air stable. All of this suggests that a convenient way to make an oxidatively stable n-type material is to ligate an electropositive metal fragment to a highly electron-deficient ligand with a low-lying π^* state and reduce this molecule. The electron in the ligand π^* orbital should then delocalize into the metal ion to stabilize the resulting charge. This should be a much stronger effect than the one generated by inductive interactions with electron-deficient centers, as, for instance, in azaaromatics.

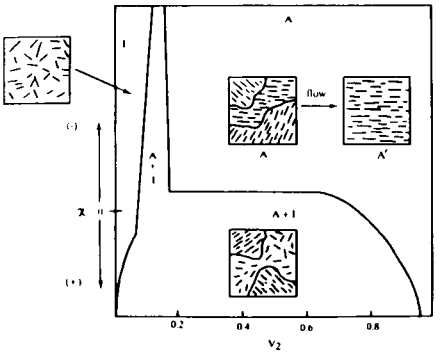

FIGURE 26. Phase diagram for a rigid rod polymer. A — anisotropic phase; I — isotropic phase; V_2 = volume fraction of polymer; interaction parameter generally becomes more negative with increase in temperature.

Some indication of the way to proceed can be seen in the series of Ru^{+2} tris complexes with electron-deficient bidentate ligands, where the reduction potential for $Ru^{+2}/+1$ changes from $-1.5 \rightarrow -1.1 \rightarrow -0.36 \rightarrow -0.14$ V (SCE) as the ligand changes from bipyridyl[112] to bipyrazine[113] to 2-pyridyl azobenzene[114] to 2-pyridyl azo 4′-nitrobenzene, respectively. We are presently synthesizing organometallic polymers based on this concept with the goal of making air-stable n-conductors.

In summary, many air- and water-stable polycationomers have been made with significant conductivity. Stabilization has been achieved by delocalization of charge over at least three or four monomer units or macrocycles and protection of sites where there is a large concentration of charge. Charged species in organic materials are still very reactive though, and the ceiling on stable conductivity is probably somewhere around 200°C. Polyanionomers are very unstable in the atmosphere, except when they are placed in a ladder polymer below a critical concentration; one of the best hopes for air-stable n-materials are electron-deficient complexes between a transition metal and ligating polymers.

B. Processing Conducting Polymers

1. Rigid Rod Polymers — Nascent Morphology and Liquid Crystal Processing

The first conducting polymers that were made were relatively nonprocessible and these included the highly crystalline rigid rod polymers, polyacetylene and poly *p*-phenylene. Although very low molecular weight oligomers of both of these materials will melt below their decomposition temperature, they are infusable at higher molecular weights. This is not unexpected, since the entropy of melting and dissolution for rigid rod materials is quite small relative to flexible polymers. Only solvents that have an exothermic energy of interaction with the polymer can dissolve them into a one-phase liquid.

Figure 26 is the typical phase diagram for a rigid rod polymer and a solvent[115,116] and consists of three important regions from the viewpoint of processing: the isotropic phase, where the rigid rods have no preferred orientation in dilute solution, the anisotropic phase containing only nematic liquid crystal domains (LC), and the biphasic region that contains both LC and isotropic phases. As might be imagined, the polymer concentration at which the anisotropic phase forms increases with decrease in molecular length. In solutions of molecules which undergo a thermally induced coil-to-rod transition, the narrow biphasic region closes off at the top and an isotropic solution exists at higher temperatures.

The biphasic region consists of a narrow part where the polymer concentration of the isotropic and LC phase is similar and a wide biphasic region where the polymer concentration of the anisotropic phase is much larger than in the isotropic phase. In the range of exothermic mixing the polymer solvent interaction parameter, X, is negative and high concentrations

of polymer will form the LC phase. As is most often the case, the interaction parameter is positive or zero (athermal) for the mixture and the system must be processed in the wide biphasic region. Processing is quite difficult since the morphology in this region consists of a physically interconnected gel network of fibrous polymer which resembles a cross-linked rubber in mechanical properties. The courseness and interconnectivity of the network will depend on whether the phase separation is occurring in the metastable (nucleation and growth regime) or the unstable regime (spinodal decomposition). Since polymer solutions also exhibit high viscosities, the equilibrium morphology as determined by the tie lines is sometimes never reached.

If the polymer can crystallize, as is the case for most rigid rod-conjugated polymers (polyacetylene % crystallinity >90%), the high polymer concentrations in the nematic phase promote crystallization. This network is ultimately infusable and the polymer must attain its final use in this state; polyacetylene is an example of this behavior. Polyacetylene is prepared from an organometallic catalyst solution in thin films when dissolved acetylene gas is polymerized to a rigid polymer chain structure. Since the polymer-polymer π interaction is very cooperative and strong in this case, the reaction mixture is well within the wide biphasic region and the expected fibrous foam morphology develops. The foam does not collapse when the solvent is removed because of the high physical cross-linking density and the very high modulus of the extended chain fibers. This morphology is actually quite useful in many applications which require a high surface area, such as electrochemical redox where rapid transport is desired (storage batteries) and sensors. In many respects the polyacetylene foam resembles a ceramic xerogel that is prepared by alkoxide polymerization,[117] except that the ceramic gel is much more brittle and will deform only elastically while the organic can be stretch oriented several hundred percent. Final processing of the polyacetylene usually involves heating the as-polymerized *cis* isomer to *circa* 150°C in nitrogen to convert it into the *trans* form.

An even more difficult material to work with when it is directly synthesized from organometallic coupling of aromatic units is poly *p*-phenylene. When these synthetic methods are used the accumulation of significant molecular weight is slow and crystallization into agglomerated particulates takes place before any gel can form. This powder can be compression sintered in the manner of ceramic powders[37] at 250°C into plaques which have some mechanical strength and, subsequently, can be oxidized chemically or electrochemically to high conductivities.[37] These methods must be used to prepare the material for useful purposes such as battery elements. The molding powder, even though it is infusable, is not as immobile as a true ceramic powder and, especially with processing aids such as polyethylene, can be extruded into oriented fiber.[118] These fibers, however, are quite brittle and thus have no commercial use.

The insolubility of these redox polymers is quite interesting in itself, since one would expect that polyionomers would be readily solvated by polar solvents. Chemical cross-links formed either during the polymerization or doping process have been invoked to explain this behavior. Alternatively, the metallic bonds (sandwich complexes between neutral and radical cation segments, e.g.) between stacks of polymer chains might be so strong and the solvation energies of delocalized carriers so small that dissolution is not preferred.

The solution to the problem of insolubility, of course, is to prepare rigid rod polymers that have the potential for interaction with solvents in a exothermic fashion as has been done with the Aramid polyamide systems.[115] This approach was first tried with the phthalocyanine-stacked polymers which were readily dissolved in strong acids such as chlorosulfonic to form LC solutions, which could be spun in the anisotropic region of the phase diagram to produce high strength fibers that could be oxidized to 100-Ω^{-1} cm^{-1} conductivity in the chain direction.[26] The mechanism of solvation was thought to be reversible protonation of the nitrogens on the phthalocyanine and the consequent potential for ionic dissolution. Cospinning from the same acid LC dope was also possible with poly *p*-benzamide and poly-

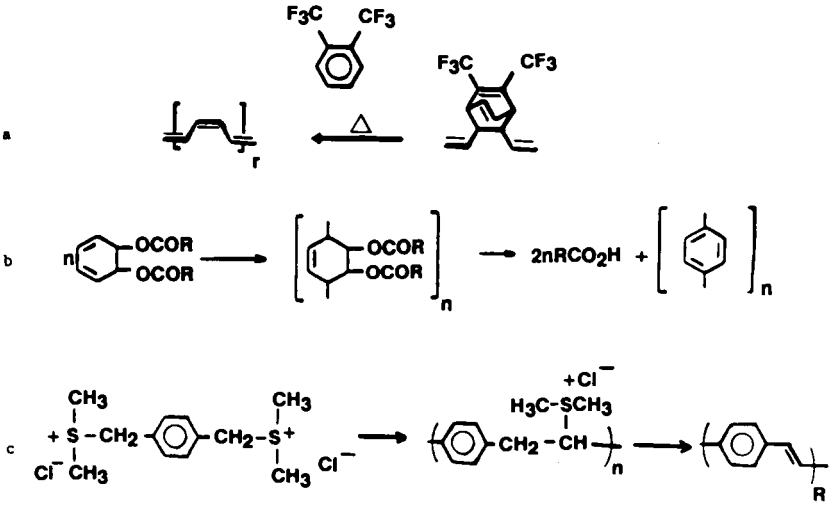

FIGURE 27. Processible precursor polymers. (a) Durham route to polyacetylene;[120] (b) biotech route to polyphenylene;[121] (c) precursor synthesis of poly *p*-vinylene phenylene (see Gagnon[177]).

benzobisthiozole to make higher strength fibers. The fibers were two phase and thus the conductivity of the oxidized phthalocyanine phase was maintained by a perculation mechanism.

At the same time several unique ladder polymers were made by condensation polymerization in polyphosphoric acid directly to high molecular weight liquid crystals.[27] The polyphosphoric acid served the dual purpose of solvating the growing polymer and reacting with the water released during the polymerization process. Depending on how the dope is processed, fibers or biaxially oriented films can be produced by extraction of the solvent. These polymers were designed solely with the objective of mechanical reinforcing applications and their structure was thus not optimized to successfully support environmentally stable radical cations or anions. More precisely, groups such as imidazole nitrogens and carbonyl groups which promote protonation solvation are not too stable to radical ions. Thus, except for the important exception mentioned in the previous section, both the p and n materials' conductivity decayed over time. It was also of interest that polybenzobisthiazole could not be oxidized or reduced because of its very tight nonintercalating crystal structure.[109]

The liquid crystal method of processing offers a great deal of promise if heat-labile solubilizing groups can be introduced into the monomer and then thermolyzed from the polymer to produce a structure more suitable for carrier stability. Alternatively, some aza-aromatic ladders might be developed that can be both protonated and still stabilize carriers in the unprotonated form. The close approach of molecular layers that is inherent to ladders suggests that appropriate molecular design might lead to intrinsic semimetals like graphite.

2. Insoluble Polymers by Thermolysis of Soluble Precursors

Many clever techniques are now available to make soluble polymers that can be cast into films and later thermalized to the insoluble highly conjugated structures that can be doped to the conductive state. There is a correspondingly large effort in preceramic polymers for the same reasons.[119]

The most successful of these precursors for polyacetylene is the polymer based on 3,6-bis(trifluoromethyl)pentacyclo[6.2.0.$0^{2,4}$.$0^{3,6}$.$0^{5,7}$]dec-9-ene (Figure 27a). The solubility of the precursor permits purification, characterization of the precursor in solution, and casting into continuous films. The material has a strong tendency to eliminate the aromatic

bis(trifluoromethyl)benzene and form *cis* and ultimately *trans* polyacetylene upon heating to 140°C. The *cis* polyacetylene that is formed initially is quite amorphous and shows a significant number of midgap states related to the structural disorder. Although conversion to *trans* occurs during doping the conductivity is still quite good. The fully oriented and crystallized *trans* polyacetylene from the precursor still cannot be doped to a higher conductivity than *trans* polyacetylene produced in fiber form direct from the Ziegler route, though.

Polyphenylene now can also be produced from esters of 5,6-dihydroxy hexa-1,3-diene precursor polymer that are quite soluble organic solvents (Figure 27b). Fibers and films made from the precursor can be heated to above 140°C to eliminate the respective organic acid and aromatize the ring. Mostly, poly *p*-phenylenes can be obtained up to 60% crystallinity.[121] Since the monomer is polymerized to the precursor polymer by means of a free radical coupling, copolymerization with other unsaturated monomers is possible.

An especially versatile precursor route to conjugated alkene-type polymers is by thermolysis of a sulfonium precursor polyelectrolyte[32] (Figure 27c). The poly *p*-phenylene derivative has been the most extensively studied in this class of polymers. The polymer is, unlike polyacetylene, stable in air because of its higher oxidation potential and has a higher bandgap of about 2.0 vs. 1.5 eV for polyacetylene. The polymer produced from the precursor by heating between 300 and 400°C is also quite pure, having a room temperature conductivity of only $10^{-15}\ \Omega^{-1}\ cm^{-1}$ and a spin concentration of only 1 ppm, behaving in close approximation to an intrinsic semiconductor. The precursor can be very easily oriented under thermolysis to an all-*trans* polymer with high crystallinity and chain axis alignment. Electron energy loss measurements with simultaneous measurement of momentum reveal that the valence band width is on the order of 2 eV.[122] This implies significant interaction between mer π orbitals in the chain and possibly perpendicular to the chain direction. The conductivities in the chain direction that are obtained upon doping saturate at the very high values of $5000\ \Omega^{-1}\ cm^{-1}$ even in the presence of known sp^3 defects. If, as in the case of Naarman polyacetylene,[5] these can be eliminated, similar very high conductivities might be obtained. Unfortunately, the present material does not exhibit air-stable conductivities.

The preparation of the precursor from the sulfonium complex has an important advantage in the making of highly ordered material. Because of the polyelectrolyte effect the precursor has a very extended chain conformation in solution and achieves a nematic type of orientation when partially converted. This prealignment promotes crystallization into crystals which are quite large in the interchain direction (300 Å). This very large lateral crystal size could be responsible for the enhanced conductivity.

The success achieved with the latter method points the way to attempt synthesis of polyanionomer precursors with very localized point charges that are true liquid crystals rather than just extended polyelectrolytes. Precursors of this type could be spun into fibers or cast into films very conveniently from water solution in a highly ordered nematic state, and then converted to completely extended chain material with very large crystal size both in the chain and lateral packing direction. Considering the very high conductivities recently observed with polyacetylene there is no reason not to believe that materials with conductivies greater than copper or gold could be made if the overall crystal grain could be made large enough. Under proper conditions the counterions probably organize into a superlattice and do not scatter conduction electrons. Very large polymer crystals of very great perfection have only been made by solid-state polymerization of monomer crystals.[123] Unfortunately, defects are evidently very disruptive to very high conductivities in polymers; because of the very anisotropic bonding the lattice defect extends over a much larger space than a vacancy or dislocation in copper, for instance.

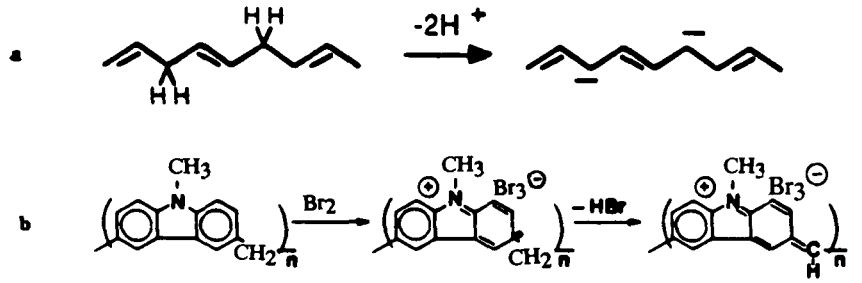

FIGURE 28. (a) Proton abstraction as a route to conducting polymers;[125] (b) hydride abstraction route to conducting polymers.[31]

3. Hydronium and Hydride Abstraction Route from Precursor to Conductor

Another method that has been used successfully to produce conducting polymers from precursors is by hydride extraction from a flexibilizing methylene linkage.[31] Heteroaromatics such as carbazole readily polymerize through the electron-rich 3,6-positions, with formaldehyde in acid solution to produce high molecular weight poly-3,6-carbazole methylene, which is soluble in a wide variety of solvents and can be cast into amorphous films of good mechanical strength with a glass transition temperature of 148°C. One hydrogen on the methylene group is very labile and can be removed as hydride ion by a number of oxidizing agents including bromine, nitrosonium cation, and triphenyl methane cation either in solution, in which the complex is soluble, or in solid films (Figure 28a). The structure that is generated is a quinoidal cation that can resonate through the methine linkage; however, NMR reveals that the hydride abstraction is only 80% complete.

The conductivities of the films are air stable, but only $10^{-2}\ \Omega^{-1}\ cm^{-1}$. ESR shows spin concentrations both in dilute solution and in the solid state of only 10^{-3}/mer, which is more evidence for nonradical cation carriers.

One of the difficulties with this complex, as reference to Figure 28 will indicate, is that the charge density on the polymer is too high when only one carbazole is linked to each methylene unit. The electrostatic repulsion potential between adjacent units on the same and adjacent chains will retard hopping in the manner of a Wigner lattice. There is also considerable steric hindrance between hydrogens 2 and 8′ on adjacent carbazoles which will twist the structure out of plane.

In order to reduce the charge density in the oxidized copolymer we also coupled 3,3′-*N*,*N*′-bicarbazyl with methylenes[124] and obtained a precursor polymer which could be cast into films and oxidized in the same way. Conductivities one order of magnitude higher ($10^{-1}\ \Omega^{-1}\ cm^{-1}$) were found as expected. The dimer methylene compound also was rather interesting in that it would form compatible blends with the fully biaryl-linked polymer, offering the possibility of improving the mechanical properties without too much sacrifice of the conductivity.

A proton also can be abstracted from a methylene group by means of a strong base to generate a delocalized radical anion.[124] For example, poly(*p*-phenylene pentadienylene), a soluble precursor polymer, can be deprotonated by a strong base such as *n*-butyl lithium, with the evolution of butane gas to yield a delocalized carboanion that has a conductivity of $1\ \Omega^{-1}\ cm^{-1}$ in the solid state (Figure 28b). At the maximum degree of reduction there was slightly less than one radical anion per repeat unit.

4. Solutions of Conducting Polymers in Exotic Solvents

Most conducting polymers that are doped in the solid state cannot be redissolved. This observation led to the development of a mixed solvent of AsF_3 and AsF_5 that was able to both oxidize and dissolve polyphenylene sulfide to conducting blue solutions that could be

cast in inert atmosphere to p-type films that had conductivities of 200 Ω^{-1} cm^{-1}.[28] Apparently, the pentafluoride oxidized the polymer to the radical cation which then dissolved in the highly polar trifluoride. Once the film had been cast it could not be redissolved because of extensive cross-linking and ring fusion to benzothiophene.

Even though polyacetylene has now been found to be soluble in this solvent mixture,[28] there will probably be little commercial use for it because of its high corrosiveness. The soluble precursor routes seem to be a much more practical way of casting films and spinning fibers.

We had observed that polycarbazoles underwent further polymerization when they were exposed to iodine vapor, and this suggested to us that liquid iodine might be a useful polymerization solvent for conducting polymers. In its liquid state (113.6 to 184°C) iodine is an excellent solvent for both carbazole monomers and polymers[30] and many other substances. The liquid is highly polarizable and ionizes mostly as $2I_2 = I^+ + I_3^-$, which gives the liquid a significant conductivity.

The iodonium ion is a strong oxidant and can oxidize carbazole to radical cations which can couple to 3,3′-dimers, reoxidize, and continue to polymerize to high polymer. Normally, bicarbazole radical cations are quite stable in normal organic solvents and show no tendency to couple. Iodonium evidently oxidizes the dimer to the diimine dication which can continue to polymerize. The reaction of 3,6-dibromocarbazole starts as soon as a solid mixture of the carbazole and the iodine are fused with a heat of polymerization of -21 kcal/mol of monomer. When the polymerization was completed the viscous solutions were cast on substrates at temperatures between 120 and 130°C to evaporate the iodine, leaving a tough conductive film with an air-stable conductivity of 1 Ω^{-1} cm^{-1}. The elemental analysis for the *N*-methyl carbazole polymer was consistent with one triiodide ion per three monomer units — the same composition that had been observed by gaseous iodine oxidation of a cast film of the carbazole produced by the usual nickel coupling technique.

NMR of the methyl diiodo carbazole polymerization in molten iodine revealed that polymerization took place through the 3,6-position and that the methyl group remained intact. The very fact that an NMR signal was observed argues for the instability of the radical cation in liquid iodine, since any radical present would couple with the proton and effectively destroy the NMR signal. Once the solution was concentrated into a film, however, a large part of it became insoluble and a small amount of methyl group was cleaved off. Evidently, when the polymer becomes concentrated bimolecular reactions which produce defects can take place more readily.

5. Copolymers, Grafting, and Side Chain Modification

One of the techniques commonly used in polymer science to modify the solubility is copolymerization between monomers or grafting between several polymeric segments. Once it was realized that polyacetylene was not going to be processible by ordinary methods, efforts were made to copolymerize with more soluble polymer segments in the hope that this component would bring the more rigid polyacetylene segment into solution. In one synthesis styrene was anionically polymerized to a living polystyryl anion which was then reacted with a titanium alkoxide to produce an catalytic end active in acetylene polymerization. When acetylene was admitted to the reaction a diblock copolymer was produced that was quite soluble and of significant molecular weight[126a] (Figure 29a).

A variant on this process consisted of preparing active sites on a polystyrene or polyisoprene[126b] chain and then growing the polyacetylene chain from this point in the manner of a graft polymer (Figure 29b). The highly colored solutions produced in this fashion probably consisted of micellar aggregates that were kept in solution by the styrene or isoprene tails. Films prepared by casting the isoprene-modified polymer had oxidized conductivities of up to 10 Ω^{-1} cm^{-1}. A bicontinuous phase structure must have been present in this film

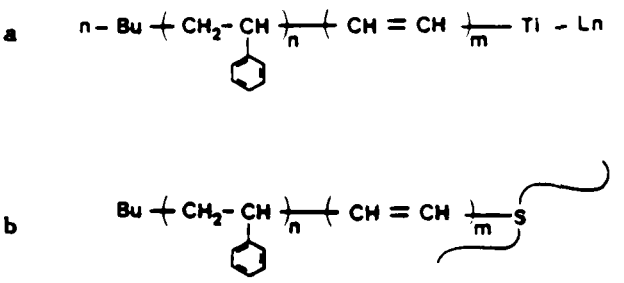

FIGURE 29. Copolymerization schemes for producing processible polyacetylene-type conducting polymers. (a) Block copolymer; (b) graft.[35]

in order to explain the high DC conductivity. The graft method could be of interest in practical application if employed with more environmentally stable varieties of conducting polymers. As we explain below, a variant of this technology has now been exploited to a commercial product.

Experimental commercial products now introduced on the market by both BASF[147] and Polaroid[14] employ water-stable colloidal emulsions of polypyrrole charge transfer complexes. Sterically stabilized, monodisperse, 1500-Å polypyrrole complex particles can be made by polymerizing and oxidizing a pyrrole suspension with ferric chloride.[127] This water-based polypyrrole latex is applied to surfaces in the manner of house paint where, upon drying, it probably sinters partially to produce an interconnected network with air-stable conductivities of 5 Ω^{-1} cm^{-1}. The simplicity and very low toxicity of processing by this method opens up many applications in static dissipation, electrocatalytic surfaces, electrochromic displays, etc.

The best way to prepare the latex is to dissolve a cationic polymerization initiator such as ferric chloride in a water solution of partially hydrolyzed polyvinylacetate (HPVA) in water. When pyrrole monomer is added to this mixture it is emulsified by the HPVA into small pyrrole particles. The presence of the N-H group on pyrrole is essential for hydrogen bonding to the emulsifier, since this process is ineffective with *N*-methyl pyrrole. The pyrrole is oxidized to radical cation by the ferric ion and this then initiates polymerization with neutral pyrrole. Enough ferric ion is also added to oxidize the resulting polymer to one charge per 3 mers, the optimum oxidation level for polypyrrole. The resulting latex can be washed free of ferrous ion to yield a water or, by solvent exchange, a polar organic, solvent suspension that is sterically stabilized by adsorbed HPVA.

Polaroid has taken this process one step further and has claimed replacement of the usual small counterion with a polyelectrolyte anion, most probably the hydrolyzed PVA. A material with a polymeric counterion is a major advance, since the likelihood of the counterion migrating under an applied field is much reduced. This property is critical in diode stability involving a junction of two polymers where migration of counterions would destroy the junction.

BASF, thinking along similar lines, has been issued a patent[127] where a suspension of pyrrole in an emulsifier is continuously impacted against an electrode in a turbulent flow and anodically polymerized in a continuous reactor. It is not known how the Polaroid process is related to this since the description has not appeared in the open literature. Polyacetylene has also been produced by BASF in emulsion form and both polypyrrole and polyacetylene are now consequently commercially available in large sheets or rolls of various thicknesses for applications.

The water solubility of conducting polymers, once thought to be impossible, has now

been proven with some very exciting possibilities for applications.[22] The process involves first making a 3-thiophene-alkylsulfonate ester (Table 5) which then can be electrochemically polymerized to a 2,2′-linked polythiophene radical cation soluble in acetonitrile. This material was a sufficiently strong oxidant to be reduced by sodium iodide with the cleavage of the ester to form the neutral sodium salt of the sulfonic acid. The sodium salt was water soluble and could be cast into films of high ionic conductivity in the presence of water. These films electrochemically oxidize above 1 V (SCE) or bromine oxidize to produce zwitterionic-type films with conductivities of 10 Ω^{-1} cm^{-1}. Oxidation could also be carried out in solution with nitrosonium ion or bromine to produce air-unstable solutions. The lack of stability of oxygen is a bit disappointing, but structural modifications on this basic scheme should solve this problem since oxidized polythiophene polymers are already close to being air stable in water. Perhaps the introduction of electron-donating alkoxy groups with acid ends into the 3-position could help alleviate this situation. Trying the same scheme with pyrrole instead of thiophene wold also help to solve the stability problem.

The making of zwitterionic conductors of this type is especially important since the counterion migration problem is completely solved in a direct fashion. Reducing the charge density in the structure by alternate copolymerization with unsubstituted or nonzwiterrionic-substituted monomers might improve conductivity and environmental stability. The potential for the electrochemically controlled release of the commercially important cationic drugs is high, since the sodium ion in the neutral form can be exchanged with the ammonium-type drug cations. Water and oxygen and biocompatibility problems still must be solved before this promise becomes reality. Electrochemical control of ion exchange and ion gates is also a possible application.

The activity in the polythiophene system has not been limited to what has just been discussed. The discovery that substitution at the 3-position did not noticeably destroy conductivity through steric effects has led to an explosion of new high molecular weight, soluble polythiophene derivatives. Since polythiophene and 3-methyl thiophene are known to be insoluble materials, the secret to success is to make the 3 side chain long enough to overwhelm the strong π-π bonding between thiophene chains. Table 5 is a compendium of the various materials of this sort that have been recently synthesized.[40-44] A material of special note in this series is the $-CH_2O[CH_2]_2O[CH_2]_2OMe$ derivative which has a room temperature conductivity greater than 1000 Ω^{-1} cm^{-1} and air stable to 210°C.

Polymers with this side chain length must be phase separated into a bicontinuous polyether phase and stacked thiophene phase in order to maintain the connectivity and DC conductivity of the thiophene phase. The conductivity actually seems to improve as the side chain lengthens, even though the amount of conductive matter in the film is decreasing. Similar effects are seen in polyurethane block copolymers[129] where the ordering of the crystalline hard segment phase improves with increasing length of the polyether soft segment by reduction in the amount of phase-mixed material. The structure of the thiophene materials is different from the urethane case in that the soft segment is in the side chain rather than in the polymer backbone, as in the case of urethane block polymers. This must severely limit the morphological possibilities.

Ideally, the direction of the sulfur must alternate from side to side down the polymer chain. In order to accomplish this and maximize packing at most, one stack of polythiophene will form as a very thin lamella. Volume filling and surface energy effects will force the thiophene units to alternate in direction, planarize, and constrain themselves to the narrow lamella which will twist through the structure in fibrous form. Just as in segmented block copolymers, there will be random interconnection through costacking of accidently overlapping fibers. This morphology must be quite similar to the one generated when highly conducting polypyrrole complexes are formed in the presence of soap-like counterions.

If the above morphology does indeed occur in these materials, one can take the concept

to its final conclusion and prepare a superlattice consisting of an alternate lamellar structure of conductor and insulator of molecularly determined thickness and very anisotropic electrical properties. One can imagine light, electric field, swelling, and mechanically induced modulation of interlamellar spacing and consequent changes in diffraction of light (modulated rugate filters, color displays, nonlinear optical effects, and optical transitors, sensors, etc.) and electrical conductivity. Preparation of such films will probably be best accomplished by some modification of LB multilayer generation techniques.[130]

Random copolymer films of thiophene and methyl methacrylate have good solubility in many solvents, can be cast into films, and, provided that the methacrylate content is not too high, exhibit high conductivities.[44] The potential for making a true block-like morphology exists in these sorts of polymers if the thiophene and interconnecting block can be made highly incompatible in the absence of a cosolvent. In this way the lamella thickness that is probably typical for the side chain-substituted material can be increased.

6. Composites of Conducting Polymers

The phase incompatibility of a conducting polymer with another polymer can be used quite effectively to produce composites of improved mechanical properties. Both low-density polyethylene[131] and polybutadiene[44] have been impregnated with titanium catalyst with or without a supporting solvent and used as matrices in which to polymerize acetylene gas. This process occurred quite readily in low-density polyethylene above its melting point and in the polybutadiene above its glass transition because of the high diffusivity of the acetylene gas at these temperatures. Since the polyacetylene phase separated into a fibrillar phase within this matrix, the composite could be oxidized to high conductivity close to that observed for pure polyacetylene. This is not unexpected since the holes in the porous form of polyacetylene were simply being filled with polymer. The mechanical properties of these films were, of course, greatly improved over unmodified polyacetylene in that high ductility was maintained even after complex formation.

Composites could also be made electrochemically.[123] The procedure was to place cast a polyvinylchloride or other film on an electrode that would swell, but not dissolve, in an electrolyte of choice. Pyrrole was then loaded into the solution and permitted to swell the polymer layer and migrate to the electrode surface where it was anodically polymerized in the usual fashion. Since the polymerization and oxidation started at the electrode surface, the morphology of the film was quite interesting in that a conducting film first formed completely covering the electrode between the matrix polymer and the electrode surface. Fibrous polypyrrole complex then grew through the film perpendicular to the surface until it emerged on the electrolyte side of the film. The lateral growth rate across the electrolyte side of the film was quite slow and the electropolymerization could be stopped before interconnection of the conducting polymer occurred. The free-standing film that was removed from the substrate exhibited the mechanical ductility of the matrix polymer but conducted only on one side!

One of the driving forces for preparing films by the composite method was to improve mechanical properties like impact strength, yield, and fracture strength, and in this sense the effort has been successful; however, the other objective was to improve the environmental stability of the conducting phase through retardation of the diffusion of oxygen or water, and this was only partially successful. Of course, now with the development of ultrastable polymer complexes, this is probably not a relevant concern except in the case of n-type materials.

IV. SOME MORE APPLICATIONS OF CONDUCTING POLYMERS

A. Linear Optical Properties of Polymeric Conductors

One of the features of conducting polymers that we have treated only very briefly is

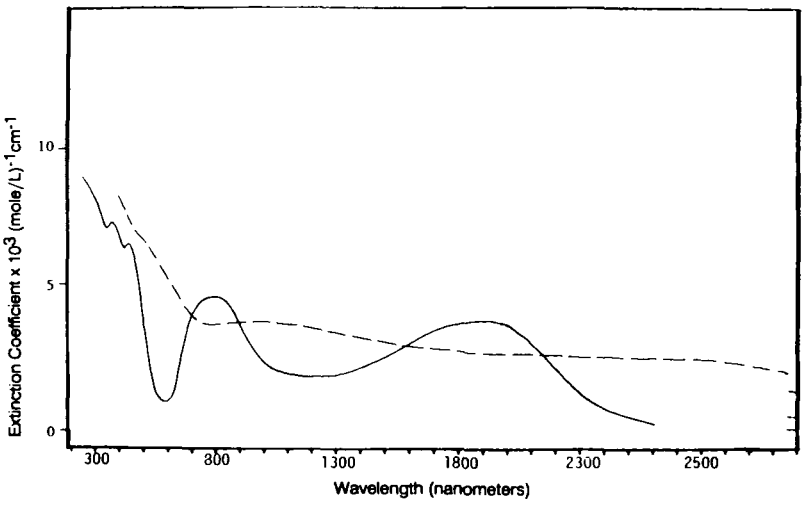

a

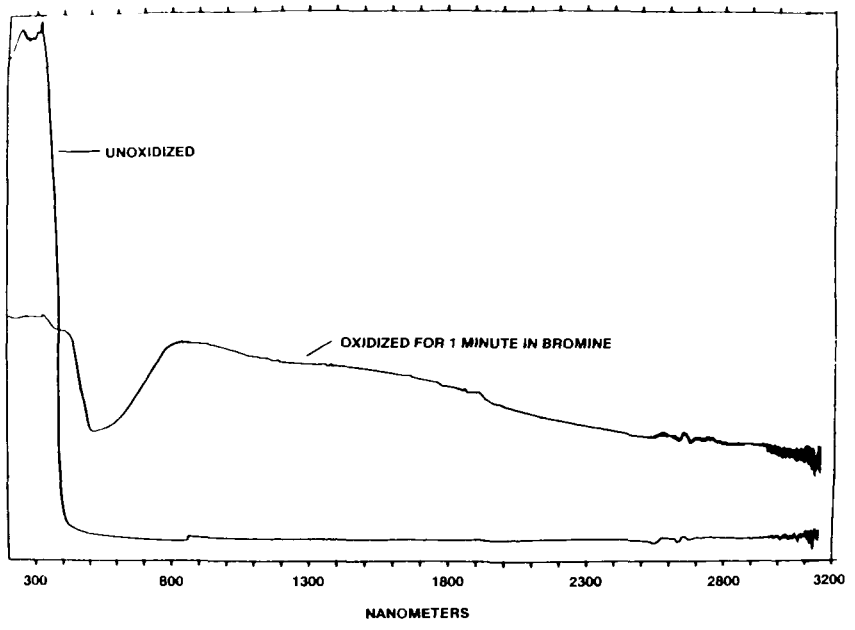

b

FIGURE 30. (a) Spectroscopy of dimeric and polymeric forms of 3,3′-linked forms of carbazole and their complexes. Dotted line — poly-(*n*-methyl carbazole) (PNMCZ) complexed with iodine at 50°C, and solid line — monotetrafluoroborate complex of *N,N′*-dimethyl 3,3′-dicarabazyl radical cation (nujol mull).[86] (b) Unoxidized and oxidized PNMCZ T.[178]

optical properties. When a polymer is either oxidized or reduced the electronic and vibrational spectrum exhibit significant changes due to the presence of the charged species. All the basic features of the spectrum of amorphous-conducting polymers can be understood even in the dimer. Figure 30a is an electronic spectrum of the radical cation of *N,N′* dimethyl 3,3′-linked carbazole dimer in various physical states and a bromine-oxidized film of the polymeric form (Figure 30b). The counterions are, respectively, BF_4^- and Br_3^-, which do not contribute to the spectrum above 400 nm.

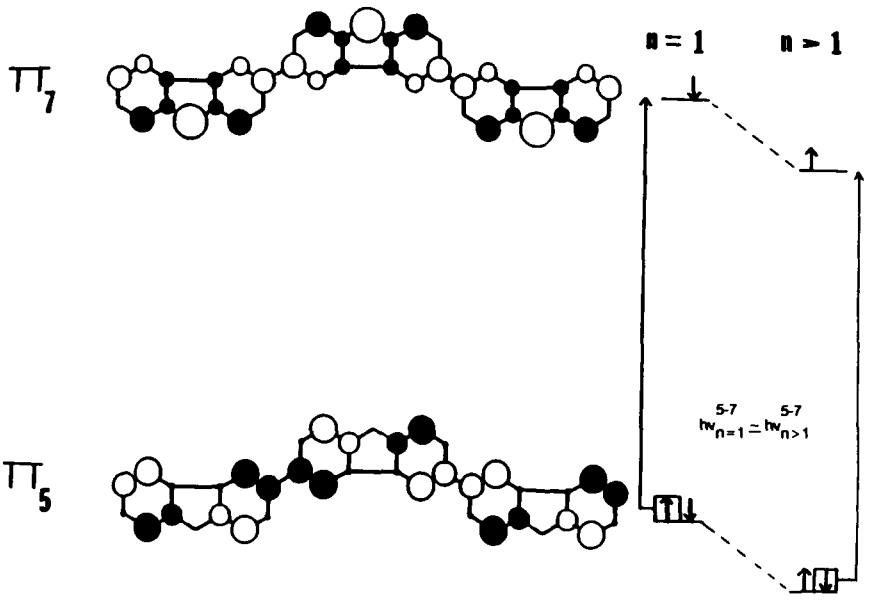

FIGURE 31. Molecular orbital diagram for the ground and excited states expected for 3,3'-linked carbazole radical cation species showing the $\pi_5 \rightarrow \pi_7$ transition.[86]

There are two near-infrared (IR) transitions of importance that develop in the spectrum of the dimer complex at 800 and at 1900 nm.[84] The same two transitions also appear in the polymer complex, but the first transition is shifted to 900 nm and the long wavelength transition is broadened extensively out into the mid-IR. In fact, the latter transition extends completely across the IR out to at least 400 cm^{-1}.[84] Extensive model compound work and theoretical calculations[134] reveal that the 800-nm transition is the $\pi_5 \rightarrow \pi_7$ intramolecular transition that appears in monomeric carbazole radical cation (Figure 31). Upon polymerization both these orbitals are stabilized by favorable overlaps at the 3 carbons and thus, as expected, not much change in this transition is seen with polymerization.

The transition at 1900 nm is seen both in the solid state and in concentrated solutions of the dimer radical cation, but not in the monomer. Surprisingly, in dilute solution the band disappears.[84] The $\pi_5 \rightarrow \pi_7$ transition is seen regardless of physical state. The electron spin resonance signal also decreases as the material is concentrated coincident with the appearence of the 1900-nm band. The interpretation is that the long wavelength band represents an intramolecular charge redistribution of the radical cation across a dimeric unit. The disappearance of the band in a dilute solution of the dimer complex suggests that an intermolecular sandwich complex forms at higher concentration between radical cation dimers which forces the dimers into coplanarity across the biaryl bond, facilitating the transition.

Bands in this frequency range are quite common in mixed valent complexes discussed in Section II.D. The charge transferred in this transition may either be symmetric or asymmetric depending on whether the excess charge is localized on one unit or resonant across the bonds connecting the two units. In the case of the Creutz-Taube ion, the ground state is symmetric and the transition that appears around 1800 nm is assigned to a symmetric transition from a binding state involving metal d orbitals and the π^* pyrazine bridge orbitals to a nonbonding state involving no bridge orbitals and opposite amplitudes on the metals.[95,96] In long linear chains of the Ru(+2) complex the d $\rightarrow \pi^*$ transition that appears in the monomer at 500 nm shifted to 726 nm in the hexamer and significantly broadened due to narrow band formation. No long wavelength transition appears in the polymer until the chain of $[Ru(+2)\mu\text{-pyrazine}]_n$ is oxidized; the maximum intensity of the band at 1800 nm is obtained at half-oxidized condition and no band appears when all the Ru(+2) has been oxidized to Ru(+3).[97]

In the carbazole polymer complexes the appearance of the band in the near IR is strongly suggestive of very easy thermally induced charge transfer between monomer units. In fact, in the Hush theory[135] of mixed valence charge transfer the thermal activation energy of this transfer asymmetric ground-state mixed valent compound is about one fourth the optical transition energy. In carbazole the extent of intrachain delocalization is evidently sufficient to permit interchain hopping. It is doubtful whether the strong mid-IR absorbance is due to "free carriers" in the metal sense, since the complex is quite amorphous. A more likely explanation is that the very low energy transitions are caused by a high density of localized states near the Fermi level. It should be mentioned that the presence of a long wavelength IR band does not necessarily mean that the material will be a good conductor. Good intermolecular packing is also a requirement.

When polypyrrole is electrochemically oxidized very similar behavior to that seen in carbazoles is observed at the highest oxidation levels of the polymer (one charge/3 mers), in that new bands at 620 and 1300 nm are seen. These transitions are assigned according to an interpretation involving an extended band model, where the 620-nm band is the transition from the valence band to the empty antibonding bipolaron band and the 1300-nm transition is the valence to empty bonding bipolaron band[136] (refer to Figure 11). Considering the amorphous state of the polymer and the similarity to polycarbazole complexes, this author does not see why an explanation based on simple radical cation transitions would not be just as effective.

The optical spectrum of amorphous polythiophene derivatives changes in exactly the same way as pyrrole and carbazole materials in that two bands again appear at 800 and 1730 nm.[42] The two bands appear together even at the lowest levels of oxidation and simply grow in intensity at the same frequencies, with about the same half-widths until the highest oxidation levels where the higher frequency band increases slightly in frequency. Again, even though explanations involving extended band theory have been advanced, these same two bands have been found in solutions of carbazole dimer radical cation at moderate concentrations where no band formation is possible. Understanding the source of these transitions is important, since one of the best chances for application of conducting polymers will be in the area of electrochemically induced color changes for displays. At this point it would be relevant to do accurate oscillator strength calculations on radical cations and anions of dimeric and trimeric species to more firmly establish the source of the transitions and to guide the chemist in the design of amorphous materials.

An especially interesting thiophene-type polymer was synthesized several years ago by annelating the 3- and 4-positions with a benzene ring.[55] The polyisothianaphthene complexes produced by the usual electrochemical polymerization through the 2,2′-positions showed a minimum in its absorption in the visible at 520 nm and a peak in the near-IR at 2200 nm, and thus, in its most conducting form (50 Ω^{-1} cm^{-1}) appeared as a light-green film. Unfortunately, there was some degradation in the properties of the oxidized film upon atmosphere exposure. Upon reduction to the neutral form the near-IR transitions disappeared and a single large transition appeared in the visible at 860 nm. The transition in the neutral polymer is at very low energy for a $\pi \rightarrow \pi^*$ transition of an aromatic compound of such small ring size. It is theorized that there is a competition between the aromaticity within the thiophene ring and the benzene ring. Upon polymerization the aromatic circuit in the thiophene ring can be broken to drive the double bonds into the bithiophene linkage to produce a polyacetylene-like structure, but with much less bond alternation. This resonance form contains a fully aromatic benzene ring. This, of course, will decrease the separation between π and π^*.

We have also observed good electrical conductivity in polycarbazole complexes that have a mixture of 3,9′- and 3,3′-linkages.[56] Upon bromine or nitrosonium oxidation a very strong

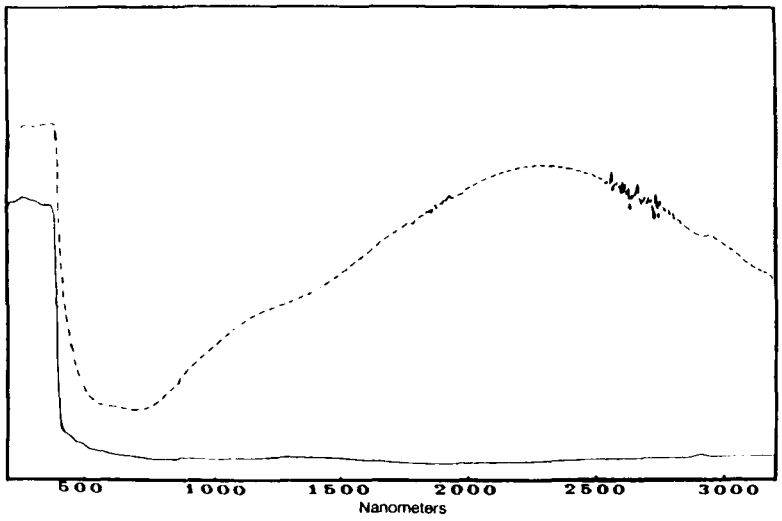

a

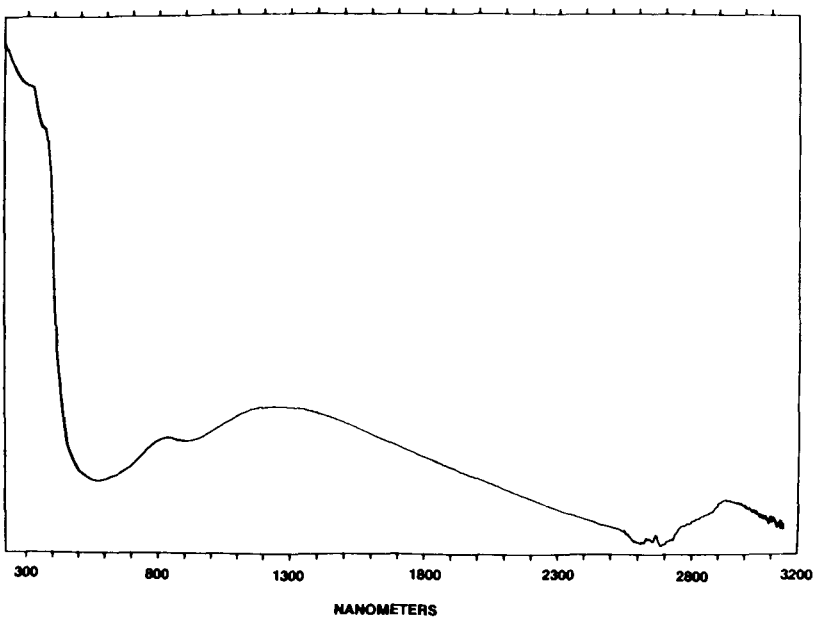

b

FIGURE 32. (a) Electronic spectrum of bromine-oxidized film of a mixed 3′3′- and 3,9′-linked carbazole made from coupling 3,6-diiodocarbazole showing minimum in absorption in the visible — dotted line; unoxidized — solid line.[56] (b) Same as (a) but a polymer of 3-methoxy 6-iodo carbazole that has been bromine oxidized.[178]

near-IR band at 2300 nm and shoulder at 1100 nm are seen (Figure 32a). The absorption minimum appears at 600 nm and the film is a light green for 10-μm-thick films with an initial conductivity of 1 Ω^{-1} cm^{-1}. The conductivity deteriorates with time, though, because of reaction of the radical cation at exposed 6-ends. Upon protecting these ends with methoxy groups air-stable conductivities of 0.01 Ω^{-1} cm^{-1} were obtained with the spectrum shown in Figure 32b.[137] In both cases the spectrum contains the absorptions from the monomer

Table 6
APPLICATIONS FOR TRANSPARENT CONDUCTORS

Visibly transparent films that reflect IR transmission
Top electrical contact on heterojunction solar cells that permits transmission of solar radiation to junction with little attenuation
Gas sensors that work by redox of gases at semiconductor surface permitting change in conductivity with transparency maintained for spectroscopic examination
Resistance heating layers for windshields to prevent frost formation
Light-transmitting electrodes in optoelectronics and waveguides for nonlinear optical applications
Photocathode in photoelectrochemical cells
Antistatic surface layers on temperature control coatings in orbiting satellites
Surface layers in electroluminescent applications

Adapted from Dawar, L. and Joshi, J. C., *J. Mater. Sci.*, 19, 1, 1984.

in Figure 33b.[137] In both cases the spectrum contains the absorptions from the monomer radical cation (1100 or 900 nm) and the mixed valence charge transfer (2300 or 1700 nm).

Visibly transparent conductors are important in many applications which are listed in Table 6 and thus they should be sought after; however, significant effort is being directed toward more efficient preparation of the indium tin oxide alloys which are already both cheap and conveniently prepared, and have conductivities of $10^4\ \Omega^{-1}\ cm^{-1}$. The advantage that conducting polymers have over the inorganic materials is that they can be switched between the different opacities when a voltage is applied. For instance, one could imagine that a conducting polymer's visible opacity or color on a windshield or canopy could be adjusted between transparent or different colors depending on the applied voltage. One of the chief limitations of conducting polymers in applications such as this is the relatively low switching speed (0.001 s) between high and low oxidation states because of a dependence on counterion diffusion rates. Successful resolution of this problem will come through design of polymeric counterions, in intimate contact with the electronically conducting polymer, that can either trap or release small ions over small distances in response to the redox cycle.

B. Photoconductivity and Devices

When light strikes a polymer with extended π orbitals electron hole pairs are created that may either stay bonded as excitonic structures, which have a very short lifetime because of almost immediate recombination, or may diffuse away from each other to produce long-lived carriers. As we have seen, there is very strong electron-phonon coupling in materials, such as polyacetylene and poly *p*-phenylene vinylene, and at least in highly crystalline materials charges probably propagate as localized disturbances such as charged solitons, polarons, and bipolarons. When these conjugated polymers are excited by a short (<ps) flash of light from a laser their absorption spectrum can be measured in a time-resolved fashion at time scales as short as 1 ps after the event.[138] These photoinduced absorption measurements reveal that polaron states are occupied within 1 ps at both the near-valence band and near-conduction band levels in the gap (a polaron exciton) by lattice relaxation of the true extended conduction band electron and valence band hole states when the material is irradiated at sufficiently high energy. In materials such as polydiaceylenes with long enclosing side chains, the two defects are constrained to one chain and will recombine within about a nanosecond with a luminescence equal to the energy difference between the bonding and antibonding states in the gap. As the chain length increases nonradiative decay to the ground state becomes more probable.

Unlike polydiacetylenes with long side chains, polyacetylene has an interchain π-π interaction on the order of 0.1 eV. This means that the polaron exciton is not confined and can decompose by charge separation into different chains. Eventually two polarons of the same charge will find each other and annihilate into a bipolaron which can have a lifetime

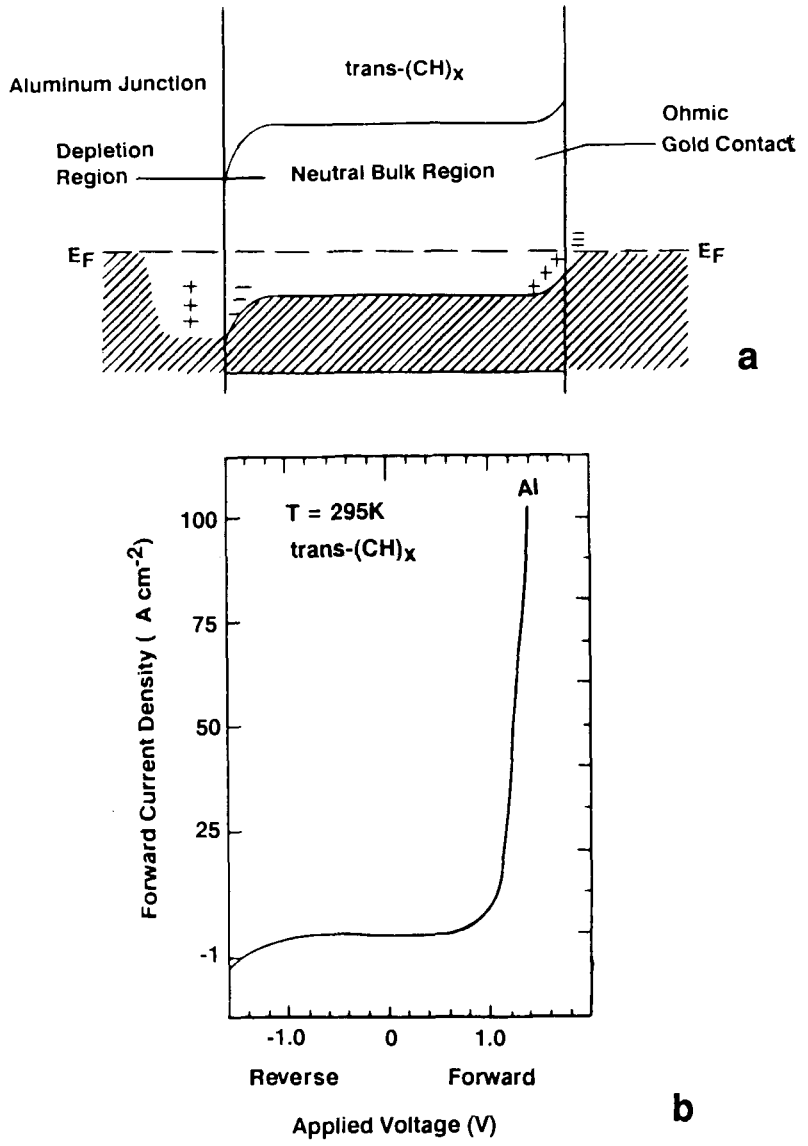

FIGURE 3 . (a) *Trans*-polyacetylene Schottkey barrier structure; (b) room-temperature dark current density vs. applied voltage rectification characteristics of Schottky barrier diode with aluminum metal.[19]

as long as milliseconds in a highly crystalline sample. This carrier will eventually decay by recombination with the oppositely charged species at a defect center. This discussion shows the importance of having good interchain interactions in order to maintain a high concentration and diffusion length for photogenerated carriers. Morphologically, this means a large lateral coherence length and a minimization of chain defects within crystals. It is obvious that conducting polymers have not achieved very high degrees of order when compared to inorganic crystals and thus would not be expected to exhibit very good properties in photovoltaic cell operation, for example.

One of the first requirements of device fabrication, for instance, a solar cell, is to fabricate a junction so that an electrostatic field can be generated within the region of charge pair generation by absorbed photons. The oppositely charged carriers will then migrate in opposite directions, preventing recombination, and inducing a current to flow in an external circuit. Figure 33a shows the energy band structure that might form when a p-conductor such as

lightly oxidized polyacetylene is placed in contact with a low work function metal to make a Schottkey barrier. Since the Fermi energy of the metal is initially higher than the semiconductor, electrons will flow down the chemical potential gradient into the semiconductor conduction band and holes from the metal valence band in the opposite direction. At the same time buildup of negative electrostatic charge on the semiconductor side occurs in a narrow region called the depletion layer where the mobile carrier concentration is extremely low. In polyacetylene this would result in anion counterions being stripped of their carriers. Because of this electrostatic charge the bands of the semiconductor bend down to create an energy barrier for further electron flow into the semiconductor conduction band. Eventually, the chemical potential equalizes across the barrier and the system is in equilibrium.

The complete device is fabricated by evaporating a high work function metal such as gold on the opposite face of the semiconductor to make an ohmic contact. The current voltage characteristics (IV) of such a polyacetylene Schottkey barrier with various metals is shown in Figure 33b and is an example of rectifying behavior where the current will flow in the forward direction (negative bias on metal electrode), but only little in the reverse bias direction.[168] The reverse bias current will be a function only of the thermal or photopromotion of electrons into the conduction band and subsequent flow down the barrier (or for holes, up the barrier). The objective in a solar cell is to tune the band gap to the peak of the solar spectrum (1.5 eV) so that maximum number of carriers are generated by absorption in the shortest possible distance, allowing them to diffuse out of the junction into the external circuit before recombination. The best possible situation requires a high carrier mobility with a minimum width of the depletion zone. Polyacetylene seems to be an ideal solar cell material since its absorption spectrum follows the solar spectrum very well. In the case of a solar cell the top ohmic electrode would be a transparent conductor like indium-tin oxide.

The photoinduced absorption measurements indicate that extended states are not long lived and will rapidly collapse into much more localized structures that must traverse the depletion layer with its high concentration of unshielded counterions. The transport must then resemble a hopping or tunnelling between shallow traps which is indeed verified by detailed capacitance measurements on the Schottkey device as a function of temperature. As expected, the photovoltaic conversion efficiencies of such a device are quite low (1%) because of the considerable trapping of photogenerated carriers.[139] This level of efficiency is certainly not competitive, with hydrogenated amorphous silica solar cells which are easily fabricated and are 13% efficient.[140]

A more serious concern has also been voiced as to whether p-n bipolar devices can ever be made from charge transfer solids with large concentrations of counterions.[141] Several experiments on molecular conductors have shown that the depletion layer thickness is independent of applied voltage and of quite high resistance. Since voltage modulation of this thickness is essential for bipolar transitor operation these applications seem to be ruled out for conducting polymers. In fact, many of the excellent Schottkey barrier properties exhibited by molecular and polymeric cells seem to be solely an effect of a surface-charged layer of only 10 Å in thickness in the polymer that is highly dependent on residual oxygen. This is also complicated by the high mobility of O_2^- under the interface electric field which will generate unstable operating characteristics and history effects. Resolution of these problems will occur when a truly wide band polymeric semiconductor conductor can be found that, in essence, behaves like silicon and dopes to high conductivities with only minute amounts of acceptors and donors.

Some attempts have been made to fabricate conducting polymers into more complicated devices in spite of these difficulties. Thus, there are examples of a model FET-type transitor based on poly(*N*-methyl pyrrole)[142] and a heterojunction formed from a contact between a reduced polythiophene and an oxidized polypyrrole.[53] Figure 34 shows a very clever transitor-like device employing polyaniline. Significant power gain is developed even at 10 kHz

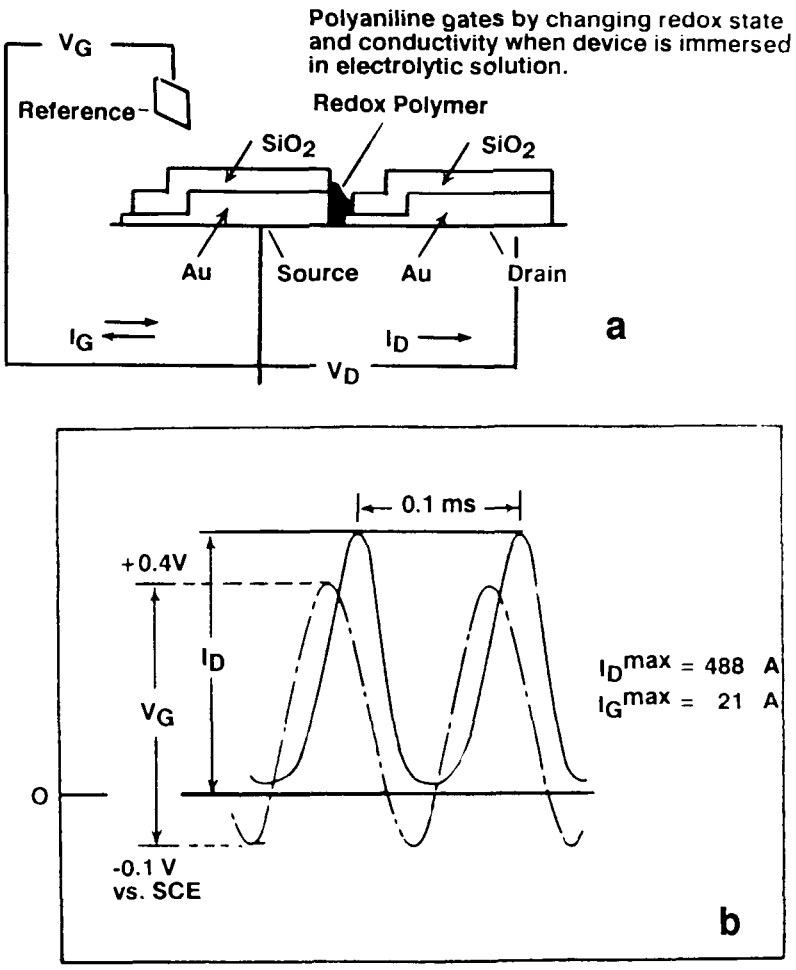

FIGURE 34. (a) Device structure employing a conducting redox polymer as a gate. Circuit is on when polyaniline is oxidized, off when reduced to the neutral state; (b) gate potential (V_G), gate current (I_G), and drain current (I_D) at 10 kHz for an ultrasmall gap polyaniline-based transitor, drain voltage V_D = 100 mV. Blank experiments show that the I_G and I_D measured for the polyaniline-based device are at least 99% due to redox and the resulting change in the conductivity of the polyaniline.[143]

because of the small amount of "gate" polymer that must undergo redox at each cycle. The device responds to 10^{-10} C of charge.[143]

C. Nonlinear Optical Properties of Conducting Polymers

In this area conjugated, extended aromatic, and organometallic polymers have outstanding potential for commercialization. Possible devices include modulated optical waveguides for fast optical logic, laser eye and sensor protection, harmonic generation, and many others.[62] Conjugated polymers such as polyacetylene, polydiacetylene, and ladder polymers similar to those discussed above have been shown to be superior to inorganic crystals both in the speed and magnitude of the effects and stability to high light fluences, and are in possession of highly anisotropic linear refractive indices which are essential for techniques such as phase matching. Consideration of complicated effects involving phase matching requires more background than this author can cover here and thus, the discussion will be limited to molecular mechanisms and some simple effects such as intensity-dependent refractive index, depending only on a third-order susceptibility, χ^3.

When certain materials are exposed to high intensity light, even nonresonant with any electronic transition, physical constants such as the refractive index change. Generally, there are many mechanisms contributing to such a physical effect, each of them acting on a different time scale. Simple local heating which will change the density of the material in the beam can respond in the nanosecond time scale and will obviously change the refractive index.[144] On even a faster picosecond time scale, lattice vibrational relaxations can couple with excited electron polarizations to produce localized defect states within the gap such as polaron exitons as discussed above. Stationary extended, electronic states that decay into these more localized states can be accessed by multiphoton absorbances. Here, the first increment of photon energy excites a virtual nonextended polarization of the molecule in the gap; the second increment of photon energy excites this state, which exists only in the electric field of the photon, into a stationary band state from which it will decay. The virtual excitations, being purely electronic, are excited in the order of femtoseconds. Typically, the faster the process the smaller its perturbance on molecular constants such as refractive index.

The usual intensity-dependent refractive index behaves as

$$n = n_o + n_2 I \tag{17}$$

where n_0 is the low intensity refractive index, n_2 is the nonlinear factor, and I is the light intensity. The nonlinear refractive index is related to the third-order susceptibility, X^3, by

$$n_2 = 16\pi\chi 10^7 \chi^3 / n_o^2 c \tag{18}$$

where c is the speed of light, χ^3 is in esu, and n_2 is in cm^2/W. The third-order susceptibility written above is a complex number and has a real part related to a real refractive index change and an imaginary part related to nonlinear absorption. The susceptibility is related to the polarization, p_i, induced in the molecule by electric field components E_i by

$$p_i = \chi^1_{ij} E_j + \chi^3_{ijkl} E_j E_k E_l \tag{19}$$

where χ^1 is the linear polarization.

Most conducting polymers have centrosymmetric structure and, therefore, the second-order susceptibility does not appear in the expression. As an example of the order of magnitude of the effect that can be generated in unoriented polyacetylene,[61] a nonresonant χ^3 of 4×10^{-10} esu was measured at 1.06 μm for third harmonic generation. If the third harmonic generation susceptibility is on the same order as the susceptibility defining a refractive index change, the expected refractive index coefficient is 5×10^{-7} cm^2/MW. Since the nonlinear effects are strongly polarized in the chain axis direction, an oriented sample would give an order-of-magnitude-larger effect. The value above compares well with that found in inorganic semiconductors. Resonant effects are of course stronger, since the field will induce a much larger perturbation in the π cloud; resonant χ^3 values of 5×10^{-8} esu are found. However, these are much smaller than those found in GaAs/GaAlAs superlattices (10^{-1} esu).[145]

The nonresonant values of the polymer electronic susceptibility are still too low for practical device application. For example, one would like to change coupling lengths in optical waveguides at power levels in the 10^4-MW/cm^2 range, producing a refractive index change in the cladding in the third decimal place.[146] For practical device application the effect generated must originate from a picosecond electronic process. Nanosecond processes are highly mixed with thermal effects which can have $\chi^3 > 10^{-2}$ esu, overwhelming any electronic effect and leading to damage and history effects. Polymers will then have to be produced with nonresonant electronic susceptibilities better than 10^{-7} esu. The basic concept

in the waveguide applications is that certain guided modes will propagate in a guide only if the refractive index of the media surrounding the guide is less than that of the guide itself. If the refractive index difference becomes too small (e.g., by a nonlinear change in the refractive index) the mode will leak out of the guide. An intensity-limiting behavior of this sort and, in some cases, self-focusing of the mode lead to applications in optical switching, bistability, modulation, and logic.

At the present time there is very active investigation into bringing the value of the susceptibility into a more useful nonresonant range. For polyene structures such as polyacetylene the following relation is predicted:[61]

$$\chi^3 = [(e^4a^3\sigma)/(90\pi^3)](W/E_g)^6 \tag{20}$$

where E_g is the band gap, a is the unit cell size, σ is the chain cross section, W is the band width, and W/E_g is the delocalization length. This relation predicts that the nonresonant susceptibility should increase very rapidly with decrease in band gap for extended states in a rigid band. In polyacetylene-like structures the gap decreases when the degree of bond alternation decreases. The increase in χ^3 is logical, since an extended one-dimensional free electron cloud should be more polarizable than an alternate bond network which clearly sees the nuclear potential.

Since the nonlinear optical properties depend so strongly on the chain conjugation, there might be some small improvements in the χ^3 if polyacetylene or other conjugated material was crystallized to a greater extent, but this increase would not be large. Initially, it was hoped that ladder polymers with more extended two-dimensional π networks might show larger effects; however, this has not been observed in the important picosecond regime.[147] ENDOR measurements have also revealed that the extent of delocalization is complete after one or two repeats of a ladder polymer structure and that consequently no further improvements in χ^3 are to be expected with increased degree of polymerization.[148]

A rather thorough study of the χ^3(3rd harmonic generation) behavior of polyacetylene in the band gap[61] has revealed that strong enhancements of this susceptibility occur at the two-photon absorption and the three-photon absorption (Figure 35).[61] The χ^3 observed at 0.65 eV (2000 nm) exceeds 10^{-9} esu and is the highest nonresonant value ever measured for any material. The actual chain χ^3 is probably an order of magnitude higher than this because of the porous morphology and unoriented nature of the film measured. These values are only two orders of magnitude away from the values required for practical device fabrication. It also must be remembered that the χ^3 for third harmonic generation is probably smaller than the χ^3 for refractive index change, since the latter value is a sum of many different processes.

The multiphoton transition probabilities increase with the single-photon transition probability. Therefore, one strategy for increasing the strength of the multiphoton processes might be to employ 1-d polymers with more polarizable atoms with strong first-order transition probabilities. Coupled d-π^* transitions in the Ru(+2)pyrazine hexamer mentioned in Section II.D have oscillator strengths on the order of 160,000 cm^{-1} and are probably completely valence delocalized.

The observation of soliton and polaron exitons in conjugated conducting polymers is a hopeful sign, since there is then the possibility that NLO mechanisms similar to those that operate in quantum well structures might occur.[145] For instance, in normal semiconductors at low temperature excitons are excited by energies close to the bandgap; however, they are not stable and rapidly delocalize (or ionize) into electron hole pairs through interactions with longitudinal optical phonons in $t < 0.4$ ps. They are not seen at room temperature because the screening effect of thermally generated free carriers prevents their formation even for a short time. In multiple quantum well structure excitons are confined to two dimensions and are more strongly bound and thus can be seen as sharp resonances of large oscillator strength

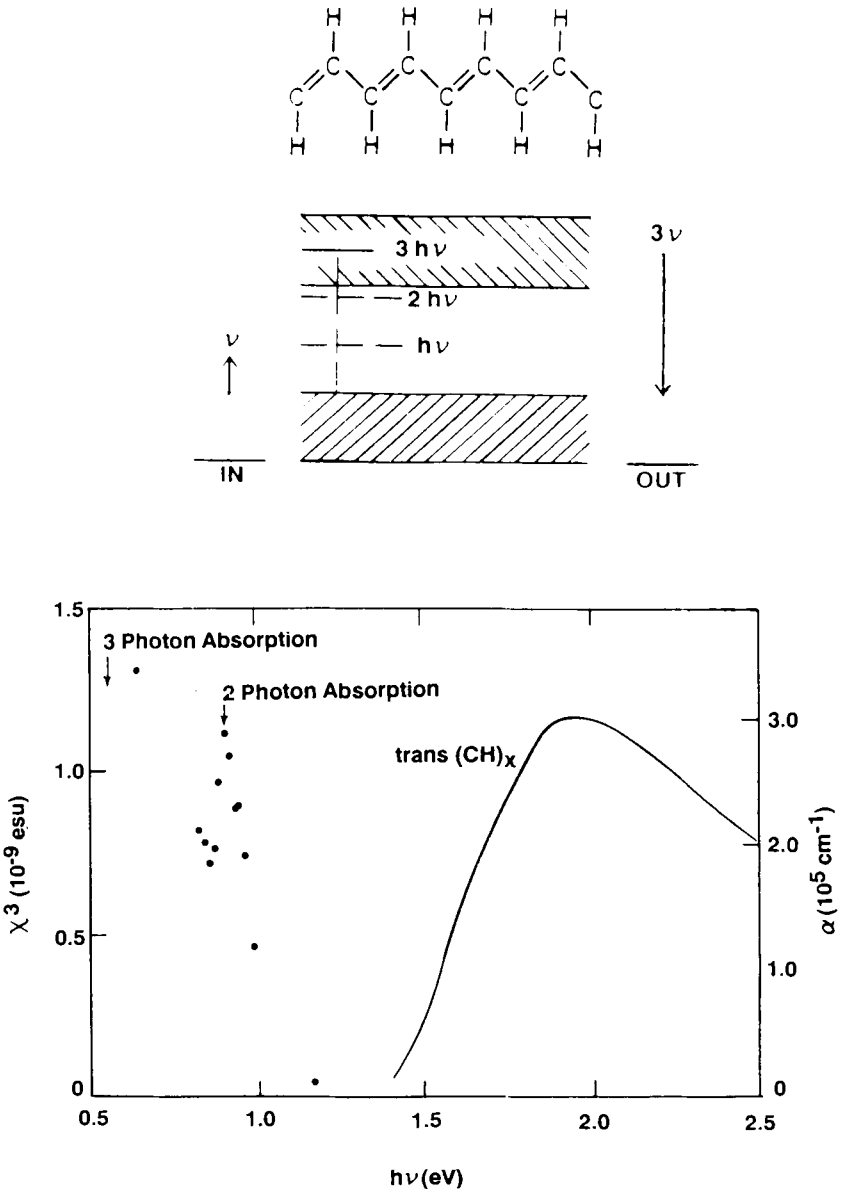

FIGURE 35. (a) Schematic diagram showing the measurement of one, two, and three photon contributions to the third harmonic intensity in *trans*-polyactetylene; (b) closed circles of χ^3 of *trans*-polyacetylene. The dashed line is the χ^1 of *trans*-polyacetylene shown for comparison. The solid line is the χ^3 of the nominally *cis*-polyacetylene.

close to the band edge even at room temperature. If a laser is tuned close to this resonance excitons are generated, exist for about 0.4 ps, and then decay into electron hole pairs. Since exciton generation is a faster process then decay (<150 fs), the exciton concentration will continue to build until a critical concentration is reached when all the space in the lattice is occupied (similar to the close packing of positronium atoms). Because of large size of the exciton this requires only a relatively weak irradiation. At this point the collection of boson-like particles (actually composite fermions) interacts and decomposes into a sea of electrons and holes where the formation of subsequent excitons is prevented by free carrier screening. The practical consequence of this is the disappearance of the exciton resonance or bleaching

at the exciting frequency at only 580 W/cm^2! The system recovers to the ground state in several nanoseconds by free carrier recombination, ready for the next pulse.

Applied electric fields also have a strong effect on this process in that they can destabilize the exciton by literally pulling the pair of charges apart. Large fields are not required, since the binding energies of the exciton are so low. The applications in electrooptic modulation are obvious and actually have been proven.

By analogy excitons in conducting polymers should be highly confined in one dimension, have a strong binding energy, and thus should be observed at room temperature. This is quite true; in fact, due to the strong electron-phonon coupling, they are $\approx$0.1 eV more stable than free carriers as compared to the 10^{-3} eV found in quantum well inorganic semiconductors. These are the polaron excitons mentioned above that can be accessed only by exciting free carriers which subsequently interact with a phonon and stabilize. Conceivably, actual phonon-uncoupled excitons might exist in the band edge, but the blurring of the band edge by structual disorder masks this. Even if these states could be generated by a direct transition, the transition would saturate at a much higher power than in quantum well structures, since fast decay of the exciton into an exciton polaron state would just deplete the exciton state with no increase in screening by free carrier generation, this latter factor being the most important in bleaching the exciton absorbance in GaAs.

The solution to this problem is to make polymers where the phonon electron coupling is much weaker so that energetic phonons will destroy the exciton and not stabilize it. Making a much more ordered structure would also be necessary so as to sharpen the gap and bring out the excitonic features. This probably means making the structure more two dimensional so as to retain exciton confinement, but minimize Peierles-type distortions which couple so well to the electrons. Ladder polymers have some potential in this regard, but are still much too disordered and probably will not harbor truly delocalized carriers.

Another mechanism of nonlinearity that could be utilized for conducting polymers would be making use of plasma excitations of the conduction band electrons. In this regard nonresonant $\chi^3 = 5 \times 10^{-8}$ esu had been observed for a TTF-type stacked charge transfer complex with iodine. This organic metal demonstrated the largest nonlinearity perpendicular to the stack direction, in the direction of highest electrical conductivity.[149]

D. Electrochemical Devices — Batteries and Chemical Sensors

As we have seen in Section III.C, the organic salt-like nature of most conducting polymers precludes some applications such as bipolar transitors; however, this very capability to store and release large amounts of charge by an electrochemical redox process makes them candidates for storage battery applications. Since the density of conducting polymers is relatively small, they should achieve a very high specific energy density. This figure of merit is calculated for polypyrrole in the following way for a polypyrrole anode:[17]

$$(C_4H_3N)_x + xy\ LiClO_4 = [(C_4H_3N)^{+y}(ClO_4)_y] + xy\ Li^+$$

The theoretical energy density of this reaction is the charge capacity/kilogram multiplied by the cell voltage, V:

$$E(Wh/kg) = (VyF)/kg\ of\ reactants \tag{21}$$

where F = faraday constant and y = 0.33. Since the voltage of a slowly discharged polypyrrole cell is 3.25 V the theoretical energy density is E = 287 Wh/kg. This number must be adjusted for the container, collector, and electrolyte weight which leads to a practical value of E_p = 57 Wh/kg. This value can be compared to E_p = 40 and 35 Wh/kg for the lead acid and nickel cadmium battery. One might think that further improvements might be

gained by using a polymer cathode also, but this is not practical considering the limited stability of polymeric anions, the greater density of polymer relative to Li, and the higher charge density storage on Li. There is a report, however, that *n*-polyacetylene might actually be more stable in a secondary battery than *p*-polyacetylene.[150]

This value of the energy density puts the polymer battery in the competitive range, but there are several other factors that must be taken into account to make a battery fully competitive. Upon recharge the battery must have a high coulombic efficiency so that the charging current is not dissipated into heat or worse. The electrode material must also not degrade over time when the battery is deeply discharged and recharged at a high rate over many cycles. A practical goal here is to be able to take the battery to deep discharge over at least 400 cycles.

These latter factors eliminate polyacetylene as a battery material. Normal film samples of polyacetylene will sustain only a very slow rate of constant current charge-discharge (microamps/square centimeter)[151] and have only poor coulombic efficiency (50%) in lithium perchlorate/propylene carbonate. The slow charge and discharge rate may be related to the necessity for the counterion to intercalate into a highly crystalline structure; this process will, of course, be slow until a phase transition to an ion channel-type network occurs. Improvements in charge and discharge rates to milliamps/square centimeter can be induced by foaming the polyacetylene to create a large surface area. The coulombic efficiencies also increase to 85%.

One of the sources of coulombic inefficiency was oxidation of the solvent through a catalytic surface action of the polyacetylene.[50] Polyacetylene also self-discharges over time. For these reasons efforts have shifted to secondary batteries made with aromatic and heteroaromatic polymers.

The morphology of the battery electrode is, of course, highly important for charge and discharge rates. Ideally, a porous structure is to be preferred for rapid ion exchange. When polypyrrole charge transfer complex is formed quickly on an electrode by electrochemical oxidation of pyrrole at higher voltage than normally used, a porous rough film develops on the electrode.[152] For the more porous electrode 100% coulombic efficiency is maintained up to current densities of 0.5 mA/cm^2 — quite a respectible behavior, much improved over a more solid film. The performance of polypyrrole after 500 cycles of 100% deep discharge is also very good in that only 15% of the energy density is lost. The self-discharge is also negligible.[153]

Some of the best performances so far have been obtained from polyaniline secondary batteries, again with lithium cathodes. Polyaniline has many advantages in that it can be deposited cheaply on surfaces by electrochemical oxidation of aniline in aqueous media. Films synthesized from HBF_4 solutions seem to provide the best characteristics,[48] the objective here being to minimize the counterion size and increase diffusion rates. Ion size does not have as strong an effect in polypyrrole systems, since lithium ion diffuses in to neutralize the film during discharge.[154] The energy densities for the best prepared of these batteries appears to be around 340 Wh/kg.[192,193]

The future for eventual commercialization of either the polypyrrole or polyaniline secondary battery system looks bright. The specific energy density, retention of specific energy on deep recycle, and self-discharge are all very competitive. Improvement in energy density per unit volume is the remaining requirement[47] for penetration into the storage battery market that is dominated by improved versions of the lead acid battery.[155] In smaller markets such as powering small detectors, hearing aids, and pacemakers, there is already a possibility of commercialization. In fact, Sieko Electronics Components and Bridgestone Corporation have started sales of a polyaniline-lithium battery for these applications. Expected lifetime of the battery is expected to exceed 5 years.[156] Further improvements in design and safety will be possible once solid or viscous polymer electrolytes of high ionic conductivity and stability are developed for batteries such as this.

Related to the battery in many ways is the fuel cell. In this system electric current is generated by flowing a gas or liquid over a catalytic electrode that can induce a redox process that generates either electrons or holes for an external circuit while converting the fuel.[157] Highly efficient fuel cells employing hydrogen as an electron generator and oxygen as a hole generator have been used in the space program. The product of the reaction, water, is obviously very useful in this environment.

One half-reaction has been demonstrated for a polyacetylene/oxygen electrode in a fuel cell configuration.[158] The secret to success in this system was to perform the oxidation of the polyacetylene by bubbling oxygen over a piece of polyacetylene in concentrated fluorboric acid. The high proton concentrations assured that the superoxide counterion was rapidly protonated to hydrogen peroxide before it could attack the polyacetylene chain. The hydrogen peroxide then oxidized the polyacetylene again to produce water, leaving the polymer cations with fluorborate counterions.

The other half-cell in this experimental demonstration was a piece of lead that ionized to Pb(+2) releasing electrons to the polyacetylene. It was thus possible to carry out the net reaction:

$$0.01 \times Pb + [CH^{0.02+}(BF_4)^{-}_{0.02}]_x \rightarrow (CH)_x + 0.01 \times Pb(BF_4)_2$$

In principle, with an appropriate electrocatalytic surface an organic compound, hydrogen, or hydrazine might be used as fuels.

Another electrochemical-type application for conducting polymers is in the area of electrocatalysis. A typical approach in this case is to electropolymerize a monomer such as pyrrole[159] or biphenyl[160] to the conducting polymer complex in the presence of an electrocatalytic agent such as a metal porphyrin. The metal complex is incorporated into the conducing polymer film and often exhibits a much simplified behavior relative to solution because of the elimination of bimolecular effects. The concept is that since the electrochemical potential of the conducting polymer can be continuously varied, it might be possible to switch the catalytic species between several stable oxidation states which would catalyze reactions in a highly selective fashion.

Phthalocyanine metal complexes are very interesting from this point of view since they can show multiple redox processes. For instance, the cobalt metallocene shows seven separate levels of oxidation.[161] The practical result of this is that oxygen has been bound to the iron metallocene in a reversible fashion at potentials 0.8 V less negative than without catalyst in a polypyrrole film.[159] This effect has also been reproduced in electropolymerized poly *p*-phenylene films. An interesting feature of the latter result is that the polymer is in its neutral form at these voltages. In principle, these complexes could be used to catalyze oxygen insertion reactions into organic compounds.

Another possible application for conducting polymers that uses their capability to do reversible redox is sensors. The scope of this subject is immense, more than 1000 articles per year appearing.[162] Sensor systems have been designed for scores of ions, gases, and even small organic molecules and macromolecules of biological interest. A redox sensor for example, a gas is just the reverse of the catalytic system discussed above. When oxygen binds to the metallocene its oxidation state will change. Depending on how well the sensor molecule is coupled to the conducting polymer matrix the polymer matrix might be reduced, an effect which could be picked up by the external circuit. More precisely, one could think of a modification of the ISFET concept. In an ISFET (ion-specific field effect transitor) ion absorption and migration are used to polarize or depolarize the gate on an FET, which will, of course, modulate the current at the drain of the transistor. One can imagine a similar situation where one would place the neutral form of a fairly wide gap polymer semiconductor on the gate of the FET and polarize it. Upon exposure to an oxidizing gas the conductivity

of the gate would increase, causing depolarization and a change in the channel width of the underlying semiconductor.

The final electrochemical concept to be discussed is the photoelectrochemically induced reactions. At the present time there is much work going on in the area of light-induced photocatalysis where a metal complex can be excited into a state where charge is transferred to a ligand by a d-π^* charge transfer.[163] In this photoexcited state the charged ligand will perform reductions not possible in the ground state. In a similar fashion a semiconductor such as GaAs can be placed in solution where a liquid junction and band bending will occur in much the same way as in the case of the Schottkey barrier. Depending on the direction of band bending either holes of electrons will migrate to the surface under the influence of the electric field of the junction where they can perform reactions. The difficulty is that GaAs is unstable in the presence of holes and water and the catalytic properties of these semiconductors deteriorates very rapidly due to surface oxide formation. Coating semiconductor electrodes with air- and water-stable conducting polymers should retard this corrosion process and, in addition, transport the hole to the solution interface where it can react. The band bending of the polymer at the semiconductor interface and the solution interface then become important. In one recent example of this technology polyaniline has been coated onto the ITO front face of an ITO heterojunction. The degradation of the catalytic activity of the semiconductor was reduced a considerable extent by this treatment.[164] Recent experiments have shown that polyaniline does form a junction at the solution semiconductor junction and will generate a photoresponse when it is irradiated.[165]

V. CONCLUDING REMARKS

In the last few years many excellent reviews, books, and summaries of conference proceedings have been written[166-170] on the subject of conducting polymers, and the reader should consult them for greater details. What this author has tried to do here is provide some background and assessment of the field up to the end of 1987. The last 2 years have seen

1. Polymers with high molecular weight that are soluble in both the neutral and charge transfer complex form and can be cast into films with high conductivity over long periods in air
2. The route to water-soluble conducting polymers and the synthesis of zwitterionic conductors established
3. Ultrahigh conductivity polyacetylene complexes that apparently behave as true metals with attainable conductivities better than copper on a volume basis and also exhibit rather good air stability
4. The demonstration that conjugated conducting polymers have the highest known nonresonant, nonlinear susceptibility of any material
5. The development of conducting polymer latex systems that are being presented commercially

Prior to some of these developments it looked like conducting polymers would not live up to the expectations that had been created for them in the late 1970s; however, through some clever chemistry, promise has been restored and actual commercial applications will be forthcoming in greater abundance.

ACKNOWLEDGMENTS

I wish to thank Bob Lyle, Garry Wnek, and Juey Lai for reviewing this manuscript and Dave Herrera, Jack Trevino, and Jackye Moravits for help with the figures and tables.

REFERENCES

1. **Francois, G. L., Walker, E., Jorda, J. L., Yvon, K., and Fischer, P.,** Structure of high temperature superconductor $Ba_2YCu_3O_7$ by X-ray and neutron powder diffraction, *Solid State Commun.*, 63(12), 1149, 1987; **Anderson, P. W. and Abrahams, E.,** Superconductivity theories narrow down, *Nature*, 327, 363, 1987.
2. **Kittel, C.,** *Introduction to Solid State Physics*, 5th ed., John Wiley & Sons, New York, 1976, 359.
3. Articles within *J. Phys.*, 44, (Colloq. C3, Suppl. 6), June 1983.
4. **Geiss, R. H., Thomas, J., and Street, G. B.,** Electron microscope study of the structural behavior of halogenated $(SN)_x$, *Synth. Metals*, 1, 257, 1979/1980.
5. **Basescu, N., Liu, Z., Moses, D., Heeger, A. J., Naarmann, H., and Theophilou, K.,** High electrical conductivity in doped polyacetylene, *Nature*, 327, 403, 1987.
6. **MacKenzie, J. D.,** Applications of the Sol-Gel method: some aspects of initial processing, in *Science of Ceramic Chemical Processing*, Hench, L. L. and Ulrich, D. R., Eds., John Wiley & Sons, New York, 1986.
7. **Simpson, M. and Smith, P.,** *Chem. Br.*, 23, 37, 1987.
8. **Eckertova, L.,** *Physics of Thin Films*, Plenum Press, New York, 1977.
9. **Glang, R.,** *Handbook of Thin Film Technology*, Maissel, L. and Gland, R., Eds., McGraw-Hill, New York, 1970.
10. **Rizkalla, H. and Wellinghoff, S. T.,** Inherent ductility in amorphous tantalum oxide films, *J. Mater. Sci.*, 19, 3895, 1984.
11. **Claussen, N. and Ruhle, M.,** *Advances in Ceramics*, Vol. 3, Heuer, A. H. and Hobbs, L. W., Eds., American Ceramic Society, Columbus, OH, 1981, 137.
12. **Pietro, W. J., Ellis, D. E., Marks, T. J., and Ratner, M. A.,** Building blocks for molecular and macromolecular metals, electronic structure of group IVA phthalocyanine monomers and cofacially-joined dimers, *Mol. Cryst. Liquid Cryst.*, 105, 273, 1984.
13. **MacDiarmid, A. G. and Heeger, A. J.,** Organic metals and semiconductors: the chemistry of polyacetylene, $(CH)_x$, and its derivatives, *Synth. Met.*, 1, 101, 1979/1980.
14. Technical Data Bulletin, Polaroid ICP-117.
15. **Muenstedt, H., Naarman, H., and Kohler, G.,** Electrical conductivities of modified polyacetylene and polypyrrole, *Mol. Cryst. Liquid Cryst.*, 118, 129, 1985.
16. **MacDiarmid, A. G., Mammone, R. J., Krawczyk, J. R., and Porter, S. J.,** Reduction potentials: key to doping phenomenon in polyacetylene, *Mol. Cryst. Liquid Cryst.*, 105, 89, 1984.
17. **Wegner, G.,** Conducting organic materials: present status and scope, *Angew. Makromol. Chem.*, 145/146, 181, 1986.
18. **Wellinghoff, S. T., Deng, Z., Kedrowski, T. J., Dick, S. A., Jenekhe, S. A., and Ishida, H.,** Electronic conduction mechanisms in polycarbazole iodine complexes, *Mol. Cryst. Liquid Cryst.*, 106, 289, 1984.
19. **Kanicki, J.,** Metal-polyacetylene Schottky barrier diodes, *Mol. Cryst. Liquid Cryst.*, 105, 203, 1984.
20. **Foot, P. J. S., Mohammed, F., Calvert, P. D., and Billingham, J.,** Diffusion in conducting polymers, *J. Phys. D*, 20, 1354, 1987.
21. **Pearson, J. R. A.,** *Mechanics of Polymer Processing*, Elsevier, London, 1985.
22. **Patil, A. O., Ikenoue, Y., Wudl, F., and Heeger, A. J.,** Water soluble conducting polymers, *J. Am. Chem. Soc.*, 109, 1858, 1987.
23. **Shirakawa, H., Louis, E. J., MacDiarmid, A. G., Chiang, C. K., and Heeger, A. J.,** Synthesis of electrically conducting organic polymers: halogen derivatives of polyacetylene, *J. Chem. Soc. Chem. Commun.*, p. 578, 1977.
24. **Nigrey, P. J., MacDiarmid, A. G., and Heeger, A. J.,** Electrochemistry of polyacetylene: electrochemical doping of polyacetylene films to the metallic state, *J. Chem. Soc. Chem. Commun.*, p. 594, 1979.
25. **Calvert, P.,** *Nature*, 304, 487, 1983.
26. **Inabe, T., Lomax, J. F., Marks, T. J., Lyding, J. W., Kannewurf, C. R., and Wynne, K. J.,** Processible, oriented, electrically conductive hybrid molecular/macromolecular materials, *Macromolecules*, 17, 260, 1984.
27. **Kim, O.,** Ladder polymers as new conductors, *Mol. Cryst. Liquid Cryst.*, 105, 161, 1984.
28. **Frommer, J. E., Elsenbaumer, R. L., and Chance, R. R.,** *Polymers in Electronics*, Davidson, T., Eds., ACS Symp. Ser., American Chemical Society, Washington, D.C., 1983; *Org. Coat. Appl. Polym. Sci. Proc.*, 48, 552, 1983.
29. **Aldissi, M.,** Chain rigidity-processability correlation in inherently conducting polymers, *Polym. Plast. Technol. Eng.*, 26(1), 45, 1987.
30. **Jenekhe, S. A., Wellinghoff, S. T., and Reed, J. F.,** Synthesis of highly conducting heterocyclic polycarbazoles by simultaneous polymerization and doping in liquid iodine, *Mol. Cryst. Liquid Cryst.*, 105, 175, 1984.

31. **Jenekhe, S. A., Wellinghoff, S. T., and Deng, Z.,** Electronically conducting complexes of poly(3,6 N-methylcarbazole methylene), *Synth. Metals,* 10, 281, 1985.
32. **Bradley, D. D. C.,** Precursor-route poly(p-phenylenevinylene): polymer characterization and control of electronic properties, *J. Phys. D,* 20, 1389, 1987.
33. **Feast, W. J., Taylor, M. J., and Winter, J. N.,** Precursor routes to polyacetylene: the microstructure of the precursor polymers, *Polymer,* 28, 593, 1987.
34. **Miyata, S. and Ozio, T.,** Electrically Conductive Composite Molded Bodies, Ger. Offen. DE 3,544,95, 1986.
35. **Reynolds, J. R.,** Advances in the chemistry of conducting polymers: a review, *J. Mol. Electron.,* 2(1), 1, 1986.
36. **Aksay, I. A.,** Microstructure control through colloidal consolidation, *Adv. Ceram.,* 9, 94, 1984.
37. **Ivory, D. M., Miller, G. G., Sowa, J. M., Shacklette, L. W., Chance, R. R., and Baughman, R. H.,** Highly conducting charge transfer complexes of poly p-phenylene, *J. Chem. Phys.,* 71(3), 1501, 1979.
38. **Heimenz, P. C.,** *J. Polym. Sci. C,* 27, 253, 1969.
39. **Ugelstad, J., Kaggerud, K. H., Hansin, F. K., and Berge, A.,** Absorption of low molecular weight compounds in aqueous dispersions of polymer-oligomer particles. II, *Makromol. Chem.,* 180, 737, 1979.
40. **Bryce, M. R., Chissel, A., Kathirgamananathan, P., Parker, D., and Smith, N. R.,** Soluble conducting polymers from 3-substituted thiophenes and pyrroles, *J. Chem. Soc. Chem. Commun.,* p. 467, 1987.
41. **Sato, M., Tanaka, S., and Kaeriyamz, K.,** Soluble conducting polythiophenes, *J. Chem. Soc. Chem. Commun.,* p. 873, 1986.
42. **Sato, M., Tanaka, T., Kaeriyama, K., and Tomonaga, F.,** Poly(3-butylthiophene) and poly(3-benzylthiophene) films, *Polymer,* 28, 1071, 1987.
43. **Sato, M., Tanaka, S., and Kaeriyama, K.,** Poly(3-dodecyl-2,5-thiophenediyl), a soluble and conducting polymer K, *Makromol. Chem.,* 188(7), 1763, 1987.
44. **Huang, W. and Park, J. M.,** Processible conductive copolymers of 3-methylthiophene and methylmethacrylate, *J. Chem. Soc. Chem. Commun.,* p. 857, 1987.

45a. **Reilly, J. J., Thomas, S. J., and Lin, W.,** Characterization of hybridized conductive fiber reinforced thermoplastics, *SAMPE J.,* 23(1), 22, 1987.

45b. McGraw-Hill's Report on High Performance Materials, McGraw-Hill, New York, November 30, 1987.

46. **Muenstedt, H., Koehler, G., Mochwald, H., Naegele, D., Bittihn, R., Ely, G., and Meissner, E.,** Rechargeable polypyrrole/lithium cells, *Synth. Met.,* 18(1 to 3), 259, 1987.
47. **Bittihn, R.,** Problems related to polymer battery design, *Springer Ser. Solid State Sci.,* 63, 206, 1985.
48. **Yamamoto, T., Zoma, M., Hishinama, M., and Yamamoto, A.,** Lithium secondary cells using LiX (X = ClO_4, BF_4) as electrolyte and poly(2,5 pyrrolylene) and poly(2,5 thienylene) as positive electrodes, *J. Appl. Electrochem.,* 17(3), 607, 1987.
49. **MacDiarmid, A. G., Yang, L. S., Huang, W. S., and Humphrey, B. D.,** Polyaniline electrochemistry and applications to rechargeable batteries, *Synth. Met.,* 18(1 to 3), 393, 1987.
50. **Schlenoff, J. B. and Chien, J. C. W.,** The cyclic voltammetry of pristine, isomerized, deuterated, and partially hydrogenated p-type polyacetylene, *J. Electrochem. Soc.,* 134(9), 2179, 1987.
51. **Passiniemi, P. and Osterholm, J. E.,** Electrochemical cells employing polyacetylene cathodes in non-aqueous solution, *Mol. Cryst. Liquid Cryst.,* 121(1 to 4), 215, 1985.
52. **Passiniemi, P. and Osterholm, J. E.,** Critical aspects of organic polymer batteries, *Synth. Methods,* 18(1 to 3), 637, 1987.
53. **Aizawa, M., Yamada, T., Shinohara, H., Akagi, K., Shirakawa, H.,** Electrochemical fabrication of a polypyrrole-polythiophene p-n junction, *J. Chem. Soc. Chem. Commun.,* p. 1315, 1986.
54. **Kaneko, M. and Yamada, A.,** Photoresponse of a Schottky junction polythienylene film, *J. Polym. Sci.,* 23, 629, 1985.
55. **Wudl, F., Kobayashi, M., Colaneri, N., Boysel, M., and Heeger, A. J.,** Novel organic conductors: effect of structure and band gap, *Mol. Cryst. Liquid Cryst.,* 118, 199, 1985.
56. **Racchini, J. R., Wellinghoff, S. T., Schwab, S. T., and Herrera, C. D.,** Synthesis and studies of poly(3,9-carbazolyl), a new conductive polymer displaying high optical transmittance in the visible, *Synth. Metals,* 22(3), 273, 1988.
57. **Jarzebski, Z. M.,** Preparation and physical properties of transparent conducting oxide films, *Phys. Status Solids A,* 71, 13, 1982.
58. **Dawar, L. and Joshi, J. C.,** Semiconducting transparent thin films: their properties and applications, *J. Mater. Sci.,* 19, 1, 1984.

60a. **Blankespoor, R. L. and Miller, L. L.,** Polymerized 3-methylthiophene: a processible material for the controlled release of drugs, *J. Chem. Soc. Chem. Commun.,* p. 90, 1985.

60b. **Miller, L. L. and Zhou, Q. X.,** Poly(N-methylpyrrolylium) poly(styrenesulfonate). A conductive, electrically switchable cation exchanger that cathodically binds and anodically releases dopamine, *Macromolecules,* 20, 1594, 1987.

61. **Etemad, S., Baker, G. L., Jaye, D., Kajzar, F., and Messier, J.,** Linear and nonlinear optical properties of polyacetylene, in *Proc. SPIE Int. Soc. for Optical Engineering,* Vol. 682, Khanarian, J., Ed., SPIE, Bellingham, WA, 1982, 44.
62. **Garito, A. F., Teng, C. C., Wong, K. Y., and Zammani, K.,** Molecular optics: nonlinear optical processes in organic and polymer crystals, *Mol. Cryst. Liquid Cryst.*, 106, 219, 1984.
63. **Agrawal, G. P., Cojan, A., and Flytzanis, C.,** Non-linear optical properties of one-dimensional semiconductors and conjugated polymers, *Phys. Rev. B,* 17(2), 776, 1978.
64. **Rustagi, K. C.,** Dispersion and polarization dependence of mobile carrier nonlinearities, *Appl. Phys. Lett.*, 44(12), 1121, 1984.
65. **Sproull, R. L.,** *Modern Physics: The Quantum Physics of Atoms, Solids, and Nuclei,* 2nd ed., John Wiley & Sons, New York, 1967.
66. **Torrance, J. B.,** The difference between metallic and insulating salts of tetracyanoquinodimethane (TCNQ): how to design an organic metal, *Acc. Chem. Res.*, 12(3), 79, 1979.
67. **Lahti, P. M., Obruzut, J., and Karasz, F. E.,** Use of the Pariser-Parr-Pople approximation to obtain practically useful predictions for electronic spectral properties of conducting polymers, *Macromolecules,* 20, 2023, 1987.
68. **Slater, J. C.,** Energy band calculations to 1972, in *A.I.P. Handbook,* McGraw-Hill, New York, 1972, 9-31.
69. **Grant, P. M. and Batra, I. P.,** Electronic structure of conducting π-electron systems, *Synth. Metals,* 1, 193, 1979/1980.
70. **Rudge, W. E. and Grant, P. M.,** Orthogonalized plane wave band structure of polymeric sulfur nitride, *Phys. Rev. Lett.*, 35, 1799, 1975.
71. **Feldblum, A., Bigelow, R. W., Gibson, H. W., Epstein, A. J., and Tanner, D. B.,** Nearly metallic $[CH(I_3)_y]_x$ — importance of solitons, crystal order, hopping and band conduction, *Mol. Cryst. Liquid Cryst.*, 105, 191, 1984.
72. **Kivelson, S.,** Electron hopping in a soliton band: conduction in lightly doped $(CH)_x$, *Phys. Rev. B,* 25(6), 3798, 1982.
73. **Shante, V. K. S.,** Hopping conduction in Quasi-one-dimensional disordered compounds, *Phys. Rev. B,* 16(6), 2597, 1977.
74. **Bredas, J. L., Chance, R. R., and Silbey, R.,** Comparative theoretical study of the doping of conjugated polymers: polarons in polyacetylene and polyparaphenylene, *Phys. Rev. B,* 26(10), 5843, 1982.
75. **Bredas, J. L., Themans, B., Fripiat, J. G., and Andre, J. M.,** Highly conducting polyparaphenylene, polypyrrole, and polythiophen chains: an ab-initio study of the geometry and the electronic structure modifications upon doping, *Phys. Rev. B,* 29(12), 6761, 1984.
76. **Bredas, J. L., Street, G. B., Themans, B., and Andre, J. M.,** Organic polymers based on aromatic rings (polyparaphenylene, polypyrrole, and polythiophene): evolution of the electronic properties as a function of the torsion angle between adjacent rings, *J. Chem. Phys.*, 83(3), 1323, 1985.
77. **Shacklette, L. W., Chance, R. R., Ivory, D. M., Miller, G. G., and Baughman, R. H.,** Electrical and optical properties of highly conducting charge-transfer complexes of poly (p-phenylene), *Synth. Metals,* 1, 307, 1979.
78. **Perlstein, J. H., VanAllan, J. A., Isett, L. C., and Reynolds, G. A.,** Chemistry of the mixed valent charge-transport process: the design of organic molecules for organic metals, *Ann. N.Y. Acad. Sci.*, 61, 1978.
79. **Soos, Z. G.,** Theory of π-molecular charge-transfer crystals, *Annu. Rev. Phys. Chem.*, 25, 121, 1974.
80. **Berlinsky, A. J.,** Organic metals, *Contemp. Phys.*, 17(4), 331, 1976.
81. **Shchegolev, I. F.,** Electric and magnetic properties of linear conducting chains, *Phys. Status Solids,* 12, 9, 1972.
82. **Barlett, N., McCarron, E. M., and McQuillan, B. W.,** Novel graphite salts and their electrical conductivities, *Synth. Metals,* 1, 221, 1979/1980.
83. **Wellinghoff, S. T., Kedrowski, T., Jenekhe, S. A., and Ishida, H.,** Synthesis and characterization of highly conducting environmentally stable iodine complexes of a soluble poly N-methyl 3,3′ carbazolyl, *J. Phys.*, 44, C3-677, 1983.
84. **Wellinghoff, S. T., Deng, Z., Reed, J. F., and Jenekhe, S. A.,** The role of polymer cations in the polymerization and electrical conductivity of polycarbazole, *Mol. Cryst. Liquid Cryst.*, 118, 403, 1985.
85. **Wellinghoff, S. T., Deng, Z., and Jenehke, S. A.,** Copolymers and blends of carbazole conducting polymers, *Mol. Cryst. Liq. Cryst.*, 121, 368, 1985.
86. **Racchini, J. R., Wellinghoff, S. T., and Jenehke, S. A.,** Protective group synthesis of poly-N-hydro-(3,6 carbazolyl), *Synth. Metals,* 22(3), 291, 1988.
87. **Ambrose, J. A., Carpenter, L. L., and Nelson, R. F.,** Electrochemical and spectroscopic properties of cation radicals, *J. Electrochem. Soc.*, 122(7), 876, 1975.
88. **Ambrose, J. A. and Nelson, R. F.,** Electrochemical and spectroscopic properties of carbazole cation radicals, *J. Electrochem. Soc.*, 115, 1159, 1968.

89. **Deng, Z.,** private communication, University of Minnesota, Minneapolis.
90. **Enkelmann, V., Gockelmann, K., Wieners, G., Monkenbusch, N.,** Radical cation salts of arenes: structure, properties and model character for conducting polymers, *Mol. Cryst. Liquid Cryst.*, 120, 195, 1985.
91. **Chien, J. C. W. and Babu, G. N.,** Electronic transport and paramagnetic properties of acetylene-carbon monoxide copolymers, *J. Chem. Phys.*, 82(1), 441, 1985.
92. **Fischer, K. and Hanack, M.,** Synthese und Eigenschaften von (Phthalocyaninato) germanium-Schwefel-verbindingen, *Chem. Ber.*, 116, 1860, 1983.
93. **Hanack, M.,** Synthesis and properties of conducting bridged macrocyclic metal complexes, *Mol. Cryst. Liquid Cryst.*, 105, 133, 1984.
94. **Creutz, C. and Taube, H.,** Binuclear complexes of ruthenium ammines, *J. Am. Chem. Soc.*, 95(4), 1086, 1973.
95. **Zhang, L. T., Ko, J., and Ondrechen, M. J.,** Electronic structure of the Creutz-Taube ion, *J. Am. Chem. Soc.*, 109, 1666, 1987.
96. **Ondrechen, M. J., Ko, J., and Zhang, L. T.,** A model for the optical absorbtion spectrum of (μ-pyrazine)decaamminediruthenium (+5): what hath Creutz and Taube wrought?, *J. Am. Chem. Soc.*, 109, 1672, 1987.
97. **von Kameke, A., Tom, G. M., and Taube, H.,** μ-Pyrazine polynuclear mixed-valence species based on trans ruthenium tetraammines, *Inorg. Chem.*, 17(7), 1790, 1978.
98. **Magnuson, R. H., Lay, P. A., and Taube, H.,** Mixed-valence pyrazine-bridged binuclear complexes of osmium ammines, *J. Am. Chem. Soc.*, 105, 2507, 1983.
99. **Reynolds, J. R., Lillya, C. P., and Chien, J. C. W.,** Intrinsically electrically conducting poly(metal tetrathiooxalates), *Macromolecules*, 20, 1184, 1987.
100. **Dirk, C. W., Bousseau, M., Barrett, P. H., Moraes, F., Wudl, F., and Heeger, A. J.,** Metal poly(benzodithiolenes), *Macromolecules*, 19, 266, 1986.
101. **Monkman, A. P., Bloor, D., Stevens, G. C., and Stevens, J. C. H.,** Electronic levels of polyaniline, *J. Phys. D*, 20, 1337, 1987.
102. **Wnek, G. E.,** A proposal for the mechanism of conduction in polyaniline, *Am. Chem. Soc. Polym. Prepr.*, 27(1), 277, 1986.
103. **Glarum, S. H. and Marshal, J. H.,** The *in-situ* ESR and electrochemical behavior of poly(aniline) electrode films, *J. Electrochem. Soc.*, 134(9), 2160, 1987.
104. **Eley, D. D., Isack, F. L., and Rochester, C. H.,** The kinetics of iodine polymerization. XIII. An infrared study of iodine catalyzed polymerization of *n*-butyl ether, *J. Chem. Soc.*, p. 872, 1968.
105. **Haink, H. J., Adams, J. E., and Huber, J. R.,** Electronic structure of diphenyl amine, iminobibenzly, acridine and carbazole, *Ber. Bunsenges. Phys. Chem.*, 78(5), 437, 1974.
106. **Billingham, N. C., Calvert, P. D., Foot, P. J. S., and Mohammad, F.,** *Polym. Deg. Stab.*, in press.
107. **Vogel, F. L.,** Some applications for intercalation compounds of graphite with high electrical conductivity, *Synth. Metals*, 1, 279, 1979/1980.
108. **Denisevich, P., Papir, Y. S., Kurkov, V. P., Current, S. P., Schroeder, A. H., and Suzuki, S.,** Processible polymers of high conductivity, *Am. Chem. Soc. Polym. Prepr.*, 24(2), 330, 1983.
109. **Ulrich, D. R.,** Multifunctional macromolecular ultrastructures: introductory comments specialty polymers, 86, *Polymer*, 28, 533, 1987.
110. **Schoch, K. F., Jr. and Bartko, J.,** Spectroscopic analysis of ion-irradiated poly(phenylene sulphide), *Polymer*, 28, 557, 1987.
111. **Melby, L. R., Harder, R. J., Hertler, W. R., Mahler, W., Benson, R. E., and Mochel, W. E.,** Substituted quinodimethanes. II. Anion-radical derivatives and complexes of 7,7,8,8-tetracyanoquinodimethan, *J. Am. Chem. Soc.*, 84, 3374, 1962.
112. **Caldararn, H., DiArmond, M. K., Hanck, K. W., and Sahian, V. E.,** EPR of electrochemically generated Rh(O) complexes, *J. Am. Chem. Soc.*, 98(15), 4455, 1976.
113. **Crutchley, R. J. and Lever, A. B. P.,** Ru(II) Tris(bipyrazl) dication — new photocatalyst, *J. Am. Chem. Soc.*, 102, 7129, 1980.
114. **Krause, R. and Krause, K.,** Chemistry of bipyridl like ligands. III. Complexes of Ru(II) with 2((4-nitrophenyl)azo pyridine), *Inorg. Chem.*, 23, 2195, 1984.
115. **Ciferri, A.,** Ultra-high modulus fibers from solution and melt spinning, *Int. J. Polym. Mater.*, 6, 137, 1978.
116. **Flory, P. J.,** Statistical thermodynamics of semi-flexible chain molecules, *R. Soc. London Proc.*, A234, 60, 1956; Phase equilibria in solutions of rod-like particles, *R. Soc. London Proc.*, A234, 73, 1956.
117. **Yoldas, B. E.,** Hydrolytic polycondensation of alkoxysilanes and modification of polymerization reactions, *J. Polym. Sci. Polym. Chem. Ed.*, 24, 3475, 1986.
118. **Stamm, M.,** Synthesis and characterization of conducting oriented fibres of poly-p-phenylene, *Mol. Cryst. Liq. Cryst.*, 105, 259, 1984.
119. **Wynne, K. J. and Rice, R. W.,** Ceramics via polymer pyrrolysis, *Annu. Rev. Mater. Sci.*, 14, 297, 1984.

120. **Bott, D. C., Brown, C. S., Winter, J. N., and Barker, J.,** Order and disorder in durham polyacetylene, *Polymer*, 28, 601, 1987.
121. **Ballard, D. G. H., Courtis, A., Shirley, I. M., and Taylor, S. C.,** *J. Chem. Soc. Chem. Commun.*, p. 954, 1983.
122. **Fink, J.,** *Synth. Metals*, in press.
123. **Patel, G. N., Chance, R. R., Turi, E. A., and Khanna, Y. P.,** Energetics and mechanism of the solid state polymerization of diacetylenes, *J. Am. Chem. Soc.*, 100(21), 6644, 1978.
124. **Deng, Z.,** Electronic Conduction Mechanism in Polycarbazole Complexes, M. S. thesis, University of Minnesota, Minneapolis, 1985.
125. **Gordon, B. and Handcock, L. F.,** Proton abstraction as a route to electrically conductive polymers, *Polymer*, 28, 585, 1987.
126a. **Galvin, M. E. and Wnek, G. E.,** *Polym. Bull.*, 13, 109, 1985.
126b. **Aldissi, M.,** Soluble conducting poly(acetylene) block copolymers, *J. Chem. Soc. Chem. Commun.*, p. 1347, 1984.
127. **Armes, S. P., Miller, J. F., and Vincent, B.,** Aqueous dispersions of electrically conducting monodisperse polypyrrole particles, *J. Colloid Interface Sci.*, 118(2), 410, 1987.
128. **Naarman, H. et al.,** Ger. Offen., DE 3, 307, 954, CA 101, 211896.
129. **Camargo, R. E.,** Kinetics and Phase Segregation Studies on the RIM Polymerization of Urethane Elastomers, Ph.D. thesis, University of Minnesota, Minneapolis, 1984.
130. **Day, D. and Lando, J. B.,** Morphology of crystalline diacetylene mononlayers polymerized at gas water interfaces, *Macromolecules*, 13, 1478, 1980.
131. **Galvin, M. E. and Wnek, G. E.,** Characterization of polyacetylene/low density polyethelene composites prepared by *in-situ* polymerization, *J. Polym. Sci. Polym. Chem.*, 21, 2727, 1983.
132. **Rubner, M. F., Tripathy, S. K., Georger, J., Jr., and Choewa, M.,** Structure property relations of polyacetylene-polybutadiene blends, *Macromolecules*, 16, 870, 1983.
133. **DePaoli, M. A., Waltman, R. J., Diaz, A. F., and Bargon, J.,** Conductive composites from poly(vinyl chloride) and polypyrrole, *J. Chem. Soc. Chem. Commun.*, p. 1015, 1984; **Bargen, J.,** *Stud. Org. Chem. (Amsterdam)*, 25, 349, 1986.
134. **Bigelow, R. W.,** A theoretical study of the radical cations of carbazole and N-alkyl carbazoles: optical and photoelectron spectra, *J. Mol. Struct. (Theochem.)*, 122, 133, 1985.
135. **Hush, N. S.,** Intervalence-transfer absorption. II. Theoretical considerations and spectroscopic data, *Prog. Inorg. Chem.*, 8, 391, 1967.
136. **Bredas, J. L., Scott, J. C., Yakushi, K., and Street, G. B.,** Polarons and bipolarons in polypyrrole: evolution of the band structure and optical spectrum upon doping, *Phys. Rev. B*, 30, 1023, 1984.
137. **Wellinghoff, S. T. and Schwab, S. T.,** Synthesis and studies of poly(6-methoxy, 3,9 carbazolyl) and its charge transfer complexes, submitted.
138. **Friend, R. H., Bradley, D. D. C., and Townsend, P. D.,** Photo-excitation in conducing polymers, *J. Phys. D*, 20, 1367, 1987.
139. **Kanicki, J.,** Metal-polyacetylene Schottky barrier diodes, *Mol. Cryst. Liquid Cryst.*, 105, 203, 1984.
140. **Sakai, Y., Matsumura, M., Nakato, Y., and Tsubomura, H.,** Effect of metal/p-doped a-Si:H junctions on the photovoltage of a-Si:H solar cells, *J. Appl. Phys.*, 62(8), 3424, 1987.
141. **Simon, J., Tournilhac, F., and Andre, J.,** Bipolar junction formation in the case of molecular materials, *J. Appl. Phys.*, 62(8), 3304, 1987.
142. **Potember, R. S., Hoffman, R. C., Hu, H. S., Cocchiaro, J. E., Viands, C. A., Murphy, R. A., and Poehler, T. O.,** Conducting organics and polymers for electronic and optical devices, *Polymer*, 28, 574, 1987.
143. **Turner Jones, E. T., Chyan, O. M., and Wrighton, M. S.,** Preparation and characterization of molecule based transistors with a 50nm source drain separation with use of shadow deposition technique — toward faster, more sensitive molecule based devices, *J. Am. Chem. Soc.*, 109(18), 5526, 1987.
144. **Umeton, C., Cipparrone, G., and Simoni, F.,** Power limiting and switching with nematic liquid crystal films, *Opt. Lett.*, p. 312, 1987.
145. **Chemie, D. S., Miller, D. A. B., and Smith, P. W.,** Nonlinear optical properties of GaAs/GaAlAs multiple quantum well material: phenomena and applications, *Opt. Eng.*, 24(4), 556, 1985.
146. **Stegeman, G. I. and Seaton, C. T.,** Third order non linear guided wave optics, *SPIE*, 682, 179, 1986.
147. **Lo, S. K. and Jenehke, S. A.,** Honeywell, Inc., private communication.
148. **Dalton, L. R., Thomson, J., and Nalwa, H. S.,** The role of extensively delocalized π-electrons in electrical conductivity, non linear optical properties and physical properties of polymers, *Polymer*, 28, 543, 1987.
149. **Huggard, P. G., Blau, W., and Schweitzer, D.,** Large third order optical nonlinearity of organic metal α-[bis(ethylenedithio)tetrathiofulvalene] triiodide, *Appl. Phys. Lett.*, 51, 2183, 1987.
150. **Shacklette, L. W., Toth, J. E., Murthy, N. S., and Baughman, R. H.,** *J. Electrochem. Soc.*, 132, 1529, 1985.

151. **Padula, A., Scrosati, B., Schwarz, M., and Pedretti, U.,** The kinetics and cyclability of various types of polyacetylene electrodes in non-aqueous lithium cells, *J. Electrochem. Soc.*, 131(12), 2761, 1984.
152. **Osaka, T., Naoi, K., Ogano, S., and Nakamura, S.,** Dependence of film thickness on electrochemical kinetics of polypyrrole and on properties of lithium/polypyrrole battery, *J. Electrochem. Soc.*, 134(9), 2096, 1987.
153. **Muenstedt, H., Koehler, H., Moehwald, H., Naegleli, D., Bitthin, R., Ely, G., and Meissner, E.,** Rechargeable polypyrrole lithium cells, *Synth. Metals*, 18(1 to 3), 259, 1987.
154. **Kaufman, J. H., Kanazawa, K. K., and Street, G. B.,** Gravimetric electrode voltage spectroscopy: in situ mass measurement during electrochemical doping of conducting polypyrrole, *Phys. Rev. Lett.*, 53, 2461, 1984.
155. **Mahoto, B. K., Brilmeyer, G. H., and Bullock, K. R.,** Performance testing of advanced lead acid batteries for electric vehicles, *J. Power Sources*, 16(2), 107, 1985.
156. *McGraw-Hill's Report on Performance Materials*, McGraw-Hill, New York, November 16, 1987.
157. **Bockris, J. O. M. and Srinivasan, S.,** *Fuel Cells: Their Electrochemistry*, McGraw-Hill, New York, 1969.
158. **Mammone, R. L. and McDiarmid, A. G.,** p-Doping of $(CH)_x$ to the metallic regime with gaseous oxygen, *J. Chem. Soc. Faraday Trans.* 1, 81, 105, 1985.
159. **Bull, R., Fan, R., and Bard, A. J.,** Polymer films on electrodes, *J. Electrochem. Soc.*, 130, 1636, 1983.
160. **McAleer, J. F., Ashley, K., Smith, J. J., Bandyopadhyay, S., Ghoroghchain, J., Eyring, E. M., Pons, S., Mark, H. B., Jr., and Dunmore, G.,** Electrochemistry and properties of poly p-phenylene formed from the anodic oxidation of biphenyl in aprotic solvents, *J. Mol. Electron.*, 2, 183, 1986.
161. **Bull, R., Fan, F. R., and Bard, A.,** Polymer films on electrodes. VII. Electrochemical behavior at polypyrrole-coated Pt and Ta electrodes, *J. Electrochem. Soc.*, 129, 1004, 1982.
162. **Meyerhoff, M. E. and Fraticelli, Y. M.,** Ion selective electrodes, *Anal. Chem.*, 54, 27, 1982.
163. **Kalyanasundarum, K.,** Photophysics of molecules in micellar form in surfactent solutions, *Coord. Chem. Rev.*, 46, 159, 1979.
164. **Hayashi, Funaoka, T., and Tetsuya, Y.,** Characterization of photoelectrochemical cells with ITO/p-Si heterojunctions coated with conducting polymers, *Nippon Kagaku Kaishi*, 2, 152, 1987.
165. **Kaneko, M. and Nakamura, H.,** Photoresponse of a liquid junction polyaniline film, *J. Chem. Soc. Chem. Commun.*, p. 346, 1985.
166. **Frommer, J. E. and Chance, R. R.,** Electrically conducting polymers, in *Encyclopedia of Polymer Science and Engineering*, Vol. 5, 2nd ed., John Wiley & Sons, New York, 1986, 462.
167. **Skotheim, B., Ed.,** *Handbook of Conducting Polymers*, Vol. 2, Marcel Dekker, New York, 1986.
168. **Kuzmany, H., Ed.,** Electronic properties of polymers and related compounds, *Spring. Ser. Solid State Sci.*, p. 63, 1985.
169. **Mort, J. and Pfister, G., Eds.,** *Electronic Properties of Polymers*, John Wiley & Sons, New York, 1982.
170. **Cotts, D. B. and Reyes, Z.,** *Electrically Conductive Organic Polymers for Advanced Applications*, Noyes Publications, Park Ridge, NJ, 1987.
171. **Slater, J. C.,** *Phys. Rev.*, 445, 794, 1934.
172. **Wegner, G.,** The state of order and the relevance of phase, *Mol. Cryst. Liquid Cryst.*, 106, 269, 1984.
173. **Smyrl, W. and Deng, Z.,** unpublished data.
174. **Marks, T. J., Schoch, K. F., Jr., and Kundalkar, B. R.,** *Synth. Metals* 1(3), 337, 1980.
175. **Hanack, M.,** *Chimia*, 37, 238, 1983.
176. *Chem. Eng. News*, June 22, 1987.
177. **Gagnon, D. R., Capistran, J. D., Karasz, F. E., Lenz, R. W., and Antoun, S.,** *Polymer*, 28, 567, 1987.
178. **Wellinghoff, S. T. and Schwab, S. T.,** submitted.

Taylor & Francis
Taylor & Francis Group
http://taylorandfrancis.com

Chapter 5

POLYMER ELECTROLYTES

James S. Tonge and Duward F. Shriver

TABLE OF CONTENTS

I. Introduction 158
   A. Polyelectrolytes 158
   B. Polymer Electrolytes 160

II. Review of Fundamentals 161
   A. Preparation of Polymer-Salt Complex Formation 161
   B. Factors Influencing Polymer-Salt Formation 161
      1. Nature of Polar Groups 162
      2. Lattice Energy of Salt 162
      3. Cohesive Energy Density of Polymers 166
      4. Phase Equilibria 167
   C. Structure 169

III. Ion Transport 172
   A. Conductivity Measurements 173
      1. General Principles 173
      2. DC Conductivity 174
      3. AC Conductivity 175
   B. Ion Transport Models 179
      1. Configurational Entropy Model 181
      2. Time-Dependent Percolation Theory 184
   C. Observed Conductivities 185
      1. Influence of Morphology 185
      2. Influence of Salt Concentration 187
   D. Transference Numbers and Ion Pairing 188
      1. Transference Numbers 188
         a. Potential Gradient 189
         b. Chemical Gradient 190
         c. Spin Gradient 192
      2. Ion Association 193

IV. Applications 194
   A. Electrochemical Stability 195
   B. Batteries 195
   C. Other Electrochemical Devices 199
      1. Photoelectrochemical Cells 199
      2. Sensors 199
      3. Electrochemical Transistor Action 199
      4. Electrochromic Display 200
      5. Solid-State Electrochemistry 200

V. Summary 200

Acknowledgment 200

References 200

I. INTRODUCTION

Solid-state ionics, and more specifically solid electrolytes, include both inorganic and polymeric systems. The field of inorganic solid electrolytes has been studied since the turn of the century and has been extensively reviewed.[1-20] The focus of this review is on a new class of polymeric materials which contains salts dissolved in polar polymers.

There is considerable recent research and development in the field of conducting polymers[21-24]including (1) electronic conductors such as doped polyacetylene,[23,24] polyaniline,[25] polythiophene,[26] polypyrrole,[27] or poly(paraphenylene);[28] (2) ionically conducting polymer electrolytes which are the subject of this chapter; (3) polymers which are mixed electronic/ionic conductors.[29,30] After a brief discussion of solvent-swollen polyelectrolytes we discuss electrolytes composed of salts in polymers but which contain no small, discrete solvent molecules.

A. Polyelectrolytes

The term polyelectrolyte is usually reserved for macromolecules with fixed ionizable groups.[31-33] They are also known as poly-ions or ionomers. The fixed charges can be positive or negative, giving rise to polyacids and polybases, examples of which are given in Table 1. In general, small counterions such as H^+, Na^+, OH^-, or Cl^- are associated with the fixed ionic charges on the polymer to maintain electroneutrality (Figure 1). In addition, polymers such as poly(amino acid) contain both acidic and basic groups on the same chain and these are termed polyampholytes.

In the absence of a solvent the small counterions in conventional polyelectrolytes are firmly bound due to the strong coulombic attraction of the array of oppositely charge fixed ions.[34] The conductivity of the polyelectrolytes increases dramatically on exposure to moisture, because the counterions are shielded from the backbone charge by hydration and they behave as simple ions in an aqueous solution.[35] The increase in ionic conductivity associated with increased water uptake makes this type of material ideal for humidity sensors.[36,37]

The perfluorinated polyethylene sulfonates and carboxylates, commonly referred to as Nafion and Flemion which were originally developed as ion exchangers, are finding a variety of electrochemical applications.[38] On addition of water to Nafion, the sulfonate and its associated cation spontaneously form an aquated phase of ion clusters within the insulating polymer matrix. This phenomenon of ion clustering has been demonstrated by X-ray[39] and neutron scattering.[40] The ion clustering is also reflected in the development of percolation paths with higher cation and water self-diffusion coefficients than predicted for conventional polymers such as poly(styrene sulfonate).[41-43] Nafion has excellent chemical stability and therefore is used as a membrane separator in chlor-alkali cells.[44] It also has the potential for use in hydrogen-air fuel cells[45] and advanced batteries.[46-48]

Insoluble polyelectrolyte complexes are formed by the combination of polycationic and

Table 1
EXAMPLES OF POLYELECTROLYTES

Name	Formula
Polyacids	
Poly(acrylic acid)	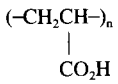
Poly(methacrylic acid)	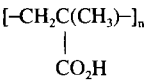
Poly(vinylsulfonic acid)	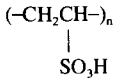
Poly(*p*-styrenesulfonic acid)	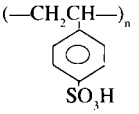
Poly(metaphosphoric acid)	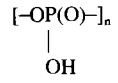
Polybases	
Poly(vinyl-trimethylammonium chloride)	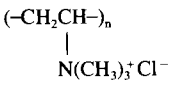
Poly(*N*-methylvinylpyridinium chloride)	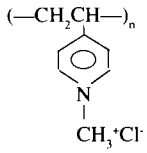
Poly(methyldiallyl sulfonium methylsulfate)	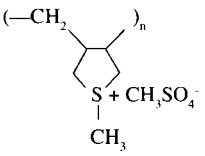
Poly(vinylbenzyl-trimethylphosphonium chloride)	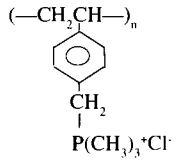

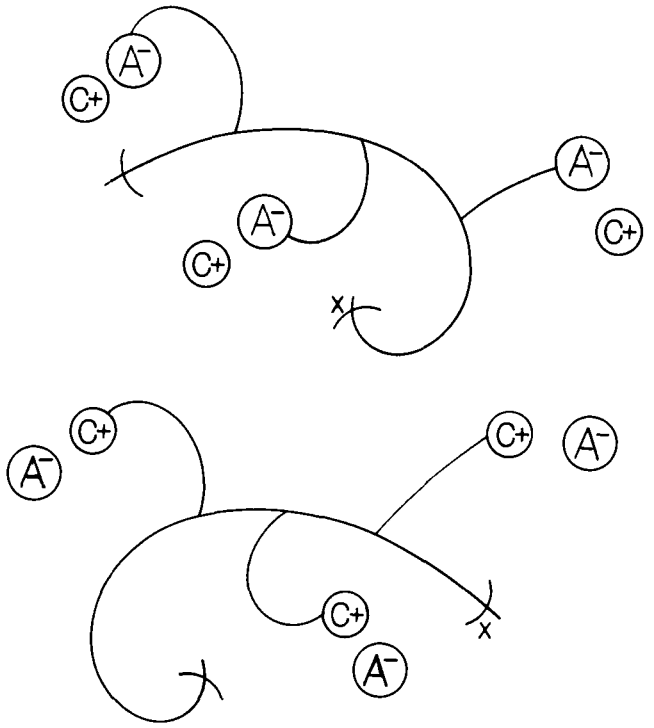

FIGURE 1. Pictorial representation of (A) polyacids and (B) polybases.

polyanionic electrolytes, such as poly(sodium styrene sulfonate) with a poly(tetra-alkylammonium chloride).[49] The inorganic ions remaining in the polyelectrolyte complex display higher mobility than in the individual polyelectrolytes. As with the simple polyelectrolytes the presence of a high dielectric solvent, such as water, is essential for high ionic mobility. The polyelectrolyte complexes have found widespread use in dialysis, battery separators, and biomedical uses.[49]

Related to the solvated polyelectrolytes systems are the gelled polymer electrolytes, consisting of a neutral polymer host, such as poly(vinylidene fluoride),[50,51] poly(acrylonitrile),[52-54] and poly(vinyl acetals),[55] a salt, and a high dielectric solvent. As with the polyelectrolytes, high dielectric constant and low viscosity solvents promote high ionic conductivity.[50] The solvated or gelled polyelectrolytes and polymer-salt complexes behave similarly to the parent solvent with a similar voltage stability window. A large solvent content results in soft polymer gels with poor mechanical properties, but the mechanical properties of the gels can be improved by cross-linking. Systems with water as the solvent and poly(vinyl alcohol) as the polymer are used as battery separators[56] and hydrogen sensors.[57]

B. Polymer Electrolytes

It was recognized in the mid-1960s that potassium salts form complexes with poly(ethylene oxide), PEO (**1**),[58,59] and poly(propylene oxide), PPO (**2**),[60] but it was not until 1973 that these materials were found to exhibit appreciable ionic conductivity.[61,62] These complexes also show increases in conductivity upon addition of high-dielectric, low-viscosity solvents.[63] Since the early studies on PEO a wide variety of PEO and PPO salt complexes have been prepared and characterized.[22,64-72] That work led to the design of a second generation of solvent-free polymer-salt complexes with optimized ionic conductivities and mechanical properties.[73-77] These polymer-salt complexes are the subject of the remainder of this chapter.

$(OCH_2CH_2)_n$

1

CH_3
|
$(OCH_2CH)_n$

2

II. REVIEW OF FUNDAMENTALS

In recent years considerable physical data have been collected on polymer electrolytes, and theoretical models to describe ion transport in these materials have been developed. In this section we outline the principles of formation and the models for ion transport in the polymer electrolytes that are not swollen by low molecular weight solvents.

A. Preparation of Polymer-Salt Complex Formation

Polymer-salt complexes may be prepared by several different methods. The most common method entails the use of a solvent for the solid polymer and salt.

$$PEO(s) + LiSO_3CF_3(s) \quad CH_3CN \quad P(EO_xLiSO_3CF_3)(soln)$$

The nomenclature used in this example and throughout the review designates the number of polymer repeat units per salt formula unit by the subscript on the polymer acronym. For example, $P(EO_4LiSO_3CF_3)$ corresponds to four C_2H_4O units per $LiSO_3CF_3$. The resulting polymer electrolyte solution can be cast on a smooth surface followed by evaporation of the solvent to produce a thin film. Since moisture can be absorbed by most polymer electrolytes, it is common to carry out the entire process with anhydrous solvents and dry starting materials and to exclude atmospheric moisture by working under a dry nitrogen or argon atmosphere. If the polymer and its salt complex are insoluble, as in the case of cross-linked networks, complexes can be produced by dipping a film of the polymer into a solution containing the appropriate amount of salt. This method of synthesis illustrates the mobility of both the cation and anion of the salt in the polymer film. In principle there is a distribution of the salt between the solvent and the polymer film, but in some cases the salt strongly partitions to the polymer phase.

Solvent-free methods are also used to prepare polymer electrolytes. As an example, complexes of poly(ethylenesuccinate), PESc, and $LiBF_4$ were prepared by mixing the finely divided salt with the molten polymer at 125°C.[78] Similarly, cold grinding and hot pressing of the constituents have been used.[79]

Recently, experiments were reported in which $P(EO_nLiSO_3CF_3)$ was heated in vacuum and deposited from the vapor state onto a surface.[80] As might have been anticipated, this method leads to pyrolysis of the polymer with a drastic reduction of the polymer's molecular weight.

B. Factors Influencing Polymer-Salt Formation

From the early studies on PEO-salt complexes and other polymer-salt complexes, some general principles governing complex formation have become apparent. We briefly list these concepts and then illustrate them in detail.

1. Polymers that form salt complexes have polar groups (Lewis bases) such as ether or ketonic oxygen, amines, and organic sulfides. As will be discussed in more detail these polar groups coordinate to the cations of the salt. So far attempts to solvate the anion have received little attention.
2. For a given cation the salts having a low lattice energy are most likely to form polymer-salt complexes. The salts usually comprise univalent alkali metal ions with large anions, e.g., $CF_3SO_3^-$, I^-, CF_3COO^-, $H_2PO_4^-$, etc.

3. Polymers with a low cohesive energy density and high flexibility have the greatest tendency to interact with salts.

1. Nature of Polar Groups

As the role of the polyether chain became apparent many groups sought to produce highly conducting polymer electrolytes by incorporating the polyether chains in various other organic and inorganic polymers, and networks.[81-89]

As described later in this review, studies of ion transport mechanisms led to the view that amorphous polymers with high chain flexibility form the most conducting polymer-salt complexes. This led to the synthesis of amorphous polymers, such as network polyethers and comb polymers,[73-77] that form amorphous polymer-salt complexes. These complexes have higher conductivity at room temperature than the PEO complexes. In the network polymers cross-linking prevents crystallization of PEO. The comb polymers consist of short polyether chains attached to a highly flexible, low T_g, inorganic backbone (–P=N– and –Si–O–). Although the polymer backbones in the polyphosphazenes and polysiloxanes contain potential coordinating groups, nitrogen and oxygen, respectively, the backbonding between P and N, or Si and O reduces the basicity of N and O such that complex formation is generally not favored. Recently, a third approach has been to randomly interrupt the OC_2H_4 repeat unit of PEO with OCH_2 units; again, crystallinity is suppressed and good conductivity is achieved at room temperature.[81]

In the search for systems containing donor atoms analogous to the oxygen containing the polyethers, polymer-salt complexes containing $(CH_2CH_2NH)_n$[82] and $(CH_2CH_2S)_n$[83] have been studied. The polyalkylsulfides are very restricted in the number of salts that form complexes, the best being soft cations such as Ag^+. Poly(ethylene imine), $(C_2H_4NH)_n$, shows extensive intra- and interchain hydrogen bonding, but this does not appear to disfavor polymer-salt complex formation. Infrared spectra indicate that the polymer forms hydrogen bonds with the anion in P(EINaSO$_3$CF$_3$) complexes.[84] As with PEO, the highly crystalline-pure PEI shows a reduction in crystallinity on complex formation, and there is also evidence for salt-rich crystalline phases in P(EI·NaI) complexes.[85]

A number of different linear polymers with various polar groups have been employed in the preparation of polymer electrolytes. The majority of these are based on polyethers. Table 2 shows a representative cross section of the type of polymer host and Figure 2 gives representative conductivity data.

2. Lattice Energy of Salt

In order to identify the thermodynamic terms that favor polymer-salt complex formation, it is instructive to consider the thermochemical cycle in Figure 3. When comparing the tendencies of polymers and salts to form complexes the variation in entropy terms is likely to be small, and we therefore focus on the more accessible enthalpy terms. The endothermic processes in the thermochemical cycle are (1) salt vaporization and dissociation and (2) polymer vaporization. These must be offset by the exothermic processes: cation complexation by the polymer (3), and by the condensation of the cation-polymer complex with the anion to form a solid polymer-salt complex (4).[128]

Enthalpies for step 1 taken from measured or estimated lattice energies are presented in Table 3, for a group of alkali metal salts. Along with each entry in this table there is an indication of whether or not the salt forms a complex with PEO. Moving down a column the cation is fixed but the anion varies, thus, the enthalpy of cation polymer interaction 1 remains constant. At the top of each column the lattice energy is too high to be offset by the favorable energy terms 3 and 4, which lead to polymer-salt complex formation. Upon moving down the column the lattice enthalpies decrease and below a given lattice enthalpy complex formation is observed.[64,129] Thus, polymer-salt complex formation for salts of a particular cation is favored by a large anion.

Table 2
HOST POLYMERS USED FOR ELECTROLYTE FORMATION

Name	Monomer unit	Ref.
Linear Polymers		
Poly(ethylene oxide)	$(CH_2CH_2O)_n$	61
Poly(propylene oxide)	$\begin{matrix} CH_3 \\ \vert \\ (CH_2CHO)_n \end{matrix}$	86
Poly(ethylenimine)	$(CH_2CH_2NH)_n$	84, 85
Poly(methylene sulfide)	$[(CH_2)_pS]_n$ (p = 2,5)	83
Poly(ethylene succinate)	$(CH_2CH_2OCO_2CH_2CH_2CO_2)_n$	87, 88
Poly(ethylene sebecante)	$[(CH_2)_2O_2C(CH_2)_8CO_2]_n$	89
Poly(*N*-methylaziridine)	$[CH_2\text{-}CH_2\text{-}N(CH_3)]_n$	90
Poly(ethylene adipate)	$[OCH_2CH_2O_2C\text{-}(CH_2)_4]_n$	91
Poly(β-propiolactone)	$(CH_2CH_2CO_2)_n$	92
Poly(epichlorohydrin)	$[CH_2CH(CH_2Cl)O]_n$	64
Poly(vinyl acetate)	$[CH_2CH(OCH_3)]_n$	93
Comblike and Branched Polymers		
Poly[bis(methoxyethoxyethoxy) phosphazene] $\{NP[O(CH_2CH_2O)_xCH_3]_2\}_n$ (χ = 1, 2, 7, 12, and 17)		73, 94
Poly(methoxypolyethylene oxide)methyl siloxane $[SiO(CH_3)(OCCH_2CH_2O)_2xMe)]_n$		75, 76
Poly(methoxypolyethylene glycol monomethacrylate) $\{CH_2C(CH_3)[CO_2(CH_2CH_2O)_xCH_3]\}_n$		95—97
Poly[diethoxy(3)methylitaconate] $\{CH_2C[CH_2CO_2(CH_2CH_2O)_xCH_3][CO_2(CH_2CH_2O)_xCH_3\}_n$ n = 1—5		98, 99
Poly(methoxyethoxyethoxybutadiene) $\{CH_2CH_2CH[O(CH_2CH_2O)_2CH_3]CH_2\}_n$		100
Branched poly(ethylenimine)		84
Polyether/Polymer Blends		
Poly(2-sulfoethyl methacrylate) lithium salt	$\begin{matrix} CH_3 \\ \vert \\ (-CH_2-C-) \\ \vert \\ CO_2CH_2CH_2SO_3^-Li^+ \end{matrix}$	101
Poly[2-(4-carboxyhexafluoro-butanoyl-oxy) ethyl methacrylate] lithium salts	$\begin{matrix} CH_3 \\ \vert \\ [(-CH_2-C)-] \\ \vert \\ CO_2CH_2CH_2OC-(CF_2)_3CO_2^-Li^+ \end{matrix}$	101
Polystyrene	$[CH_2CH(C_6H_5)]_n$	79
Poly(vinyl pyrrolidone)	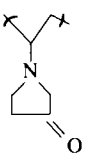	102

Table 2 (continued)
HOST POLYMERS USED FOR ELECTROLYTE FORMATION

Name	Monomer unit	Ref.
Poly(diallyldimethylammonium chloride)	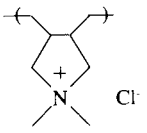	103
Poly(styrene-sulfonate) sodium salt	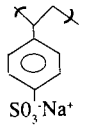	104
Poly(methacrylic acid)	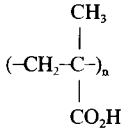	103
Nafion 117	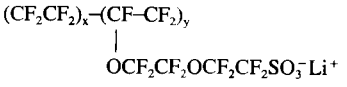	106
Flemion	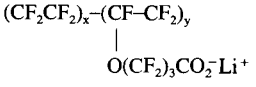	107
Poly(acrylate)/polybrene salt	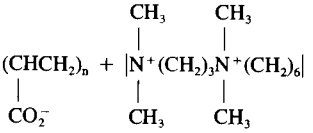	34
Poly(2-acylamino-2-methyl propane sulfonate)/polybrene salt	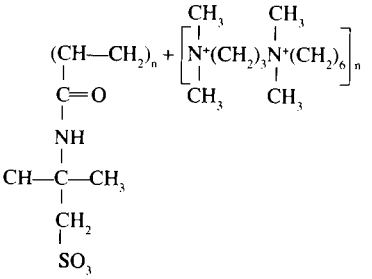	34

Table 2 (continued)
HOST POLYMERS USED FOR ELECTROLYTE FORMATION

Name	Monomer unit	Ref.
Copolymers		
Poly(propylene oxide-co-tetramethylene oxide)	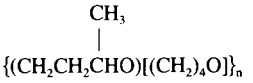	107
Poly(propylene oxide-co-urethane urea)	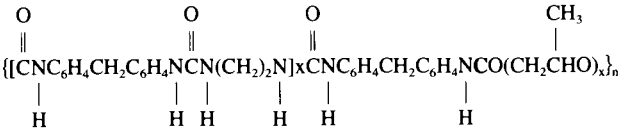	108
Poly(dioxolane-co-trioxane)	$[(CH_2O)_2(CH_2CH_2O)]_n$	109
Oxymethylene-linked poly(oxyethylene)		81
Poly[lithium methacrylate-co-oligo(oxyethylene) methacrylate]	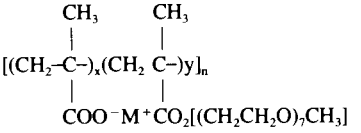 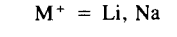	110, 111
Poly(dimethyl siloxane-co-ethylene oxide)	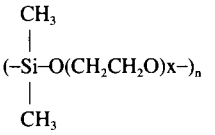	112
Cross-linked Polymers		
PEO		
Methods of cross-linking		
Radiation induced		113
Di-isocyanates		114
Tri-isocyanates		115
$POCl_3$		116
Si, Cd, B, or Ti, e.g., use CH_3SiCl_3		117,118
Al, Zn, or Mg, e.g., use $Al(C_8H_{17})_3$		119
PPO di-isocyanate		120
Poly(dimethysiloxane-co-ethylene oxide)		
Di-isocyanate		121
Triacetoxy and triethoxy-silanes		122
Poly(methoxypolyethylene oxide) methyl siloxane		

Table 2 (continued)
HOST POLYMERS USED FOR ELECTROLYTE FORMATION

Name	Monomer unit	Ref.
Benzoyl peroxide (radical)		75
Heat treatment		76
Poly (α-methacryloyl-ω-methoxypoly(oxyethylene)) cross-linked with 3,6,9-trioxaundecamethylene dimethyacrylate		123
Poly [bis(methoxyethoxyethoxy)phosphazene] cross-linked with PEG		74
Poly(acrylonitrile-butadiene-styrene-methoxyoligo-ethylene oxide)		
Thermally		124, 125
Radical		124, 125
Self-Ionizable Networks		
Cross-linked	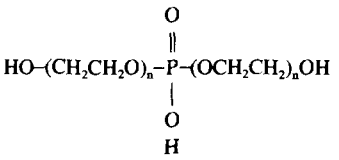	126
Cross-linked	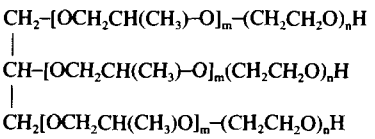	126
Where ROH groups in the above two polymers are converted to $ROSbCl_5^- Li^+$ $ROOC(CF_2)_3COO^-Li^+$		
Interpenetrating Networks		
Combination of PEO Diglycidylether of bisphenol A PPO triamine		127

In view of the mounting evidence for cation-anion interaction in the solvent-free polymer electrolytes, it is surprising that this simple analysis works as well as it does.

3. Cohesive Energy Density of Polymers

Polymers such as nylon with high cohesive energy density exhibit a reduced tendency to form complexes with salts. From the thermochemical cycle, Figure 3, this may be seen to originate from the highly endothermic enthalpy of vaporization for the parent polymer.

There are indications that steric factors play a role in the formation of polymer-salt complexes. Thus, it is thought that highly flexible polymers can achieve favorable conformations for coordination with a wide variety of cations. Similarly, the steric hinderance caused by the additional methyl group in PPO, compared to PEO, has been invoked as the difference in solvating power between the two polymers.[22] The reduction in solvation is illustrated by the inability of PPO to complex large alkali metal (K^+, Rb^+, Cs^+) salts.[22]

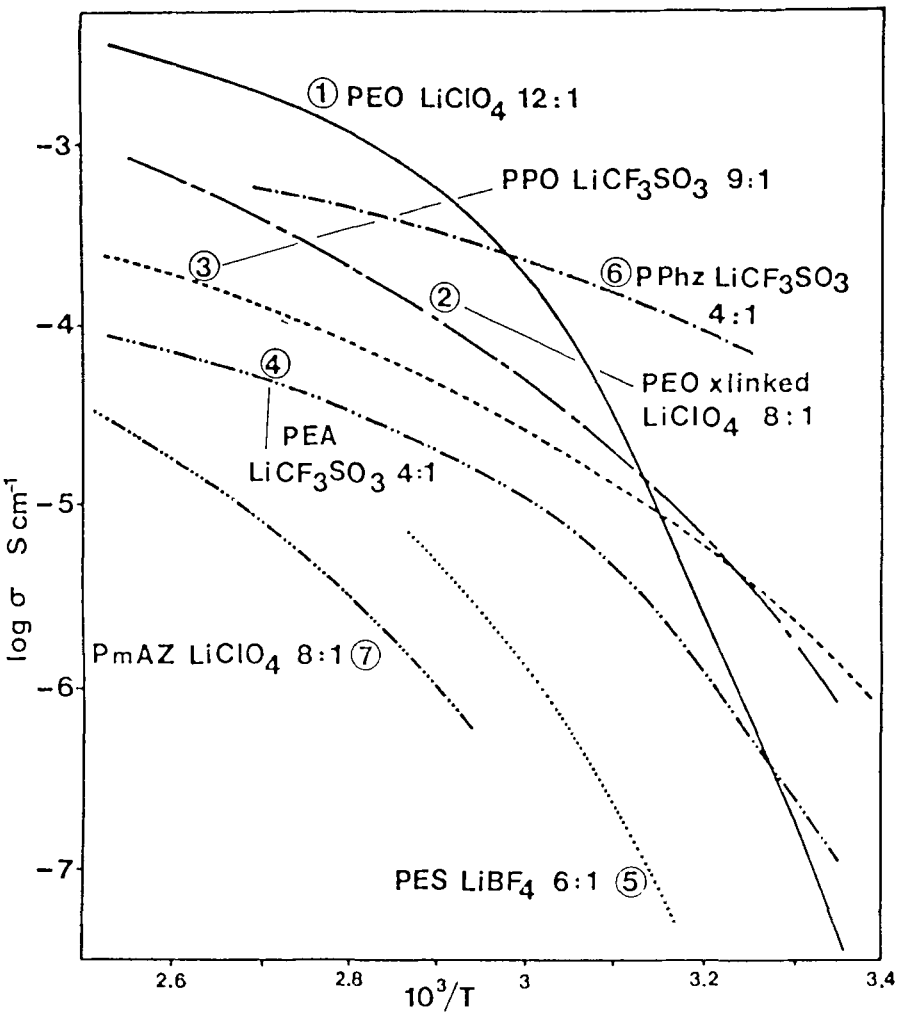

FIGURE 2. Conductivity vs. 1/T for a series of polymer-salt complexes. (1) $P(EO_{12}LiClO_4)$; (2) cross-linked PEO_8LiClO_4; (3) $P(PO_9LiSO_3CF_3)$; (4) poly[(ethylene adipate)$_4LiSO_3CF_3$]; (5) poly(ethylenesuccinate)$_6$-$LiBF_4$; (6) poly{[bis(methoxyethoxyethoxy)phosphazene]$_4LiSO_3CF_3$}; and (7) poly[(*N*-methylaziridine)$_8LiClO_4$].

4. Phase Equilibria

For some polymer-salt systems two or more phases may coexist, such as crystalline polymer, amorphous polymer, crystalline complex, amorphous complex, and crystalline salt. The determination of phase diagrams for these systems is complicated by kinetics of crystallization, molecular weight inhomogeneity of the polymer, and the lack of complete crystallization in most polymer systems. Despite these complications a variety of techniques including DSC,[130-133] X-ray diffraction,[134,135] optical microscopy,[136] and NMR[137,138] have been successfully employed to determine the phase diagrams and formulas for polymer-salt complexes.

For pure PEO the crystalline phase accounts for approximately 80% of the available volume, with the remainder being taken up by a dispersed amorphous phase. On the addition of NaSCN to PEO, an amorphous polymer-salt complex is formed until the saturation of the amorphous phase occurs. At this point a crystalline complex is formed of approximate stoichiometry 3.5:1 oxygen/cation.[136] The phase diagram of $P(EO_nNaSCN)$ of Lee and

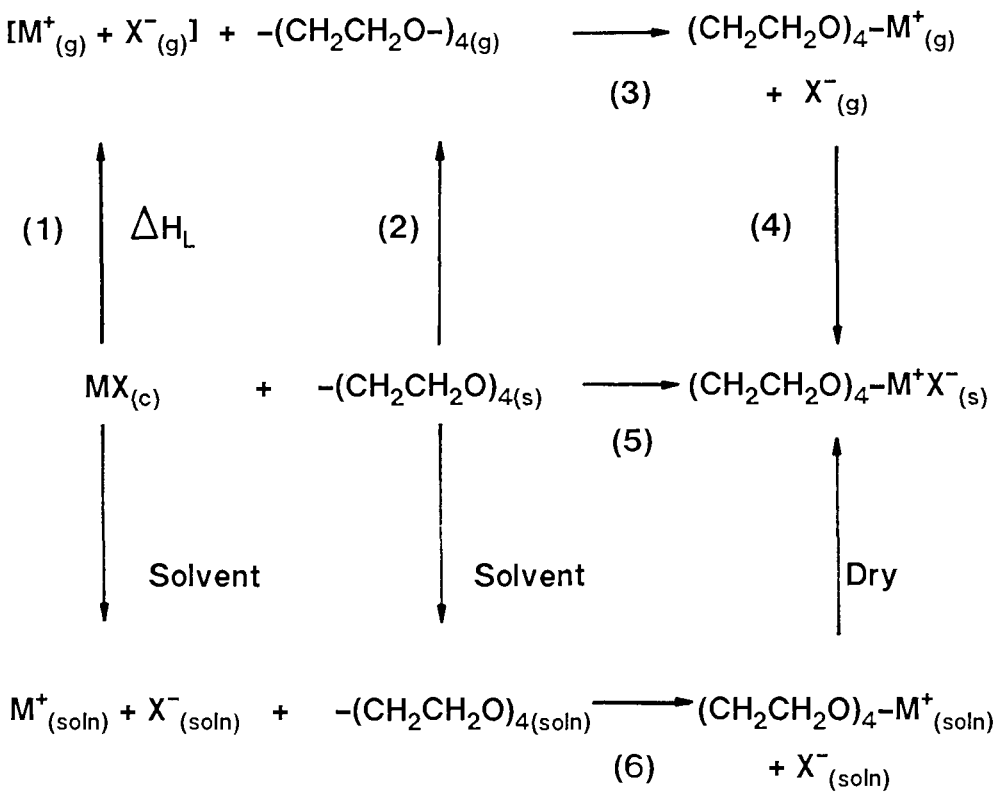

FIGURE 3. A thermodynamic cycle for cation solvation in PEO with a 4:1 (oxygen/cation) mole ratio.

Table 3
SALTS THAT FORM COMPLEX POLYMERIC ELECTROLYTES WITH PEO

	Li^+	Na^+	K^+	Rb^+	Cs^+
	No	No	No	No	No
F^-	1036[a]	923	821	785	740
	Yes[b]	No[c]	No	No	No
Cl^-	853	786	715	689	659
	Yes	Yes	No	No	No
Br^-	807	747	682	660	631
	Yes	Yes	Yes	Yes	Yes
I^-	757	704	644	630	604
	Yes	Yes	Yes	Yes	Yes
SCN^-	807	682	619	616	568
	Yes	Yes	Yes	Yes	Yes
$SO_3CF_3^-$	725	650	605	585	550
	Yes	Yes	Yes	Yes	Yes
ClO_4^-	723	648	602	582	542

[a] The lattice energies of the salts in kJ/mol.
[b] Yes indicates polymer-salt complex formation.
[c] No indicates the absence of complex formation.

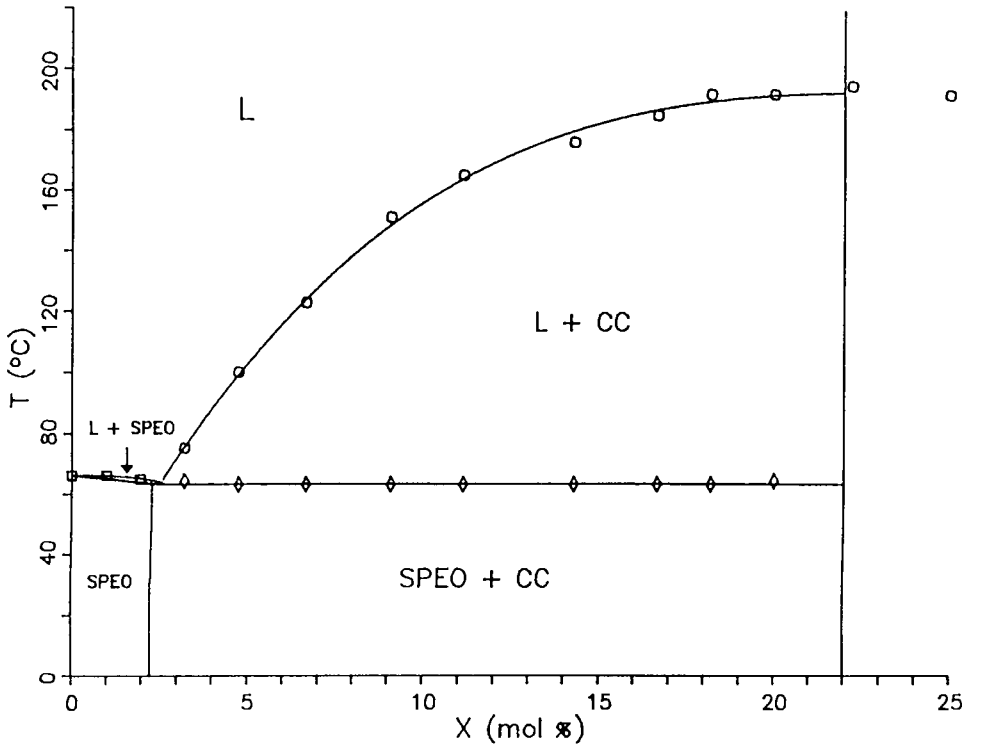

FIGURE 4. Binary phase diagram for the P(EO-NaSCN) system, where L = liquid, CC = crystalline complexes, and SPEO = semicrystalline PEO. Transition temperatures were determined by DSC and optical microscopy.

stoichiometry 3.5:1 oxygen/cation.[136] The phase diagram of $P(EO_nNaSCN)$ of Lee and Crist[136] is shown in Figure 4. The stoichiometries of crystalline PEO complexes are given in Table 4.

Since the rates of crystallization can be slow, polymer properties are sometimes found to be dependent on the thermal history of the system. In $P(EO_nNH_4SCN)$ complexes the rate of crystallization of the metastable amorphous phase was dependent on the salt stoichiometry; the 8:1 and 6:1 (polymer/salt) complexes remained amorphous for weeks, while the 4:1 salt regained its crystalline component within days.[68] A similar metastable phase has been observed in $P(EO_nNaI)$ salts.[30]

Wright noted that the morphology of PEO salt complexes varies depending on whether the complex is cast from solution or from the melt.[142] The solution cast complexes form folded chain lamellae and well-defined spherulites, while the thermally crystallized $P(EO_nNaSCN)$ adopts a "banded or shish-kebab" morphology which he suggests is due to extension of the molecular conformation.[143]

C. Structure

Our understanding of polymer-salt complex formation as well as ion transport would be greatly improved by detailed structural data on the polymer electrolytes. Because of the lack of high quality single crystals of the polymer-salt complexes, precise X-ray structural data are lacking. As a result, approximate structural inferences have been made from X-ray data on oriented fibers, as well as spectroscopic methods such as infrared (IR), Raman, NMR, and extended X-ray fine structure (EXAFS).

From an X-ray study on $P(EO_4KSCN)$ Hibma suggests that the potassium ion is coordinated to oxygen atoms from more than one polyether chain.[135] In a more recent study of $P(EO_3NaI)$

Table 4
STOICHIOMETRY OF CRYSTALLINE COMPLEXES OCCURRING IN PEO SALT COMPLEXES

Polymer salt	Stoichiometry	Ref.
$PEO_xLiCF_3SO_3$	x = 3	134
	x = 3.3	132
	x = 3.5	137, 138
	x = 4	131
PEO_xLiCLO_4	x = 6, 3, 2[a]	134
	x = 3	133
PEO_xLiAsF_6	x = 3, 6	134
	x = 6—6·4, 21—28	132
PEO_xLiBF_4	x = 4	139
	x = 2·5, 16—20	132
PEO_xLiPF_6	x = 6·2, 22—28	132
$PEO_xLiAlCl_4$	x <1[a]	132
PEO_xNaSCN	x = 3[a]	135
	x = 3·5	136
PEO_xKSCN	x = 4	135
PEO_xRbSCN	x = 4	140
PEO_xRbI	x = 4	140
PEO_xHgCl_2	x = 4	141
PEO_xNH_4SCN	x = 4	68
$PEO_xNH_4SO_3CF_3$	x = 4[a], 8[a]	68

[a] Postulated stoichiometries.

the smaller Na^+ ion was suggested to reside within the helix of a single polyether chain. The coordination environment of the cation was described as three ether oxygens and two iodide ions.[144]

IR and Raman spectroscopic studies on PEO salt complexes provide information on the cation polymer interaction, ion pairing, and polymer conformation.[128,145-147] Vibrational bands associated with the cation vibrating within an ether solvent cage are observed in the far-IR, typically around 400 cm^{-1} for Li^+, 200 cm^{-1} for NH_4^+, 180 cm^{-1} for Na^+, and 150 cm^{-1} for K^+.[148-152] In accordance with these solution values, a broad-IR active band is observed at *circa* 420 cm^{-1} in $P(EO_nLiX)$, and 190 cm^{-1} with $P(EO_nNaX)$.[128,146] The sharp cation-dependent far-IR bands for $P(EO_nNaX)$ indicate a well-defined $Na^+..O_n$ environment. The $NaBF_4$, NaI, and NaBr PEO complexes exhibit little anion dependence for their cation cage modes. This was taken as an indication that the anion is outside the first coordination sphere of the cation. As discussed later in this review, evidence is accumulating in favor of the importance of ion pairing and more complex ion-ion interaction. A more thorough investigation of the cation modes in the far-IR may be helpful for establishing cation-anion interaction. For certain P(EO·NaX) complexes (BH_4^-, SCN^-, and BD_4^-) distinct anion dependence is found in the far-IR bands.[147]

Internal modes in a polyatomic anion are often sensitive to ion pairing.[153] Similarly, a study of the internal vibrational modes of BH_4^- and BF_4^- in PEO shows a loss of symmetry in the BH_4^-, indicative of an anion-cation interaction.[147] The strong anion-cation interaction is supported by the low ionic conductivity observed in $P(EO_nNaBH_4)$ compared to $P(EO_nNaBF_4)$. Similar Raman spectra are obtained for complexed and pure PEO. An exception to this is a strong new band at 865 cm^{-1} characteristic of all PEO complexes studied.[145] In a similar system, the crown ether alkali metal-salt complexes, an intense polarized band near 865 to 870 cm^{-1} was assigned to the totally symmetric metal-oxygen

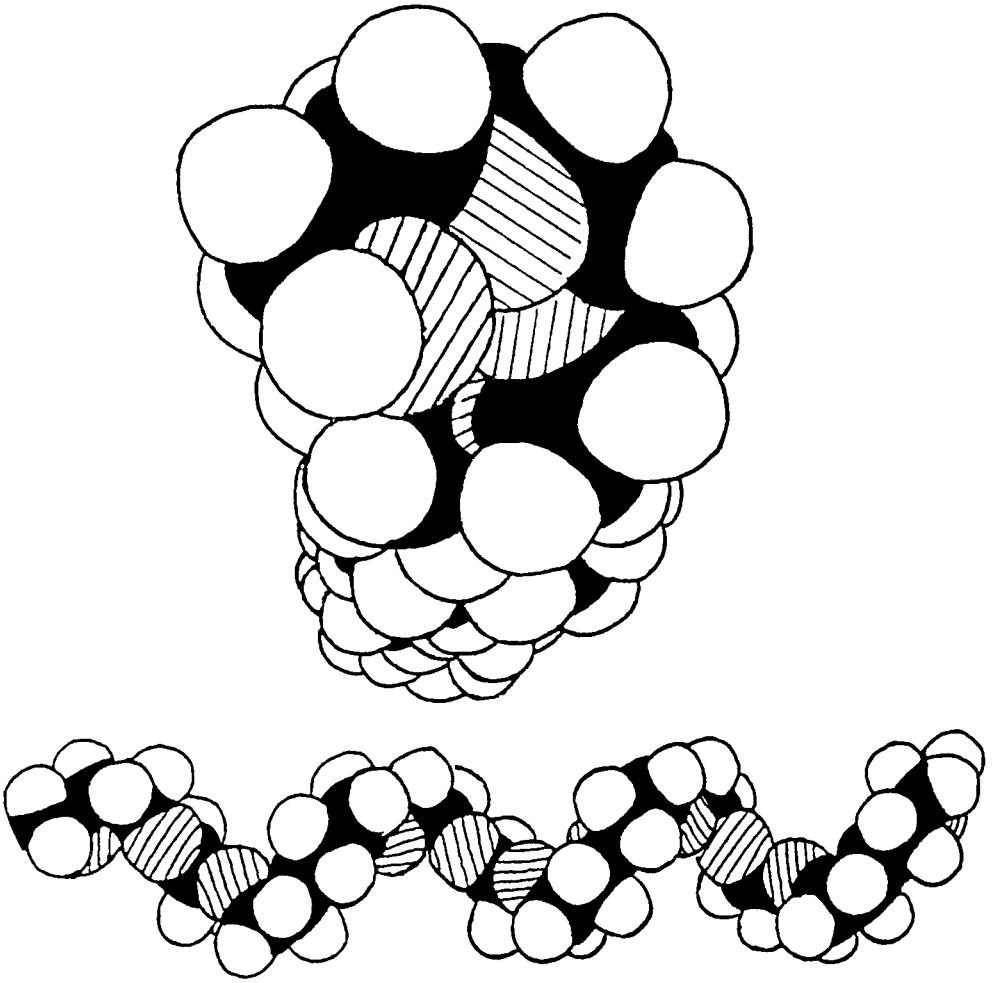

FIGURE 5. Space filling molecular models depicting the T_2GT_2G conformation established for PEO. Upper diagram, side view; lower diagram, end view.

breathing motion.[154] Based on the analogous crown ether work and the IR inactivity, the new band was tentatively assigned to a metal-oxygen symmetric stretch which is strongly mixed with CH_2 rock.

In Raman studies carried out on P(PO·NaSCN), the low frequency mode at 239 cm^{-1} (torsional or bending motion of the polymer backbone) proved sensitive to the presence of NaSCN.[155] This band narrows and shifts on dissolution. The SCN^- stretching modes also indicate ion pairing in $P(PO_nNaSCN)$. The authors believe that ions move via an ion-pair exchange which leads to the observed broadening of the anion stretching frequencies.

IR and Raman spectroscopic data plus X-ray repeat unit data and space-filling molecular models have been used to infer the conformation of pure semicrystalline PEO[156-158] (Figure 5); however, the more recent data cited above indicate that ion pairing may be more important than was assumed in this early structure model.

Relatively little structural data are available for polymer-salt complexes other than PEO. A study of poly(ethylene glycol) plasticized with poly(vinylpyrrolidone) indicated coordination of the ketonic oxygen to the cation, and hydrogen bonding between the glycol end groups and the anion.[102] IR spectroscopic data on poly(ethylene imine) (PEI) salt complexes show that complex formation leads to a breakup of the N–H– –N hydrogen bonding in the parent polymer.[84]

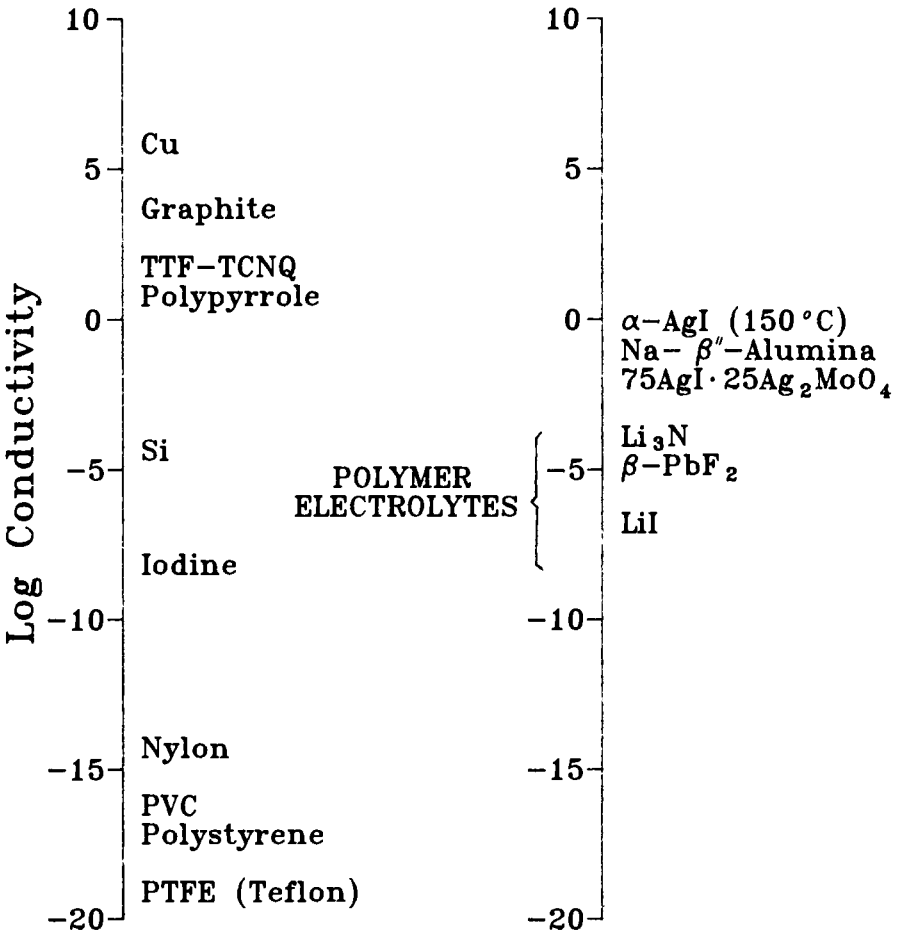

FIGURE 6. A log conductivity scale for typical electronic (left) and ionic (right) conductors at 25°C.

A very important use of IR spectroscopy in polymer electrolyte characterization is the detection of residual water. This application is based on the data of Edgell and co-workers[159] for the determination of moisture in nonaqueous solvents.

In principle EXAFS could provide information on the coordination sphere of an ion in a polymer electrolyte; however, the EXAFS spectra of rubidium salts in PEO[140] give broad, unresolved features and it is perhaps unwise to infer too much from these data.

NMR spectroscopy is a very promising tool for the investigation of polymer structure. The potential scope for studies of this type is greatly increased by the availability of magic angle spinning techniques. For example, chemical shift and relaxation measurements have implicated the sites of cation solvation in comb-like polymers,[160,161] and the structure of a silicone polymer host has been inferred from ^{29}Si NMR. Aside from structural information, NMR has been very useful for defining the dynamics of ion and polymer motion. These aspects will be discussed in Sections III.C.1 and III.D.1.c.

III. ION TRANSPORT

A comparison of the polymer electrolytes with other electrical conductors (Figure 6) reveals that these polymer systems display conductivities that are comparable to those of semiconductors. In this section the theory and measurement of AC impedance and other techniques

for conductivity determination will be discussed. AC impedance spectroscopy is the most important of these techniques, so we describe it in greater detail. This is followed by a description of the effect of crystallinity, salt concentration, temperature, and pressure on the ionic conductivity.

A. Conductivity Measurements

1. General Principles

At low frequencies, electrical conduction in solids occurs via the long-range migration of electronic (electrons or electron holes) or ionic charge carriers. Conduction by one or other type of charge carrier usually predominates in a material. The specific conductivity, σ, which is the sum of the electronic, σ_{el}, and ionic, σ_{ion}, conductivities is given by

$$\sigma = \sigma_{el} + \sigma_{ion} \tag{1}$$

For any given material the specific conductivity is related to the number of charge carriers, n_i, charge, q_i, and mobility, u_i, of i by

$$\sigma = \sum_i n_i q_i u_i \tag{2}$$

The conductivity of most inorganic solid electrolytes and crystalline polymer electrolytes follows an Arrhenuis equation of the form

$$\sigma = A/T \exp(-E_a/kT) \tag{3}$$

where E_a is the thermal activation energy and A a preexponential factor which includes the carrier concentration.

The mobility of an ion (u_i) is related to the number of carriers per unit volume (n) of charge q by

$$u_i = \sigma_i/nq \tag{4}$$

and has dimensions of $cm^2\ V^{-1}\ s^{-1}$.

The transference number of a charge species i (t_i) is defined as the ratio of the mobility of a carrier divided by the sum of the mobilities of all charge-carrying species. When concentration gradients are absent the transference number is given by the corresponding quotient of ion conductivities:

$$t_i = I_i \Big/ \sum_{j=1}^{m} I_j = \sigma_i \Big/ \sum_{j=1}^{m} \sigma_j \tag{5}$$

where the sum of the transference numbers equals 1 $\left(\sum_{j=1}^{m} t_j = 1\right)$ and is dimensionless.

The diffusion coefficient for a mobile species can be related to the conductivity via the Nernst-Einstein equation,

$$\sigma/D = nq^2/k_B T \tag{6}$$

where D is the diffusion coefficient. Studies of diffusion in solids can be carried out by various techniques: radiotracer, DC and AC methods with varying electrode choices, and electrochemical and NMR methods to be discussed in Section III.D.1.

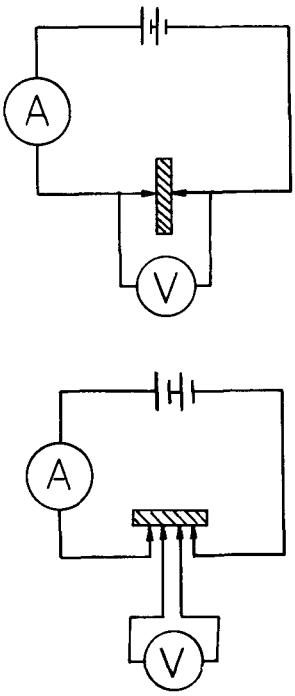

FIGURE 7. Circuit diagrams for (A) two-probe and (B) four-probe DC conductivity measurements.

2. DC Conductivity

The study of conductivity of metals is facilitated by the small resistance that generally exists between the sample and the probe electrodes. Thus, the DC conductivity of a sample can be ascertained by measuring the constant current in the external circuit on the application of a known potential across the sample. The total conductivity (σ) for a sample of length l and cross-sectional area A is

$$\sigma = \frac{I}{V} \cdot \frac{\ell}{A} \tag{7}$$

where I and V are the current and voltage, respectively. A simple representation of a two-probe cell is given in Figure 7A. In the collection of precise data it is common to employ a four-probe arrangement, Figure 7B, which compensates for the interfacial resistance and related effects.

By contrast, if a DC potential is applied to an ionic conductor, using standard inert metal electrodes such as Pt, the mobile ions are unable to cross the electrode/electrolyte interface; hence, charge accumulation and depletion occur. Electrodes giving rise to this type of charge buildup are termed blocking or irreversible. A capacitative response is obtained in this system which is characterized by the capacitance C, accumulated charge q, and applied field E:

$$C = q/E \tag{8}$$

The charge buildup at the electrode/electrolyte interface results in a charge double layer and the associated capacitance is designated C_{dl}. The creation of an electrical double layer influences the electrical response of a system. The current/time profiles for ionic conductors with blocking and reversible electrodes are shown in Figure 8.

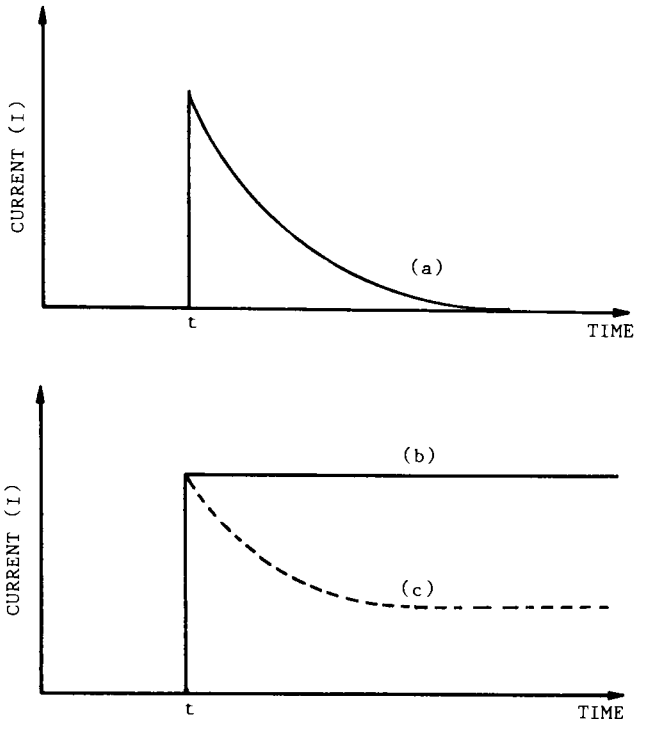

FIGURE 8. Typical current/time profiles for polymer electrolytes with (a) blocking electrodes, (b) totally reversible electrodes, and (c) electrodes reversible to one of the mobile species only.

In principle ion-reversible electrodes might be employed for DC conductivity measurements on polymer electrolytes, but the required electrodes that are reversible with respect to both cations and anions are generally unavailable.[162] The lack of truly reversible electrodes and the polarization of the electrolyte at the electrode-electrolyte interface have led to the widespread use of AC techniques that permit the separation of bulk and interfacial responses.

3. AC Conductivity

The AC analog of ohms law (E = IR) is

$$E = IZ \tag{9}$$

where E and I are waveform amplitudes for the potential and current, respectively, and Z is the impedance. Figure 9 represents a typical voltage sine wave E applied across a given circuit and the resultant AC current waveform I. The traces differ in both their amplitude and phase. In the case of a purely resistive network, the waveforms are in phase but differ in amplitude. Vector analysis provides a convenient method for chacterizing AC waveforms. A current waveform vector is shown in Figure 10. Figure 10A illustrates the current vector in terms of a phase angle, θ, and the magnitude of I. An alternative approach which is more convenient for numerical analysis is to use the real, I′, and imaginary, I″, components of the current, as shown in Figure 10B. Using these conventions, any AC current vector can be defined as the sum of the real and imaginary components:

$$I^* = I' + jI'' \tag{10}$$

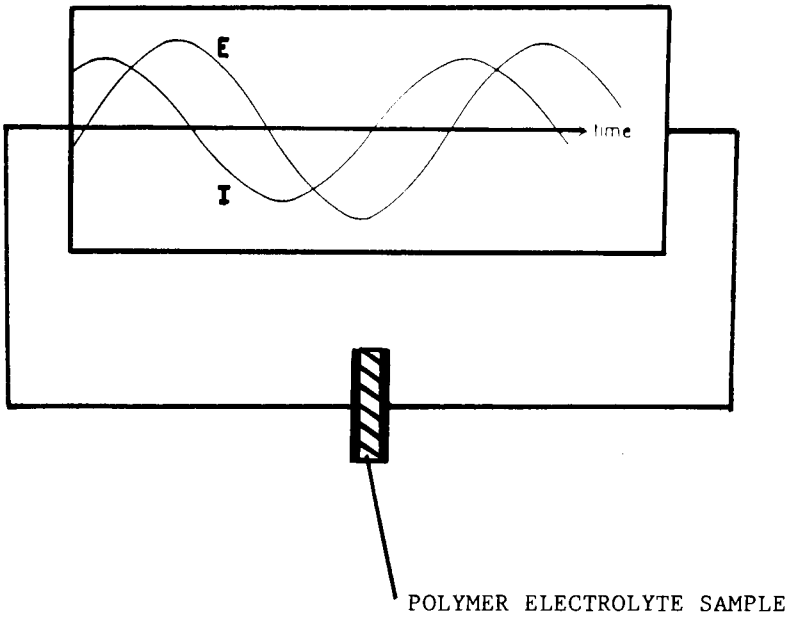

FIGURE 9. AC waveforms for an applied potential E and a result current I. The current sine wave can be described by the equation $I = A\sin(\omega t + \theta)$, where I = instantaneous surrent, ω = frequency in radians, A = maximum amplitude, and θ = phase shift in radians.

where I* denotes the total complex current and $j = \sqrt{-1}$. Similarly, a complex potential, E*, and complex impedance, Z*, can be expressed as the sum of their imaginary and real components:

$$Z^* = Z' + jZ'' \tag{11}$$

From analysis of the vector geometry, the magnitude of the impedance vector can be expressed as

$$Z = [(Z')^2 + (Z'')^2]^{1/2} \tag{12}$$

and

$$\tan\theta = Z''/Z' \tag{13}$$

or

$$Z'' = |Z|\sin\theta, \qquad Z' = |Z|\cos\theta \tag{14}$$

As previously stated a pure resistor has current and voltage in-phase, in a zero-phase angle, and no imaginary component. A capacitor, on the other hand, has a current that leads the voltage by 90°, hence it has no real component. In ionic conductors the capacitance due to the bulk electrolyte, C_b, and the electrode-electrolyte interface leads to a displacement of applied potential and measured current. The frequency response of a solid electrolyte between two metallic electrodes can be modeled as a series or parallel combination of resistor-capacitor networks (see Figure 11). From the analysis of the complex impedance spectrum it is possible to obtain values for the resistors and capacitors that model a particular material. The most

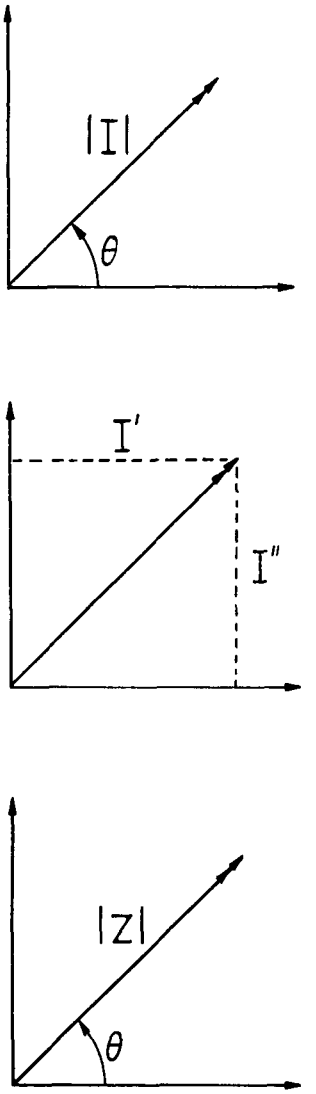

FIGURE 10. Vector analysis of the AC waveforms in terms of (A) the magnitude of the current |I| and phase angle θ; (B) real, I′, and imaginary, I″, components of the current; and (C) the magnitude of the impedance |Z| and the phase angle θ. $Z'' = |Z|_{\sin\theta}$; $Z' = |Z|\cos\theta$.

common application of impedance spectroscopy is to determine the bulk resistivity, R_b, from a plot such as Figure 11A. The value of R_b is used to determine the ionic conductivity together with measured values of the electrode area and electrolyte thickness by Equation 7.

The characteristic semicircular arcs and straight lines obtained in the complex plane Figure 11 can be related to various processes (e.g., ionic conduction, double layer capacitance, interfacial resistance, or Warburg diffusion). Consider first the case of a conductance cell with ion-blocking electrodes (Figure 11A). The high frequency semicircle is due to the bulk capacitance C_b plus leakage through a parallel resistance, R_b. At lower frequencies a spur associated with C_{dl} is seen.

Macdonald[163] has given a similar treatment for a cell with reversible electrodes. In this

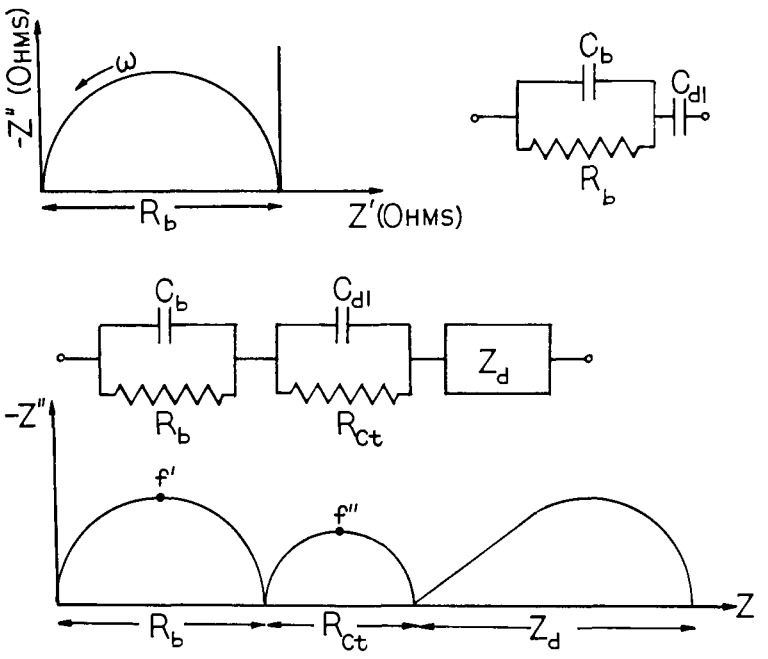

FIGURE 11. Complex impedance diagrams and equivalent resistor/capacitor circuits for polymer electrolytes with (A) blocking electrodes and (B) cation-reversible electrodes. Analysis of (B) gives the cation transference number, $t_+ = 1/(1 + Z_d(O)/R_b)$, where $Z_d = R_b(\mu_-/\mu_+)$ (tanh α)/α and $\alpha^2 = i2\pi f l^2/D_s$. When α goes to zero, Z_d will be $Z_d(O) = R_b(\mu_-/\mu_+)$. Further analysis of the RC circuits gives $R_bC_b2\pi f' = R_{dl}C_{dl}1\pi f'' = 1$, and $C_b = \epsilon A/l$, where l, A, and ϵ are the thickness, cross-sectional area, and dielectric constant, respectively, and μ is the mobility.

case the impedance plot consists of three arcs see (Figure 11B). The highest frequency arc has just been described. At somewhat lower frequencies in Figure 11B a second arc is associated with the capacitance C_{dl} and resistance R_{dl} of the electrical double layer. At still lower frequencies a linear response at 45° (slope = 1) is observed which is due to the concentration gradients in the electrolyte caused by the amount of charge transfer at the electrode in half a cycle. The resulting electrical response is modeled by function called the Warburg impedance; at still lower frequencies the impedance may deviate from the Warburg impedance and return to the real axis. This low frequency dip in impedance may be due to finite diffusion layer thickness at steady state or due to a finite electrolyte thickness. It is possible by analysis of the magnitude of the various circuit elements described above to estimate values of the diffusion constant D_s and the transport numbers t_i.

Equivalent circuits provide useful descriptions of the bulk response of electrode-electrolyte systems, but they do not yield insight at the molecular level. Microscopic models have been devised to describe the dielectric response of materials. In Debye's original model[164] for dielectric relaxation in polar liquids, a single relaxation time τ_0 was used to describe the dipolar reorientation that leads to the C_b term discussed above. The Debye model leads to a semicircular arc centered on the real axis for the dielectric spectrum of bulk materials, whereas the observed arc is generally centered below the real axis (see Figure 12A). Attempts at modifying Debye's simple model to more closely describe real systems have been made. Cole and Cole[165] introduced a distribution of relaxations rather than a single relaxation. This gives a broader arc in the complex plane whose center is depressed below the real axis (Figure 12B). The model of Cole and Cole leads to an impedance that is independent of frequency. This concept of constant phase element has been extensively discussed by Jonscher,[166,167] Macdonald,[168-170] and others.[171,172]

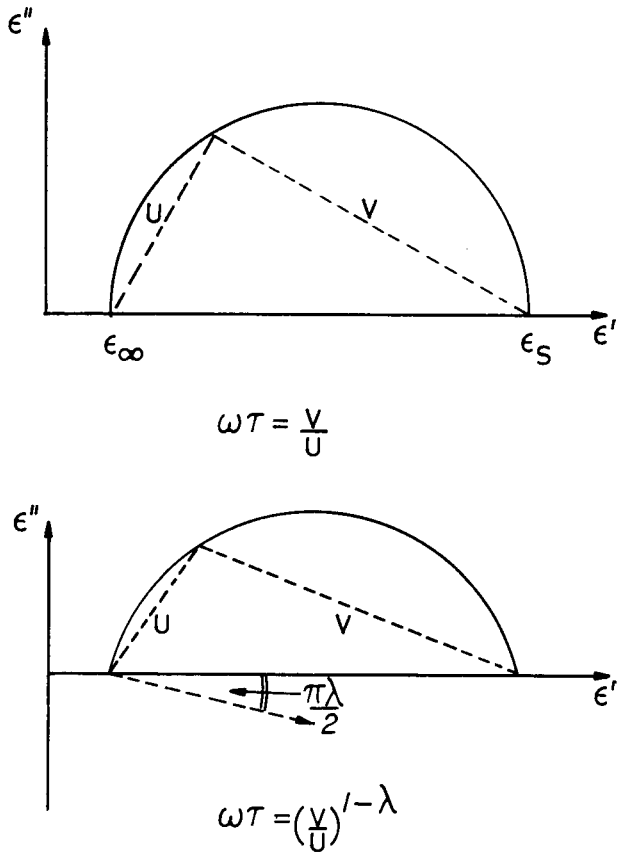

FIGURE 12. Cole-Cole plots of real and imaginary parts of the perittivity for a system with (A) a single relaxation time and (B) a distribution of relaxation times.

B. Ion Transport Models

In the early studies of PEO salt complexes it was suggested that cations reside inside the single[86] or double helices[173] of the polyethers chain. Cation hopping thruogh the helices was thought to be the mechanism for ion transport. In apparent agreement with this interpretation Arrhenius behavior (Equation 3) was observed for the temperature dependence of the conductivity. As described below, however, this mechanism is no longer accepted. The first indications of a different mechanism came from the studies of Armand and co-workers[86] on the amorphous polymer-salt complexes formed between PPO and various salts.

The conductivity data could be fit by the Vogel-Tamman-Fulcher, VTF, equation:

$$\sigma = \sigma_o \exp[-B/(T - T_o)] \tag{15}$$

where B is an apparent activation energy and T_o is a fitting parameter. Since expressions of the form of Equation 15 are characteristic of ion and atom transport in fluid media, it became apparent that the simple hopping model for ion transport in the polyethers might not be appropriate. Subsequent NMR measurements showed that the ion transport in PEO-salt complexes occur in the amorphous regions and not in the crystalline regions.[137-138] Similarly, experiments with dopant ions that form immobile ion pairs indicated that ion transport was not occurring down the presumed helical path.[147] A wide variety of experiments now agree with the concept that ion transport in most, if not all, of the polymer-salt complexes

occurs by a liquid-like mechanism in which the segmental motions of the polymer are responsible for ion transport.

Because Equation 15 is so widely used to describe ion transport in polymer electrolytes, we give background on its development and the development of related expressions. The VTF equation is an empirical relation originally developed to describe viscosity of supercooled liquids.[174-176] The viscosity, η, was found to be of the form

$$\eta = C \exp[+B/(T - T_o)] \tag{16}$$

which when combined with the Stokes-Einstein relation for diffusion of polymers, D,

$$D = k_B T/6\Pi r_i \eta_i \tag{17}$$

where r_i is the radius for diffusion, gives

$$D = c_1 T^{1/2} \exp[-B/(T - T_o)] \tag{18}$$

The VTF form (Equation 15) can be obtained by a combination of Equation 18 with the Nernst-Einstein Equation 6. It should be noted that Equation 17 applies to diffusion of ions in a continuous medium, and the T_o is a fitting parameter. T_o, also labeled T_∞ is the temperature at which relaxation times become infinite.[177]

A parallel but conceptually simpler semiempirical relation, the free volume model, was developed in the study of fluidity of simple hydrocarbon liquids.[178] In the free volume model the average free volume per molecule, v_f, is defined by

$$v_f = \bar{v} - v_o \tag{19}$$

where v_o is the van der Waals volume of the molecule or segmental motion and $\bar{v}$ is the average volume per molecule in the liquid. On suggestions by Fox and Flory,[179,180] Doolittle[178] found that the fluidity, ϕ, of hydrocarbon liquids could be satisfactorily represented by

$$\phi = A \exp(-bv_o/v_f) \tag{20}$$

where b is a constant of order unity. Batschinsky[181] had previously suggested that viscosity is nearly independent of temperature at constant volume (i.e., $\phi = \eta$), hence the viscosity decreases linearly with free volume. Williams, Landel, and Ferry (WLF) developed the Doolittle idea further for liquid hydrocarbons to include relaxation processes which characterize polymers and other glass-forming materials.[177] They defined a shift ratio, a_T, which is the ratio of any relaxation process (e.g., viscosity, diffusion, conductivity, etc.) at temperature T to its value at some reference temperature, T_s. Through appropriate choice of T_s a universal plot of $\log(a_T)$ as a function of $(T - T_s)$ can be obtained. It was observed that the best fits are obtained in a 100-K region above the T_g for any particular polymer studied and that $(T_s - T_g) = 50$ K. An analytical expression for a_T can be inferred by modifying the VTF Equation 15 to

$$\log a_T = \text{const} + \log[\eta(T)/\eta(T_s)] \tag{21}$$

which implies to within an additive constant

$$\log a_T = \frac{-C_1(T - T_s)}{(C_2 + T - T_s)} \tag{22}$$

Equation 22 is the usual form of the WLF equation containing universal constants, C_1 and C_2. A plot of $(T - T_s)/\log(a_T)$ against $(T - T_s)$ gives a straight line from which the universal values of C_1 (8.9) and C_2 (101.6 K) can be obtained. It also follows from comparison of the VTF and the WLF that $C_2 = (T_s - T_o)$. As T_s is normally 50 K above T_g and T_o is approximately 50 K below T_g, then

$$\log a_T = \frac{-17.44(T - T_g)}{(51.6 + T - T_g)} \tag{23}$$

Although the WLF treatment was not based on free volume it can be derived from the Doolittle Equations 20 and 23 by using

$$v_f = v_g[0.025 + \alpha(T - T_g)] \tag{24}$$

where v_g is the volume at T_g and α is the thermal expansivity and normally taken as $4.8 \times 10^4\ K^{-1}$. Williams et al.[177] believed the success of their model was due to "the nature of the volume change and its effect on the rates of molecular rearrangement which are essentially the same for supercooled systems, polymeric and nonpolymeric mixtures, independent of molecular structure".

Insight into the various free volume treatments was provided by Cohen and Turnbull's[182] adaptation of the model to describe molecule transport in a hard-sphere liquid. The spheres achieve gas kinetic velocities but are confined to a cage made up of immediate neighbors. When a fluctuation in density of the neighbors opens a hole a molecule may move into it, and diffusion results if another molecule takes its original place. Thus, in this treatment, diffusion is not an activated process but instead the result of fluctuations in free volume.

The polymer electrolytes which involve strong ion-polymer and ion-ion interaction present a much greater degree of complexity than the hard-sphere liquid of Cohen and Turnbull or even the polymers considered by Williams et al. In an effort to bridge the gap Cheradame[183] has extended a free volume model[184] to include ion pairing and an Arrhenius-type activated motion, giving rise to

$$\sigma = \sigma_o \exp\left(\frac{-\gamma v^*}{v_f} - \frac{\Delta E}{RT}\right) \tag{25}$$

where ΔE is taken as

$$\Delta E = E_a + E_b + W/\epsilon \tag{26}$$

where ϵ is the dielectric constant, W is the dissociation energy of the salt, E_a is the potential barrier to displacement of the polymer segment, and E_b, though not defined, is the activation energy for ion hopping. In a somewhat different treatment of this same problem Watanabe[129] and co-workers show that deviations from the WLF treatment (Equation 23) become progressively greater with increasing lattice energy of the dissolved salt. The inference is that ion dissociation decreases for the small cation-small anion combinations that give rise to higher lattice energies.

1. Configurational Entropy Model

There are basic conceptual problems in the application of free volume models for ion transport in amorphous media. Angell, in particular, has argued that the free volume concept of an ion jumping into a hole is not realistic for ion transport in molten salts.[185] Instead he

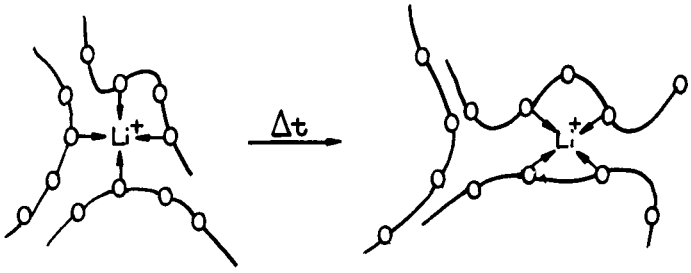

FIGURE 13. A pictorial representation of the migration of a lithium ion assisted by polymer segmental motion.

prefers a configurational model in which ion motion is viewed as occurring by the cooperative rearrangement of an ion and its surroundings. Similarly, estimates by Papke and co-workers[128] of the energy for an alkali metal to jump from one coordination site into a vacant hole vastly exceed the apparent activation energy for ion conductivity.

A more energetically acceptable model is that of the polymer and associated ions undergoing cooperative fluctuations that lead to ion transport (Figure 13).[128,186] The original configurational entropy model devised by Gibbs and co-workers[187,188] and discussed by Goldstein[189] and Angell[185,186,190,191] invokes a configurational ground state at a temperature T_o. Below this temperature no further entropy can be lost through configurational motion. However, above T_o the segmental motions of a polymer set in and associated with this process is a configurational entropy S_c. Adam and Gibbs[188] have shown that the WLF functional dependence of polymer properties can be derived from the configurational entropy model. They obtained the probability W(T) for the cooperative polymer rearrangements that lead to mass transport, which can be written

$$W = A \exp(-\Delta\mu S_c^*/k_B T S_c) \tag{27}$$

where $\Delta\mu$ is a free energy barrier per mole which impedes the rearrangement and S_c^* is the minimum configurational entropy required for rearrangement. Taking the thermodynamic definition of entropy

$$S_c(T) - S_c(T_o) = \int_{T_o}^{T} \Delta C_p/T \cdot dT \tag{28}$$

where C_p is the heat capacity change going from glassy to liquid states, and where $S_c(T_o)$ disappears. Substitution of Equation 28 into Equation 27 gives a VTF or WLT form derived from entropy. The exact nature of these models depends on the assumptions made for ΔC_p. Adams and Gibbs assumed it to be independent of T and obtained

$$W(T) = A \exp(-\Delta\mu S_c^*/k_B T \Delta C_p \ln T/T_o) \tag{29}$$

and by relating W to the inverse relaxation time obtained the WLF form

$$-\log a_T = a_1(T - T_s)/(a_2 + T - T_s) \tag{30}$$

with a_1 and a_2 defined in terms of Δu, ΔC_p, T_s, and T_o; a_2 is weakly temperature dependent. The VTF form of Equation 29 can be derived here by writing

$$\ln T/T_o = (T - T_o)/T_o \qquad \text{when} \qquad T/T_o \rightarrow 1 \tag{31}$$

then

$$W = A \exp \frac{(-K_\sigma)}{(T - T_o)} \tag{32}$$

where

$$K_\sigma = \Delta\mu S_c^*/k_B \Delta C_p \tag{33}$$

which is to say that close to T_o the VTF form of the configuration holds an ΔC_p is constant. By using an experimentally observed relationship ($C_p = B_1/T$) the VTF Equation 32 can be derived, but now K_σ is given by Equation 34.[185]

$$K_\sigma = \frac{\Delta\mu S_c^* T_o}{k_B B_1} \tag{34}$$

The Adam and Gibbs model is more useful in that it permits some microscopic interpretations unlike the empirical VTF or WLF, but it still only models polymer motion in a very general way.

Other points which arise from the Adam and Gibbs model have been discussed more thoroughly elsewhere[192] and will be just briefly outlined here.

1. The effect of pressure on apparent activation energy from Equation 34 is

$$\frac{\partial K\sigma}{\partial P_T} = \frac{S_c^* \Delta V T_o}{k_B B_1} \tag{35}$$

   where ΔV is the volume of activation. This predicts that the conductivity should decrease with increasing pressure, which is also apparent from free volume and as been observed for polymer electrolytes.
2. The Gibbs and DiMarzio[187] model suggests that T_g becomes independent of chain length for relatively low molecular weight polymers. For PEO as well as most polymers an increase in chain length is accompanied by a rapid rise in viscosity. Thus, low molecular weight polymers might give the most conductive electrolytes, however, dimensional stability would be lost and the material would no longer be a solid.
3. The T_g shows a linear salt concentration, x, dependence (i.e., as more salt is added, T_g increases). The conductivity can now be written as

$$\sigma = A'x \exp[-K\sigma/(T - cx - C_o)] \tag{36}$$

   The maximum conductivity is associated with an optimum salt concentration x_m fixed by $\frac{\partial\sigma}{\partial\chi} = 0$. This maximum is observed for the simple amorphous salt complexes of PPO,[86] MEEP (methyoxyethoxyethoxypolyphosphophazene),[73] polysiloxanes,[161] and network polymers,[202] but breaks down for semicrystalline PEO and PESc[87] salt complexes where the carrier number is no longer linear (see Section III.C).
4. The lower T_o (or T_g) the higher the conductivity at any temperature T above T_o. The polymer with a lower T_o is farther into a liquid regime and, hence, the ions are more mobile.

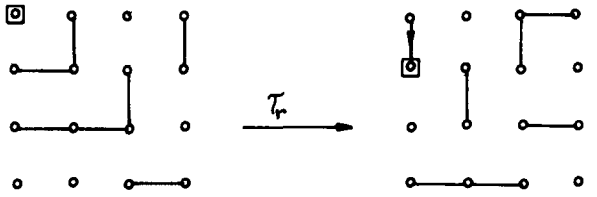

FIGURE 14. Percolation on a dynamic lattice, with renewal time τ_r.○, Lattice site; □, hopper; (—), available path.

5. The highly crystalline complexes still possess configurational motion and, hence, there is still strong coupling of ion motion. Microwave studies in the 10- to 70-GHz region on crystalline-pure PEO, P(EO·NaSCN), and P(EO·$NaBH_4$) at room temperature[193,194] show strong conductive response due to local segmental motion of the polymer (β relaxation).[104] The lower frequency spectrum, below 0.1 GHz, is dominated by ionic motion.

The close correlation between the volume and entropy in polymers is the explanation given[190] for the success of the VTF equation in describing ion transport in polymers.

2. Time-Dependent Percolation Theory

The free volume and excess entropy models discussed so far lack macroscopic detail. A step in the direction of more detailed models has been taken by Ratner and Nitzan,[195-199] who devised the time-dependent bond percolation theory. In a static percolation model the hoppers are all independent and move on a lattice made up of a regular array of fixed sites of which fractions, f, are allowed paths (Figure 14). There exists a certain threshold number of available paths above which there is a continuous connected route for the hopper to move through the lattice. This condition permits DC conductivity. Below this threshold number of paths (percolation limit) the DC conductivity drops precipitously. This static percolation model is appropriate for two-phase systems. For example, Berthier[137,138] used static percolation to describe semicrystalline PEO complexes in which the conducting amorphous phases are interspersed with nonconducting crystalline regions.

In order to describe the local liquid-like motion of the ions in a polymer which is rapidly changing conformation above T_g, Ratner and Nitzan's[195-199] dynamic percolation model introduces the idea that the available paths (or bonds in the authors' terminology) are constantly opening and closing (i.e., renewing at a rate λ on the time scale τ_r, where $\tau_r = 1/\lambda$. The physical picture is that the renewal process corresponds to conformation changes in the polymer and surrounding ions that lead to ion transport. To date simulations have been restricted to a one-dimensional dynamic lattice for which several interesting points have arisen:

1. If there are any available sites (i.e., $f > 0$) and if the observation times are large with respect to both the renewal time and the hopping rate, ω ($\tau_{obs} \gg \tau_r > 1/\omega$), then diffusion occurs and there is no percolation threshold. The ion will be stopped only as long as it takes the polymer to create a new available path. The result is that the mean squared displacement of the ion $\langle x^2 \rangle$ will be proportional to the observation time.
2. If τ_r is short such that $1/\omega \gg \tau_r$, then the ion motion is nonpercolating (i.e., hopping at a rate ωf in a homogeneous system). Conversely, if τ_r is long, such that $1/\omega \ll \tau_{obs} < \tau_r$, then the system reverts to a simple static percolation model and in a one-dimensional system the motion is no longer diffusive, and $\langle x^2 \rangle = fa^2/(1 - f)^2$, where a is the hop distance.

3. It can be shown that the diffusion coefficient and hence, conductivity of a system described by dynamic percolation can be related to a static percolation system by

$$D_{dg}(\omega) = D_{st}(\omega - i\lambda) \quad (37)$$

It is therefore possible to convert well-studied static systems to dynamic systems and also investigate frequency-dependent properties.

The three charactertistic parameters of the dynamic percolation model f, ω, and λ are used by Ratner et al. to describe the microscopic features observed in solvent free polymer electrolytes (SFPE) such as the pressure-dependent conductivity and polymer chain length on the variation of counterion, stoichiometry changes, effect of plasticizers, and cross-linking. A very great strength of this model is that it provides an interpretation of high frequency conductivity data. The dynamic percolation model nicely fits frequency-dependent studies of the conductivity and dielectric response in the KHz through GHz range for polymer electrolytes around room temperature[193,194] and lower frequency data for polymer electrolytes at low temperatures.[200]

At room temperature PEO and PEO complexed with NaSCN show very similar responses above 10 GHz (Figure 15). The interpretation is that in this frequency regime the conductivity is dominated by the high segmental motion of the polymer. In the case of $P(EO_8NH_4SO_3CF_3)$ ion motion also appears to contribute to the conductivity (Figure 16).

Below 10 MHz the conductivity of pure PEO drops rapidly, whereas that of the polymer-salt complexes flatten out (Figures 15 and 16).

The totally amorphous $P(EO_8NH_4SO_3CF_3)$ shows a flat conductivity response below 10 MHz, which contrasts with a moderate drop in conductivity observed for the analogous crystalline complex (Figure 16). A qualitative explanation of the flat region is that it represents purely diffusive motion of the cation facilitated by the higher frequency segmental motion of the polymer. In other words, the low-frequency conductivity plateau represents case (1) from above for which $\tau_{obs} >> \tau_r > |/\omega$. The lines through the data points in Figure 16 represent a fit of the dynamic percolation theory to the frequency-dependent conductivity data under the assumption of a single relaxation time for the amorphous $P(EO_8NH_4SO_3CF_3)$. Inhomogeneous polymers often display multiple relaxations. For example, two well-separated relaxation times were necessary in the case of the partially crystalline sample of $P(EO_8NH_4SO_3CF_3)$.

C. Observed Conductivities

1. Influence of Morphology

PEO is a semicrystalline solid composed of two phases at ambient temperature. It is therefore necessary to consider the effect of this semicrystalline inhomogeneity on the transport properties.

Berthier[137,138] employed ^1H, ^7Li, and ^{19}F NMR to probe the polymer, cations, and anions, respectively, in $P(EO_nLiSO_3CF_3)$. The temperature dependence of the broad ^1H signal due to the crystalline phase shows the melting of pure PEO and the gradual dissolution of crystalline polymer-salt phases. The narrow ^1H signal due to the amorphous phase shows a gradual increase with temperature. A very important conclusion from this study was that the ions in the amorphous phase are responsible for the ionic conductivity in polymer electrolytes.[137] Similar behavior was observed for $P(EO_{10}NaI)$.[130]

A quantitative study of charge carrier concentration, mobility, and ultimately modeling the conductivity in PEO is difficult because of the simultaneous presence of different phases. Phase diagrams have been used by several authors[131-141] to explain the temperature-dependent conductivities obtained for a variety of PEO lithium, sodium, and ammonium salts com-

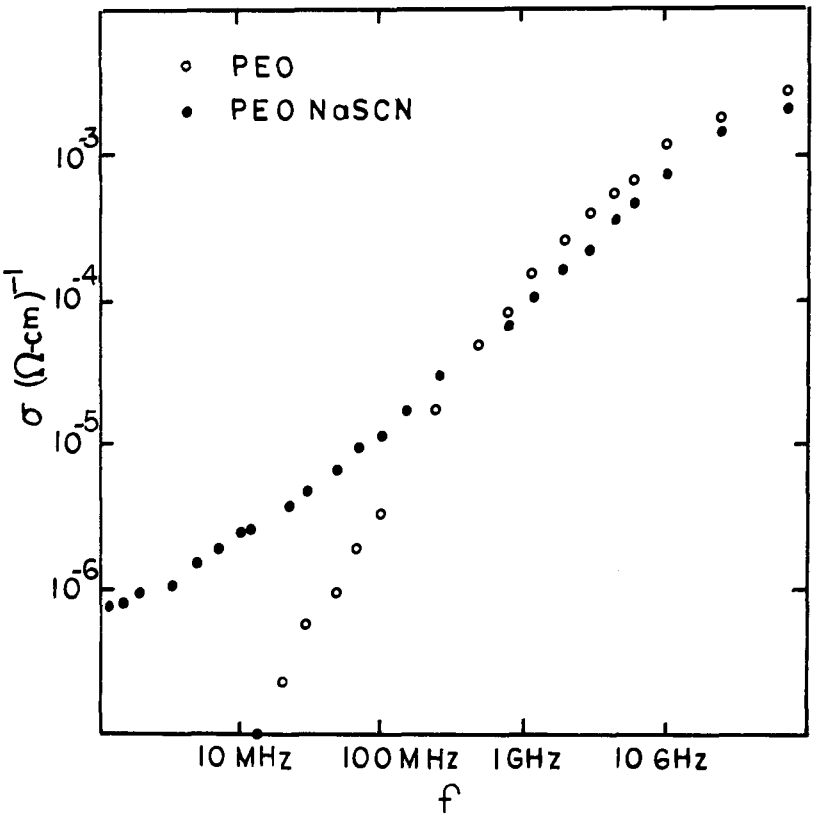

FIGURE 15. Log conductivity vs. frequency for pure PEO and $P(EO_{4.5}NaSCN)$.

plexes. To demonstrate the underlying principles a recent study by Lee and Crist[136] on PEO_nNaSCN will be described. At compositions below the formation of crystalline complex, Figure 17, and below the melting point of pure crystalline PEO, the conductivity is dominated by percolation of the ions in the dispersed amorphous regions and gives a linear log(σ) vs. 1/T (Arrhenius behavior) plot. The abrupt melting of the pure crystalline PEO, observed by DSC, results in an increase in conductivity. As the PEO melts it dilutes the amorphous phase causing a fall in T_g of the amorphous region. The resulting increase in ion mobility gives increased conductivity. As the temperature is raised further, the salt-rich crystalline complex dissolves in the amorphous phase. This dissolution is marked by a broad endotherm in the DSC. In this region the increase in conductivity due to a greater number of carriers (salt from the crystalline complex) is moderated by the accompanying increase in T_g up to the melting point of the crystalline complex, at which point the entire sample becomes amorphous. Above this melting point the sample is totally amorphous and it exhibits a curved log(σ) vs. 1/T plot (VTF behavior) (Figure 17).

The thermal history of a PEO complex is an important factor in determining the degree of crystallinity and, hence, the conductivity. If the complexes are cooled quickly from the melt a metastable totally amorphous phase can form depending on the kinetics of recrystallization. The increased ionic conductivity of the metastable amorphous phase of $P(EO_nNH_4SO_3CF_3)$ over the semicrystalline sample can be seen in Figure 18.[193] A metastable phase was also seen in $P(EO_{10}NaI)$ whose lifetime depends on the heat treatment.[130] If the sample was heated to the melting point of the complex, 450 K, the metastable phase persisted down to 280 K for an extended time period, whereas the metastable phase was less persistent at 280 K when the pretreatment temperature was only 410 K.

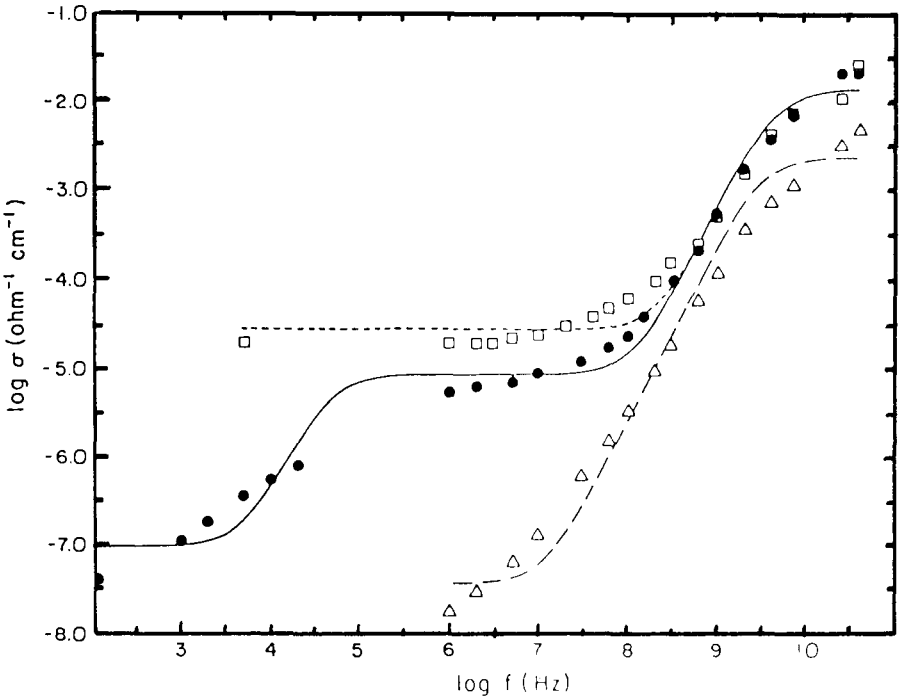

FIGURE 16. Room temperature conductivity/frequency plots for $P(EO_8NH_4SO_3CF_3)$: amorphous, □; crystalline, ●; pure PEO; Δ. The lines correspond to the least-squares fit of the dynamic percolation theory to experimental points.

2. Influence of Salt Concentration

The conductivity of polymer electrolytes is found to be strongly dependent on concentration. As we have seen in the previous section, changes in salt concentration can lead to a succession of phases in partially crystalline polymer-salt complexes. This leads to a complicated dependence of the conductivity on the salt concentration.

The effect on conductivity on increasing salt concentration is most readily seen in the totally amorphous polymer-salt complexes. In the majority of studies a maximum in conductivity is reported at moderate salt concentrations[73,202] (see Figure 19). This can be explained in terms of two opposing effects of salt concentration. At very low salt concentration the effect of added salt is to increase the number of charge carriers, and a conductivity increase results (Equation 4, see Section III.A.1); however, as salt is added the polymer-salt complex becomes more rigid due to a decrease in polymer segmental motion and this is reflected in an increase in T_g. As discussed in Sections III.C.1 and III.C.2, reduced segmental motion leads to reduced ion mobility and eventually this effect dominates with a resulting decrease in conductivity upon further addition of salt. Cheradame and co-workers[183,202] have shown that the influence of salt concentration on conductivity is less dramatic at high temperatures (Figure 20). The exact role of ion pairing or clustering throughout this concentration region is yet to be determined. The counterpart of decreased segmental motion for polymer electrolytes is the increased viscosity in fluid electrolytes. Jones and Dole developed a widely used empirical relation between viscosity and conductivity for liquids.[203]

Robitaille and Fauteux[134] reported isothermal ion conductivity vs. mass fraction salt for $P(EO_nLiX)$ ($X = SO_3CF_3^-$, AsF_6^-, $C10_4^-$) in which the characteristic maximum at low salt concentrations has satellite maxima or shoulders. While lower in magnitude than the generally observed maximum, and somewhat temperature dependent, these peaks occur at a salt concentration close to the eutectic (or monotectic) points. While no explanation of

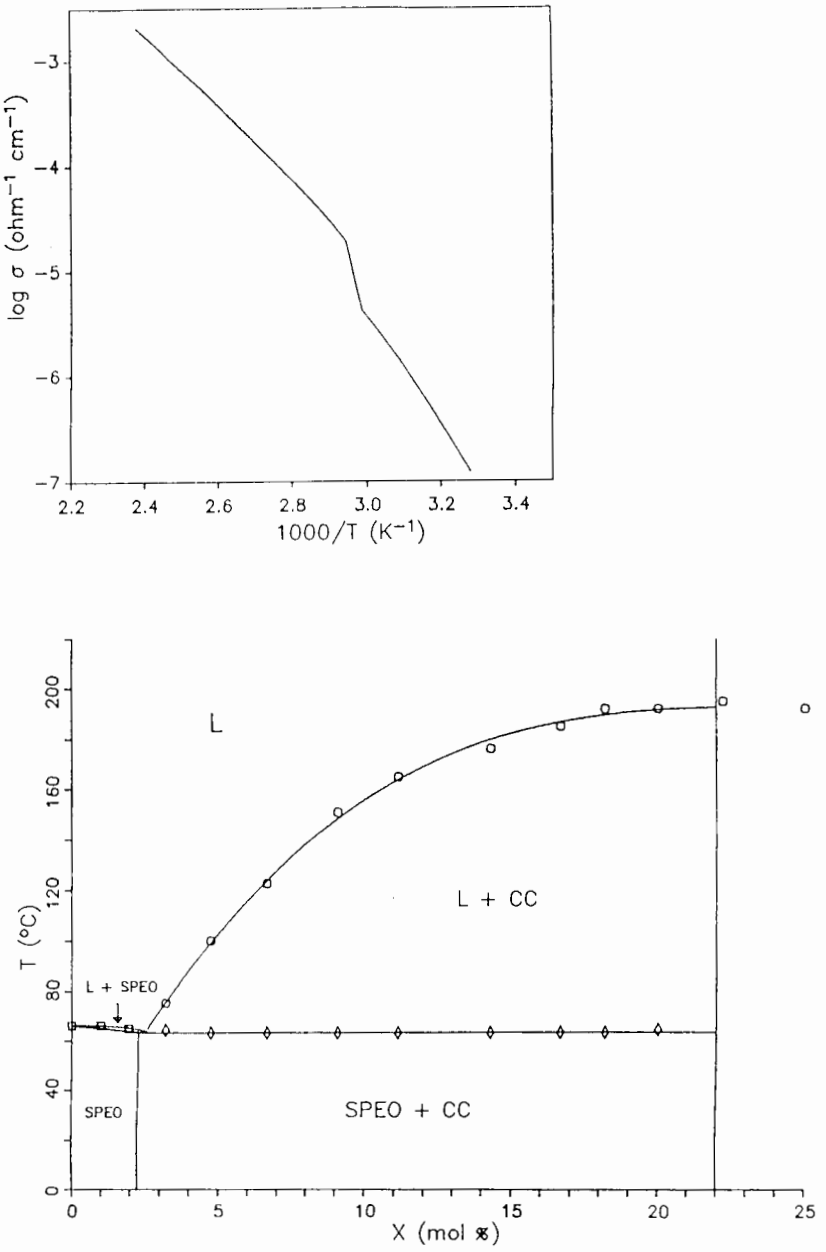

FIGURE 17. Log conductivity vs. 1/T for P(EO_8NaSCN) taken at the composition indicated by the arrow in the phase diagram. The linear portion on the right is observed below the melting point of PEO, the central rapid rise occurs in the liquidus, and the upper portion represents the conductivity in the amorphous polymer-salt complex.

their origin was given, presumably the formation of crystalline complexes reduces the amount of salt in the amorphous phase giving rise to an increased conductivity.

D. Transference Numbers and Ion Pairing

1. Transference Numbers

A wide range of techniques has been applied to measure transference numbers in polymer electrolytes. In general, both ions and electrons or electron holes contribute to the conductivity

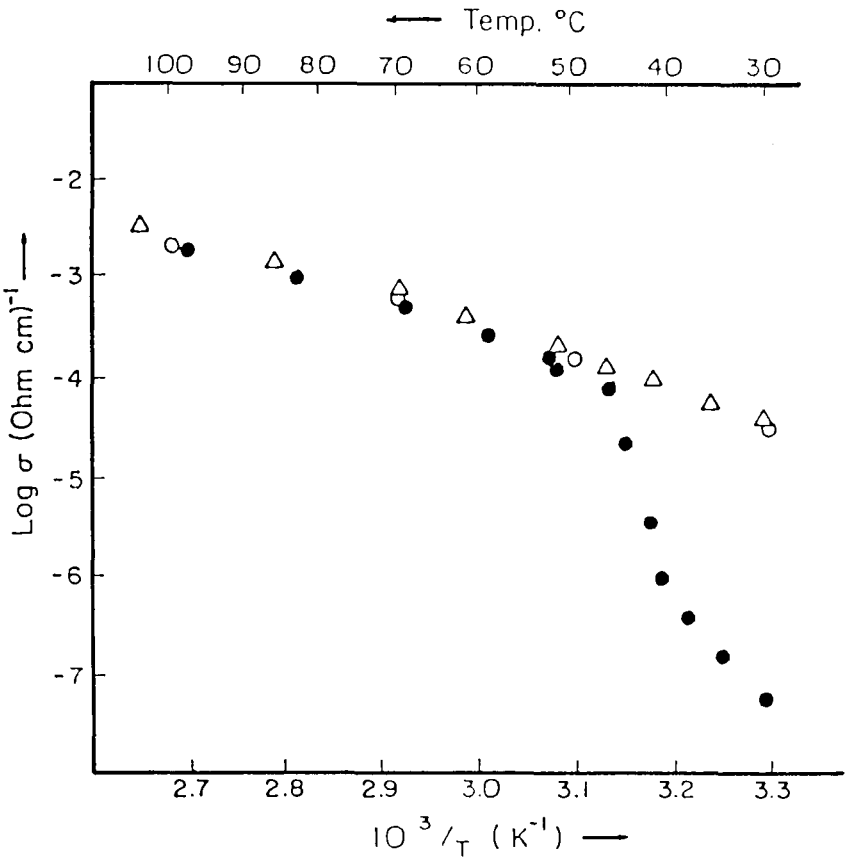

FIGURE 18. Variable temperature/conductivity plots for $P(EO_8NH_4SO_3CF_3)$: cooling and re-heating curves for the quenched amorphous polymer (Δ, ○) and heating curve for a sample of electrolyte which is crystalline at room temperature.

of a solid (Equation 5). It has been shown, however, that the electronic conductivity in a typical polymer electrolyte is very low,[204] so for most polymer electrolytes the parameters of interest are the fraction of charge carried by the cation t_+ and the anion t_-. The measurement of t_+ or t_- is not trivial, in part because different experimental techniques are sensitive to different mobile species.

The methods by which transport numbers are directly measured generally involve creating a gradient in electrical potential, chemical potential, radiotracer, or nuclear spin, and then analyzing the response of the system as a function of time.

a. Potential Gradient

In this general technique a potential driving force is applied across a polymer electrolyte and the passage of ions is monitored gravimetrically or by monitoring the current decay with time. The classic Tubandt's method[205] involves a cell in which the electrolyte pellets are sandwiched between weighed electrodes which are reversible to the cations. A known DC current is passed for some finite time t. The cell is then separated and the electrodes are again weighed. Transport numbers are inferred from moles of deposited material at an electrode divided by the total equivalents of current passed (see Figure 21).[162] This technique has been utilized in the laboratories of Watanabe[88] and of Cheradame.[206]

For example, Watanabe used an asymmetric cell arrangement with lithium and platinum electrodes and P(ESc·$LiClO_4$)[88] or poly[(β-propiolactone) $LiClO_4$][92] as the electrolytes. Ex-

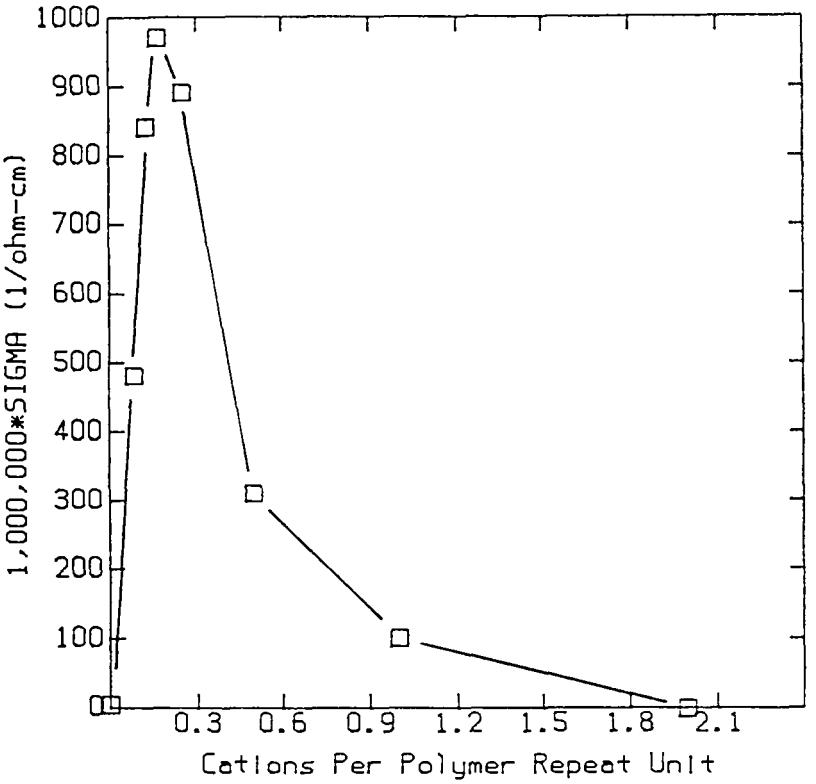

FIGURE 19. Electrical conductivity at 70°C vs. composition of $[AgSO_3CF_3)_xMEEP]_n$ complexes.

perimental difficulties in separating the electrodes from the elastomeric complexes have restricted widespread use of this simple technique in the field of SFPEs.[206]

Polarization experiments to determine transference numbers are based strictly on the electrical response of a system.[218,219] Usually the experiment involves the application of a constant voltage or current. For example, a small constant potential may be applied to a cell having reversible electrodes with respect to one ion (in this example the cation). The evolution of the current is followed with time. Both anions and cations contribute to the initial current, but as a concentration gradient builds up across the electrolyte, due to the lack of a source and sink for the anion, the current reaches a limiting value, where the cation migration is the sole contribution. When the instantaneous current is corrected for double-layer capacitance, and both instantaneous and steady-state current are corrected for electrode-electrolyte interfacial resistance, the ratio of currents yields t_+. A similar galvanostatic procedure can be employed. Unfortunately, the corrections are only approximate so this appealingly simple technique is subject to large errors. A somewhat related time-of-flight method has been proposed.[212]

AC impedance spectroscopic measurements of t have been performed with a cell equipped with electrodes which are reversible with respect to one ion. This technique is based on the very low frequency feature in the complex impedance spectrum (Figure 11B).[72,76,207-210,220]

b. Chemical Gradient

A method has been described which is based on the measurement of the potential across a concentration cell as a function of time.[214] As ions migrate the concentrations begin to equalize and potential of the cell drops. The electrolyte in this concentration cell consists of two slabs of polymer electrolyte having different salt concentrations:

$$Li|P(EO_mLiX)|P(EO_nLiX)|Li$$

If t_- is concentration and activity independent, it is related to the open circuit voltage, V_{oc}, and the mean activity, $a\pm$, by Equation 38:

$$t_- = -F/(2RT)\ dV_{oc}/d\ln(a\pm) \tag{38}$$

In general, it is also necessary to independently measure the mean activities for the ions in the two polymer electrolyte samples.

The migration of an electroactive ion in a solvent can be monitored by electrochemical methods.[221] Murray and co-workers[222] applied electrochemical methods to the measurement of transport rates for electroactive complex cations, such as $[Ru(ppy)_3]^{2+}$ in $P(EO_{16}LiSO_3CF_3)$. The electrochemical techniques hold great promise for probing the influence of polymer and salt concentration on the rate of diffusion of low concentrations of electroactive ions in polymer-salt complexes.

The use of radioactive-labeled charge carries is a powerful method in the determination of transference numbers. In radiotracer analysis work on $P(EO_8NaSCN)$ the diffusion of radioactive $^{22}Na^+$ and $S^{14}CN^-$ through PEO was monitored.[215,223] This was achieved by introducing the labeled salt on one side of the electrolyte, allowing time for diffusion, then microtoming the sample and analyzing the various sections for the concentration of tracer ions by scintillation counting.

A similar experiment has been reported in which the mobility of I^- through $P(EO_8LiX)$ (where X = ClO_4^-, AsF_6^-, or $SO_3CF_3^-$) was measured by an ion-selective electrode, Ag_3SI.[224] The experiment involved a lithium reference electrode, Ag_3SI iodide-sensing electrode, and the electrolyte consisted of films of $P(EO_xLiI)$ and $P(EO_xLiX)$ having equal thickness. The time-dependence of anion homogenization was determined by the increase of I^- at the Ag_3SI electrode/electrolyte interface.

c. Spin Gradient

Translational diffusion coefficients of mobile nuclei can be measured by the Stejskal-Tanner pulsed field gradient (PFG) NMR spin-echo technique.[225] This method, which has proven successful with solid electrolytes, involves applying field gradient pulses between two radio frequency (rf) pulses. In the absence of gradient pulses the first rf pulse rotates the magnetization through 90°. The second rf pulse rotates and rephases the magnetizations causing a spin-echo amplitude. If there is no diffusion the second gradient pulse negates the effect of the first gradient pulse and the echo amplitude remains unchanged. If, however, the nuclei are mobile and diffusion occurs within the time interval between gradient pulses, then incomplete phasing is observed in the form of a reduced echo amplitude. From the ratio of the two spin echos it is possible to calculate diffusion coefficient. The transference number is computed from diffusion coefficients for cation and anion by the relation:

$$t_+ = \frac{D_+}{D_+ + D_-} \tag{39}$$

Unlike the electrical methods this experiment is sensitive to the diffusion of both charged and uncharged species.

Table 5 presents transference numbers determined for a variety of polymer electrolytes by the techniques we have discussed. A survey of this table reveals that the majority of the cation transference numbers are below 0.5. Furthermore, the most recent data obtained with Tubandt and NMR PFG methods, which are better than many of the earlier techniques, give t_+ values in the range 0.2 to 0.4. These values are in line with transference numbers in

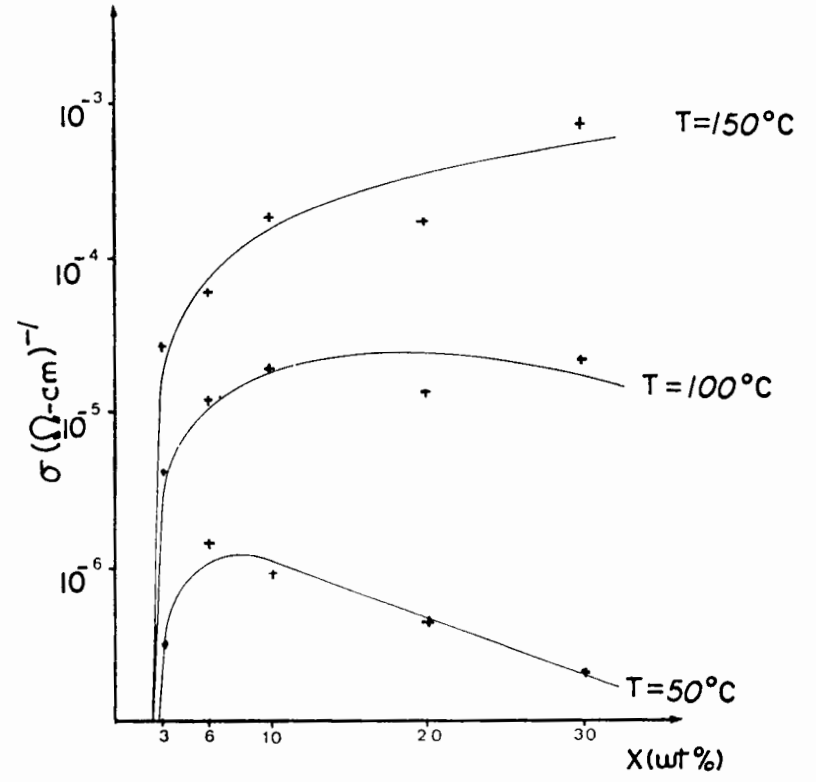

FIGURE 20. A plot at different temperatures of the log conductivity vs. concentration (wt %) of $NaBPh_4$ in cross-linked PPO.

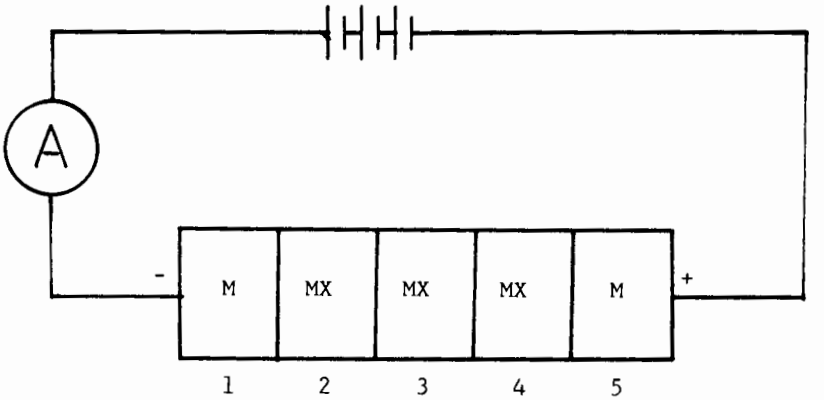

The transport number of M may be inferred as

$$t_{M^+} = \frac{(\text{equivalents of M gained by pellet 5})}{(\text{total equivalents of current passed})}$$

FIGURE 21. A schematic representation of a Tubandt cell experiment.

Table 5
TRANSFERENCE NUMBERS FOR POLYMER-SALT COMPLEXES

Polymer salt complex	Method of measurement	t^+	T[a]	Ref.
$PESc_nLiClO_4$[b]	Tubandt	1	(90)	88
$Poly(\beta\text{-propiolactone})_nLiClO_4$	Tubandt	1	(90)	92
Cross-linked $PEO_{20}AgClO_4$	Tubandt	0.23	(80)	206
Cross-linked $PEO_{36}KClO_4$	Tubandt	0.20	(90)	206
Cross-linked $PEO_{36}NaClO_4$	Tubandt	0.17	(92)	206
Cross-linked $PEO_{59}LiClO_4$	Tubandt	0.37	(95)	206
Cross-linked $PEO_{20}LiClO_4$	Tubandt	0.23	(90)	206
Cross-linked triblock-copolymer $PEO/PPO_{10}LiClO_4$	Tubandt	<0.02	(86)	206
$PEO_{39}DSNa$[c]	Tubandt	>0.97	(108)	206
PEO_8LiClO_4	Ac impedance	0.27	(112)	207
$PEO_{16}MgCl_2$	Ac impedance	>0.005	(100)	208
$PEO_{20}PbBr_2$	Ac impedance	0.6—0.7	(140)	72
$PEO_{4.5}LiSCN$	Ac impedance	0.55	(110)	209
Siloxane-PEO-copolymer$_nLiClO_4$	Ac impedance	0.55	(18)	76
$PEO_{16}LiSO_3CF_3$	Ac impedance	0.47	(85)	210
$PEO_{16}LiSO_3CF_3$	Chronoamperometry	0.35	(85)	210
PEO_4NaSCN	Potentiostatic polarization	0.6	(90)	211
$PESc_{12.5}LiSCN$	Polarization	0.92—0.99	(90)	212
PEG_4NaPSS[d]	Polarization	1	(29)	211
$PEO_4LiSO_3CF_3$	Polarization	0.6	(100)	211
$PEO_4LiSO_3CF_3$	Galvanostatic polarization	0.6	(100)	213
PEO_8LiI	Concentration cell	0.34	(90)	214
$PEO_8LiSO_3CF_3$	Concentration cell	0.70	(90)	214
PEO_8LiClO_4	Concentration cell	0.25	(90)	214
PEO_8NaSCN	Radiotracer	0.5[e]	(30)	215
PEO_6LiClO_4	PFG NMR	0.23	(80—100)	216
PEO_8LiClO_4	PFG NMR	0.18	(80—122)	216
$PEO_{20}LiClO_4$	PFG NMR	0.17	(50)	216
		0.28	(122)	216
$PEO_8LiSO_3CF_3$	PFG NMR	0.34	(155)	217
		0.41	(175)	217

[a] measurement temperature °C.
[b] n = 8—50.
[c] $CH_3(CH_2)OSO_3Na$.
[d] Poly(styrenesulfonate).
[e] Calculated from values given in reference.

both aqueous and polar organic electrolytes.[226] The general interpretation attached to the lower values of t_+ than t_- in water and polar organic solvents is that heavy solvation lowers the mobility of the cation. The quality of the transport number measurements is highly variable so it is unwise to interpret broad trends from the data in Table 5.

2. *Ion Association*

Ion association appears to be assured in polymer electrolytes because of the low dielectric constants of the host polymers and range of salt concentrations generally studied. In line with these ideas, we have cited evidence for ion pairing from X-ray fiber data and vibrational spectroscopy (Section III.D.2). Similarly, recent work on cross-linked dimethylsiloxane-ethylene oxide copolymer indicates the presence of two types of ^{23}Na ions, bound and mobile.[122,227] The number of mobile ions increased at the expense of the bound ions in this

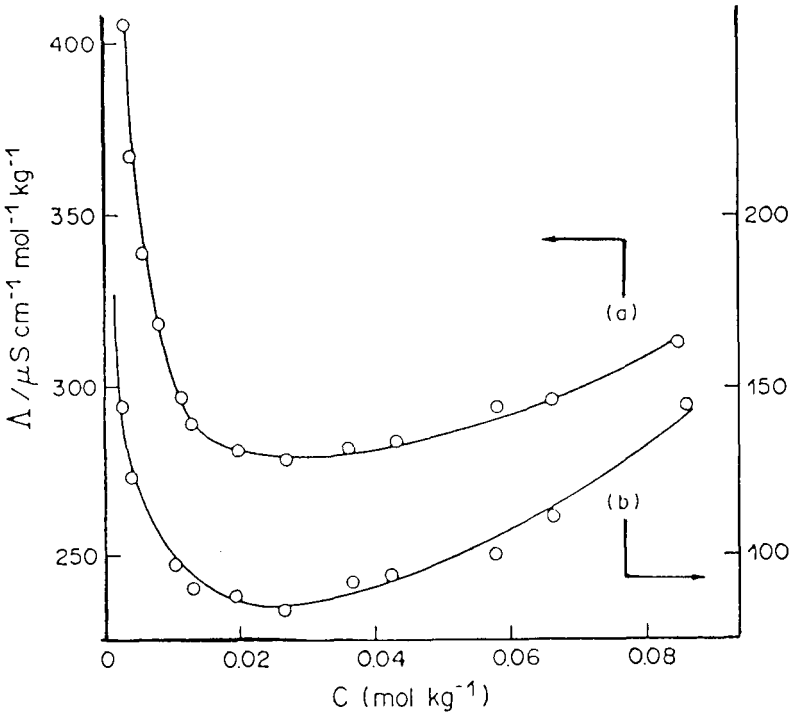

FIGURE 22. Molal conductance as a function of concentration for (a) $LiClO_4$ and (b) $LiSO_3CF_3$ in PEO molecular weight 400 at 25°C.

amorphous copolymer between −120 and 100°C. Since these systems are totally amorphous the bound ions must originate from either some strong anion-cation or polymer-cation interaction. The authors were not able to discriminate between these two possible interactions.

An excellent perspective on ion-ion interaction was provided by recent conductance studies on liquid low molecular weight PEO_nLiX (X = ClO_4^- and $SO_3CF_3^-$).[228] As shown in Figure 22, the equivalent conductance is high at low salt concentrations. At slightly higher concentrations the equivalent conductance falls steeply and monotonically which is attributed to a decrease in the degree of dissociation (ion pair formation). In this and previous studies of ions in low dielectric solvents,[229] the minimum in the conductance is attributed to the formation of ion pairs. After going through a minimum the equivalent conductance increases again and goes through a broad maximum in the range of eight other oxygens per LiX. Similar concentration-dependent conductance and viscosity measurements have been carried out on tetra(ethyleneglycol)dimethyl ether with $LiClO_4$ and $LiBF_4$.[230]

A clear understanding of the mobile species and nature of the conductance maximum has yet to be developed. We have already pointed out (Section III.C.2) that around this maximum T_g is increasing rapidly, so the increased viscosity (i.e., decreased segmental motion) appears to lead to the turn down in conductivity. The exact role of ion-ion interactions in this concentration range is less clear. Currently, it is thought that the theoretical treatments devised for molten salts will prove useful in describing these coulombic interactions.

IV. APPLICATIONS

Much of the research in the area of polymer electrolytes has been motivated by their potential applications in batteries and other electrochemical devices. Two important parameters for the utilization of an electrolyte are its conductivity and its electrochemical stability.

Table 6
POTENTIAL DOMAIN OF VARIOUS POLYMER-SALT COMPLEXES

Complexes[d]	Working electrode	T (°C)	E (V)	Ref.
PEO_9NaTf[a]	Pt	80	5.8	231
PEO_9LiTf[a]	Pt	100	4.8	232
PEO_8LiTf[a]	Pt	138	5.0	233
$MEEP_4LiTf$[b]	Pt	RT	4.6	234
$MEEP_4LiTf$	Pt	60	4.8	234
$MEEP_4LiTf$	GC[c]	60	5.2	234
$BPEI_{20}NaTf$	Pt	60	5.2	234
PPO_9LiTf	Pt	60	4.8	234
PPO_9LiTf	GC	60	5.2	234
X-linked siloxane 7.5% LiTf	Pt	60	4.1	234
X-linked siloxane 7.5% LiTf	GC	60	4.5	234

[a] No IR compensation.
[b] Thin-layer cell.
[c] Glassy carbon.
[d] Tf = $SO_3CF_3^-$

We have already discussed the conductivity at some length. In the following section we take up electrochemical stability and then discuss some of the applications.

A. Electrochemical Stability

A significant part of the potential range for a typical organic electrolyte represents a region of thermodynamic instability but very slow electrochemical decomposition rates. Thus, the practical stability range is determined by the time scale of the measurement and the catalytic influence of various electrode surfaces.

One approach to the study of electrochemical stability is cyclic voltammetry.[221] The time scale for this experiment as it is practiced in most experiments on polymer electrolytes is on the order of minutes. Thus, it does not detect extremely slow processes that may be important for the shelf-life of a product. Some results obtained by this method are collected in Table 6, from which it can be seen that the potential range of stability for various polyether electrolytes is quite broad.

Complex impedance spectroscopy provides another electrical method for studying the stability of a polymer electrolyte against specific electrode materials. The complex impedance experiment can, for example, be performed with alkali metal electrodes. Changes in the charge transfer resistance with time will then indicate the buildup of a resistive layer at the electrode-electrolyte interface. If these measurements are to be meaningful, careful attention must be paid to the elimination of reactive impurities such as air, moisture, casting solvent, polymer stabilizers, and residual polymerization catalysts. Measurements of this type were carried out with PEO salt complexes in contact with lithium electrodes.[235] A resistive layer builds up at the electrode/electrolyte interface which is similar to that observed in cells employing polar organic electrolyte solutions.[236] The growth of this film was only observed above 100°C. Another indication of the stability of the electrolyte can be obtained from the cycling behavior of secondary cells.[237,238]

B. Batteries

The traditional role of polymers in batteries has been as container materials or electrode separators. More recently carbon-filled polymers have been used as structural materials in composite electrodes. In the 1970s and 1980s conducting polymers have been investigated

as electrolytes and active electrode materials. The most promising systems at the present time are thin-film cells employing inorganic electrode materials and polymer electrolytes.

In a battery consisting of two chemical reactants (electrodes) separated by an electrolyte, the electrolyte should conduct ions but have infinite resistance with respect to electronic conductivity. The potential developed by the battery, V, is dependent upon the Gibbs energy for the electrode reactions, ΔG

$$V = -\Delta G/(nF) \tag{40}$$

where n is the number of elementary charges carried by the ions and F is Faraday's constant. Therefore, electrode reactions with the most negative ΔG provide the greatest potential, and the focus in high energy density battery development is to employ light electrodes that have a highly negative ΔG of reaction.

Some current favorites are the lithium negative electrode and positive electrodes consisting of TiS_2 or V_6O_1[3] that exhibit highly negative ΔG for the formation of lithium insertion compounds, such as Li_xTiS_2. Initial potentials on the order of 3 V can be achieved with such cells and sustained potentials on the order of 2.3 V are possible. Although the high reactivity of the electrode materials gives rise to favorable energy densities, it puts large demands on the chemical stability of the electrolyte. The initial thrust of the British, Canadian, and French groups was to develop power sources for electric vehicles.[237,238] This remains an active goal, but attention has broadened to include smaller specialty batteries as well. Some features that are cited as advantages and problems with these advanced batteries are given below.

1. The apparent large stabilty window of polyether-salt complexes with respect to lithium and cathode materials permits the use of highly energetic electrodes. The long-term battery applications will require considerable testing to discern the influence on electrolyte stability of impurities and catalytic reactions at electrodes.
2. The high flexibility of the polymer electrolyte materials appears to permit them to accomodate large changes in volume which occur on charging and discharging, while still maintaining intimate electrode/electrolyte contact. The operational volume changes of the electrodes are significant (Li 100%, LiAl 50%, TiS_2 11%, and V_6O_{13} 10%) and this typically leads to interfacial fracture when rigid ceramic electrolytes are used. Balanced against the advantage of flexibility is the requirement that the polymer have sufficient integrity to separate the positive and negative electrodes.
3. The high resistance of the electrolyte remains a problem, but this has been mitigated by the fabrication of thin film batteries (Figure 23). In this way it should be possible to reduce the internal resistance of the battery by employing a high surface-to-thickness ratio.[237,239] The thin-film design might also free the engineer from the conventional battery shapes and it could give rise to power sources which form an integral part of the device structure. An example is the thin-film batteries studied by Owen, and their proposed use in integrated circuits and smart credit cards.[240]
4. The absence of liquids or fragile ceramic/electrode interfaces reduces leakage problems and sensitivity to mechanical shock, which is a desirable property for many types of portable power sources.
5. The shelf life of the polymer electrolyte batteries appears to be favorable as a result of the low reactivity of the electrolyte with the electrodes and low electronic conductivity of the electrolytes.
6. The growth of lithium dendrites has led to serious problems in secondary cells employing lithium-negative electrodes in conjunction with liquid nonaqueous electrolytes. It appears dendrites are less serious for the polymer electrolyte cells and, unlike ceramic

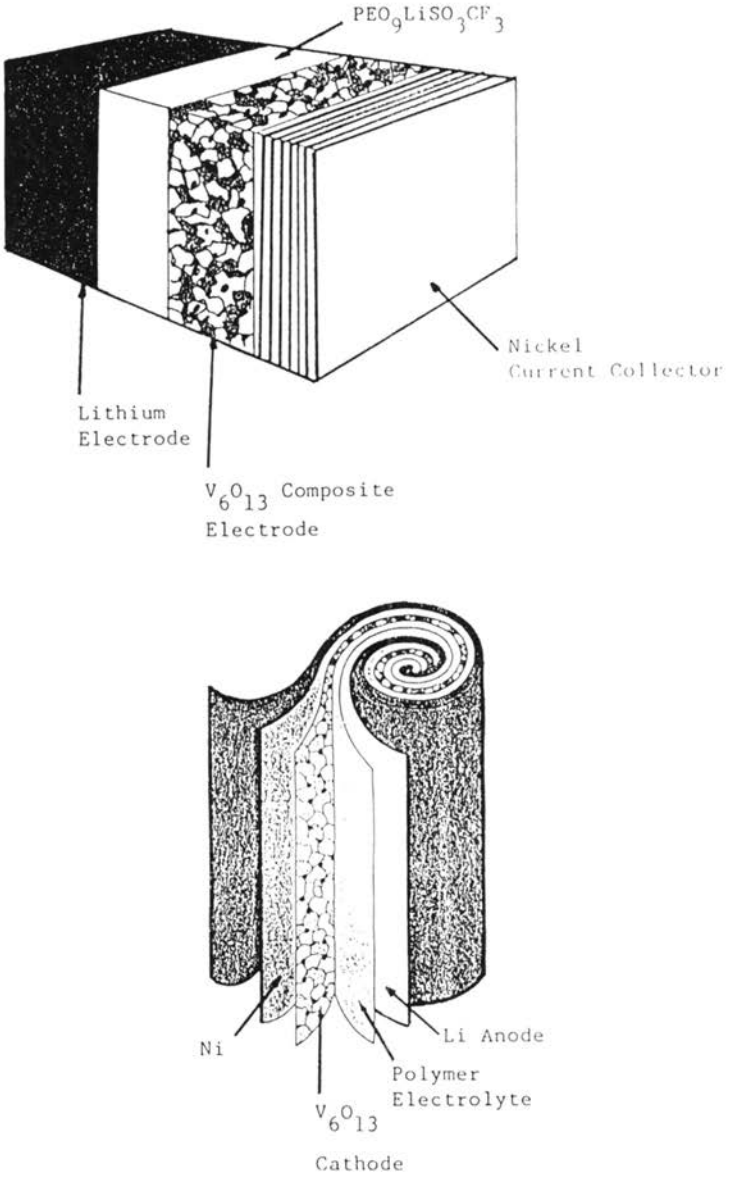

FIGURE 23. Examples of thin-film solid-state cell configurations for batteries based on polymer electrolytes. Typical thicknesses are Li foil 5 to 75 μm, polymer electrolyte 25 to 50 μm, and composite electrode 57 to 75 μm.

electrolytes, the polymer exhibits a self-healing phenomenon when a dendrite does form.

7. The low conductivity of the polymer electrolytes can be partially offset by the thin-film design mentioned previously, but thin current collectors and efficient packaging will also be required to maintain a favorable energy-to-weight ratio. Some of the most detailed testing with PEO-based electrolytes reported to date were carried out at 80 to 100°C and gave 0.5 to 1.0 mA/cm^2 and energy density of 87 Wh/kg for a Li/TiS_2 cell with 50 to 160-μm-thick electrolyte.[238] The performance at lower temperatures was not very favorable. The amorphous polyether electrolytes should improve the low temperature operation of these electrolytes. The potential applications for polymer

electrolyte batteries would be greatly broadened if conductivities around 10^{-3} Scm^{-1} can be achieved.

8. The large anion component to the ionic conductivity is also a problem in that it results in the polarization of the cell. In a battery made up of a metal negative electrode and an intercalation compound as the positive, the mobility of anions in the electrolyte results in a concentration polarization. Assuming an ideal solution, this polarization results in a limiting current i_{lim}

$$i_{lim} = \frac{4RT}{F} \cdot \frac{\sigma_+}{l} \tag{41}$$

where σ_+ is the cationic conductivity. Beyond this current salt depletion occurs at the cathodic interface. In a cell with current i the onset of depletion occurs at a time t where

$$t = \frac{clF}{8RT} [i/i_{lim}] \; 1/4\Pi RT\sigma_- \tag{42}$$

where c = concentration and σ_- = anion conductivity. Thus, a lower σ_- results in a larger t and more efficient energy systems.

Reports have appeared on two different lithium/PEO rechargeable batteries:

$$Li/P(EO \cdot LiX)/TiS_2 \qquad \text{Cell 1}$$

$$Li/P(EO \cdot LiX)/V_6O_{13} \qquad \text{Cell 2}$$

where X^- is usually ClO_4^- or $SO_3CF_3^-$.

Cells of type I or II are generally tested in the 80 to 140°C range to overcome crystallinity problems. Open circuit voltages are typically over 3 V with 70 to 99% energy efficiencies on discharging at 0.1 to 1.5 mA/cm^2.[238,241] Losses in capacity are seen on repeated cycling, but these are usually associated with the cathode materials rather than the polymer electrolyte. In a comparative study[242] using a LiAl anode polymer electrolyte cells were shown to have comparable if not superior coulombic efficiencies compared to organic liquid electrolytes. Gauthier and co-workers[239] have demonstrated that these small batteries can be scaled up with a variety of cathode materials, namely, MnO_2, TiS_2, FeS_2, and FeS, without significant loss of performance. The encouraging results obtained to date for a number of similar systems have appeared in the patent literature,[243-248] including rechargeable batteries employing a sodium anode.[249,250]

The use of PEO complexes as battery electrolytes has been extended to include alkaline earth metals (Mg and Ca) as well as Zn and Al anodes.[251] While the intrinsic energy denisty is lower than lithium batteries, the large divalent salts tend to form amorphous complexes with PEO and show good operational characteristics. With a Mg anode and a range of cathode materials at ambient temperatures (TiS_2, V_6O_{13}, MnO_2, NiO_2, CoO_2, MoO_2, MoO_3, V_2O_5, and WO_3) initial open-circuit voltages of 1.4 to 2.0 V were obtained. Similar voltages were obtained when Ca, Zn, and Al anodes were employed.[251]

Slightly more exotic systems which combine the two emerging technologies of electronic and ionically conducting polymers are cells based on polyacetylene and PEO.[252] This type of cell

$$(CH)_x/P(EO \cdot LiX)/(CH)_x \qquad \text{Cell 3}$$

is an example of a true polymer battery.[253,254]

In efforts to extend the range of batteries containing polymer electrolytes, new cathode materials other than those mentioned have been tried — $Li_xNa_yTiS_2$,[255] MoS_3,[248] and PbI_2/Pb[256] — but the best results to date have been reported for TiS_2 and V_6O_{13}.

A newer class of batteries is also being investigated which is not hampered by the low temperature crystallinity problems of PEO, and is better suited to ambient temperature operation. These batteries incorporate polymer electrolytes based on cross-linked dimethylsiloxane-polyethylene oxide copolymer,[257-259] a triblock copolymer of PEO, PPO, and polyurethane,[260] PEO plasticized with PEG, and polyphosphazenes.[233,261]

C. Other Electrochemical Devices

1. Photoelectrochemical Cells

A common problem with photoelectrochemical cells employing liquid electrolytes is the photocorrosion of the semiconductor interface. Skotheim has replaced convention liquid electrolytes with a polymer electrolyte in a number of photogalvanic cells.[262-264] Initial results show a high overpotential for charge transfer between the semiconductor and the polymer electrolyte.[265] To surmount this problem Skotheim initially covered the semiconductor with a platinum layer upon which he grew, electrochemically, an electronically conducting polypyrrole film. The platinum and polypyrrole together serve as an electron transfer catalyst.

The efficiency of the photogalvanic conversion, even using electrocatalyst, was only 2 to 4%. The high internal resistance of the cell is the main factor in limiting these efficiencies. The resistive loss is due to the semicrystalline PEO complex used as electrolyte; therefore, improved performance would be expected with amorphous highly conducting electrolytes such as the polyphosphazenes or siloxanes.

In conjunction with his photoelectrochemical studies, Skotheim[266] used solid polymer electrolytes containing pyrrole to grow polypyrrole *in situ*. It was also possible to study the reduction and oxidation of the polypyrrole under ultrahigh vacuum using photoelectron spectroscopy techniques.[266]

2. Sensors

The sensor applications of SFPE materials has been quite limited to date. The moisture sensitivity of ionic conductivity in polymer electrolytes makes them candidates for humidity sensors. One such device comprising $P(EO_nLiClO_4)$ was constructed with a capping porous hydrophobic polymer[poly(ethylene)].[267,268] The small pore size of the polyethylene provides permeability to water vapor while protecting the electrolyte. This sensor shows high sensitivity at low humidity.

A hydrogen sensor developed at Allied[57] consists of proton conductor poly(vinyl alcohol), H_3PO_4, and water. A film of the polymer is metallized on two sides; across one side a reference gas sample of known hydrogen concentration is passed, while the test gas of unknown hydrogen concentration is passed across the other. By calibrating the voltage to a known concentrations of hydrogen, accurate values of the hydrogen concentration can be obtained. A similar device could be envisaged using the solvent-free protonic conductor $P(EO_n{\cdot}H_3PO_4)$.[269,270]

3. Electrochemical Transistor Action

Transistor action was demonstrated by Chao and Wrighton[271] for an all-solid-state electrochemical device composed of molecular materials. The device involves poly(3-methylthiophene) on Pt microelectrodes. This electroactive polymer is coated with $P(EO_{16}LiSO_3CF_3)$. The device can be cycled by doping the poly(3-methylthiophene) between a conducting state (oxidized, "on") and an undoped insulating state (reduced, "off") by cycling the applied potential. The oxidation of the neutral poly(3-methylthiophene) occurs with the insertion of a triflate anion from the electrolyte; the redox scheme is shown in Figure 24. The device is

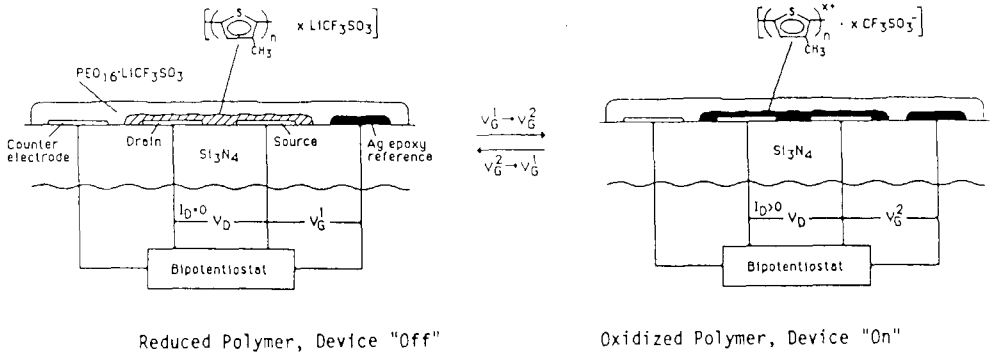

FIGURE 24. Solid-state microelectrochemical transistor using poly(3-methylthiophene) and $P(EO_{16}LiSO_3CF_3)$.

turned on at a potential of +0.4 V vs. Ag. On exceeding +0.6 V there is a change in electrolyte structure due to depletion of anions with a sevenfold increase in the electrolyte resistance. The switching times are slow at approximately 5 s, compared to 5 μs for a comparable solution of electrolytes. The slow switching appears to originate from slow diffusion in the electronic polymer and not from the electrolyte conductivity.

4. Electrochromic Display

Electrochromic display (ECD) devices traditionally comprise a liquid electrolyte and a electrochromic material such as WO_3 or IrO_x. The color of these materials can be switched by reduction and reoxidation. As with the photogalvanic cells, there are corrosion problems as well as fabrication and storage problems with liquid electrolytes. These may be overcome by construction of an all-solid-state device. One such display was constructed using polyelectrolytes, such as poly(styrenesulfonic acid) and poly(ethylene sulfonic acid) with WO_3 as the electrochromic material, or Nafion with Turnbull's blue.[272,273] Inganas has demonstrated the possibility of electrochromic devices constructed of a polypyrrole/P(EO·salt) blend.[274]

5. Solid-State Electrochemistry

In addition to the foregoing developmental work on applications for polymer electrolytes, these electrolytes can be employed as a solvent for a wide variety of electrochemical experiments. For example, the study of kinetic electrochemistry in these materials has been described, and electrochemical experiments in high vacuum are feasible.[266]

V. SUMMARY

The investigation of polymer electrolytes over the last decade has provided a wide range of new materials. The best room-temperature electrolytes that are free of low molecular weight solvents are made from amorphous polymers, developed for electrolyte applications, such as cross-linked PEO networks, comb polymers, and poly(oxymethylene-oxethylene). Segmental motion in the polymer host appears to provide a local liquid-like mechanism for ion transport in these materials. A dynamic percolation theory was developed to model the liquid-like frequency-dependent ion transport. Although many applications can be envisioned for polymer electrolytes, battery applications are receiving the primary attention and encouraging results on test cells have been reported.

ACKNOWLEDGMENT

We appreciate the support of the ONR, DOE, and NSF-MRL program for our research on various aspects of polymer electrolytes.

REFERENCES

1. **Hagenmuller, P. and Van Gool, W.,** *Solid Electrolytes,* Academic Press, New York, 1978.
2. **Mahan, G. D. and Roth, W. L., Eds.,** *Superionic Conductors,* Plenum Press, New York, 1976.
3. **Hladik, J.,** *Physics of Electrolytes,* Vol. 1 and 2, Academic Press, New York, 1972.
4. **Subbarao, E. C.,** *Solid Electrolytes and Their Applications,* Plenum Press, New York, 1980.
5. **West, A. R.,** Ionic conductivity and solid electrolytes, in *Solid State Chemistry and Its Applications,* John Wiley & Sons, New York, 1984, 452.
6. **Vashishta, P., Mundy, J. N., and Shenoy, G. K., Eds.,** *Fast Ion Transport in Solids: Electrodes and Electrolytes,* North-Holland, New York, 1979.
7. **Van Gool, W., Ed.,** *Fast Ion-Transport in Solids, Solid State Batteries and Devices,* North-Holland, Amsterdam, 1973.
8. **Bates, J. B. and Farrington, G. C., Eds.,** *Fast Ionic Transport in Solids,* North-Holland, Amsterdam, 1981.
9. **Kleitz, M., Sapoval, B., and Ravaine, D., Eds.,** *Solid State Ionics,* North-Holland, Amsterdam, 1983.
10. **Boyce, J. B., DeJonghe, L. C., and Huggins, R. A.,** *Solid State Ionics,* Vol. 1 and 2, North-Holland, Amsterdam, 1986.
11. **Sequeira, C. A. C. and Hooper, A.,** *Solid State Batteries,* Martinus Nijhoff, Dordrect, 1985.
12. **Poulsen, F. W., Andersen, N. H., Clausen, K., Skaarup, S., and Sorensen, O. T.,** *Transport-Structure Relations in Fast Ion and Mixed Conductors,* Proc. RISO 6th Int. Symp. Metal Material Science, 1985.
13. **Linford, R. G. and Hackwood, S.,** Physical techniques for the study of solid electrolytes, *Chem. Rev.,* 81, 327, 1981.
14. **Farrington, G. C. and Briant, J. L.,** Fast ionic transport in solids, *Science,* 204, 1371, 1979.
15. **Shriver, D. F. and Farrington, G. C.,** Solid ionic conductors, *Chem. Eng. News,* p.43, May 20, 1985.
16. **Ingram, M. D. and Vincent, C. A.,** Solid state ionics, *Chem. Br.,* March, 235, 1984.
17. **McGeehin, P. and Hooper, A.,** Review: fast ion conduction materials, *J. Mater. Sci.,* 12, 1, 1977.
18. **Rickert, H.,** Solid ionic conductors: principles and applications, *Angew. Chem. Int. Ed. Engl.,* 17, 37, 1978.
19. **Steele, B. C. H.,** Mass transport in materials incorporated in electrochemical energy conversion systems, *Solid State Ionics,* 12, 391, 1984.
20. **Glasser, L.,** Proton conduction and injection in solids, *Chem. Rev.,* 75, 21, 1975.
21. **Blonsky, P. M., Clancy, S., Hardy, L. C., Harris, C. S., Spindler, R., Tonge, J. S., and Shriver, D. F.,** Solvent-free polymer electrolytes and mixed ionic conductors, *Chemtech,* 17, 758, 1987.
22. **Armand, M. B.,** Polymer electrolytes, *Annu. Rev. Mater. Sci.,* 16, 245, 1986.
23. **Shirakawa, H., Louis, E. J., MacDiarmid, A. G., Chaing, C. K., and Heeger, A. J.,** Synthesis of electrically conducting organic polymers: halogen derivatives of polyacetylene, $(CH)_x$, *J. Chem. Soc. Chem. Commun.,* p. 578, 1977.
24. **Epstein, A. J. and Conwell, E. M., Eds.,** *Proc. Int. Conf. on Low Dimensional Conductors,* Gordon & Breach Science Publishers, London, 1982.
25. **MacDiarmid, A. G., Chiang, J.-C., Halpern, M., Huang, W.-S., Mu, S.-L., Somasiri, N. L. D., Wu, W., and Yaniger, S. I.,** "Polyaniline": interconversion of metallic and insulating forms, *Mol. Cryst. Liquid Cryst.,* 121, 173, 1985.
26. **Kossmehl, G. and Chatzitheodorou, G.,** Electrical conductivity of poly(2,5-thiophenediyl)AsF_5-complex, *Makromol. Chem. Rapid Commun.* 2, 551, 1981.
27. **Diaz, A. F. and Kanazawa, K. K.,** Electrochemical polymerization of pyrrole, *J. Chem. Soc. Chem. Commun.,* p. 635, 1979.
28. **Ivory, D. M., Miller, G. G., Sowa, J. M., Schacklette, L. W., Chance, R. R., and Baughman, R. H.,** Highly conducting charge-transfer complexes of poly(paraphenylene), *J. Chem. Phys.,* 71, 1506, 1979.
29. **Hardy, L. C. and Shriver, D. F.,** PEO-sodium polyiodide conductors: characterization, electrical conductivity, and photoresponse, *J. Am. Chem. Soc.,* 108, 2887, 1986.
30. **Jernigan, J. C., Chidsey, C. E. D., and Murray, R. W.,** Electrochemistry of polymer films not immersed in solution: electron transfer on an ion budget, *J. Am. Chem. Soc.,* 107, 2824, 1985.
31. **Lundberg, R. D.,** Ionomers, in *Kirk-Othmer Encyclopedia of Chemical Technolgy,* Suppl. Vol., 3rd ed., Grayson, M. and Eckroth, D., Eds., Wiley-Interscience, New York, 1984, 546.
32. **Eisenberg, A. and King, M.,** *Ion-Containing Polymers,* Academic Press, New York, 1977.
33. **Holliday, L., Ed.,** *Ionic Polymers,* Halsted Press, New York, 1975.
34. **Toyota, S., Nogami, T., and Mikawa, H.,** Lithium ion conductors of polyion complexes dispersed with $LiClO_4$ and their application to solid-state batteries, *Solid State Ionics,* 13, 243, 1984.
35. **Anderson, C. F. and Morawetz, H.,** Polyelectrolytes, in *Kirk-Othmer Encyclopedia of Chemical Technology,* Vol. 18, Grayson, M. and Echroth, D., Eds., Wiley-Interscience, New York, 1982, 495.

36. **Hirata, M., Inoue, S., and Yosomiya, R.,** Humidity dependence of the electric characteristics of quaternized poly(vinylpyridine) perchlorate complexes, *Angew. Makromol. Chem.*, 131, 125, 1985.
37. **Crowley, J. L., Wallace, R. A., and Bube, R. H.,** Ionic transport in a sulfonated polystyrene-polyethylene copolymer, *J. Polym. Sci. Polym. Phys. Ed.*, 14, 1769, 1976.
38. **Eisenberg, A. and Yeager, H. L., Eds.,** *Perfluorinated Ionomer Membrane*, ACS Symp. Ser. No. 180, American Chemical Society, Washington, D.C., 1982.
39. **Yeo, S. C. and Eisenberg, A.,** Physical properties and super molecular structure of perfluorinated ion exchange containing (nafion) polymers, *J. Appl. Polym. Sci.*, 21, 875, 1977.
40. **Duplessix, R., Escoubes, M., Rodmacq, B., Volino, F., Roche, E., Eisenberg, A., and Pineri, M.,** *Water Soluble Polymers*, Rowland, S. P., Ed., ACS Symp. No. 127, American Chemical Society, Washington, D.C., 1980, chap. 29.
41. **Hsu, W. Y., Barkley, J. R., and Meakin, P.,** Ion percolation and insulator-to-conductor transition in Nafion perfluorosulfonic acid membranes, *Macromolecules*, 13, 198, 1980.
42. **Yeager, H. L., Twardowski, Z., and Clarke, L. M.,** A comparison of perfluorinated carboxylate and sulfonate ion exchange polymers. I. Diffusion and water sorption, *J. Electrochem. Soc.*, 129, 324, 1982.
43. **Twardowski, Z., Yeager, H. L., and O'Dell, B.,** A comparison of perfluorinated carboxylate and sulfonate ion exchange polymers. II. Sorption and transport properties in concentrated solution environment, *J. Electrochem. Soc.*, 129, 328, 1982.
44. **Dotson, R. L. and Woodward, K. E.,** Electrosynthesis with perfluorinated ionomer membranes in chlor-alkali cells, in *Perfluorinated Ionomer Membrane*, Eisenberg, A. and Yeager, H. L., Eds., ACS Symp. Ser. No. 180, American Chemical Society, Washington, D.C., 1982, 311.
45. **See Yeo, R. S.,** Applications of perfluorosulfonated polymer membranes in fuel cells, electrolyzers, and load levelling devices in *Perfluorinated Ionomer Membrane*, Eisenberg, A. and Yeager, H. L., Eds., ACS Symp. Ser. No. 180, American Chemical Society, Washington, D.C., 1982, 452.
46. **Weininger, J. L. and Russell, R. R.,** Corrosion of the ruthenium oxide catalyst at the anode of a solid polymer electrolyte cell, *J. Electrochem. Soc.*, 125, 1482, 1978.
47. **Yeo, R. S. and Chin, D.-T.,** A hydrogen-bromine cell for energy storage applications, *J. Electrochem. Soc.*, 127, 549, 1980.
48. **Will, F. G.,** Bromine diffusion through Nafion perfluorinated ion exhange membrane, *J. Electrochem. Soc.*, 126, 36, 1979.
49. **Bixler, H. J. and Michaels, A. S.,** Polyelectrolyte complexes, in *Encyclopedia of Polymer Science and Technology*, Vol. 10, Mark, H. F., Gaylord, N. G., and Bikales, N. M., Eds., Wiley-Interscience, New York, 1969, 765.
50. **Tsuchida, E., Ohno, H., and Tsunemi, K.,** Conduction of lithium ions in polyvinylidene fluoride and its derivatives, *Electrochim. Acta*, 28, 591, 1983.
51. **Tsunemi, K., Ohno, H., and Tsuchida, E.,** A mechanism of ionic conduction of poly(vinylidene-fluoride)-lithium perchlorate hybrid films, *Electrochim. Acta*, 28, 833, 1983.
52. **Watanabe, M., Kanba, M., Matsuda, H., Tsunemi, K., Mizoguchi, K., Tsuchida, E., and Shinohara, I.,** High lithium ionic conductivity of polymeric solid electrolytes, *Makromol. Chem. Rapid Commun.*, 2, 741, 1981.
53. **Watanabe, M., Kanba, M., Nagaoka, K., and Shinohara, I.,** Ionic conductivity of hybrid films based on polyacrylonitrile and their battery application, *J. Appl. Polym. Sci.*, 27, 4191, 1982.
54. **Watanabe, M., Kanaba, M., Nagaoka, K., and Shinohara, I.,** Ionic conductivity of hybrid films composed of polyacrylonitrile, ethylene carbonate, and $LiClO_4$, *J. Polym. Sci. Polym. Phys. Ed.*, 21, 939, 1983.
55. **Armand, M. B.,** Polymer electrolytes: conductivity and stability domain, *Lithium Non-Aqueous Battery Electrochemistry*, Yeager, E. G., Schumm, B., Blomberg, G., Blankenship, D. R., Leger, V., and Akridge, J., Eds., Electrochemical Society, Pennington, NJ, 1980, 261.
56. **Dodin, M. G.,** Non-equilibrium electrolyte permeability in poly(vinyl alcohol) membranes, *Polymer*, 22, 788, 1981.
57. **Polak, A. J., Petty-Weeks, S., and Beuhler, A. J.,** Applications of novel proton-conducting polymers to hydrogen sensing, *Sensors and Actuators*, 9, 1, 1986.
58. **Blumberg, A. A., Pollack, S. S., and Hoeve, C. A. J.,** A poly(ethylene oxide)-mercuric chloride complex, *J. Polym. Sci. Part A*, 2, 2499, 1964.
59. **Lunberg, R. D., Bailey, F. E., and Callard, R. W.,** Interaction of inorganic salts with poly(ethylene oxide), *J. Polym. Sci. Part A*, 1(4), 1563, 1966.
60. **Moacanin, J. and Cuddihy, E. F.,** Effect of polar forces on the viscoelastic properties of poly(propylene oxide), *J. Polym. Sci.*, C14, 313, 1966.
61. **Fenton, D. E., Parker, J. M., and Wright, P. V.,** Complexes of alkali metal ions with PEO, *Polymer*, 14, 589, 1973.
62. **Wright, P. V.,** Electrical conductivity in ionic complexes of poly(ethylene oxide), *Br. Polym. J.*, 7, 319, 1975.

63. **Weston, J. E. and Steele, B. C. H.,** Effects of preparation on properties of lithium salt-poly(ethylene oxide) polymer electrolytes, *Solid State Ionics,* 7, 81, 1982.
64. **Shriver, D. F., Papke, B. L., Ratner, M. A., Dupon, R., Wong, T., and Brodwin, M.,** Structure and ion transport in polymer-salt complexes, in *Fast Ionic Transport in Solids,* Bates, J. B. and Farrington, G. C., Eds., North-Holland, Amsterdam, 1981, 83.
65. **Rietman, E. A., Kaplan, M. L., and Cava, R. J.,** Lithium ion-poly(ethylene oxide) complexes. I. Effect of anion on conductivity, *Solid State Ionics,* 17, 67, 1985.
66. **Fontanella, J. J., Wintersgill, M. C., Calame, J. P., and Andeen, C. G.,** Electrical and differential scanning calorimetry studies of poly(ethylene oxide) complexed with alkaline-earth thiocyanates, *J. Polym. Sci. Phys. Ed.,* 23, 113, 1985.
67. **Stevens, J. R. and Mellander, B.-E.,** Poly(ethylene oxide)-alkali metal-silver halide salt systems with high ionic conductivity at room temperature, in *Transport-Structure Relations in Fast Ion and Mixed Conductors,* Proc. RISO 6th Int. Symp. Metal Material Science, 1985, 359.
68. **Stainer, M., Hardy, L. C., Whitmore, D. H., and Shriver, D. F.,** Stoichiometry of formation and conductivity response of amorphous and crystalline complexes formed between poly(ethylene oxide) and ammonium salts: $PEO_x{\cdot}NH_4SCN$ and $PEO_x{\cdot}NH_4SO_3CF_3$, *J. Electrochem. Soc.,* 131, 784, 1984.
69. **Armand, M. B., Kadiri, F. E., and Moursli, C. E.,** Bis Perhalogen Oacyl-Orsul Fonyl-Imides of Alkali Metals, Their Solid Solutions With Plastic Materials and Their Use to the Constitution of Conductor Elements for Electrochemical Generators, U.S. Patent 4,505,997, March 1985.
70. **Armand, M. B., Kadiri, F. E., and Moursli, C. E.,** Tetra-Alkynyl Or-Aluminates of Alkali Metals, Their Solid Solutions with Plastic Materials and Their Use for the Constitution of Conductor Elements for Electrochemical Generators, U.S. Patent 4,542,081, September 1985.
71. **Wasson, J. R., Bolster, D. E., and Hatfield, W. E.,** Fast ion conductors: lithium ionomers and salts-polymer-based materials, *Electrochem. Soc. Ext. Abr. 83-1,* Abstr. 491, 749, 1983.
72. **Yang, L.-L., Huq, R., and Farrington, G. C.,** Preparation and properties of PEO complexes of divalent cation salts, in *Solid State Ionics,* Vol. 1 and 2, North-Holland, Amsterdam, 1986, 291.
73. **Blonsky, P. M., Shriver, D. F., Austin, P., and Allcock, H. R.,** Poly-phosphazene solid electrolytes, *J. Am. Chem. Soc.,* 106, 6854, 1984.
74. **Tonge, J. S. and Shriver, D. F.,** Increased dimensional stability in ionically conducting polyphosphazenes systems, *J. Electrochem. Soc.,* 134, 269, 1987.
75. **Fish, D., Khan, I. M., and Smid, J.,** Poly(methoxyheptaethyleneoxide) methylsiloxane/$LiClO_4$ complexes as solvent free polymer electrolytes for high energy density storage devices, *Polym. Prepr.,* 27, 325, 1986.
76. **Hall, P. G., Davies, G. R., McIntyre, J. E., Ward, I. M., Bannister, D. J., and LeBrocq, K. M. F.,** Ion conductivity in polysiloxane comb polymers with ethylene glycol teeth, *Polym. Commun.,* 27, 98, 1986.
77. **Killis, A., LeNest, J. F., Gandini, A., and Cheradame, H.,** Dynamic mechanical properties of crosslinked polyurethanes containing sodium tetraphenylborate, *J. Polym. Sci. Polym. Phys. Ed.,* 19, 1073, 1981.
78. **Papke, B. L.,** Vibrational Spectroscopy Structure, and Ion Transport in Complexes of PEO with Alkali Metal Salts, Ph.D. thesis, Northwestern University, Evanston, IL, 1982.
79. **Gray, F. M., MacCallum, J. R., and Vincent, C. A.,** PEO-$LiSO_3CF_3$-polystyrene electrolyte systems, *Solid State Ionics,* 18/19, 282, 1986.
80. **Ito, Y., Syakushire, K., Hiratani, M., Miyachi, K., and Kuda, T.,** Structure and ionic conductivity in evaporated thin films of PEO complexed with $LISO_3CF_3$, *Solid State Ionics,* 18/19, 277, 1986.
81. **Craven, J. R., Mobbs, R. H., and Booth, C.,** Synthesis of oxymethylene-linked poly(oxyethylene) elastomers, *Makromol. Chem. Rapid Commun.,* 7, 81, 1986.
82. **Chiang, C. K., Davis, G. T., and Harding, C. A.,** Polymeric electrolytes based on poly(ethyleneimine) and lithium salts, *Solid Siate Ionics,* 18/19, 300, 1986.
83. **Clancy, S., Shriver, D. F., and Ochrymowycz, L. A.,** Preparation and characterization of polymeric solid electrolytes from poly(alkylene sulfides) and silver salts, *Macromolecules,* 19, 606, 1986.
84. **Harris, C. S., Ratner, M. A., and Shriver, D. F.,** Ionic conductivity in branched polyethyleneimine $NaSO_3CF_3$ complexes. Comparisons to analogs complexes made with linear poly(ethyleneimine), *Macromolecules,* 20, 1778, 1987.
85. **Chiang, C. K., Davis, G. T., Harding, C. A., and Takahashi, T.,** Poly(ethylene imine)-sodium iodide complexes, *Macrocolecules,* 18, 825, 1985.
86. **Armand, M. B., Chabagno, J. M., and Duclot, M. J.,** Poly-ethers as solid electrolytes, in *Fast Ion Transport in Solids: Electrodes and Electrolytes,* Vashishta, P., Mundy, J. N., and Shenoy, G. K., Eds., North-Holland, New York, 1979, 131.
87. **Dupon, R., Papke, B. L., Ratner, M. A., and Shriver, D. F.,** Ion transport in polymer electrolytes formed between poly(ethylene succinate) and $LiBF_4$, *J. Electrochem. Soc.,* 131, 586, 1984.
88. **Watanabe, M., Rikukawa, M., Sanui, K., Ogata, N., Kato, H., Kobayashi, T., and Ohtaki, Z.,** Ionic conductivity of polymer complexes formed by poly(ethylene succinate) and $LiClO_4$, *Macromolecules,* 17, 2902, 1984.

89. **Watanabe, M., Rikukawa, M., Sanui, K., and Ogata, N.,** Effects of polymer structure and incorporated salt species on ionic conductivity of polymer complexes formed by aliphatic polyester and alkali metal thiocyanate, *Macromolecules,* 19, 188, 1986.
90. **Armand, M. B.,** Polymer solid electrolytes—an overview, *Solid State Ionics,* 9/10, 745, 1983.
91. **Armstrong, R. D. and Clarke, M. D.,** Lithium ion conducting polymeric electrolyte based on poly(ethylene adipate), *Electrochem. Acta,* 29, 1443, 1984.
92. **Watanabe, M., Togo, M., Sanui, K., Ogata, N., Kobayashi, T., and Ohtaki, Z.,** Ionic conductivity of polymer complexes formed by poly(β-propiolactone) and $LiClO_4$, *Macromolecules,* 17, 2908, 1984.
93. **Wintersgill, M. C., Fontanella, J. J., Calame, J. P., Greenbaum, S. G., and Andeen, C. G.,** Electrically conducting poly(vinylacetate), *J. Electrochem. Soc.,* 121, 2208, 1984.
94. **Tonge, J. S., Blonsky, P. M., Shriver, D. F., Allcock, H. R., Austin, P. E., Neenan, T. X., and Sisko, J. T.,** Effect of sidechain length and crosslinking on ionic conductivity in polyphosphazene solid electrolytes, in *Lithium Batteries,* Vol. 87-1, Dey, A. N., Ed., Electrochemical Society, Pennington, NJ, 1987, 533.
95. **Bannister, D. J., Davies, G. R., Ward, I. M., and McIntyre, J. E.,** Ionic conductivities of poly(methoxypolyethylene-glycol monomethacrylate) complexes with $LiSO_3CF_3$, *Polymer,* 25, 1600, 1984.
96. **Xia, D. W., Soltz, D., and Smid, J.,** Conductivities of solid polymer electrolyte complexes of alkali metal salts with polymers of methoxypolyethylene glycol methacrylates, *Solid State Ionics,* 14, 221, 1984.
97. **Xia, D. W. and Smid, J.,** Solid polymer complexes of polymethacrylates carrying pendant oligo-oxyethylene(glyme) chains, *J. Polym. Sci. Polym. Lett. Ed.,* 22, 617, 1984.
98. **Cowie, J. M. G. and Martin, A. C. S.,** Ionic conductivity of poly(diethoxy(3)methylitaconte) containing $LiClO_4$, *Polym. Commun.,* 26, 298, 1985.
99. **Cowie, J. M. G., Ferguson, R., and Martin, A. C. S.,** Glass transition temperatures in poly(di-propyleneglycol)itaconate)-salt mixtures, *Poly. Commun.,* 28, 130, 1987.
100. **Bell, S. E. and Bannister, D. J.,** Polymers with alkoxy side groups from poly(butadiene) by solvomercuration-demercuration, *J. Polym. Sci. Polym. Lett. Ed.,* 24, 165, 1986.
101. **Bannister, D. J., Davies, G. R., Ward, I. M., and McIntyre, J. E.,** Ionic conductivities for PEO complexes with lithium salts of monobasic and dibasic acids and blends of PEO with lithium salts of anionic polymers, *Polymer,* 25, 1291, 1984.
102. **Spindler, R. and Shriver, D. F.,** Physical and spectroscopic properties of ternary polymer electrolytes composed of poly(vinylpyrrolidone), poly(ethylene glycol), and $LiCF_3SO_3$, *Macrocolecules,* 19, 347, 1986.
103. **Hardy, L. C. and Shriver, D. F.,** Chloride ion conductivity in a plasticized quaternary ammonium polymer, *Macromolecules,* 17, 975, 1984.
104. **Hardy, L. C. and Shriver, D. F.,** Preparation and electrical response of solid polymer electrolytes with only one mobile species, *J. Am. Chem. Soc.,* 107, 3823, 1985.
105. **Tsuchida, E., Ohno, H., Tsunemi, K., and Kobayashi, N.,** Lithium ionic conduction in poly(methacrylic acid)-PEO complexes containing $LiClO_4$, *Solid State Ionics,* 11, 227, 1983.
106. **Tsuchida, E. and Shigehara, K.,** Lithium ion conducting polymeric hybrids, *Mol Cryst. Liquid Cryst.,* 106, 361, 1984.
107. **Watanabe, M., Nagaoka, K., Kanba, M., and Shinohara, I.,** Ionic and conductivity of polymeric solid electrolytes based on PPO or poly(tetramethylene oxide), *Polym. J.,* 14, 887, 1982.
108. **Watanabe, M., Oohaski, S., Sanui, K., Ogata, N., Kobayashi, T., and Ohtaki, Z.,** Morphology and ionic conductivity of polymer complexes formed by segmental polyether poly(urethaneurea) and $LiClO_4$, *Macromolecules,* 18, 1945, 1985.
109. **Giles, J. R. M., Booth, C., and Mobbs, R. H.,** Examination of ionic conduction in an oxyalkane copolymer, in *Transport-Structure Relations in Fast Ion and Mixed Conductors,* Proc. RISO 6th Int. Symp. Metal Material Science, 1986.
110. **Kobayashi, N., Uchiyama, M., and Tsuchida, E.,** Poly(lithium methacrylate-co-oligo(oxyethylene)methacrylate) as a solid electrolyte with high ionic conductivity, *Solid State Ionics,* 17, 307, 1985.
111. **Kobayashi, M., Hamada, T., Ohno, H., and Tsuchida, E.,** Poly[oligo (oxyethylene) methacrylate-co-sodium methacrylate] as a polymeric solid electrolyte with sodium ion conduction, *Polym. J.,* 18, 661, 1986.
112. **Nagaoka, K., Naruse, H., Shinohara, I., and Watanabe, M.,** High ionic conductivity in poly(dimethylsiloxane-co-ethylene oxide) dissolving $LiClO_4$, *J. Polym. Sci. Polym. Lett. Ed.,* 22, 659, 1984.
113. **MacCullum, J. R., Smith, M. J., and Vincent, C. A.,** The effect of radiation-induced crosslinking on the conductance of $LiClO_4$-PEO electrolytes, *Solid State Ionics,* 11, 307, 1984.
114. **Watanabe, M., Nagano, S., Sanui, K., and Ogata, N.,** Ionic conductivity of network polymers from PEO containing $LiClO_4$, *Polym. J.,* 18, 809, 1986.
115. **Killis, A., LeNest, J. F., Gandini, A., Cheradame, H., and Cohen-Addad, J. P.,** Correlation among transport properties in ionically conducting cross-linked networks, *Polym. Bull.,* 6, 351, 1982.

116. **Giles, J. R. M. and Greenhall, M. P.,** Ionic conducting in phosphate-ester-crosslinked poly(ethylene glycols) complexed with $LiCF_3SO_3$, *Polym. Commun.*, 27, 360, 1986.
117. **Armand, M. B., Muller, D., and Chabagno, J. M.,** Ion Conducting Macromolecular Material for Making Electrolytes or Electrodes, Eur. Pat. Appl. EP. 163, 576, December 4, 1985.
118. **Giles, J. R. M., Knight, J., Booth, C., Mobbs, R. H., Owens, J. R., Craven, J. R. and Kelly, I. E.,** Polymeric electrolytes, PCT Int. Appl. WP 8601, 643, March 13, 1986.
119. **Armand, M. B. and Muller, D.,** Ion conducting macromolecular material, European Patent Appl. EP 149, 393, 1985.
120. **Watanabe, M., Sanui, K., Ogata, N., Inoue, F., Kobayashi, T., and Ohtaki, Z.,** Ionic conductivity and mobility of PPO networks dissolving alkali metal thiocyanates, *Polym. J.*, 17, 549, 1985.
121. **Bouridah, A., Dalard, F., Deroo, D., Cheradame, H., and LeNest, J. F.,** Poly(dimethylsiloxane)-PEO based polyurethane networks used as electrolytes in Li electrochemical solid state batteries, *Solid State Ionics*, 15, 233, 1985.
122. **Adamic, K. J., Greenbaum, S. G., Wintersgill, M. C., and Fontanella, J. J.,** Ionic conductivity in solid, crosslinked dimethysiloxane-ethylene oxide copolymer networks containing sodium, *J. Appl. Phys.*, 60, 1342, 1986.
123. **Fish, D., Xia, D. W., and Smid, J.,** Solid complexes of $LiClO_4$ with crosslinked polymers of α-meth-acryloyl-ω-methoxypoly(oxy ethylene)s. Conductivities and morphology, *Makromol. Chem. Rapid Commun.*, 6, 761, 1985.
124. **LeMehaute, A., Crepy, G., Marcellin, G., Hamaide, T., and Guyot, A.,** Polymer electrolytes: the route towards solid polymer electrolytes with stable electrochemical performances upon long term storage, *Polym. Bull.*, 14, 233, 1985.
125. **Guyot, A., Hamaide, T., LeMehaute, A., Crepy, G., and Marcellin, G.,** New composite polymeric electrolytes, *Polym. Prepr.*, 26, 112, 1985.
126. **Cheradame, H. and LeNest, J. F.,** Self ionizable networks as solid electrolytes, in *Ist Int. Symp. on Polymer Electrolytes*, Abstr. 16, St. Andrews University, St. Andrews, Scotland, 1987.
127. **Chiang, C. K., Bauer, B. J., Briber, R. M., and Davis, G. T.,** Synthesis of ionic conducting interpenetrating polymer networks, *Polym. Commun.*, 28, 34, 1987.
128. **Papke, B. L., Ratner, M. A., and Shriver, D. F.,** Conformation and ion-transport models for the structure and ionic conductivity in complexes of polyethers with alkali metal salts, *J. Electrochem. Soc.*, 129, 1694, 1982.
129. **Watanabe, M., Itoh, M., Sanui, K., and Ogata, N.,** Carrier transport and generation processes in polymer electrolytes based on poly(ethylene oxide) networks, *Macromolecules*, 20, 569, 1987.
130. **Minier, M., Berthier, C., and Gorecki, W.,** Differential scanning calorimetry of sodium iodide poly(ethylene oxide) complexes, *Solid State Ionics*, 9/10, 1125, 1983.
131. **Sorensen, P. R. and Jacobsen, T.,** Phase diagram and conductivity of the polymer electrolyte: PEO_r-$LiCF_3SO_3$, *Polym. Bull.*, 9, 47, 1983.
132. **Fateux, D., Lupien, M. D., and Robitaille, C.D.,** Phase diagram conductivity and transference number of PEO-NaI electrolytes, *J. Electrochem. Soc.*, 134, 2761, 1987.
133. **Ferloni, P., Chiodelli, G., Magistris, A., and Sanesi, M.,** Ion transport and thermal properties of poly(ethylene oxide)-$LiClO_4$ polymer electrolyte, *Solid State Ionics*, 18/19, 265, 1986.
134. **Robitaille, C. D. and Fauteux, D.,** Phase diagrams and conductivity characterization of some PEO-LiX electrolytes, *J. Electrochem. Soc.*, 133, 315, 1986.
135. **Hibma, T.,** Structural aspects of poly(ethylene oxide) salt complexes, *Solid State Ionics*, 9/10, 1101, 1983.
136. **Lee, Y. L. and Crist, B.,** Phase behavior and conductivity in PEO-NaSCN systems, *J. Appl. Phys.*, 60, 2683, 1986.
137. **Berthier, C., Gorecki, W., Minier, M., Armand, M. B., Chabagno, J. M., and Rigaud, P.,** Microscopic investigation of ionic conductivity in alkali metal salts-PEO adducts, *Solid State Ionics*, 11, 91, 1983.
138. **Minier, M., Berthier, C., and Gorecki, W.,** Thermal analysis and NMR study of a PEO complex electrolyte: $PEO(LiSO_3CF_3)_x$, *J. Phys.* 45, 739, 1984.
139. **Payne, D. R. and Wright, P. V.,** Morphology and ionic conductivity of some lithium ion complexes with PEO, *Polymer*, 23, 690, 1982.
140. **Catlow, C. R. A., Chadwick, A. V., Greaves, G. N., Moroney, L. M., and Worboys, M. R.,** An EXAFS study of the structure of rubidium PEO salt complexes, *Solid State Ionics*, 9/10, 1107, 1983.
141. **Yokoyama, M., Ishihara, H., Iwamoto, R., and Tadokoro, H.,** Structure of poly(ethylene oxide) complexes, *Macromolecules*, 2, 184, 1969.
142. **Lee, C. C. and Wright, P. V.,** Morphology and ionic conductivity of complexes of sodium iodide and sodium thiocyanate with poly(ethylene oxide), *Polymer*, 23, 681, 1982.
143. **Siddiqui, J. A. and Wright, P. V.,** Mesogenic structures in poly(ethylene oxide)-alkali-ion complexes having organic anions, *Polym. Commun.*, 28, 5, 1987.
144. **Okamura, S. and Chatani, Y.,** Crystal structure of PEO sodium iodide complex, *Polymer*, 28, 1815, 1987.

145. **Papke, B. L., Ratner, M. A., and Shriver, D. F.,** Vibrational spectroscopy and structure of polymer electrolytes, PEO complexes of alkali metal salts, *J. Phys. Chem. Solids,* 42, 493, 1981.
146. **Papke, B. L., Ratner, M. A., and Shriver, D. F.,** Vibrational spectroscopic determination of structure and ion pairing in complexes of PEO with lithium salts, *J. Electrochem. Soc.,* 129, 1434, 1982.
147. **Dupon, R., Papke, B. L., Ratner, M. A., Whitmore, D. H., and Shriver, D. F.,** Influence of ion pairing on cation transport in the polymer electrolyte formed by PEO with $NaBF_4$ and $NaBH_4$, *J. Am. Chem. Soc.,* 104, 6247, 1982.
148. **Popov, A. I.,** Alkali metal NMR and vibrational spectroscopic studies on solvates in non-aqueous solvents, *Pure Appl. Chem.,* 41, 275, 1975.
149. **Edgell, W. F.,** *Ions and Ion-Pairs in Organic Reactions,* Vol. 1, Szwarc, M., Ed., Wiley-Interscience, New York, 1972, chap. 4.
150. **Tsatsas, A. T., Stearns, R. W., and Risen, W. M., Jr.,** The nature of alkali metal ion interactions with cyclic polyfunctional molecules. I. Vibrations of alkali ions encaged by crown ethers in solution, *J. Am. Chem. Soc.,* 94, 5247, 1972.
151. **Wuepper, J. L. and Popov, A. I.,** Spectroscopic studies of alkali metal ions in dimethylsulfoxide and 1-methyl-2-pyrrolidone, *J. Am. Chem. Soc.,* 92, 1493, 1970.
152. **Edgell, W. F., Lyford, J., IV, Wright, R., Risen, W., Jr., and Watts, A.,** The intermolecular vibration of ions in solution, *J. Am. Chem. Soc.,* 92, 2240, 1970.
153. **Irish, D. E. and Brooker, M. H.,** *Advances in Infrared and Raman Spectroscopy,* Vol. 2, Clark, R. J. H. and Hester, R. E., Eds., Heyden, London, 1976, 212.
154. **Sato, H. and Kusumoto, Y.,** Highly symmetric structure of alkali metal complexes of 18-crown-6 and 15-crown-5 in liquid and crystalline states as revealed by raman spectra, *Chem. Lett.,* p. 635, 1978.
155. **Teeters, D. and Frech, R.,** Temperature dependent spectroscopic studies of PPO and PPO-inorganic salt complexes, *Solid State Ionics,* 18/19, 271, 1986.
156. **Yoshihara, T., Tadokoro, H., and Murashashi, S.,** Normal vibrations of the polymer molecules of helical conformation. IV. PEO and polyethylene-d_4 oxide, *J. Chem. Phys.,* 41, 2902, 1964.
157. **Liu, K.-J. and Parsons, J. L.,** Solvent effects of the preferred conformation of PEG, *Macromolecules,* 2, 529, 1969.
158. **Takahashi, Y. and Tadokoro, H.,** Structural studies of polyethers $(-(CH_2)_m-O-)_n$. X. Crystal structure PEO, *Macromolecules,* 6, 672, 1973.
159. **Barbetta, A. and Edgell, W. F.,** Infrared spectrophotometric determination of trace water in selected organic solvents, *Appl. Spectrosc.,* 32, 93, 1978.
160. **Barriola, A.,** unpublished data, Northwestern University, Evanston, IL, 1986.
161. **Spindler, R. and Shriver, D. F.,** Synthesis NMR classification and electrical properties of siloxane-based polymer electrolytes, *Macromolecules,* 21, 648, 1988.
162. Sequeira, C. A. C., D. C. methods of cell characterization, in *Solid State Batteries,* Martinus, Nijhoff, Dordrect, 1985, 219.
163. **Macdonald, J. R.,** Simplified impedance/frequency response results for intrinsically conducting solids and liquids, *J. Chem. Phys.,* 61, 3977, 1974.
164. **Debye, P.,** *Polar Molecules,* Chemical Catalog Co., New York, 1929.
165. **Cole, K. S. and Cole, R. H.,** Dispersion and absorption in dielectrics, *J. Chem. Phys.,* 9, 341, 1941.
166. **Jonscher, A. K.,** Physical basis of dielectric loss, *Nature,* 253, 717, 1975.
167. **Jonscher, A. K.,** New interpretation of dielectric loss peaks, *Nature,* 256, 566, 1975.
168. **Macdonald, J. R.,** Frequency response of unified dielectric and conductive systems involving an exponential distribution of activation energies, *J. Appl. Phys.,* 58, 1955, 1985.
169. **Macdonald, J. R.,** Generalization of "universal dielectric response" and a general distribution-of-activation-energies model for dielectric and conducting systems, *J. Appl. Phys.,* 58, 1971, 1985.
170. **Macdonald, J. R.,** Note on the parameterization of the constant-phase admittance element, *Solid State Ionics,* 13, 147, 1984.
171. **Scheider, W.,** Theory of the frequency dispersion of electrode polarization. Topology of networks with fractional power frequency dependence, *J. Phys. Chem.,* 79, 127, 1975.
172. **LeMehaute, A. and Crepy, G.,** Introduction to transfer and motion in fractal media: the geometry of kinetics, *Solid State Ionics,* 9/10, 17, 1983.
173. **Parker, J. M., Wright, P. V., and Lee, C. C.,** A double helical model for some alkali metal ion-poly(ethylene oxide) complexes, *Polymer,* 22, 1305, 1981.
174. **Vogel, H.,** The law of the relation between the viscosity of liquids and the temperature, *Z. Phys.,* 22, 645, 1921.
175. **Tammann, G. and Hesse, W.,** Die Abhangigkeit der Viscositat von der Temperatur bei Unterkuhiten Flussigkeiten, *Z. Anorg. Allg. Chem.,* 156, 245, 1926.
176. **Fulcher, G. S.,** Analysis of recent measurements of the viscosity of glasses, *J. Am. Ceram. Soc.,* 8, 339, 1925.

177. **Williams, M. L., Landel, R. F., and Ferry, J. D.,** The temperature dependence of relaxation mechanisms in amorphous polymers and other glass-forming liquids, *J. Am. Chem. Soc.*, 77, 3701, 1955.
178. **Doolittle, A. K.,** Studies in newtonian flow. II. The dependence of the viscosity of liquids on free-space, *J. Appl. Phys.*, 22, 1471, 1951.
179. **Fox, T. G. and Flory, P. J.,** Second-order transition temperatures and related properties of polystyrene. I. Influence of molecular weight, *J. Appl. Phys.*, 21, 581, 1950.
180. **Fox, T. G., Jr. and Flory, P. J.,** Viscosity-molecular weight and viscosity-temperature relationships for polystyrene and polyisobutylene, *J. Am. Chem. Soc.*, 70, 2384, 1948.
181. **Batschinsky, A. J.,** Untersuchungen uber die Innere Reiburg der Flussigkeiten, *Z. Phys. Chem.*, 84, 643, 1913.
182. **Cohen, M. H. and Turnbull, D.,** Molecular transport in liquids and glasses, *J. Chem. Phys.*, 31, 1164, 1959.
183. **Cheradame, H.,** A comprehensive theory of the high ionic conductivity of macromolecular networks, in *IUPAC Macromolecules,* Benoit, H. and Rempp, P., Eds., Pergamon Press, Elmsford, NY, 1982, 251.
184. **Miyamoto, T. and Shibayama, K.,** Free-volume model for ionic conductivity in polymers, *J. Appl. Phys.*, 44, 5372, 1973.
185. **Angell, C. A. and Sichina, W.,** Thermodynamics of the glass transition: empirical aspects, *Ann. N.Y. Acad. Sci.*, 279, 53, 1976.
186. **Angell, C. A.,** Fast-ion motion in glassy and amorphous materials, in *Solid State Ionics,* Kleitz, M., Sapoval, B., and Ravaine, D., Eds., North-Holland, Amsterdam, 1983, 3.
187. **Gibbs, J. H. and DiMarzio, E. A.,** Nature of the glass transition and the glassy state, *J. Chem. Phys.*, 28, 373, 1958.
188. **Adam, G. and Gibbs, J. H.,** On the temperature dependence of cooperative relaxation properties in glass-forming liquids, *J. Chem. Phys.*, 43, 139, 1965.
189. **Goldstein, M.,** Viscous liquids and the glass transition: a potential energy barrier picture, *J. Chem. Phys.*, 51, 3728, 1969.
190. **Williams, E. and Angell, C. A.,** Glass transition with negative change in expansion coefficients, *J. Polym. Sci. Polym. Lett. Ed.*, 11, 383, 1973.
191. **Angell, C. A.,** Recent developments in fast ion transport in glassy and amorphous materials, *Solid State Ionics,* 18/19, 72, 1986.
192. **Ratner, M. A. and Shriver, D. F.,** Aspects of the theoretical treatment of polymeric solid electrolytes: transport theory and models, *Chem. Rev.*, 88, 109, 1988.
193. **Ansari, S. M., Brodwin, M., Stainer, M., Druger, S. D., Ratner, M. A., and Shriver, D. F.,** Conductivity and dielectric constant of the polymeric solid electrolyte, $(PEO)_8NH_4SO_3CF_3$, in the 100 Hz to 10^{10} Hz range, *Solid State Ionics,* 17, 101, 1985.
194. **Wong, T., Brodwin, M., Papke, B. L., and Shriver, D. F.,** Dielectric and conductivity spectra of PEO complexes of sodium salts, in *Fast Ionic Transport in Solids,* Bates, J. B. and Farrington, G. C., Eds., North-Holland, Amsterdam, 1981, 689.
195. **Druger, S. D., Ratner, M. A., and Nitzan, A.,** Polymeric solid electrolytes: dynamic bond percolation and free volume models for diffusion, in *Solid State Ionics,* Kleitz, M., Sapoval, B., and Ravaine, D., Eds., North-Holland, Amsterdam, 1983, 1115.
196. **Druger, S. D., Nitzan, A., and Ratner, M. A.,** Dynamic bond percolation theory: a microscopic model for diffusion in dynamically disordered systems. I. Definition and one-dimensional case, *J. Chem. Phys.*, 79, 3133, 1983.
197. **Druger, S. D., Ratner, M. A., and Nitzan, A.,** Generalized hopping model for frequency-dependent transport in a dynamically disordered medium, with applications to polymer solid electrolytes, *Phys. Rev. B*, 31, 3939, 1985.
198. **Druger, S. D., Ratner, M. A., and Nitzan, A.,** Applications of dynamic bond percolation theory to the dielectreic response of polymer electrolytes, in *Solid State Ionics,* Vol. 1 and 2, North-Holland, Amsterdam, 1986, 106.
199. **Harris, C. S., Nitzan, A., Ratner, M. A., and Shriver, D. F.,** Particle motion through a dynamic disordered medium: the effect of bond correlation and application to polymer solid electrolytes, in Solid State Ionics, Vol. 1 and 2, North-Holland, Amsterdam, 1986, 151.
200. **Fontanella, J. J., Wintersgill, M. C., Calame, J. P., and Andeen, C. G.,** Electrical relaxation in pure and alkali metal thiocyanate complexed PEO, *Solid State Ionics,* 8, 333, 1983.
201. **Wintersgill, M. C., Fontanella, J. J., Calame, J. P., Figueroa, D. R., and Andeen, C. G.,** Dielectric relaxation in PEO complexed with alkali metal perchlorates, *Solid State Ionics,* 11, 151, 1983.
202. **Killis, A., LeNest, J.-F., Cheradame, H., and Gandini, A.,** Ionic conductivity of polyether-polyurethane networks containing $NaBPh_4$: a free volume analysis, *Makromol. Chem.*, 183, 2835, 1982.
203. **Jones, G. and Dole, M.,** The viscosity of aqueous solutions of strong electrolytes with special reference to barium chloride, *J. Am. Chem. Soc.*, 51, 2950, 1929.

204. **Dupon, R., Whitmore, D. H., and Shriver, D. F.,** Transference number measurements for the polymer electrolyte poly(ethylene oxide) NaSCN, *J. Electrochem. Soc.*, 128, 715, 1981.
205. **Tubandt, C.,** *Handbuch Der Experimental Physik*, Wien, W. and Harms, F., Eds., Akademische Verlagsgesellschaft, Leipzig, 1932, 21.
206. **Leveque, M., LeNest, J. F., Gandini, A., and Cheradame, H.,** Ionic transport numbers in polyether networks containing different metal salts, *Makromol. Chem. Rapid Commun*, 4, 497, 1983.
207. **Weston, J. E. and Steele, B. C. H.,** Effects of inert fillers on the mechanical and electrochemical properties of Li salt-PEO polymer electrolytes, *Solid State Ionics*, 7, 75, 1982.
208. **Yang, L. L., McGhie, A. R., and Farrington, G. C.,** Ionic conductivity in complexes of PEO and $MgCl_2$, *J. Electrochem. Soc.*, 133, 1380, 1986.
209. **Sorensen, P. R. and Jacobsen, T.,** Conductivity, charge transfer and transport number-An AC-investigation of the polymer electrolyte LiSCN·PEO, *Electrochim. Acta*, 27, 1671, 1982.
210. **Sorensen, P. R. and Jacobsen, T.,** Limiting currents in the polymer electrolyte: $PEO_xLiSO_3CF_3$, *Solid State Ionics*, 9/10, 1147, 1983.
211. **Shriver, D. F., Clancy, S., Blonsky, P. M., and Hardy, L. C.,** Ion transport numbers for new polymer electrolytes, in *Transport-Structure Relations in Fast Ion and Mixed Conductors*, Proc. Risoe 6th Int. Symp. Metal Material Science, 1985, 353.
212. **Watanabe, M., Rikukawa, M., Sanui, K., and Ogata, N.,** Evaluation of ionic mobility and transference number in a polymeric solid electrolyte by isothermal transient ionic current method, *J. Appl. Phys.*, 57, 123, 1985.
213. **Owen, J. R., Spurdens, P. C., Shemilt, J. E., and Steele, B. C. H.,** Limiting current effects in PEO based solid electrolytes, in *Electrochem. Soc. Extended Abstracts*, Vol. 82-1, Abstr. 712, Electrochemical Society, Pennington, NJ, 1982, 1141.
214. **Bouridah, A., Dalard, F., Deroo, D., and Armand, M. B.,** Potentiometric measurements of ionic mobilities in PEO electrolytes, *Solid State Ionics*, 18/19, 287, 1986.
215. **Chadwick, A. V., Strange, J. H., and Worboys, M. R.,** Ionic transport in polyether electrolytes, *Solid State Ionics*, 9/10, 1155, 1983.
216. **Gorecki, N., Andreani, R., Berthier, C., Armand, M. B., Mali, M., Roos, J., and Brinkman, D.,** NMR, DSC and conductivity study of PEO complex electrolyte: PEO_xLiCLO_4, *Solid State Ionics*, 18/19, 295, 1986.
217. **Bhattacharja, S., Smoot, S. W., and Whitmore, D. H.,** Cation and anion diffusion in the amorphous phase of the polymer electrolyte $PEO_8LiSO_3CF_3$, *Solid State Ionics*, 18/19, 306, 1986.
218. **Wagner, C.,** Equations for transport in solid oxides and sulfides of transition metals, *Prog. Solid State Chem.*, 10, 3, 1975.
219. **Wagner, J. B.,** Polarization studies on solid state electrolytes, in *Electrode Processes in Solid State Ionics*, Kleitz, M. and Dupuy, M., Eds., Reidel, Holland, 1976, 185.
220. **Macdonald, J. R.,** Theory of space-charge polarization and electrode discharge effects, *J. Chem. Phys.*, 58, 4982, 1973.
221. **Bard, A. J. and Faulkner, L. R.,** *Electrochemical Methods*, John Wiley & Sons, New York, 1980.
222. **Geng, L. Reed, R. A., Longmire, M. L., and Murray, R. W.,** *J. Phys. Chem.*, 91, 2908, 1987.
223. **Bridges, C., Chadwick, A. V., and Worboys, M. R.,** Radiotracer self-diffusion measurements in PEO and PPO electrolytes, in *Abstr. 1st Int. Symp. Polymer Electrolytes*, Abstr. 11, St. Andrews University, St. Andrews, Scotland, 1987.
224. **Fauteux, D., Gauthier, J., Belanger, A., and Gauthier, M.,** Iodide diffusivity in PEO thin films, in Electrochem. Soc. Meet., Abstr. 711, Montreal, May 9 to 14, 1982, 1140.
225. **Stejskal, E. O. and Tanner, J. E.,** Spin diffusion measurements: spin echoes in the presence of a time-dependent field gradient, *J. Chem. Phys.*, 42, 288, 1965.
226. **Venkatasetty, H. V.,** Transport properties and structure of non-aqueous electrolyte solutions, in *Lithium Battery Technology*, Venkatasetty, H. V., Ed., Wiley-Interscience, New York, 1984, 13.
227. **Greenbaum, S. G.,** ^{23}Na NMR Studies of Ion Conducting Polymers, presented at the Denver ACS Meeting, April 1987.
228. **MacCallum, J. R., Tomlin, A. S., and Vincent, C. A.,** An investigation of the conducting species in polymer electrolytes, *Eur. Polym. J.*, 22, 787, 1986.
229. **Marcus, Y.,** *Ion Solvation*, Wiley-Interscience, New York, 1985.
230. **Hall, P. G., Davies, G. R., Ward, I. M., and McIntyre, J. E.,** Conductivity of lithium perchlorate and lithium tetrafluoroborate in tetraethylene glycol dimethyl ether, *Polym. Commun.*, 27, 100, 1986.
231. **Armand, M. B., Duclot, M. J., and Rigaud, P.,** Polymer solid electrolytes: stability domain, *Solid State Ionics*, 3/4, 429, 1981.
232. **Sequeira, C. A. C., North, J. M., and Hooper, A.,** Stability domain of a complexed lithium salt PEO polymer electrolyte, *Solid State Ionics*, 13, 175, 1984.
233. **Palmer, D. N., Brule, J. E., Alexander, M. G., O'Neill, J. K., and Miller, J. M.,** The characteristics of thin film MEEP lithium aprotic salt ionic complexes as electrolytes for lithium secondary cell applications, presented at Phosphazene Chemistry Workshop, U.S. Naval Academy, Annapolis, MD, November 6, 1985.

234. **Reed, R. A., Murray, R. W., Tonge, J. S., Yaniv, D. R., and Shriver, D. F.,** Solid state voltammetry of ionically conducting phosphazene $LiSO_3CF_3$ complexes, *J. Electroanal. Chem.*, in press.
235. **Fauteux, D.,** Formation of a passivating film at the lithium-PEO-$LiSO_3CF_3$ interface, *Solid State Ionics*, 17, 133, 1985.
236. **Gabano, J.-P., Ed.,** *Lithium Batteries* Academic Press, New York, 1983.
237. **Tofield, B. C.,** Future prospects for all-solid-state batteries, in *Solid State Batteries*, Martinus Nijhoff, Dordrect, 1985, 423.
238. **Gauthier, M., Fauteux, D., Vassort, G., Belanger, A., Duval, M., Ricoux, P., Chabagno, J. M., Muller, D., Rigaud, P., Armand, M. B., and Deroo, D.,** Assessment of polymer-electrolyte batteries for EV and ambient temperature applications, *J. Electrochem. Soc.*, 132, 1333, 1985.
239. **Gauthier, M., Belanger, A., Fauteux, D., Harvey, P. E., Kapfer, B., Duval, M., Robitaille, C., Vassort, G., Muller, D., Chabagno, J. M., and Ricoux, P.,** Recent progress in the development of rechargeable lithium batteries based on polymer electrolytes, in *Lithium Batteries*, Vol. 86-2, Ext. Abstr. 43, Dey, A. N., Ed., Electrochemical Society, Pennington, NJ, 1986.
240. **Upton, J. R., Owen, J. R., Rudkin, R. A., Steele, B. C. H., and Benjamin, J. D.,** Thin film arrays of polymer electrolyte cells, in *Lithium Batteries*, Abstr. 44, Dey, A. N., Ed., Electrochemical Society, Pennington, NJ, 1987.
241. **Hooper, A. and North, J. M.,** The fabrication and performance of all solid state polymer-based rechargeable lithium cells, *Solid State Ionics*, 9/10, 1161, 1983.
242. **Maskell, W. C. and Owen, J. R.,** Cycling behavior of thin film LiAl electrodes with liquid and solid electrolytes, *J. Electrochem. Soc.*, 132, 1602, 1985.
243. **Hooper, A. and North, J. M.,** Battery, German Offen. DE 3,439,327, May 9, 1985.
244. **Hooper, A. and North, J. M.,** Solid State Battery, German Offen. DE 3,438,243, May 2, 1985.
245. **Hooper, A. and North, J. M.,** Electrochemical Battery, European Patent Appl. EP 123,516, October 31, 1984.
246. **Cook, J. A., Park, G. B., and McLoughlin, R. H.,** Protected Electrode Material and Its Use in Electrical Devices, European Patent Appl. EP 146,245, June 26, 1985.
247. **Cook, J. A., Park, G. B., McLoughlin, R. H., and Whitcher, W. J.,** Materials for Electrical Batteries, European Patent Appl. EP 145,498, June 19, 1985.
248. **Hitachi Maxell Ltd.,** Secondary Solid-State Laminar Battery, Japanese Kokai Tokyo Koho JP 60 49, 573, March 18, 1985.
249. **Armand, M. B. and Duclot, M.,** Electrochemical Current Generators and Materials for Their Construction, European Patent Appl. 13, 199, July 9, 1980.
250. **West, K., Zachau-Christiansen, B., Jacobsen, T., and Atlung, S. A.,** Rechargeable all-solid-state sodium cell with polymer electrolyte, *J. Electrochem. Soc.*, 132, 3061, 1985.
251. **Patrick, A., Glasse, M., Latham, R., and Linford, R.,** Novel solid state polymeric batteries, *Solid State Ionics*, 18/19, 1063, 1986.
252. **Chiang, C. K.,** Polyacetylene as an electrode in solid state batteries, *Solid State Ionics*, 9/10, 445, 1983.
253. **Berthier, C. M. and Friend, R. H.,** Composite Conductors Comprising Continuous Electronic Conducting Material and a Continuous Ionic Conducting Material, PCT Int. Appl. WO 85 02,294, May 23, 1985.
254. **Hitachi Ltd. and Showa Denko, K. K.,** Secondary Battery with Solid Electrolyte, Japanese Kakai, Tokyo, Koho JP 60 97,561, October 31, 1983.
255. **Johnson, W. B. and Worrell, W. L.,** Electrochemical cell investigations of Li_xTiS_2 and $Li_xNa_yTiS_2$ using a polymer electrolyte, *Solid State Ionics*, 5, 367, 1981.
256. **Toshiba Corp.,** Solid State Battery, Japanese Kokai Koho JP 60 47,372, August 26, 1983.
257. **Oi, M. and Suzuki, T.,** Non-Aqueous Batteries, Japanese Kokai, Tokyo Koho JP 60,216,461, October 29, 1985.
258. **Suzuki, T., Oi, M., Tsuchida, H., and Shinohara, I.,** Nonaqueous Batteries, Japanese Kokai Tokyo Koho JP 60,216,462, October 29, 1985.
259. **Oi, M. and Suzuki, T.,** Nonaqueous Batteries, Japanese Kokai Tokyo Koho JP 60,216,463, October 29, 1985.
260. **LeNest, J. F., Cheradame, H., Dalard, F., and Deroo, D.,** Electric and electrochemical properties of a lattice of polyether-based polyurethane charged with $LiClO_4$, *J. Appl. Electrochem.*, 16, 75, 1986.
261. **Semkow, K. W. and Sammells, A. F.,** Secondary solid-state SPE cells, *J. Electrochem. Soc.*, 134, 766, 1987.
262. **Skotheim, T.,** A tandem photovoltaic cell using a thin film polymer electrolyte, *Appl. Phys. Lett.*, 38, 712, 1981.
263. **Skotheim, T. and Lundstrom, I.,** Solid polymer electrolyte photovoltaic cell, *J. Electrochem. Soc.*, 129, 894, 1982.
264. **Inganas, O., Skotheim, T. A., and Feldberg, S. W.,** Photoelectrochemistry at the n-silicon/polymer electrolyte interface, *Solid State Ionics*, 18/19, 332, 1986.
265. **Sammells, A. F. and Ang, P. G. P.,** Photoelectrochemical investigation of a PEO cell, *J. Electrochem. Soc.*, 131, 617, 1984.

266. **Skotheim, T. A.,** Interfaces between electronically and ionically conducting polymers: applications to ultra high vacuum electrochemistry and photoelectrochemistry, *Synth. Met.*, 14, 31, 1986.
267. **Sadaoka, Y. and Sakai, Y.,** Humidity sensor using laminated film with lithium-doped hydrophilic polymer and hydrophobic porous polymer, *J. Mater. Sci. Lett.*, 5, 772, 1986.
268. **Sadaoka, Y., Sakai, Y., and Akiyama, H.,** A humidity sensor using alkali salt-PEO hybrid films, *J. Mater. Sci.*, 21, 235, 1986.
269. **Defendini, F., Armand, M. B., Gorecki, W., and Berthier, C.,** Solid protonic electrolytes based on PEO, in *Lithium Batteries,* Ext. Abstr. 597, Dey, A. N., Ed., Electrochemical Society, Pennington, NJ, 1986, 893.
270. **Donoso, P., Gorecki, W., Berthier, C., Defendini, F., and Armand, M.,** NMR and conductivity study of anhydrous polymer protonic conductors, in *1st Int. Symp. Polymer Electrolytes,* Abstr. 17, St. Andrews University, St. Andrews, Scotland, 1987.
271. **Chao, S. and Wrighton, M. S.,** Solid-state microelectrochemistry: electrical characteristics of a solid-state microelectrochemical transistor based on poly(3-methylthiophene), *J. Am. Chem. Soc.*, 109, 2197, 1987.
272. **Giglia, R. D.,** Electrochromic Device, British U.K. Patent Appl 2,005,856, April 25, 1979.
273. **Reddy, T. B.,** Polymeric Electrolyte for Electrochromic Display Apparatus, Belgian 860,105, April 26, 1978.
274. **Inganas, O.,** Electroactive polymer blends, in *1st Int. Symp. Polymer Electrolytes,* Abstr. 20, St. Andrews University, St. Andrews, Scotland, 1987.

Chapter 6

LANGMUIR-BLODGETT FILMS: LANGMUIR FILMS PREPARED BY THE BLODGETT TECHNIQUE

Scott E. Rickert

TABLE OF CONTENTS

I. Introduction 212
- A. Historical Background of Monolayer Studies 212
- B. Work of Irving Langmuir and Katherine Blodgett 212
- C. New Interest in Monolayers and Multilayers 212

II. Fundamental Properties of Monolayers and Multilayers 214
- A. Properties on the Water Surface 214
- B. Multilayer Properties 216

III. Current Status of Langmuir Films 217
- A. Film Fabrication/Crystal Growth 217
- B. Electronic Properties 218
- C. Diffusion Properties 218
- D. Structural Properties 219

IV. Applications of Monolayers and Multilayers 220
- A. Microelectronic Devices 221
- B. Dielectrics 222
- C. Barriers 222
- D. BioFilms 223
- E. Lubricants 223
- F. Spacers 223
- G. Optical Coatings 224
- H. Sensors 224

V. Conclusions and Future Outlook 224

References 225

I. INTRODUCTION

A. Historical Background of Monolayer Studies

Although there are three states of matter — gas, liquid, and solid — scientists have always been fascinated with the interface, or junctions between states. One of the most important interfaces is that of water with air. The process of water evaporation from large seas, lakes, or reservoirs, and its subsequent condensation and precipitation are, indeed, the key process which permits life to exist on earth.

During the 18th century, the scientist/philosopher Benjamin Franklin became fascinated with the spreading of liquid soaps (e.g., palmitates, stearates) on large bodies of water. He observed that the liquid soap seemed to "calm" or dampen the waves of an area of water far larger than that originally covered. Franklin was perhaps the first to note that the liquid soap film would have had to thin to a film one molecule in thickness in order to explain its effect on such a large area of water.

Man's fascination with this property of soap expanded in the 19th century, with noted research being performed by Lord Rayleigh and by such pioneers as Agnus Pockels. It was quickly verified that Franklin was indeed correct regarding the monomolecular nature ("monolayer") of soap films. It was further learned that the application of soap films to water reservoirs not only calmed them, but also greatly reduced the evaporation rate from the reservoir. Such soap films have gained routine use in reservoirs for this purpose today.[1]

B. Work of Irving Langmuir and Katherine Blodgett

The first comprehensive investigation of the properties of monolayers and multilayers was undertaken by a research team in the 1920s at the General Electric Corporation in Schenectady, NY, headed by Dr. Irving Langmuir. Dr. Langmuir, along with his colleague, Dr. Katherine Blodgett, became fascinated with the properties of monolayers on water surfaces.[2-4]

Langmuir focused on the properties of monolayers, while Blodgett developed the vertical dipping technique still employed to transfer these compressed monolayers onto a solid surface, and to build up multiple thicknesses of such monolayers (i.e., multilayers). When Langmuir won his Nobel Prize in Chemistry in 1931, General Electric prepared a film documentary on his work in this field. This documentary amply demonstrates the breadth of understanding these co-workers maintained regarding monolayers.

It is perhaps due to their documented understanding of the self-assembly process of monolayers that these films are often referred to as Langmuir-Blodgett films. More correctly, the films should be called Langmuir films, prepared by the Blodgett technique, but this is often shortened to Langmuir-Blodgett or LB films for convenience. Regardless of the name associated with monolayers and multilayers, the pioneering work of Langmuir and Blodgett in the 1920s began the modern age of multilayer organic films, and some of the keenest insights into the properties and potential applications of these films lie in their papers of that period. Figure 1 shows schematically the method developed by Langmuir for measuring monolayer properties on the water surface. Figure 2 shows the Blodgett method for depositing such monolayers on a rigid substance.

C. New Interest in Monolayers and Multilayers

After Langmuir and Blodgett finished their studies, the field continued to be studied by only a few investigators interested in: (1) an understanding of the physics and chemistry associated with monolayers and multilayers, (2) a method to understand other physical phenomena, or (3) a way to test new analytical surface characterization methods. For example, Kuhn utilized monolayers and multilayers to investigate the transfer of energy between dye molecules as a way to understand life processes,[5] and Lando used these films to investigate differences in solid-state polymerization between monolayer film and bulk crystals.[6]

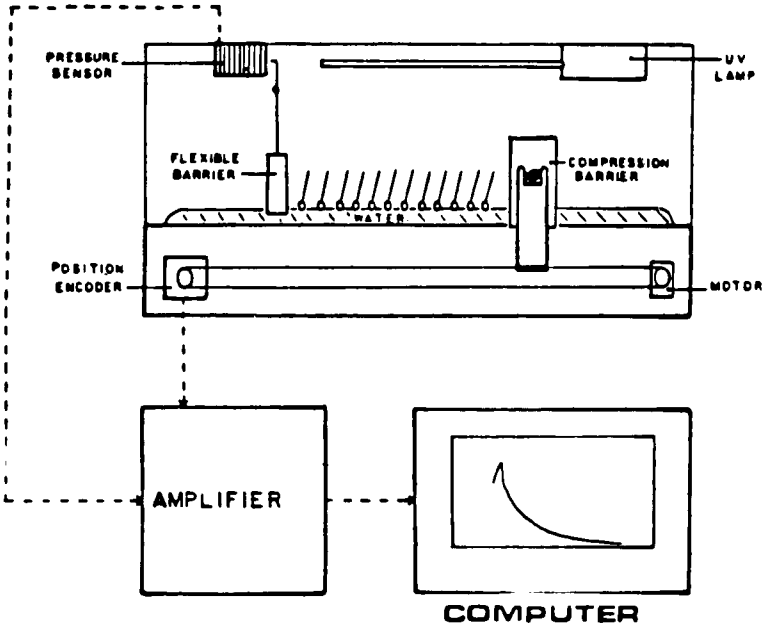

FIGURE 1. Schematic diagram of a Lauda film balance. The silicon wafer is deposited between the flexible barrier (which is also a pressure transducer) and the compression barrier.

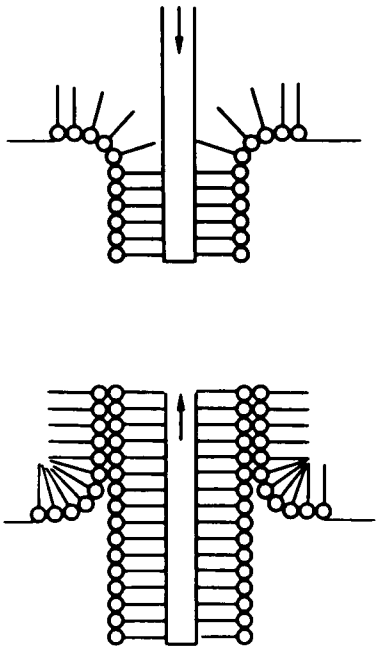

FIGURE 2. Formation of a multilayer film on a hydrophobic silicon surface by the Langmuir technique. In the first downtrip, the hydrophobic tail attaches itself to the hydrophobic surface. The upward trip causes the attachment of the hydrophilic group leading to a head-head, tail-tail structure.

It should be noted, however, that a large amount of work was also being done during this time by biochemists in the area of lipid membranes and bilayers.[7] As is so often the case, the results of this work were not successfully transferred from biochemists to chemists and chemical engineers. Fortunately, this problem has been lessened today through increased interdisciplinary activity in this field.

In the mid-1970s, the field was revitalized by the work of Barraud,[8] Ringsdorf,[9] and Roberts,[10] Barraud can be described as a physical chemist, Ringsdorf as a synthetic chemist, and Roberts as an electrical engineer. Their training led to their research focus on properties, materials, and devices, respectively. Applications of LB bilms as high-resolution electron-beam resists, field-effect transistors, and chemical and optical sensors using dye-based molecules were first demonstrated by them. These three scientific groups, along with Kuhn and Lando's groups, spurred the recent interantional interest among universities, industry, and government agencies in LB films as potentially important materials and devices.

In 1983, the Polymer Microdevice Laboratory (PML) was constructed on the campus of Case Western Reserve University, Cleveland, OH. The PML was established as an interdisciplinary research center to focus on development of reliable electronic and physical "devices", making use of conventional electronic materials, large-scale integration (LSI) technology, and LB film technology. This so-called hybrid molecular device technology (HMD) makes use of a class 10 ultraclean laboratory to purify and filter air and water used to fabricate and test LB HMDs for various applications, such as chemical and pressure sensors, perm-selective ultrathin membranes, high-mobility field effect devices, and smart interconnecting multilevel electronic devices.[11-13] Researchers in chemistry, chemical engineering, and electrical engineering collaborate closely with polymer engineers in this interdisciplinary field.

The importance of LB film fabrication in the absence of dust and other environmental contaminants has been amply documented,[14] and most research laboratories working in this area have incorporated differing aspects of this laboratory into their research programs (Plate 2*). The interdisciplinary nature of the PML is its most important attribute, but other groups have been slow to adopt this research approach. It is hoped that this will change in the future.

Several new process analysis techniques have been introduced by the PML. Among them is the development of a process window, based chiefly on the results of compressive creep studies (Figure 3).

II. FUNDAMENTAL PROPERTIES OF MONOLAYERS AND MULTILAYERS

A. Properties on the Water Surface

As already mentioned, the first application of monolayers was to retard the evaporation of lakes, ponds, and reservoirs. The exact mechanism by which this blockage of water works is still not understood, but evaporation curves taken from large bodies of water which are partially covered by such a monolayer can be fit quite accurately by assuming that all of the evaporation is coming from the uncovered areas and that no evaporation occurs from under the monolayer![15] This can only be explained as a combination of low molecular mobility (i.e., diffusion) and low water solubility within the films.

The exact state of monolayers floating on water is still not completely understood. The best current theory for conventional soap-like molecules is that they pack next to each other in a pseudo-liquid crystalline arrangement, with high mobility primarily normal to the water surface.[16] Aromatic, highly conjugated, or cross-linked molecules probably do not follow this theory because of substantially reduced lateral mobility when condensed. The two parameters which would effect a liquid crystalline monolayer state, if present, would be the bulk melting temperature of the soap used, as well as the degree of supercooling (the

*See Plate 2 following p. 120.

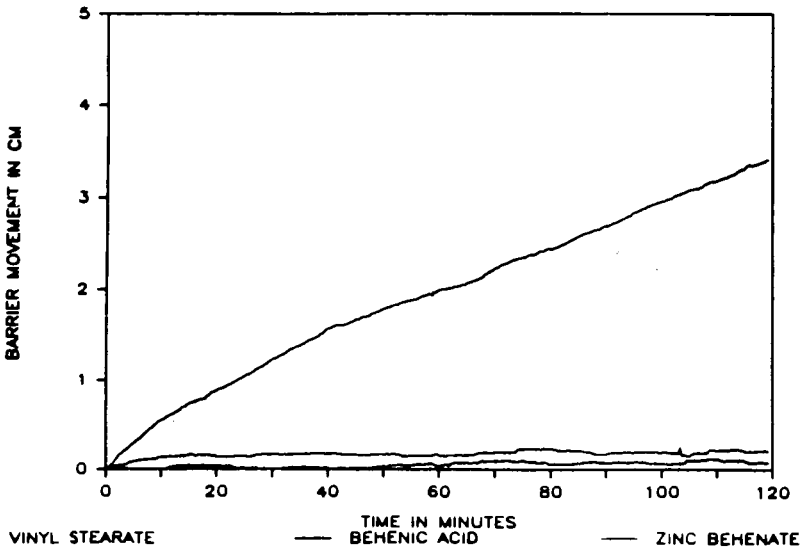

FIGURE 3. Compressive creep test of LB films.

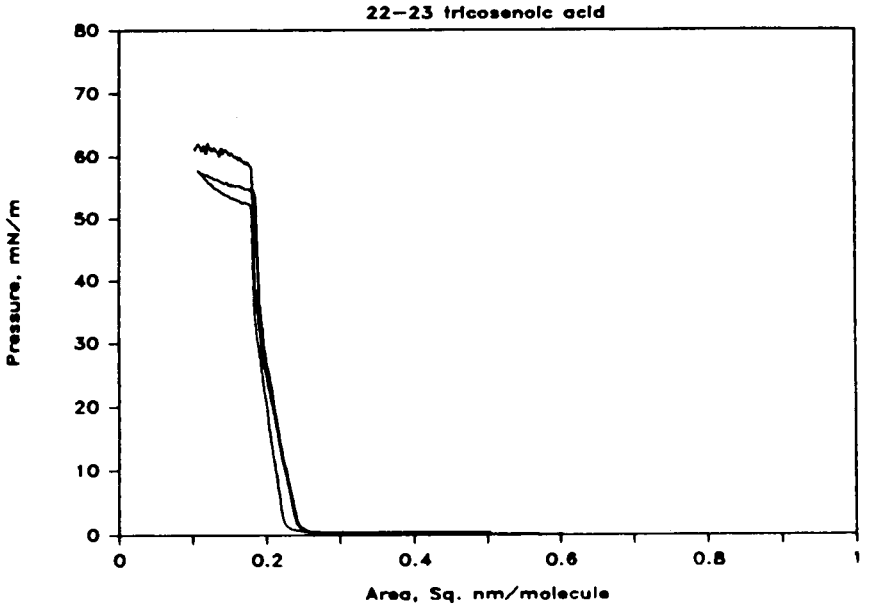

FIGURE 4. Langmuir isotherm for 23-23 tricosenoic acid.

difference in temperature between the bulk melting temperature and the monolayer temperature); i.e., the higher the degree of supercooling, the less likely is a "liquid crystalline" state on the water surface and the more likely is a rigid crystalline state on the water surface. The classic Langmuir isotherms shown in Figure 4 are a method to measure the resistance force between molecules or crystals as a function of molecular density.

A number of research groups have focused on monolayer properties through the years, developing such concepts as the co-area (area occupied per totally compressed molecule in the monolayer extrapolated to 0 pressure), equilibrium spreading pressure (pressure exerted by one molecule on another in a monolayer in equilibrium with the bulk crystal phase:

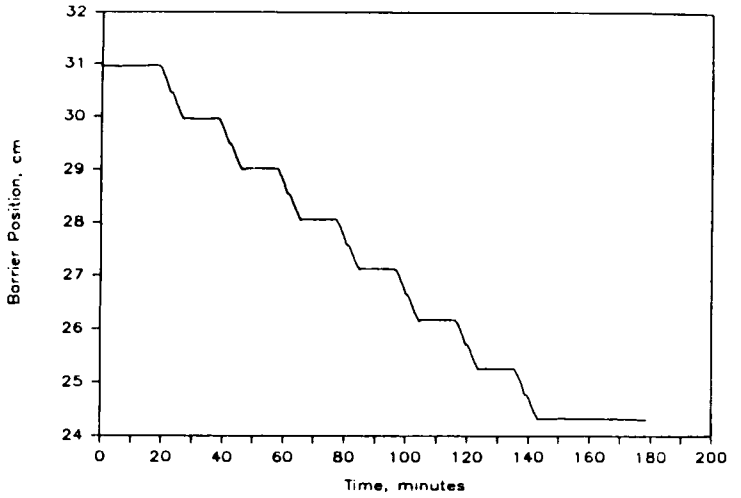

FIGURE 5. Plot of barrier position vs. time during dipping process.

usually measured by spreading a fine dispersion of crystals on a water surface and measuring the increase in pressure or decrease in surface tension at equilibrium), and monolayer viscosity (the two-dimensional resistance to movement or flow).[17] This work has generally been done independently by separate research groups other than those who worked on the physical and electronic properties of LB films, many of them from the lipid research area. Recent techniques, such as glancing angle X-ray scattering (via a high energy accelerator) and capillary wave interferometry utilizing ultraprecise laser surface scattering, allow us to not only understand the structure and dynamics of static monolayers, but also the dynamics and structure of monolayers while undergoing transfer to a solid substrate. Through the use of these methods, as well as more conventional techniques such as precise surface potential measurements (change in interfacial capacitance as a function of film density), it may be possible to develop a thorough understanding of the forces and motions within a monolayer as it forms and transfers off of a water surface to a solid substrate. This understanding is essential to developing a comprehensive processing equation for LB films.

B. Multilayer Properties

It is clear that, independent of the state of a monolayer on the water surface, the process of transferral to a solid substrate causes the monolayer to crystallize and bond tightly to the substrate. Each subsequent monolayer will crystallize on top of the underlying monolayer, thereby building up a multilayer film in thickness multiples of the original monolayer. (*Note*: a plot of barrier position vs. time during dipping will assist in determining the quality of the deposition [Figure 5].) Although there has been some controversy regarding the extent of order and retention throughout a typical multilayer, work in the PML on a wide variety of materials has clearly shown, at least with respect to these materials, that an epitaxial crystallization (i.e., oriented overgrowth of a crystalline substance on a substrate, which is also crystalline) of each new monolayer on top of the multilayer must occur when the monolayer is processed in a near-optimum manner (i.e., under conditions in the "process window").[18]

The ways in which one can describe a typical multilayer are as follows: flexible, abrasion resistant, durable, reasonable thermal stability (very chemical dependent), optically transparent, and virtually pinhole or defect free. These characteristics, coupled with the near room temperature, and atmospheric pressure fabrication technology associated with these films are in contrast to sputtered or metallized foil technology, and have generated a great deal of industrial interest in LB films grown on a wide variety of substrates, both organic

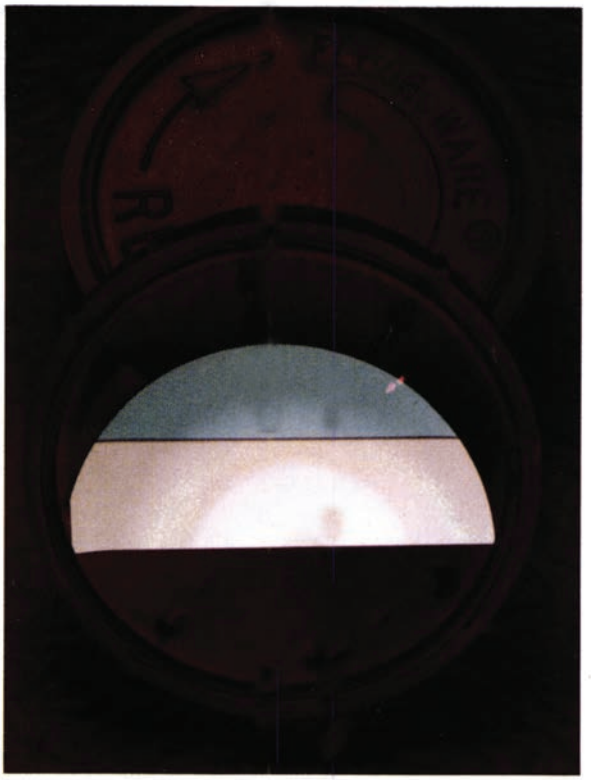

PLATE 1. W-tricosenoic acid deposited utilizing LB technique onto silicon substrate (46 layers).

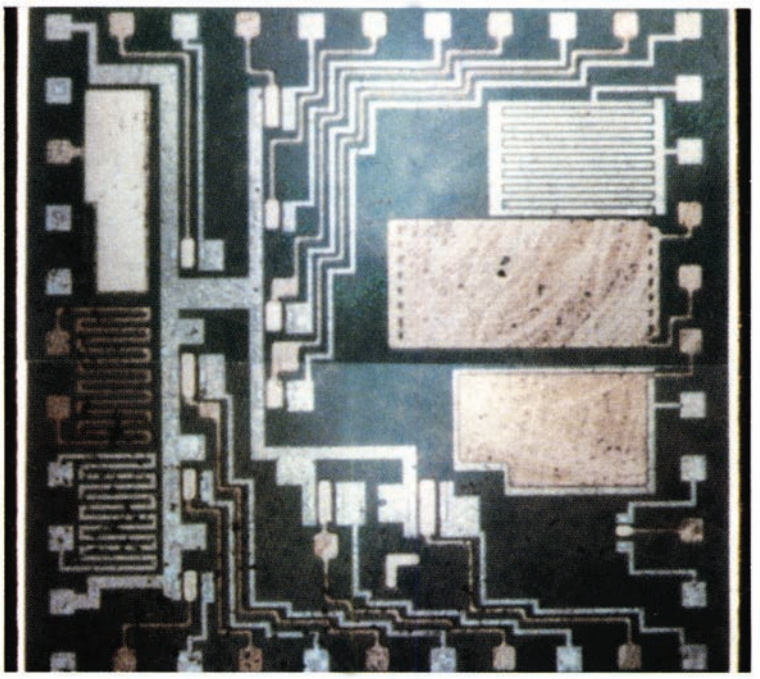

PLATE 2. A photomicrograph of a completed chip (3.3 × 3.3 mm) that contains 11 IGFET of various sizes and many other test structures.

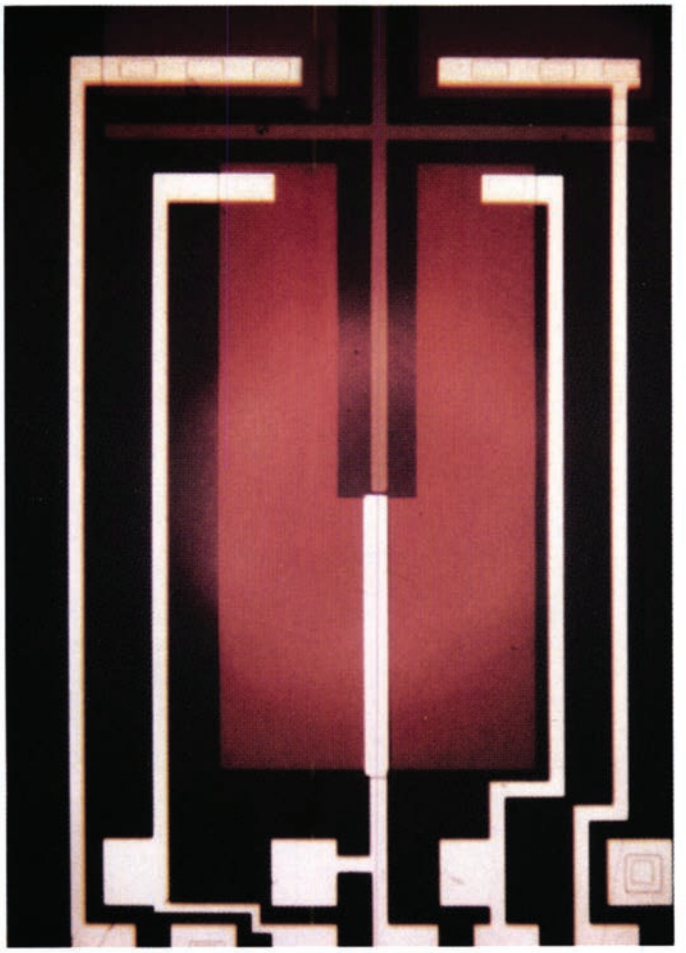

PLATE 3. Hybrid chemitransistor (CHEMFET) utilizing LB film as the sensing dielectric in the device.

and inorganic. Color plate 1* shows a typical multilayer deposited on a 2-in. silicon wafer. Notice the uniformity which is apparent in good multilayer films (bottom half of wafer is coated). Perhaps the one property which stands out in LB films is its anisotropic nature. One can literally tailor the multilayer to exhibit different optic, electronic, or magnetic properties within and through the thickness of the film. For example, one could produce a film which is a conductor through the film and an insulator across the film, or vice versa. Very few inorganic films display this capability. The exploitation of this property will probably lead to some of the greatest application developments in LB film technology.

III. CURRENT STATUS OF LANGMUIR FILMS

A. Film Fabrication/Crystal Growth

LB films are usually fabricated by following the methodology listed below:

1. Prepare a 1-g/l solution of the amphiphile molecule in a dust-free volatile solvent, such as chloroform or hexane.
2. Using a microliter pipette, dispense enough materials, dropwise, onto the surface of very pure water so as to reach a molecular density of less than 50% of the co-area density (e.g., 0.4 nm^2/molecule for stearic acid).
3. After solvent evaporation gently compress the film, by means of a movable barrier, until the co-area density is reached. Near this point, a surface pressure (i.e., reduction in water surface tension) will be measurable, either directly (e.g., a floating transducer measuring displacement as the film is compressed) or indirectly (e.g., a Wilhelmy plate measuring weight gain as the film is pushed onto a half-submerged plate).
4. Continue compressing the film until the measured pressure is between 10 and 50 mN/m. At this point the monolayer is substantially compressed beyond its equilibrium spreading pressure (usually between 0 and 10 mN/m).
5. While holding the pressure constant, a solid substrate is passed vertically or horizontally through the monolayer, in an up and down motion. With each down trip and again upon the up trip, another monolayer is deposited on top of the last. Thus, an n-layer multilayer is usually produced in "n" up plus down trips.

This method is subject to infinite variations and requires substantial skill to produce near defect-free, high-quality multilayers. Typical times to learn these skills range between 6 weeks to 6 months for a skilled researcher! Critical factors for achieving high quality films using this technique include precise surface temperature, surface pressure, vibration, chemical purity, and dipping speed control, as well as sufficient substrate preparation to ensure a uniform surface energy distribution across the substrate.

B. Electronic Properties

Generally, LB films can be classified electronically as leaky capacitor materials. That is, the films are capacitors, but charge carriers are transported in all directions within the films by a variety of mechanisms. The types of charge carriers include ions, electrons, and protons (Figure 6). In many cases, due to the anisotropic crystalline structure of LB films, the transport velocity is often quite direction dependent, with charge transport most easily realized in the direction normal to the film plane, due to through-film defects.

There are specific LB films, formed usually from dye molecules and derivatives, which do exhibit electronic conduction in specific directions. Due to their highly conjugated one-

*See color plate 1 following p. 216.

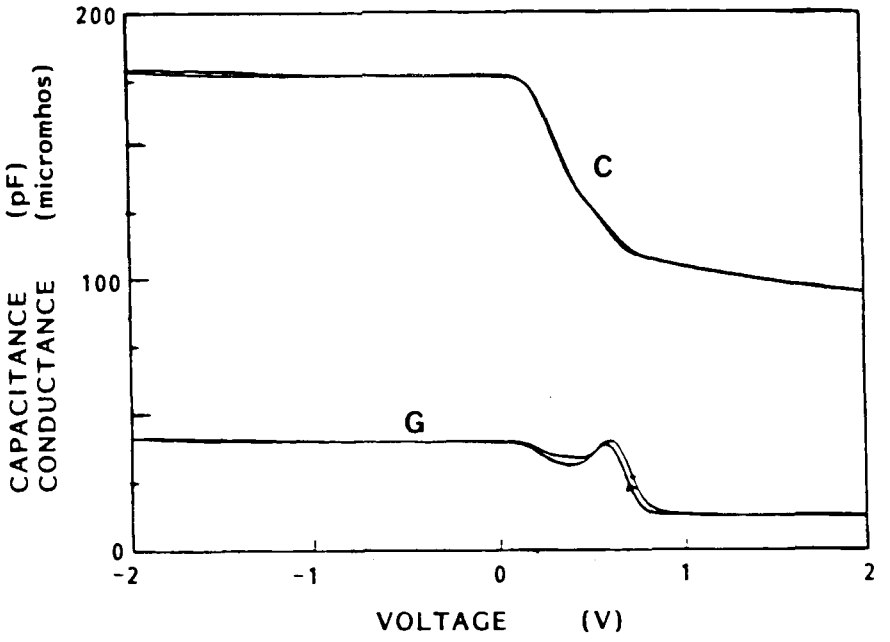

FIGURE 6. 16/8 diacetylene as a leaky capacitor.

dimensional nature, it is possible to prepare directional semiconductors and conductors from these LB films. Examples of dye molecules exhibiting this behavior are the phthalocyanines and porphyrins.[19]

C. Diffusion Properties

As already impled in the case of water evaporation control, monolayers and multilayers retard the permeation rates of most gases and liquids (excluding solvents or swelling agents for the amphiphile used). Research conducted in the PML indicate that a multilayer of poly(vinyl stearate) exhibits similar permeation rates for nitrogen as a 1-mil film or high-density polyethylene. Considering that the multilayer is approximately 0.12% of the thickness of polyethylene, this is a remarkable fact!

D. Structural Properties

LB films consist of a mosaic pattern of needle-like crystallites arranged in a random manner in the plane of the film. Each crystallite is usually on the order of 1 μm in average dimension, although wide variation from suboptical to several millimeters in diameter can be obtained through control of the crystallization process in certain circumstances (Figure 7). The crystal plane parallel to the film surface, however, is usually identical from crystal to crystal across the film. This implies that the film should exhibit anisotropic properties in such a manner as to provide uniquely different properties through vs. along the film plane. This has been observed experimentally for a wide variety of physical and chemical properties. The observed registry (or epitaxial interaction) between monolayers varies depending on the specific chemistry and process conditions chosen. It is clear that it is possible in specific cases to invoke a specific epitactic interaction leading to the development of complete order through the LB film. This can be evidenced by electron and X-ray diffraction studies.

Enkelmann and Lando have investigated the structure of a series of aliphatic amphiphilic compounds. Their studies indicate that the packing of the aliphatic molecules within the multilayer are identical to the packing seen in conventionally grown single crystals of the same molecule (Figure 8). For example, regardless of the methods chosen for multilayer

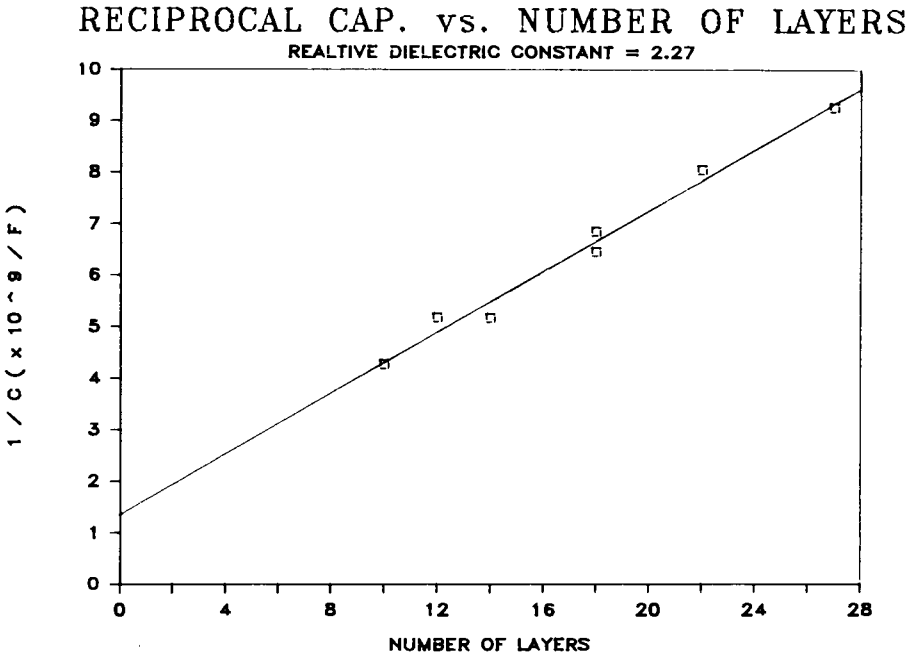

FIGURE 7. 16/8 diacetylene as insulator.

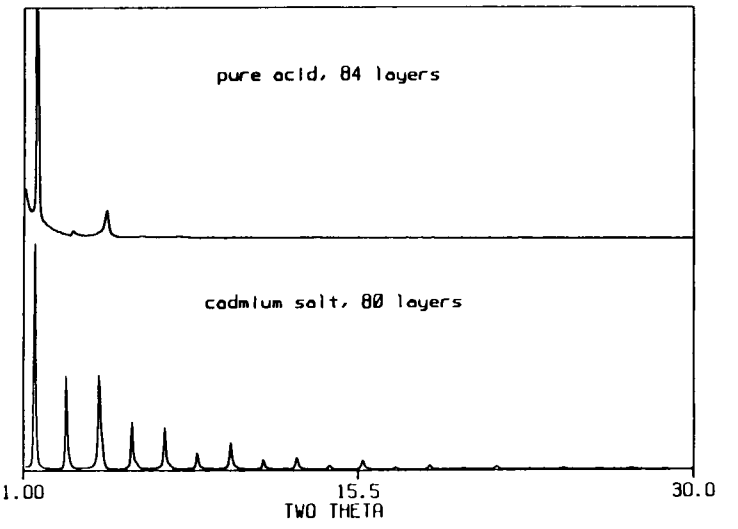

FIGURE 8. Packing of aliphatic molecules within a multilayer.

formation, or measurements indicative of deposition of two alternating head-tail/tail-head layers of poly(vinyl stearate) within the multilayer, poly(vinyl stearate) only ended up with its usual head-tail/head-tail packing.[20] (*Note*: the "head" refers to the polar end, and the "tail" refers to the apolar end of the amphiphilic molecule.) This observation has been verified within our group in many cases, including our attempts to grow a pyroelectric crystal from an LB film. In no case was it possible to grow a film which did not exhibit the identical molecular packing evidenced by an X-ray single crystal or powder study of the same material.[21]

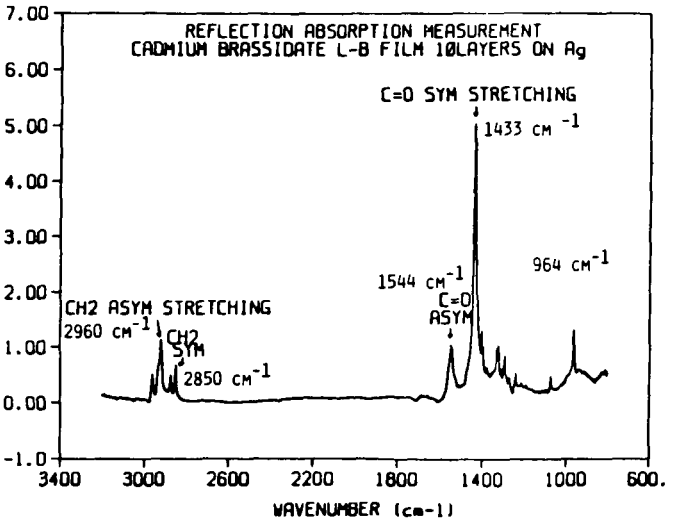

FIGURE 9. FTIR reflection absorption spectra of cadmium brassidate film deposited by the Langmuir technique. The thickness of the film is 30 nm.

FTIR surface studies are also quite useful in structural analyses of LB films (Figure 9). Their use, however, is restricted to experts in surface techniques, and one should not expect as well that conventional FTIR instruments provide useful information regarding LB films.

IV. APPLICATIONS OF MONOLAYERS AND MULTILAYERS

As is true for crystals, in general, there are an unlimited number of applications for LB films. Some applications focus on the inherent properties of the film, such as barrier, lubricating, and insulating properties ("passive devices"). Other applications utilize an active molecular species within the film to alter either the path of light, electrons, or ions as they are transported through the film ("active devices"). Both passive and active device properties of LB films will be discussed in the subsequent sections.

A. Microelectronic Devices

One particularly important application for LB films is in the area of microelectronics. The field of microelectronics utilizes thin films of primarily inorganic semiconductors and oxides in processing electronic information. Thickness control on the order of nanometers is essential in order to reach high information and process densities. Further, the film grown must have very few defects per square micrometer in order to be processible into an electronic circuit, using very large-scale integration (VLSI) technology.

Both the type and number of inorganic thin films which can be grown successfully on silicon wafer substrates are severely limited to a handful of compounds. Fortunately, the native oxide of silicon can be used to provide both insulating and protective properties to the underlying crystal, and can be easily grown in a high-temperature oxidation furnace.

The other competitive semiconductors (i.e., germanium, gallium arsenide, cadmium sulfide, indium phosphide, gallium phosphide) do not form surface oxides which provide both the insulating and protective properties of silicon oxide. As a result, the industry has focused on attempts to grow silicon oxide, silicon nitride, and related compounds on these semiconductors, but with limited success.

LB films, due to their near-ambient processing conditions, provide a low-temperature processing alternative to silicon oxide for both silicon and alternative semiconductors. They

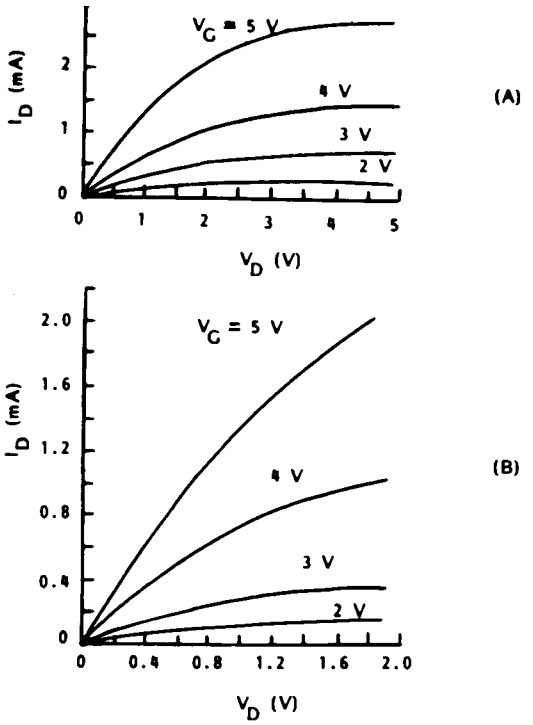

FIGURE 10. (A) The drain I-V characteristics of a typical IGFET obtained from a curve tracer; (B) I-V curves of the same device in the nonsaturation region.

have been shown to be useful as both insulating and protective coatings for semiconductor substrates (color plate 1). In addition, these films can be produced from a variety of "doped" materials to provide the exact capacitance values required for a particular application.[22]

Furthermore, LB films can play an active role by enhancing the intrinsic carrier mobility (i.e., clock speed of a chip) by about 20%. Color plate 2* shows the I-V characteristics of a typical FET made with an LB film insulator, and Figure 10 indicates the test silicon chip used to prepare such FETs (e.g., IGFETs). It is these FETs which exhibited enhanced mobility of charge carriers. Although the mechanism of this mobility enhancement is not known, it may be supposed that some electron transport must be occurring within the LB film itself. Thus, charge may be reversibly injected and withdrawn from the LB film-insulating layer as needed. It is clear that there is substantial resistance to the use of any organic material in microelectronic circuits (e.g., the long delay before use of spincast polyimides as multilevel separation layers in multilayer devices). LB film use is compounded by unfamiliarity on the part of electrical engineers with the process of film production (i.e., LB films are not spuncast!). However, the long-term limitation of their use in microelectronics relates to temperature stability.

Regardless of chemical composition, LB films are prepared from molecular crystals, not atomic crystals. As such, van der Waals forces, and not covalent or ionic forces, hold these crystals together. van der Waals (i.e., dispersion) forces are substantially weaker by nature than covalent and ionic forces, and even the best organic crystals will melt or decompose at temperatures exceeding 400°C. This number should be compared to the temperatures used in the microelectronics industry (e.g., typical oxidation furnaces [1100°C], ohmic junction furnaces [450°C]), in order to understand the magnitude of this limitation.

*See color plate 2 following p. 216.

Research at Case has shown that suitable microelectronic devices can be fabricated using LB films as insulating layers, but only when all the furnace steps in the process are done in advance.

The real delay, therefore, facing the application of LB films in this industry is in the design and acceptance of processes which either apply all of the LB films near the end of processing, or somehow protect these films from the high temperatures of the current process.

B. Dielectrics

Thin/thick-film (i.e., hybrid) devices are currently being implemented on a large scale within the microelectronics industry. These films contain resistors and capacitors which can be glued to a printed circuit board, in contrast to soldering individual cylindrical resistors and capacitors to the same board. Process time, as well as smaller product size and higher yield data, can be substantially improved by hybrid device use.

As in the case of microelectronics, hybrid devices should be composed of very thin, defect-free films stacked neatly on top of one another. Each film can act as an individual capacitor or resistor, or assemblies of different materials can be used together to make individual capacitors or resistors.

Due to the relatively relaxed purity and process standards applied to hybrid devices, it should be easier for LB films to penetrate this application area than that of conventional microelectronics. The use and process temperatures of printed circuit boards are near room temperature and should pose no limitation on the choice of LB film material.

As of yet, no concerted attempts have been disclosed on the use of LB hybrid devices, but there is no intrinsic limitation as to their application in this area.

C. Barriers

The use of monolayers as water evaporation barriers has already been discussed. What is clear is that gas and liquid penetration through any crystal, both inorganic or organic, is slow and occurs primarily through crystal defects. Since LB films are nothing more than very thin crystals, it is not surprising that such films can provide remarkable protection from gas and liquid penetration. The main problem with their use as barriers relates to very slow, uneconomic production speeds and costs. If a new process can be developed to prepare such films at much higher speeds, with inexpensive chemicals, this application can become quite important.

D. BioFilms

The original source of chemicals used in LB film production came from plants and animals, and could be categorized as lipids or phospholipids. Lipids make up the majority of all cell membranes and exist in humans in a near-liquid crystalline state or ordered disorder. Their fluid-like behavior, combined with strong hydrogen and covalent bonding forces holding them into a bilayer morphology, makes the basis for an excellent perm-selective membrane and protective coating around cells.

These authors, as well as many other investigators, have shown that a diacetylene-based phospholipid can be deposited onto a water surface to form an ordered monolayer, and this monolayer can be picked up to form multilayers by the Blodgett technique.[23]

One application for such films relates to their use as advanced biosensors. In this application, the LB film acts as a receptor for other bioactive sensing molecules, such as valinomycin. Another application involves the coating of implants with a biocompatible coating, prepared from a biological LB film material.[24]

The potential exists for LB films to have a major impact in this area, as the mechanical and thermal requirements for bioapplications are much less severe than most others.

E. Lubricants

Tribology is the science of wear, abrasion, and friction. Metal-to-metal, ceramic-to-metal, polymer-to-metal, and polymer-to-ceramic parts are constantly wearing against one another in most major appliances, automobiles, trucks, tape recorders, etc. There are two approaches to friction and wear reduction in these applications: (1) the use of liquid lubricant oils to provide a renewable thin-film liquid layer between the rubbing parts, and (2) the use of solid lubricant coatings to provide a permanent thin-film lubricant layer between the parts.

LB films can be prepared from waxen materials, such as stearates or palmitates, which are excellent liquid lubricants when dispersed in water (i.e., soaps). When in multilayer form, such films have already found potential application as magnetic tape coatings for rotary head tape machines.[25] In such an application, the tribological coating provided virtually unlimited rotary head life and substantially improved the length of time that a tape machine could be in pause position, without significant tape wear.

By careful selection of materials to be used in tribological applications, it should be possible to provide LB film solutions to many friction problems in all of the industries mentioned above.

F. Spacers

As mentioned previously, spuncast polyimides are under serious consideration as dielectric spacers between active silicon "chips" in multilevel microelectronic devices. They exhibit excellent thermal stability and can be fabricated with existing technology. Two serious questions remain, however, concerning their use as spacers: (1) what is the long-term impact of the use of amorphous spacers with a substantial concentration of unreacted chemicals within them, and (2) what is the long-term impact of the use of spacers with substantially uncontrollable thickness variation across their lateral dimensions?

LB films directly solve these two potential problem areas for polyimides. Furthermore, if polyimides are so critical for thermal stability, such chemical moieties can be used to make multilayer films. There is no intrinsic chemistry dictating the formation of LB films, other than that the molecules used must have some sort of amphiphilic character. Specific amphiphilic polyimides could be synthesized for this application.

The fabrication issue remains, however. LB films cannot be formed by conventional spincasting technology. Indeed, even if they could be formed by this route, the resulting films would exhibit the same thickness nonuniformity problems as other spuncast films. The production rates associated with spincasting are quite comparable to the Blodgett technique, so this area is an application area where production scaleup is not a problem. Indeed, there is no reason why LB films should not play a major role in the development of spacers for multilevel microelectronic devices in the future.

G. Optical Coatings

Perhaps the most interesting application for LB films relates to their use as active and passive layers in integrated and optical fiber systems. Their intrinsic polycrystallinity and mosaic structure preclude significant optical transport through the films in a wave-guiding manner. However, applications where thickness control determines how an optical coating will reflect light back into a waveguiding medium would benefit substantially from the use of these uniform multilayers. This application was originally mentioned by Langmuir in the early 1930s.

Furthermore, many optical applications require crystalline order in only one direction within a film, such as laser coatings. For these transmission applications, LB multilayers may provide a convenient method for provideing uniform thin coatings.

H. Sensors

Hybrid chemiresistors and chemitransistors (CHEMFETs) can be prepared by the use of

LB films as the sensing dielectric in the device (color plate 3*). Their sensitivity and response times to various gases compare favorably with those of conventional surface acoustic wave sensors.[26]

V. CONCLUSIONS AND FUTURE OUTLOOK

Scientific interest in Langmuir films prepared by the Blodgett technique has undergone a renaissance, with dozens of research groups across the world now actively studying potential applications for these films. This chapter has surveyed many of the potential applications, albeit briefly, but many others remain unmentioned.

What is clear is that these films possess the remarkable properties of high crystallinity, coupled with fabrication ease under mild processing conditions. What is not clear is how soon any application for LB films will be realized commercially.

There are many barriers to the introduction of a new material, especially one which is not readily visible to the naked eye. In engineering, one speaks of an "experience curve", which is the measurement of a number of critical properties of a given material as a function of actual use time in a given application. The experience curves for LB films have yet to be developed, and until that time there will remain a healthy skepticism about their practical applications among engineers.

I believe that LB films will prove very useful in many, but not all, of the applications mentioned in this chapter. However, the actual use of LB films in commercial products will take significantly longer than many who work in the field expect. Researchers should expand their development of methods of film characterization and of film properties, as well as continue introducing and testing new amphiphilic materials. It is only through these efforts that it will be possible for experience curves to be developed for specific applications.

REFERENCES

1. **LaMer, V. K., Ed.,** *Retardation of Evaporation of Monolayers,* Academic Press, New York, 1962.
2. **Blodgett, K. B. and Langmuir, I.,** Built-up films of barium stearate and their optical properties, *Phys. Rev.*, 51, 964, 1937.
3. **Langmuir, I.,** The mechanism of the surface phenomena of flotation, *Trans. Faraday Soc.*, 15, 62, 1919.
4. **Blodgett, K. B.,** Films built by depositing successive monomolecular layers on a solid surface, *J. Am. Chem. Soc.*, 57, 1007, 1935.
5. **Kuhn, H.,** Energieubertragung in monomulekularen schichten, *Naturwissenschaften,* 54, 429, 1967.
6. **Cemel, A., Fort, T., and Lando, J. B.,** Polymerization of vinyl stearate multilayers, *J. Polym. Sci. Part A-1,* 10, 2061, 1972.
7. **Tien, H. T.,** *Bilayer Lipid Membranes,* Marcel Dekker, New York, 1974.
8. **Barraud, A., Ruaudel-Teixier, A., and Rosilio, C.,** Reactions chemiques a l'état solide dans les couches monomoléculaires organiques, *Semin. Chim. Etat Solide Ann. Chim.*, 10, 195, 1975.
9. **Finkelmann, H., Happ, M., Portugall, M., and Ringsdorf, H.,** Liquid crystalline polymers with biphenyl-moieties as mesogenic groups, *Makromol. Chem.*, 179, 2541, 1978.
10. **Roberts, G. G., Pande, K. D., and Barlow, W. A.,** InP-Langmuir-film M.I.S. structures, *Electron. Lett.*, 13, 581, 1977.
11. **Fariss, G., Lando, J. B., and Rickert, S. E.,** Phase controlled surface reaction-reaction of a monolayer at the gas-water interface, *J. Mater. Sci.*, 18, 3323, 1983.
12. **Dewa, A. S., Fung, C. D., DiPoto, E. P., and Rickert, S. E.,** The study of metal-insulator-semiconductor structures with Langmuir-Blodgett insulators, *Thin Solid Films,* 132, 27, 1985.
13. **Fung, C. D. and Larkins, G. L.,** Planar silicon field-effect transistors with Langmuir-Blodgett gate insulators, *Thin Solid Films,* 132, 33, 1985.
14. **Spaulding, J.,** Electron Beam Lithography of Ultrathin Resists, M.S. thesis, Case Western Reserve University, Cleveland, OH, 1985.

*See color plate 3 following p. 216.

15. **LaMer, V. K., Ed.,** *Retardation of Evaporation of Monolayers,* Academic Press, New York, 1962.
16. **Mann, J. A.,** Pre-Langmuir-Blodgett monolayers, *Thin Solid Films,* 152, 29, 1987.
17. **Pethica, B. A.,** Experimental criteria for monolayer studies in relation to the formation of Langmuir-Blodgett multilayers, *Thin Solid Films,* 152, 3, 1987.
18. **Biddle, M. B., Rickert, S. E., and Lando, J. B.,** Constructing a processing window for a Langmuir-Blodgett film, *Thin Solid Films,* 134, 121, 1985.
19. **Roberts, G. G., Pande, K. D., and Barlow, W. A.,** InP-Langmuir-film M.I.S. structures, *Electron. Lett.,* 13, 581, 1977.
20. **Enkelmann, V. and Lando, J. B.,** Polymerization of ordered tail-to-tail vinyl stearate, *J. Polym. Sci. Polym. Chem. Ed.,* 15, 1843, 1977.
21. **Biddle, M. B.,** Molecular Engineering of Ultrathin Films Using the Langmuir-Blodgett Technique, Ph.D. thesis, Case Western Reserve University, Cleveland, OH, 1987.
22. **Shutt, J. D. and Rickert, S. E.,** Poly(diacetylene) salts as thin-film dielectrics in metal-Langmuir film-semiconductor devices, *Langmuir,* 3, 460, 1987.
23. **Scholfalvi, K. H.,** unpublished data, 1987.
24. **Brown, A. D.,** An ionophoretic chemically-sensitive solid state transducer, *Sensors Actuators,* 6, 151, 1984.
25. **Seto, J., Nagai, T., Ishimoto, C., and Watanabe, H.,** Frictional properties of magnetic media coated with LB films, *Thin Solid Films,* 134, 101, 1985.
26. **Fu, C. W. and Rickert, S. E.,** unpublished data, 1987.

Taylor & Francis
Taylor & Francis Group
http://taylorandfrancis.com

INDEX

A

AC conductivity, 175—178
Adhesion promoter, 12, 38, 41
Adhesion to substrate, 12, 38, 41
Alkyd, 76
Allyl ester, 76
Alpha particle barrier, polyimides as, 56
Aluminum chelate adhesion promoter, 41
γ-Aminopropyltriethoxy silane, 38, 41
Anisotropic etching, 13
Anthracene, 106
Aromatic polyamide, 83
Asphalt, 76
4-Azido chalcone, 27

B

Barrier
  Langmuir-Blodgett films as, 222—223
  moisture, 64, 66
Bathtub model, of device failure, 86—88
Battery, 95, 98—99, 146—149, 158, 195—199
Battery separator, 160
Beam-leaded device, 67—69
Benzophenone tetracarboxylic dianhydride (BTDA), 36
Bilayer resist, 25—27
BioFilm, 223
Biosensor, 223
Bis-γ-aminopropyltetramethyl disiloxane (GAPD), 36—37
Bis-azide, 2—3, 14—15
Bis-azide 3,3′-diazidodiphenyl sulfone, 26
Bisphenol-A, 75, 78
Bis(trifluoromethyl)pentacyclo[6.2.0.0.0.0]dec-9-ene, 128—129
Blodgett, K., 212
BTDA, see Benzophenone tetracarboxylic dianhydride
Buna-S rubber, 77
Burn-in testing process, 87, 89
Butadiene-styrene, 76
p-tert-Butyl benzoic acid, 20

C

Capillary wave interference, 216
Casting, 73
Cavity-filling process, in chip packaging encapsulation, 73—74
Ceramic packaging, 52—53
Ceramics, 94
Charge transport, in conducting polymer, see Conducting polymer, charge transport in
Chemical etching, 13
Chemical sensor, 95, 146—149
Chemical vapor deposition (CVD) encapsulation technique, 69—72
Chemiresistor, 224
Chemitransistor, 224
Chip packing encapsulation technique, 73—74
Chip-to-substrate interconnection
  beam-leaded devices, 67—69
  flip-chip bonding, 67
  tape automated bonding, 67
  wire bonding, 67—69
Chlor-alkali cell, 158
Chloride ions, protection against, 66
Chloro rubber, 77
Cholic acid, *O*-nitrobenzyl ester of, 20
CMOS device, see Complemental metal oxide silicon device
CMOS technology, see Complemental metal oxide silicon technology
Co-area, 216
Coatings, 95
Cobalt metallocene, 148
Complemental metal oxide silicon (CMOS) device, 17
Complemental metal oxide silicon (CMOS) technology, 64, 66
Complex impedance spectroscopy, 195
Conducting polymer
  applications of, 95—99, 134—149
  charge transport in
    electronic interchain, 111—117
    intrachain, by mobile defects, 107—111
    organometallic charge transfer complexes, 117—119
    proton-assisted electron, 119—120
    simple one-electron band theory of, 99—107
  chemical instability of, 96
  composite, 134
  copolymers, 131—134
  environmental stability of, 121—125
  grafted, 131—134
  hydronium and hydride abstraction route from precursor to conductor, 129—130
  insoluble polymers by thermolysis of soluble precursors, 128—129
  materials for, 94—95
  optical properties of
    linear, 134—139
    nonlinear, 142—146
  processibility of, 96—98
  processing of, 126—134
  rigid rod, 126—128
  side chain modifications, 131—134
  solutions in exotic solvents, 130—131
Conductivity
  AC, 175—178
  DC, 174—175, 184
  measurement of, 173

of polymer electrolytes, 173
Conductor, transparent, 139
Configurational entropy model, of ion transport, 181—184
Conformal coating, 74
Contact printing, 3—5
Continuous, atmospheric pressure reactor, 70
Contrast, of polymer resist, 11
Copolymer, conducting, 131—134
Copper/polyimide thin-film multilayer interconnection, 50—51, 54—55
Creutz-Taube complex, 118—119
Crystals, as moisture barriers, 64, 66
Curing agent, 75, 79—80
CVD encapsulation technique, see Chemical vapor deposition encapsulation technique
Cyclic voltammetry, 195

D

DADPE, see 4,4′-Diaminodiphenyl ether
DC conductivity, 174—175, 184
DCPA, see Poly(2,3-dichloro-1-propyl acrylate)
Deep-UV resist, 3—4, 9, 20—21
Degree of planarization (DOP), 41—43
Developer, 2
Device encapsulant, see Encapsulant
Device failure, 86—89
16/8 Diacetylene, 219
Dialysis, 160
4,4′-Diaminodiphenyl ether (DADPE), 36
2,6-Di-(4′-azidobenzol)-4-methyl cyclohexanone, 15
3,3′-Diazidobenzophenone, 20
3,3′-Diazidodiphenyl sulfone, 20—21
4,4′-Diazidostilbene, 15
o-Diazoketone, 3
5-Diazo-Meldrum's acid, 20—21
Dielectric constant, of polyimides, 39, 47, 52
Dielectric material, 57, 222
Dielectric strength, of polyimides, 39
Diffusion coefficient, 173
N,N′-Di(*n*-heptyl)-4,4′-bypyridium dibromide, 95
5,6-Dihydroxy hexa-1,3-diene, 128—129
N,N′-Dimethyl carbazole 3,3′-dicarbazolyl tetrafluoroborate, 114, 116
Dip coating, 74
Dissipation factor, of polyimides, 39
Dissolution inhibitor, 3, 14
Doolittle equation, 180—181
DOP, see Degree of planarization
Double-layer resist, see Bilayer resist
DRAM device, see Dynamic random access memory device
Drug release formulation, 99, 133
Dry developable resist, chemistry of, 22—24
Dry etching, 12—14, 44—45, 48, 57
Dynamic random access memory (DRAM) device, 66, 79

E

ECD, see Electrochromic display
Elastomer, 75, 77
Electrocatalysis, 99, 148
Electrochemical device, 146—149
Electrochemical stability, of polymer electrolytes, 195
Electrochemical transistor action, 199—200
Electrochemistry, solid-state, 200
Electrochromic display (ECD), 99, 200
Electrochromic filter, 99
Electrode
  battery, 146—147
  composite, 195
  lithium-negative, 196—197
Electrolyte, polymer, see Polymer electrolyte
Electromagnetic insulation (EMI), 98
Electromigration, 56
Electron-beam lithography, 2, 5—7
Electronic device, 95
Electronic packaging, 48—55
  high-performance requirements of, 49—50
  thin-film multilayer, 50—55
    advantages and applications of, 52—53
    demonstrations of, 55
    polyimides in, 52—55
Electronic switching system (ESS), 89
Electron resist, 3—5
  chemistry of, 15—19
  contrast of, 11
  negative, 5, 16—19
  positive, 5, 16—18
  sensitivity of, 9—10
Electron transport, proton-assisted, 119—120
Electrophotography, 95
Emeraldine, 120
EMI, see Electromagnetic insulation
Encapsulant
  inorganic, 74, 77
  organic, 74—84
  reliability of, 86—89
  temperature humidity bias accelerating testing of, 84—86
Encapsulation
  for protection, 64, 66
  techniques of
    chip-to-substrate interconnection, 67—69
    on-chip, 69—73
EP-25H, 11—12
Epichlorohydrin, 75, 78
Epoxide, 76
Epoxy
  as encapsulant, 75—79
  glob-top type, 79
  as moisture barrier, 64, 66
  preparation of, 75
Equilibrium spreading pressure, 216
ESS, see Electronic switching system
Ethylenediamine, 43

F

Failure, see Device failure
Failure unit (FIT), 89

Flemion, 158, 164
Flip-chip bonding, 67
Flow coating, 74
Fluorocarbon, 64, 66, 76
Free volume model, of ion transport, 180—181
Fuel cell, 148, 158

G

GAPD, see Bis-γ-aminopropyltetramethyl disiloxane
Glancing angle X-ray scattering, 216
Glass, as moisture barrier, 64, 66
Glass transition temperature, 11, 38
Grafting of polymers, 131—134

H

Hamiltonian, 100—101
Heat-curable silicone, 79—81
Heterojunction, 141
Hexamethyldisilazane (HMDS), 12
HMD, see Hybrid molecular device
HMDS, see Hexamethyldisilazane
Hostile environment, protection against, 66
Hot-wall plasma-assisted chemical vapor deposition, 71—72
Hot-wall, reduced-pressure reactor process, 69—70
HPVA, see Poly(vinylacetate), partially hydrolyzed
Humidity sensor, 158, 199
Hybrid molecular device (HMD), 214
Hydrazine hydrate, 43
Hydrogen sensor, 199

I

IBAE, see Ion beam-assisted etching
IC, see Integrated circuit
Impregnation coating, 74
Indene carboxylic acid, 14—15
Indium tin oxide (ITO) alloy, 99
Infant mortality failure, 87
Inorganic encapsulant, 74, 77
Integrated circuit (IC), 2
  chip dimension trends in, 64—65
  fabrication of, 2—3
  intermetal dielectrics for, 47—48
  technological trends in, 64—65
  very large-scale, 2
Interlayer dielectric, 47—55
  electronic packaging
    high-performance packaging requirements, 49—50
    polyimides, favorable properties of, 52—53
    TFML interconnections, advantages and disadvantages, 52
    TFML interconnects, processing of, 53—55
    TFML packaging, 50—52, 55
  integrated circuits, 47
Iodine, liquid, as polymer solvent, 131
Ion association, in polymer electrolytes, 193—194
Ion beam-assisted etching (IBAE), 44
Ion-beam resist, 3, 9
Ion contaminant, mobile, protection against, 64, 66
Ion etching, 13
Ion implantation, 3—4
Ion mobility, 173
Ion-specific field effect transistor (ISFET), 148
Ion transport, by polymer electrolytes, 172—194, see also Polymer electrolytes
Iron metallocene, 148
ISFET, see Ion-specific field effect transistor
Isotropic etching, 13
ITO alloy, see Indium tin oxide alloy

K

Kapton, 36, 49

L

Langmuir, I., 212
Langmuir-Blodgett (LB) film
  applications of, 220—224
  compressive creep test of, 214—215
  diffusion properties of, 218—219
  electronic properties of, 218
  fabrication of, 217—218
  multilayer properties of, 216—217
  properties on water surface, 214—216
  structural properties of, 219—220
Langmuir isotherm, 215—216
Laser ablation, 46—47, 54
Laser etching, 46—47
Latex, polypyrrole, 132
Lauda film balance, 213
LB film, see Langmuir-Blodgett film
Leucoemeraldine, 120
Lift-off stencil, 57
Lipids, 223
Lithography, see specific types
Lubricant, 223

M

MDA, see Methylene dianiline
MEEP, see Methoxyethoxyethoxypolyphosphophazene
Mercury-cadmium-tellurate temperature sensor, 73
Metalloid phthalocyanine complex, 94
Metalloid phthalocyanine iodine complex, 117
Metals
  as moisture barriers, 64, 66
  phthalocyanine complexes of, 94
Methine-linked heteroaromatic, 97
Methoxyethoxyethoxypolyphosphophazene (MEEP), 183
Methylene dianiline (MDA), 36—37
Microelectronic device, 221
Microlithography, 2, 3—8
Moisture barrier, 64, 66
Molding, 73—74
Monolayer, 212—214, see also Langmuir-Blodgett film
Monolayer viscosity, 216

MRL, 27
MRS, 26
Multichip circuit, flexible substrates for, 49
Multilayer, recent interest in, 212—214
Multilayer resist, chemistry of, 24—26

N

Nafion, 158, 164
1,2-Naphthaquinone, 14—15
Nernst-Einstein equation, 173
Nigraniline, 120
Nitrene, 15
NMR spin-echo technique, 192
Nonswelling negative photoresist, 26—27
Novolak resin, 14—15, 18, 20, 75, 78

O

ODPA-ODA, 83
ODPA-PPDA, 83
On-chip encapsulation technique
  continuous, atmospheric pressure, 70
  hot-wall plasma-assisted chemical vapor deposition, 71—72
  hot-wall, reduced-pressure reactor process, 69—70
  parallel-plate plasma-assisted chemical vapor deposition, 71
  plasma deposition, 70—72
  radiation-stimulated, 72—73
  thermal deposition, 69—70
Optical coating, 224
Optical density device, 95
Optical properties, of polymeric conductor, 134—139, 142—146
Optical switching element, solid-state, 95
Optical waveguide, 143—144
Organic aluminum chelate, 38
Organic encapsulant, 74—84
  epoxies, 75—79
  Parylene, 83—84
  polyimides, 81—83
  polyurethanes, 80—81
  silicones, 79—80
Organometallic charge transfer complex, 94, 117—119
Organosilicon polymer resist, 27
Organosiloxane polymer, see Silicone
Osmium compound, mixed valent, 118
Osmium-ruthenium dimer, 118

P

Parallel-plate plasma-assisted chemical vapor deposition, 71
Parylene, 76, 83—84
Parylene C, 84
Parylene D, 84
Parylene N, 84
Passivation material, polyimides as, 56
Patterning, of polyimide films, 42—47
PBS, see Poly(butene-1-sulfone)
PCM, see Portable conformable mask
PDPUV, 23—24
Pentafluoride, as polymerizing solvent, 130—131
PEO, see Poly(ethylene oxide)
Perfluorinated polyethylene carboxylate, 158
Perfluorinated polyethylene sulfonate, 158
Pernigraniline, 119—120
Phenolaldehyde, 76
Phenolic resin, 75
Photocatalysis, 149
Photoconductivity, 139—142
Photodefinable polyimide, 82
Photoelectrochemical cell, 199
Photogalvanic cell, 199
Photolithography, 2—9
Photonic device, 95
Photopatterning, 44—46
Photoresist, 2
  chemistry of, 14—15
  negative, 2, 26—27
  positive, 3
  sensitivity of, 9
Photosensitive polyimide, 44—46
Photosensitizer, 14
Photovoltaics, 95
Phthalocyanine, 127
Phthalocyanine-bridged polymer, 117—118
Phthalocyanine metal complex, 95, 148
PI-2080, 36
PI-2500, 39
PI-2525, 42
PI-2555, 38—39, 42
PIQ, 36, 38—39, 56
Planarization properties, of polyimide films, 41—42
Planarizing material, 57
Plasma, 13—14
Plasma-assisted etching, see Dry etching
Plasma deposition, on-chip encapsulation technique, 70—72
Plasma etching, 44
PMDA, see Pyromellitic dianhydride
PMMA, see Poly(methyl methacrylate)
PMPS, see Poly(2-methyl-1-pentene sulfone)
PNMCZ, see Poly(*n*-methyl carbazole)
Polarization, of polyimide film, 48—49
Polyacetylene, 94, 96, 98—101, 104—109, 111, 114—115
  alternate single-double bond, 100
  applications of, 95, 141—142, 147—148, 198
  in composites, 134
  in copolymers, 131—132
  in emulsion form, 132
  nonlinear optical properties of, 143—145
  photoconductivity by, 139—141
  precursors for, 128—129
  processibility of, 96—97
  reduction potentials of couples, 121
  rod polymers of, 126—127
  stability of, 96, 121—122
Polyacetylene foam, 127

Poly(2-acrylamino-2-methyl propane sulfonate)/polybrene salt, 164
Poly(acrylate)/polybrene salt, 164
Poly(acrylic acid), 159
Poly(acrylonitrile), 160
Poly(acrylonitrile-butadiene-styrene-methoxyoligoethylene oxide), 166
Poly(alkenylsilane sulfone), 27
Polyalkylsulfide, 162
Poly(allyl methacrylate-co-2-hydroxyethyl methacrylate), 19, 21—22
Poly(amic acid), 34—35, 38
Polyampholyte, 158
Polyaniline, 95, 98, 119, 124
  applications of, 141—142, 147, 149
  charge transfer complex, 119—120
Poly *p*-benzamide, 127
Polybenzimidazobenzophenanthroline, 124
Polybenzobisthiazole, 97, 127—128
Polybenzothiophene, 95
Poly[bis(methoxyethoxyethoxy)phosphazene], 163, 166—167
Poly(3-bromo-*N*-vinylcarbazole), 95
Polybutadiene, 19, 134
Poly(butene-1-sulfone) (PBS), 17, 21—22
Poly(*n*-butyl-α-chloroacrylate), 20—21
Poly(*p*-*t*-butylphenylsilane), 27
Polycarbazole, 97, 112—115, 131
  linear optical properties of, 135—138
  stability of, 122—123
Poly-3,6-carbazole methylene, 130
Poly[2-(4-carboxyhexafluoro-butanoyl-oxy)ethyl methacrylate] lithium salt, 163
Polycarbonate-triphenylamine, 95
Poly(chloromethylstyrene), 19, 21—22
Poly(chloromethylstyrene-co-styrene), 19
Poly(4-chlorostyrene), 19
Poly(4-chlorostyrene-co-styrene), 19
Polydiacetylene, 99, 139, 142
Poly(diallyldimethylammonium chloride), 164
Poly(*N*,*N*′-dibenzyl-4,4′-bipyridium), 95
Poly(2,3-dichloro-1-propyl acrylate) (DCPA), 21
Poly(diethoxy(3)methylitaconate), 163
Poly(dimethyl siloxane), 27
Poly(dimethyl siloxane-co-ethylene oxide), 165
Poly(dimethyl siloxane-co-polyethylene oxide), 199
Poly(dioxolane-co-triaxane), 165
Polyelectrolyte, 158—160
Poly(epichlorohydrin), 163
Polyethylene, 76, 134, 199
Poly(ethylene adipate), 163, 167
Poly(ethylene glycol), 171
Poly(ethylene imine), 162
Poly(ethylene oxide) (PEO), 160—161, 163, 165, see also Polymer electrolyte
Poly(ethylene sebecante), 161
Poly(ethylene succinate), 161, 163, 167
Poly(ethylene sulfonic acid), 200
Poly(ethylenimine), 163
Poly(2-fluoroethyl methacrylate), 21
Poly(glycidyl methacrylate), 19
Poly(glycidyl methacrylate-co-ethyl acrylate), 19
Poly(glycidyl methacrylate-co-styrene), 19
Poly(hexafluorobutyl methacrylate), 18, 21
Polyimide, 76
  adhesion to substrate, 38
  applications of, 34, 223
  aromatic, 83
  chemistry of, 34—39
  coefficient of thermal expansion of, 47
  curing of, 34—35
  dielectric constant of, 39, 47, 52
  dielectric strength of, 39
  dissipation factor of, 39
  as encapsulant, 81—83
  glass transition temperature of, 38
  molecular weight of, 38
  photodefinable, 82
  photosensitive, 37, 44—46
  physical properties of, 37—39
  polymerization of, 34—35
  resistance to ionizing radiation, 38
  solubility of, 38
  synthesis of, 34—35, 83
  tensile strength of, 39, 47
  thermal coefficient expansion, 82
  thermal stability of, 34, 38, 47
  types of, 35—37
  volume resistivity of, 39
  Young's modulus of, 39, 47
Polyimide/glass composite, 48
Polyimide adhesive, 48
Poly(imide-isoindoloquinazoline-5,6-dione), 36
Polyimide siloxane, 36
Polyimide thin film
  adhesion to surface, 41
  applications of, 47—57, see also Interlayer dielectric
  coating of, 40
  deposition of, 40—41, 53—54
  patterning of, 37, 42—47, 53—54
    by dry etching, 44—45, 48
    by laser ablation, 46—47, 54
    by photopatterning, 44—46
    by wet etching, 42—44, 48
  planarization by, 57
  planarization properties of, 41—43
  polarization of, 48—49
  processing of, 39—47
Poly(iron benzodithiolene), 118—120
Polyisoprene, 2—3, 14—16, 26, 131
Polyisothianaphthene, 137
Poly[lithium methacrylate-co-oligo(oxyethylene) methacrylate], 165
Polymer, conducting, see Conducting polymer
Polymer electrolyte, 160, see also Polymer-salt complex
  applications of, 194—200
  conductivity of, 173
    DC, 175
    morphology and, 185—189
    observed, 185—191

salt concentration and, 187—191
electrochemical stability of, 195
ion association in, 193—194
ion transport in, 172—194
configurational entropy model of, 181—184
free volume model of, 180—181
models of, 179—185
time-dependent percolation theory of, 184—185
preparation of, 161
structure of, 169—172
transference number of, 188—193
Polymer Microdevice Laboratory (Case Western Reserve University), 214
Polymer resist, see also specific types of resists
adhesion to substrate, 12
applications of, 2—3
chemistry of, 14—26
deep-UV resists, 20—21
dry developable resists, 22—24
electron resists, 15—20
multilayer resists, 24
photoresists, 14—15
contrast of, 11
dry and wet etch resistance of, 12—14
future of, 28
general requirements of, 9—14
glass transition temperature of, 11
negative, 2—3, 9—10
organosilicon, 27
positive, 2—3, 9—10
processing parameters of, 9
properties of, 2—14
application of for IC fabrication, 2
factors affecting, 9—12
microlithography, 3—8
resolution of, 11
sensitivity of, 9—11
thermal stability of, 11—12
Polymer-salt complex
cohesive energy density of polymer, 166, 168
lattice energy of salt, 162—166, 168
phase equilibria in, 167—169
polar groups of, 162
preparation of, 161—169
Poly(metaphosphoric acid), 159
Poly(methacrylate), 16, 18
Poly(methacrylic acid), 159, 164
Poly(methacrylonitrile), 14, 18, 21
Poly(methacrylonitrile-co-methacrylic acid), 17—18
Poly(methacrylonitrile-co-methyl-α-chloroacrylate), 18
Poly(methacrylonitrile-co-trichloroethyl methacrylate), 18
Poly[α-methacryloyl-ω-methoxypoly(oxyethylene)], 166
Poly(methoxyethoxyethoxybutadiene), 163
Poly(methoxypolyethylene glycol monomethacrylate), 163
Poly(methoxypolyethylene oxide)methyl siloxane, 163, 165
Poly(*N*-methylaziridine), 163
Poly(*n*-methyl carbazole) (PNMCZ), 116, 135—136
Poly(methyl α-chloroacrylate), 18
Poly(methyldiallyl sulfonium methylsulfate), 159
Poly(methylene sulfide), 163
Poly(methyl isopropenyl ketone), 20
Poly(methyl methacrylate) (PMMA), 10—11, 16, 18, 20—21, 134
Poly(methyl methacrylate-co-acrylonitrile), 18
Poly(methyl methacrylate-co-glycidyl methacrylate), 20
Poly(methyl methacrylate-co-indenone), 20
Poly(methyl methacrylate-co-isobutylene), 18
Poly(methyl methacrylate-co-methacrylic acid), 14, 18, 20—21
Poly(methyl methacrylate-co-methyl α-chloroacrylate), 18
Poly(methyl methacrylate-co-methyl itaconate), 18
Poly(methyl methacrylate-co-3-oximino-2-butanone methacrylate), 20
Poly(2-methyl-1-pentene sulfone) (PMPS), 18
Poly(methyl phenyl silane), 27
Poly(*N*-methyl pyrrole), 99, 141
Poly(methylstyrene), chlorinated, 21—22
Poly(methylstyrene-co-chloromethyl styrene), 19
Poly(3-methylthiophene), 199—200
Poly(*N*-methylvinylpyridinium chloride), 159
Poly(nickel tetrathioxalate), 118—119
Poly(olefin sulfone), 17—18
Poly(oxyethylene), oxymethylene-linked, 165
Polyphenylene, 95—96, 98, 100, 106, 109, 111
applications of, 148
precursors for, 128—129
rod polymers of, 126—127
Poly(phenylene pentadienylene), 130
Poly(phenylene sulfide), 97
Poly(phenylene vinylene), 139
Polyphosphazene, 199
Polyphthalocyanine, 97
Poly(β-propiolactone), 163
Poly(propylene oxide) (PPO), 160—161, 163, see also Polymer electrolyte
Poly(propylene oxide-co-tetramethylene oxide), 165
Poly(propylene oxide-co-urethane urea), 165
Polypyromellitimide, 38
Polypyrrole, 94—98, 106, 109, 111—112
applications of, 141, 146—147, 199—200
chemical instability of, 96
in composites, 134
in emulsion form, 132
formation of, 199
linear optical properties of, 137
stability of, 124
Polyquinoline, 124
Polysilane, 27
Polysiloxane, 183
Poly(siloxane methacrylate), 27
Poly(sodium styrene sulfonate), 160
Polystyrene, 14, 18—19, 76, 163
chloromethylated, 21
in copolymers, 131
monodisperse, 11

polydisperse, 11
Poly(styrene-co-*N*-(*p*-hydroxyphenyl)maleimide), 20
Poly(styrene sulfonate), 99, 158
Poly(styrene sulfonate) sodium salt, 164
Poly(styrene sulfonic acid), 159, 200
Poly(2-sulfoethyl methacrylate) lithium salt, 163
Polysulfur nitride, 94, 99
Poly(tetra-alkylammonium chloride), 160
Polythiophene, 95, 98—99, 109, 133—134
  applications of, 141
  linear optical properties of, 137
  stability of, 124—125
Poly(triallylphenyl silane), 27
Poly(2,2,2-trichloroethyl methacrylate), 18
Poly(trifluoroethyl α-chloroacrylate), 18
Poly(2,2,2-trifluoroethyl methacrylate), 21
Polyurethane, 80—82, 133, 199
Poly(vinyl acetal), 160
Poly(vinyl acetate), 95, 132, 163
Poly(vinyl alcohol), 160, 199
Poly(vinylbenzyl-trimethylphosphonium chloride), 159
Poly(vinyl carbazole), 14, 95
Poly(vinyl carbazole)-trinitrofluorenone, 95
Poly(vinyl chloride), 76, 134
Polyvinylene, 97
Poly(vinyl ether), chlorinated, 21
Poly(vinylidene fluoride), 160
Poly(vinyl phenol), 26—27
Poly(vinyl pyridine)-I_2, 95
Poly(vinyl pyrrolidone), 163, 171
Poly(vinyl stearate), 219
Poly(vinyl sulfonic acid), 159
Poly(vinyl toluene), chlorinated, 20—21
Poly(vinyl trimethylammonium chloride), 159
Poly(para-xylylene), see Parylene
Portable comformable mask (PCM), 25
Potting, 73
Printed circuit board, 222
Printing, see specific types of printing
Projection printing, 3, 5
Protoemeraldine, 120
Proximity printing, 3—5
Pyralin, 36
Pyrazoline, 95
Pyromellitic dianhydride (PMDA), 35—36
Pyromellitic dianhydride-benzidene, 83
Pyromellitic dianhydride-ODA, 83
Pyrrole, anodic polymerization of, 123

R

Radiation-stimulated deposition, 72—73
Raster scan, 6—7
Reactive ion beam etching (RIBE), 44
Reactive ion etching (RIE), 13, 44—45
Reduction potential, of polyacetylene couples, 121
Refractive index, intensity-dependent, 142—143
Reliability, of encapsulant, 86—89
Reliability testing, 86—89
Resist, see specific types of resists
Resole, 75, 78
Resolution, of polymer resist, 11
Rhodia Kermid 600, 36
RIBE, see Reactive ion beam etching
RIE, see Reactive ion etching
Rigid rod polymer, 126—128
Room-temperature vulcanized (RTV) silicone, 79
Rubber, 77

S

Scanning electron-beam lithography, 6—7
Schottkey barrier, 140—141
Screen printing, of polyimide films, 40
Semiconductor, 221
Sensitivity, of polymer resist, 9—11
Sensor, 199, 223—224, see also specific types of sensors
Shadow printing, 3, 5
Shielding, 95
Silane adhesion promoter, 41
Silicone, 76
  as encapsulant, 79
  heat-curable, 79—81
  as moisture barrier, 64, 66
  production of, 79—80
  room-temperature vulcanized, 79
Silicone-epoxy, 76
Silicone-polyimide, 76
Silicone rubber, 77
Siloxane-polyimide, 83
Solar cell, 98—99, 140—141
Solid-state electrochemistry, 200
Soliton conduction, 107—111
Solubility, of polyimides, 38
Spacer, 223—224
Spin coating, 40, 74
Spray coating, of polyimide film, 40
Stability, of conducting polymers, 121—125
Stejskal-Tanner pulsed field gradient, 192
Sulfonium precursor polyelectrolyte, 129
Superconductivity, 94

T

Tape-automated bonding (TAB), 49, 67
Tape machine, rotary head, 223
Tars, 76
TCE polyimide, see Thermal coefficient expansion polyimide
TCNQ, see Tetracyanoquinodimethane
Temperature humidity bias (THB) accelerating testing
  of encapsulants, 84—86
  of leakage current change with time, 88
  of resistance change with time, 87
  triple-track device for, 85—86
Tensile strength, of polyimides, 39, 47
Tetracyanoquinodimethane (TCNQ), 100, 106, 111, 125
Tetrathiofulvalene (TTF), 95, 99—100, 106, 111

TFML packaging, see Thin-film multilayer packaging
THB accelerating testing, see Temperature humidity bias accelerating testing
Thermal coefficient expansion (TCE) polyimide, 82
Thermal expansion, of polyimides, 47
Thermal stability, 11—12, 34, 38, 47
Thermoplastic polymer, 75—76
Thermosetting material, 74—76
Thick-film multilayer packaging, 52—53
Thin-film battery, 196—197
Thin-film multilayer (TFML) packaging, 50—55
  advantages and applications of, 52—53
  demonstrations of, 55
  polyimides in, 52—55
Thioplast, 77
Time-dependent percolation theory, of ion transport, 184—185
Transference number, 173
  measurement of
    chemical gradient methods, 190—192
    potential gradient methods, 189—190
    spin gradient methods, 192—193
  of polymer electrolytes, 188—193
Transistor, 2, 141, 148
Transistor action, electrochemical, 199—200
Transparent conductive thin film, 95
Transparent conductor, 139
Traveling wave, 101
Tribology, 223
23-23 Tricosenoic acid, 216
Trifluoride, as polymerizing solvent, 130—131
Trilayer resist, 25
Triple track conductor (TTC), 85—86
Triple track resistor (TTR), 85
Triple-track testing device, 85—86
TTC, see Triple track conductor
TTF, see Tetrathiofulvalene
TTR, see Triple track resistor
Tubandt's cell, 189—191

U

Urethane, 77
UV radiation, protection against, 66

V

Vapor deposition, of polyimide films, 41
Vector scan, 6—7
Very large-scale integration (VLSI) technology, 2, 64, 221
Vinyl polymer, 14, 16—18
Visible light, protection against, 66
VLSI technology, see Very large-scale integration technology
Vogel-Tamman-Fulcher (VTF) equation, 179—181
Voltammetry, cyclic, 195
Volume resistivity, of polyimides, 39
VTF equation, see Vogel-Tamman-Fulcher equation

W

Wafer stepper, 5
Wax, 76
Wearout, 87
Wet etching, 12—14, 42—44, 48
Wigner lattice, 111
Wire bonding, 67—69
Wiring, 95
WLF equation, 180—181

X

X-ray, generation of, 8
X-ray lithography, 2, 8—9
X-ray mask, 57
X-ray resist, 2—4, 9, 21—22
XU-218, 36

Y

Young's modulus, of polyimides, 39, 47